# Field Testing of Railroad Flatcar Bridges Volume I: Single Spans


## Final Report
## August 2007

**Sponsored by**
the Iowa Department of Transportation
and
the Iowa Highway Research Board (Project TR-498)

IOWA STATE UNIVERSITY

## About the Bridge Engineering Center

The mission of the Bridge Engineering Center is to conduct research on bridge technologies to help bridge designers/owners design, build, and maintain long-lasting bridges.

## Disclaimer Notice

The contents of this report reflect the views of the authors, who are responsible for the facts and the accuracy of the information presented herein. The opinions, findings and conclusions expressed in this publication are those of the authors and not necessarily those of the sponsors.

The sponsors assume no liability for the contents or use of the information contained in this document. This report does not constitute a standard, specification, or regulation.

The sponsors do not endorse products or manufacturers. Trademarks or manufacturers' names appear in this report only because they are considered essential to the objective of the document.

## Nondiscrimination Statement

Iowa State University does not discriminate on the basis of race, color, age, religion, national origin, sexual orientation, gender identity, sex, marital status, disability, or status as a U.S. veteran. Inquiries can be directed to the Director of Equal Opportunity and Diversity, (515) 294-7612.

**Technical Report Documentation Page**

| 1. Report No.<br>IHRB Project TR-498 | 2. Government Accession No. | 3. Recipient's Catalog No. | |
|---|---|---|---|
| 4. Title and Subtitle<br>Field Testing of Railroad Flatcar Bridges Volume I: Single Spans | | 5. Report Date<br>August 2007 | |
| | | 6. Performing Organization Code | |
| 7. Author(s)<br>Terry J. Wipf, F. Wayne Klaiber, Holly A. Boomsma, Kristine S. Palmer, Brian Keierleber, and Jim Witt | | 8. Performing Organization Report No. | |
| 9. Performing Organization Name and Address<br>Center for Transportation Research and Education<br>Iowa State University<br>2711 South Loop Drive, Suite 4700<br>Ames, IA 50010-8664 | | 10. Work Unit No. (TRAIS) | |
| | | 11. Contract or Grant No. | |
| 12. Sponsoring Organization Name and Address<br>Iowa Highway Research Board<br>Iowa Department of Transportation<br>800 Lincoln Way<br>Ames, IA 50010 | | 13. Type of Report and Period Covered<br>Final Report | |
| | | 14. Sponsoring Agency Code | |

**15. Supplementary Notes**

Visit www.ctre.iastate.edu for color PDF files of this and other research reports.

**16. Abstract**

Based on the conclusions of IHRB Project TR-444, Demonstration Project Using Railroad Flat Car Bridges for Low Volume Road Bridges, additional research on the use of RRFC bridges was undertaken.

This portion of the project investigated the following:

- Different design and rating procedures
- Additional single span configurations plus multiple span configurations
- Different mechanisms for connecting adjacent RRFCs and the resulting lateral load distribution factors
- Sheet pile abutments
- Behavior RRFCs that had been strengthened so that they could be used on existing abutments.

A total of eight RRFC bridges were tested (five single span bridges, two two-span bridges, and one three-span bridge).

Based on the results of this study a simplified design and rating procedure has been developed for the economical replacement bridge alternative. In Volume 1, this volume, the results from the testing of four single span RRFC bridges are presented, while in Volume 2 the results from the testing of the strengthened single span bridge plus the three multiple span bridges are presented.

| 17. Key Words | 18. Distribution Statement | | |
|---|---|---|---|
| bridge replacement—field testing —railroad flatcar bridges—simple spans | No restrictions. | | |
| **19. Security Classification (of this report)** | **20. Security Classification (of this page)** | **21. No. of Pages** | **22. Price** |
| Unclassified. | Unclassified. | 176 | NA |

**Form DOT F 1700.7 (8-72)** **Reproduction of completed page authorized**

# FIELD TESTING OF RAILROAD FLATCAR BRIDGES VOLUME 1: SINGLE SPANS

**Final Report**
**August 2007**

**Principal Investigator**
F. Wayne Klaiber
Distinguished Professor, Department of Civil, Construction, and Environmental Engineering Iowa State University

**Co-Principal Investigators**
Terry J. Wipf
Professor, Department of Civil, Construction, and Environmental Engineering
Iowa State University

Brian Keierleber
Buchanan County Engineer
Independence, Iowa

Jim Witt
Winnebago County Engineer
Forest City, Iowa

**Research Assistants**
Holly A. Boomsma
Kristine S. Palmer

**Authors**
Terry J. Wipf, F. Wayne Klaiber, Holly A. Boomsma, Kristine S. Palmer, Brian Keierleber, and Jim Witt

Sponsored by
the Iowa Highway Research Board
(IHRB Project TR-498)

Preparation of this report was financed in part
through funds provided by the Iowa Department of Transportation
through its research management agreement with the
Center for Transportation Research and Education,

A report from
**Center for Transportation Research and Education**
**Iowa State University**
2711 South Loop Drive, Suite 4700
Ames, IA 50010-8664
Phone: 515-294-8103
Fax: 515-294-0467
www.ctre.iastate.edu

## TABLE OF CONTENTS

## LIST OF FIGURES

## LIST OF TABLES

**ACKNOWLEDGMENTS**

The investigation presented in this final report was conducted by the Iowa State University Bridge Engineering Center under auspices of the Center for Transportation Research and Education at Iowa State University. The research was sponsored by the Project Development Division of the Iowa Department of Transportation and Iowa Highway Research Board under Research Project TR-498.

The authors wish to thank the various Iowa DOT engineers who helped with this project and provided their input and support. A special thanks is accorded to the following counties and their respective county engineers for their cooperation and assistance with the field tests: Buchanan County: Brian Keierleber, County Engineer; Delaware County: Mark Nahra, County Engineer; Winnebago County: Jim Witt, County Engineer. The input, advice, and assistance of the project Technical Advisory Committee: B. Keierleber, Buchanan County Engineer; D. Rolando, Floyd and Chickasaw County Engineer; J. Witt, Winnebago County Engineer is gratefully acknowledged.

Special thanks are extended to Doug Wood, Manager of the ISU Structural Engineering Laboratory and the numerous Civil Engineering graduate and undergraduate students for their assistance in various aspects of the project.

## EXECUTIVE SUMMARY

Based on the conclusions of TR-444, Demonstration Project Using Railroad Flatcar Bridges for Low Volume Road Bridges, additional research on the use of RRFC bridges was proposed to increase the understanding of RRFC bridges and the range of applications for which RRFC bridges could be used. Different design alternatives, such as span lengths, span configurations (single vs. multiple), longitudinal connection type, and abutment attachment were investigated through the field testing and subsequent analysis of seven additional RRFC bridges.

In Volume 1, this volume, four single span RRFC bridges were investigated; two are located in Buchanan County, Iowa (BCB2 and BCB3), one is located in Delaware County, Iowa (DCB), and one is located in Winnebago County, Iowa (WCB2). BCB2 is constructed from two 56-ft V-deck RRFCs and has a cast-in-place reinforced concrete beam. The bridge is 20'-7" wide and spans 54'-0". BCB3 is constructed from three 89-ft RRFCs that have been symmetrically trimmed to produce a bridge that has a center to center of abutments length of 66'-2" and is 26'-5 1/2" wide. The BCB3 longitudinal flatcar connection is comprised of 1 1/4" diameter bolts through the adjacent RRFC exterior girders spaced three feet on center. The DCB is constructed from two symmetrically trimmed 89-ft RRFCs. The bridge is 18'-4" wide and spans 66'-4" center to center of abutments. The DCB longitudinal connection is comprised of a 1/2 inch steel plate welded to both RRFCS at the deck level. The WCB2 bridge was constructed from three 89-ft RRFCs that had been symmetrically trimmed to produce a bridge that was 27'-0" wide and spanned 66'-4" center of abutment to center of abutment with 2'-1 3/4" overhangs at each end. The WCB2 longitudinal connection was almost identical to the connection developed for WCB1. Timber planking was again used on WCB2, a single span RRFC bridge (WINNRRFC) in Winneshiek County that had steel plates (23″ x 5/8″) welded to the bottom flanges of the main RRFC girders.

In Volume 2, three multiple span RRFC bridges were investigated: two in Buchanan County, Iowa (BCB4 and BCB5) and one in Winnebago County, Iowa (WCB3) plus a single span RRFC bridge (WINNRRFC) in Winneshiek County that has steel plates (23"x5/8") welded to the bottom flanges of the RRFC girders. BCB4 is constructed from two 89-ft RRFCs to produce a RRFC bridge that has a 40'-3" west span and a 39'-9" east span. There are also end overhangs of 4'-11" and 4'-1" at the west and east ends, respectively. The bridge is 18'-7" wide and has a reinforced concrete beam for the longitudinal connection between cars. BCB5 is constructed from two 89-ft RRFCs to produce a RRFC bridge that has a 42'-8" south span and a 43'-10" north span for a center to center of abutments length of 86'-6". The longitudinal connection is a bolted connection similar to BCB3, except with 5/8" diameter bolts; the bridge is 17'-1" wide. WCB3 is constructed from three 89-ft RRFCs and is almost identical to WCB1. The major different is that WCB3 features sheet pile abutments. The two RRFCs in the WINNRRFC were strengthened so that the original abutments at the site could be used.

To further increase the ease in which a RRFC bridge can be implemented, a simplified design procedure was developed to aid in the design of future RRFC bridges. The simplified design procedure relates a single flexural moment for the entire bridge to a target girder live load moment based on a lateral distribution factor. This factor, which is dependent on the RRFC type, longitudinal connection, and span configuration, was developed for all the different bridge configurations that were tested as part of this investigation. This procedure follows a similar methodology developed in TR-444 and is presented in Volumes 1 and 2 for simple span and multiple span bridges, respectively.

As recommended in TR-444, a rating procedure was developed for use with RRFC bridges. Using the American Association of State Highway Transportation Officials (AASHTO) allowable stress rating methodology, a rating procedure was developed to provide engineers a conventional rating procedure which uses the factors developed for the simplified design procedure. The rating procedure is discussed in both Volumes 1 and 2, with an example of the procedure presented in Volume 1 Appendix D.

# 1.0 INTRODUCTION

## 1.1 Background

Because the Mississippi River forms the eastern border of Iowa and the Missouri River forms the western border of Iowa, the state has a large number of tributary streams. Iowa has approximately 25,000 bridges that cross these tributary streams, as well as rivers and in some cases, roads. Approximately 80 percent of these bridges are on county roads and thus must be maintained by the counties [1]. According to a 2004 National Bridge Inventory report, Iowa has 5,260 structurally deficient bridges and 1,699 functionally obsolete bridges [1]. However, Iowa ranks 30th in the United States in terms of population [2]. This lower tax base limits the funds that are available for Iowa counties to repair or replace deficient and obsolete bridges. Because of this, the Bridge Engineering Center (BEC) at Iowa State University (ISU) has researched low-cost bridge alternatives for use on low-volume roads. One such alternative is the use of decommissioned railroad flatcars (RRFCs) for the superstructure in bridges.

## 1.2 Railroad Flatcar Bridges

The viability of using RRFCs as an economical alternative for low-volume road bridges was investigated in two previous research projects conducted by the ISU BEC: a 1999 feasibility study, TR-421 [3], and a 2003 demonstration project, TR-444 [4]. The use of RRFC bridges has been shown to provide an economical bridge replacement in several counties around the state of Iowa. Other advantages include the ease of construction and maintenance along with the flexibility of bridge length and abutment type. Careful RRFC selection along with proper design and construction procedures can result in RRFC bridges for low-volume roads that will successfully carry legal loads. The performance of these bridges has also been shown to be accurately modeled using grillage modeling and analysis.

### *1.2.1 RRFC Selection*

The feasibility study noted that RRFCs are decommissioned due to age, damage caused by derailments, and economics. Since derailments typically cause significant structural damage to the RRFCs, it was determined that RRFCs involved in derailments are not suitable for use in bridges. It was also recommended that the RRFCs selected for use in low-volume road bridges have a redundant cross-section, that is, multiple girders contributing to the structural strength of the RRFC. Non-redundant cross-sections, those with only one girder capable of supporting traffic loads, are acceptable only if an efficient longitudinal flatcar connection (LFC) is used to transfer loads from one flatcar to another [3].

Inspection of numerous RRFCs found that the basic configuration of most RRFCs is the same, although the size and position of the elements may be different. The elements can be classified into four categories: decking, girders, secondary members, and transverse members. Of these, the girders are the largest members, and thus, provide the majority of the load capacity. To assist in the selection of adequate RRFCs for use in bridges, selection criteria were developed. The five criteria for RRFC selection are:

1. Structural Element Sizes, Load Distributing Capabilities, and Support Locations: The RRFC should have a redundant cross-section or exterior girders with the ability to form a proper LFC and adequate strength and stability at bearing locations.

2. Member Straightness/Damage: Damaged or deformed members will not adequately carry or distribute loads. Visual inspection and string lines should be used to determine member straightness.

3. Structural Element Connections: Choose welds over rivets since rivets lose strength over time. Welds must be checked for fatigue cracks.

4. Uniform Matching Cambers: For the transverse connection, the cambers of the two adjacent RRFCs must be within a tolerance of ± 1 inch.

5. RRFC Availability: Use easily accessible RRFCs so more bridges can be built without additional design work [4].

### *1.2.2 RRFC Bridges*

Several Iowa counties have previously expressed interest in the RRFC bridge concept and have collaborated with ISU in the construction and testing of some demonstration bridges. In the 1999 feasibility study [3], a RRFC bridge in Tama County, Iowa, was tested, and in the 2003 demonstration project [4] bridges in Buchanan County, Iowa, and Winnebago County, Iowa, were designed, constructed, and tested in a collaborative effort between the counties and BEC.

#### 1.2.2.1 Tama County Bridge, Iowa

A RRFC bridge in Tama County spanning 42 ft from center to center of abutments is composed of two RRFCs placed side-by-side to create a 12 ft width. Metal gratings followed by transverse timber planks create the driving surface. Each RRFC had, as the primary longitudinal load bearing members, two exterior girders (C-sections) and two interior girders (I-sections). Multiple transverse members, including one exterior member and one interior member, had sustained significant damage prior to construction. Support conditions at the abutments were not uniform for each flatcar; hence, bridge symmetry and redundancy in load paths at the abutments was questionable [3].

Testing of the Tama County Bridge (TCB) was conducted both before and after connections between the two RRFCs were established; differences in strains and deflections from the two tests varied only slightly. Therefore, it was shown that the longitudinal connections did very little to distribute the loads between the flatcars, but, instead, the timber planks alone could effectively transfer traffic loads across the bridge width [3].

A finite element model created using beam elements verified the results obtained through the field tests conducted on the TCB. Maximum stresses found in the RRFC members were below the yield strength of the steel and the maximum deflections were also less than the American Association of State and Highway and Transportation Officials (AASHTO) maximum recommendation of ‘span’/800 for live load deflections. In conclusion, the analytical model and field tests conducted verified that the TCB could adequately carry Iowa legal loads despite the previous damage in the RRFCs [3].

#### 1.2.2.2 Buchanan County Bridge, Iowa

Buchanan County replaced an existing kingpost pony truss bridge with a single span 56-ft RRFC bridge (clear span: 51ft – 9 1/2 in.). Three 56-ft V-shaped RRFCs placed side-by-side created a 29 ft wide deck, which had a driving surface composed of pea gravel and asphalt millings. A guardrail system was also installed to provide traffic safety across the waterway. Each RRFC had a redundant cross-section consisting of an interior girder seated 8 in. below the two exterior girders, thus creating the V-shaped deck. Using visual inspection and a string line, straightness of members was ensured and the cambers of all three RRFCs were found to vary by only 1/2 in. The RRFCs were placed upon new concrete abutments using bearing plates [4].

A longitudinal reinforced concrete beam was used to connect the RRFCs. Formwork was clamped to the flanges of the adjacent RRFC exterior members, and midspan shoring was constructed. Longitudinal reinforcement was placed in the void region between the adjacent exterior girders and holes were drilled through the exterior members to insert transverse threaded rods which were tightened against the girders. The void region was then filled with concrete and allowed to cure for two weeks before the formwork was removed [4].

Three separate field load tests were performed on the Buchanan County Bridge 1 (BCB1). The first load test was conducted before the concrete beam connection was installed. The second load test was performed after the longitudinal connections between the RRFCs were constructed, and involved testing the bridge both before and after the driving surface was installed. After one year of being in service, the BCB1 was tested for the third and final time. All of the load tests involved measuring deflections and strains at critical locations in the bridge by instrumenting longitudinal and transverse members along with the bridge deck [4].

A grillage analysis of the RRFCs joined with the longitudinal reinforced concrete beam connections was performed. The results indicated that the 56-ft RRFCs could each support Iowa legal loads and that the concrete connection could sufficiently distribute the live loads to each of the three RRFCs, reducing both the maximum strains and deflections in the longitudinal girders. A laboratory connection specimen, similar to the longitudinal concrete beam connection used in the BCB1, was tested in both torsion and flexure. The results showed the connection had adequate strength for use in the BCB1. Field tests of the BCB1 verified the analytical and laboratory results; the RRFC structural members experienced stresses below the yield stress of the material and deflections were below the recommended AASHTO live load recommendations. Therefore, it was concluded that the BCB1 could sufficiently support Iowa legal traffic loads [4].

#### 1.2.2.3 Winnebago County Bridge, Iowa

Due to deterioration of the substructure, a three-span timber bridge crossing the North Fork Buffalo Creek in Winnebago County was replaced with a three-span RRFC demonstration bridge. The two lane bridge had three 89-ft RRFCs side-by-side placed upon steel piles and caps at the abutments and piers. The roadway was 26 ft – 9 in. wide with a transverse timber deck, gravel driving surface, and guardrail system.

A longitudinal reinforced concrete beam was constructed to create the connection between the RRFCs. Holes were drilled through adjacent RRFC exterior girder webs and threaded rods were inserted and bolted. Steel plates were then welded to the bottom flanges of the adjoining exterior girders. Longitudinal reinforcement was placed on top of the transverse threaded rods and the void region between the exterior girders of adjacent RRFCs was filled with concrete. After seven days of concrete curing, steel plates were welded to the adjacent RRFCs, above the concrete connection [4].

Field testing of the Winnebago County Bridge 1 (WCB1) involved instrumenting longitudinal and transverse members with strain and deflection transducers during four separate field tests. The first test was completed before the concrete connection was built between the RRFCs and before any driving surface was installed. The following two tests were conducted immediately after completion of the bridge, and the last test was performed approximately 9 months after the bridge was in service [4].

There was good agreement between the WCB1 theoretical and field test data. Theoretical data were obtained for the WCB1 by constructing a grillage model of the bridge in which the structural members were modeled as prismatic, symmetrical beam elements. Results indicated that 99.9% of the bridge bending moment was resisted by the RRFCs' interior girders. This non-redundancy assumption of the

89-ft RRFC was verified from field tests performed on the WCB1 in which exterior girders experienced nearly zero strains while interior girders had strains over 400 MII (11.6 ksi). Field tests show that the longitudinal concrete beam connections between the RRFCs, along with transverse timber planks on the bridge deck, adequately distribute the traffic loads to all RRFCs. Data from theoretical and field tests show that the RRFC stresses were well below the yield stress of the material, and deflections were below the maximum values specified by AASHTO [4].

Based upon the results from the demonstration project, it was proposed that further study of RRFC bridges be undertaken to investigate different span lengths for use with existing abutments and bridges consisting of only two RRFCs. With the data from the additional testing, the design recommendations [4] could be improved, and a rating methodology for RRFC bridges for use by county engineers and consultants could be developed.

The county engineers that participated in the demonstration project were questioned regarding their decision to continue using RRFC bridges and the benefits associated with RRFC bridges. Both Jim Witt, County Engineer for Winnebago County, and Brian Keierleber, County Engineer for Buchanan County, cited cost as the main factor for choosing to install more RRFC bridges in their counties. The RRFC bridges built in Winnebago County and Buchanan County cost approximately $27 per square foot and $35 per square foot, respectively. Both of these values are well below the typical Iowa Department of Transportation (Iowa DOT) standard slab bridge costs, which are approximately $70 per square foot. In addition to cost, Witt also explained that county forces can be used to install RRFC bridges, which saves time and money.

### 1.3 Objective and Scope of Project

Based on the recommendations for further study in the 2003 ISU RRFC demonstration project [4], a research project to continue investigating the behavior of various RRFC bridges was initiated. The primary objectives of the research were to (1) investigate variables in RRFC bridge construction to improve performance, constructability, and cost; (2) design, construct, and test four RRFC bridges implementing variables from objective (1); (3) refine the design methodology presented in the demonstration project, TR-444, and (4) develop a load rating process for RRFC bridges. The following tasks were completed to achieve the objectives:

- Inspection and selection of RRFCs for use in low-volume road bridge superstructures.
- Data collection through field testing of four RRFC bridges containing different span lengths and widths, longitudinal connection details, and abutment supports.
- Analysis of design variables.
    - Steel sheet pile wall abutments
    - Abutment bearing supports for exterior and interior girders
    - Alternative longitudinal connection details

## 2.0 BUCHANAN COUNTY BRIDGE 2 ON 290TH ST

### 2.1 Background

Buchanan County participated in previous RRFC research projects and was interested in developing the concept further. The second RRFC bridge constructed in Buchanan County crosses the Dry Creek about five miles southeast of Quasqueton, Iowa, on 290th Street; since this bridge is the second RRFC bridge tested in Buchanan County, it will be referred to as BCB2. Presented in Figure 2.1a is a map of a portion of Buchanan County showing the major highways in that portion of the county; the general location of the bridge is identified with a dashed rectangle and labeled Detail A, which is presented as Figure 2.1b; the actual location of the bridge has been identified with a dashed circle. Details on the design and construction of BCB2 are presented in Section 2.2.


a. Map of a portion of Buchanan County

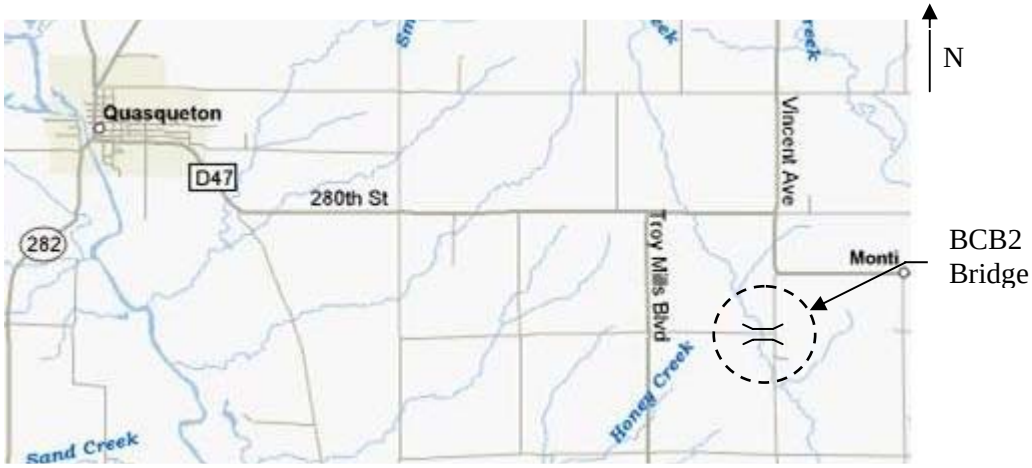


b. Detail A

**Figure 2.1. Location of the BCB2 site [5]**

## 2.2 BCB2 Design and Construction

### *2.2.1 BCB2 Design*

The BCB2, which was designed by the Buchanan County Engineering Department, is based on the BCB1 which was designed, constructed, and tested for the demonstration project, TR-444 [4]. In Table 2.1, the design characteristics of the BCB1 and BCB2 are compared. Although both bridges use 56-ft V-deck RRFCs and have a 54 ft – 0 in. span, the BCB1 consists of three RRFCs while the BCB2 consists of two. In both bridges, the LFC, which will be discussed later, is a reinforced concrete (R/C) beam; however, the BCB2 LFC is wider than the BCB1 LFC. These changes in the design resulted in the width of the bridge to decrease from 29 ft – 1 1/2 in. (BCB1) to 20 ft – 7 in. (BCB2).

**Table 2.1. BCB1 design vs. BCB2 design**

| | BCB1 | BCB2 |
|---|---|---|
| Type of RRFCs | 56-ft V-deck | 56-ft V-deck |
| Number of RRFCs | 3 | 2 |
| Span (center-to-center of abutments) | 54 ft | 54 ft |
| Bridge Width | 29 ft – 1 1/2 in. | 20 ft – 7 in. |
| LFC Width | 14 1/2 in. | 30 1/2 in. |

As may be seen in Figure 2.2a, the 56-ft RRFCs have three main girders, two exterior and one interior, and six small secondary girders, all of which are W-shaped. The main girders are connected with C-shaped transverse members. The deck has a V shape, shown in Figure 2.2d, because the elevation of the top flange of the interior girder is 8 in. lower than that of the exterior girders. Although the elevation of the top flange of the interior girder is constant along the length of the RRFC, the depth of the interior girder varies along the length of the RRFC; these dimensions are shown in Figure 2.3. Unlike the interior girder, the depth of the exterior girders is constant along the length of the RRFC. Thus, as shown in the cross-sectional view of the RRFC at midspan in Figure 2.2a, the depth of the exterior girder is 24 in. along the entire length of the RRFC.

The BCB2 abutments are nearly identical to the BCB1 abutments, which were designed for the demonstration project, TR-444 [4]. The concrete abutments are composed of a 3-ft by 3-ft cap beam with a 1-ft deep, 2-ft high backwall and are reinforced as shown in Figure 2.4a. Each concrete abutment is supported by three HP10x42 piles spaced on 9 ft – 10 1/2 in. centers. The RRFCs are positioned on the abutments as shown in Figure 2.4b; a photograph of the side view of an abutment is shown in Figure 2.4c. One difference between the BCB1 abutments and the BCB2 abutments is the type of joint at the abutments. Both BCB2 abutments have expansion joints while the BCB1 has one integral abutment and one abutment with an expansion joint. As may be seen in Figure 2.5a, the expansion joint consists of a 3/4-in. gap between the RRFC girders and the backwall. In order to prevent gravel and debris from falling into the expansion joint, a 8-in. by 1/2-in. plate was used to cover the gap.

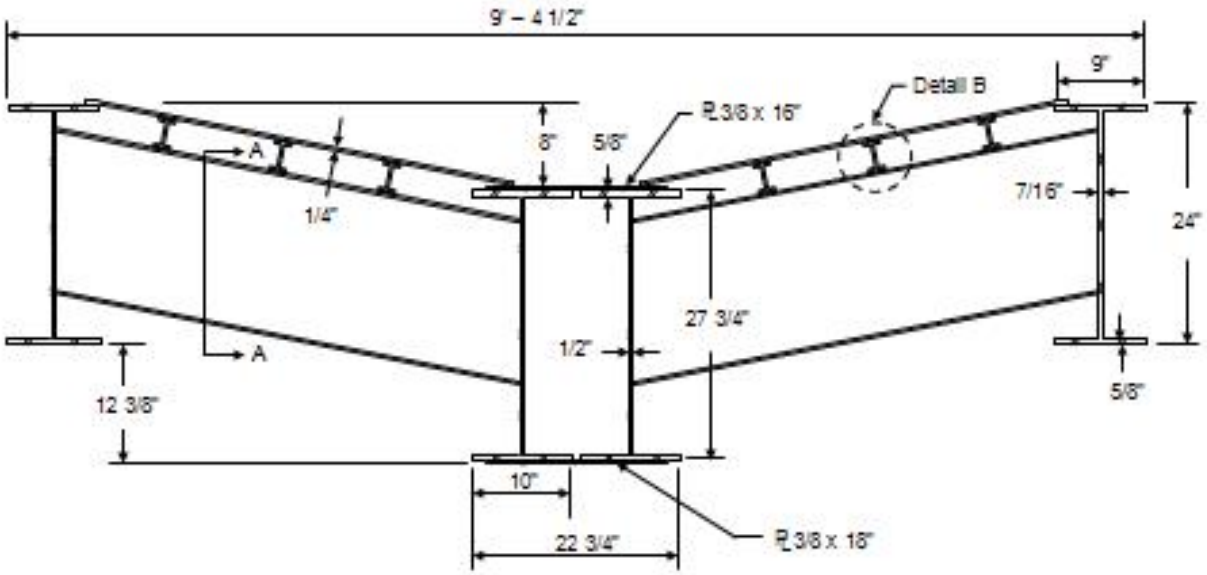


a. Cross-section at midspan

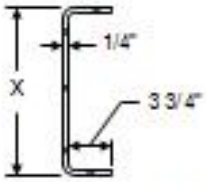


X = 12" for the Small Transverse Member.

X = 16 3/8" for the Large Transverse Member.

b. Section A - A

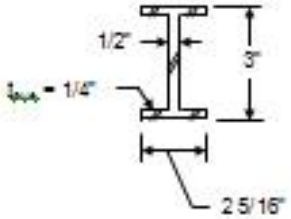


c. Detail B

d. The V-deck

**Figure 2.2. Details of the 56-ft V-deck RRFCs used in BCB2 [4]**

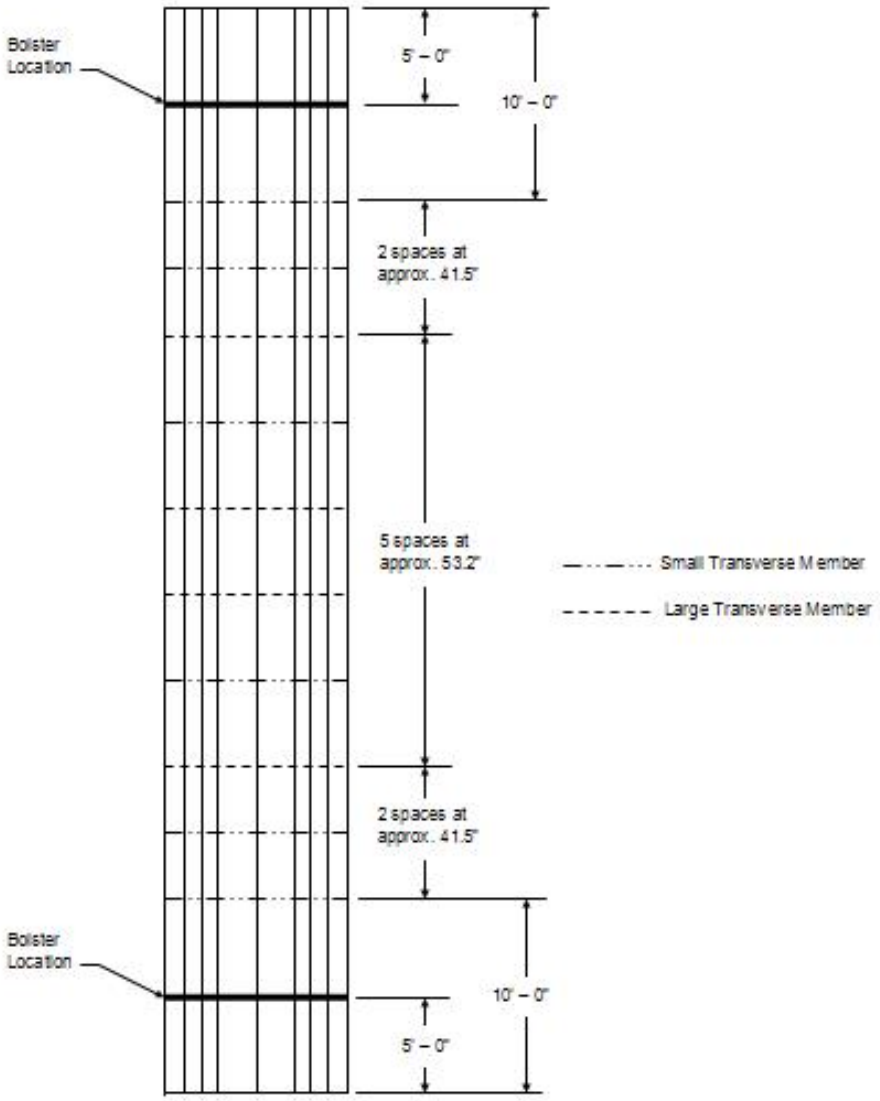


e. Locations of small and large transverse members

**Figure 2.2. Continued**

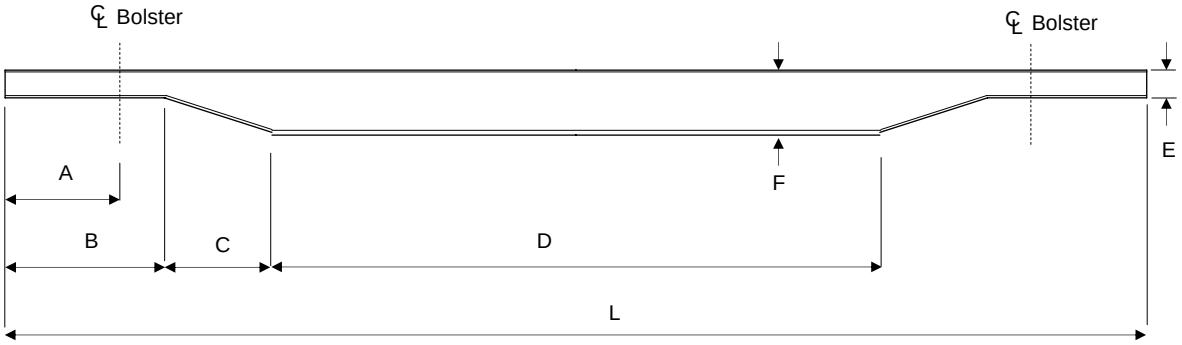


A = Distance from end to bolster
B = Minor Cross-Section Region
C = Transition Region
D = Major Cross-Section Region
L = Length of RRFC

| Bridge | Dimensions | | | | | | |
|---|---|---|---|---|---|---|---|
| | A | B | C | D | E | F | L |
| BCB2 | 5' - 0" | 7' - 2" | 8' - 9" | 24' - 2" | 1' - 1 1/4" | 2' - 3 3/4" | 56' - 0" |

**Figure 2.3. Dimensions of the interior girders in the RRFCs used in BCB2**

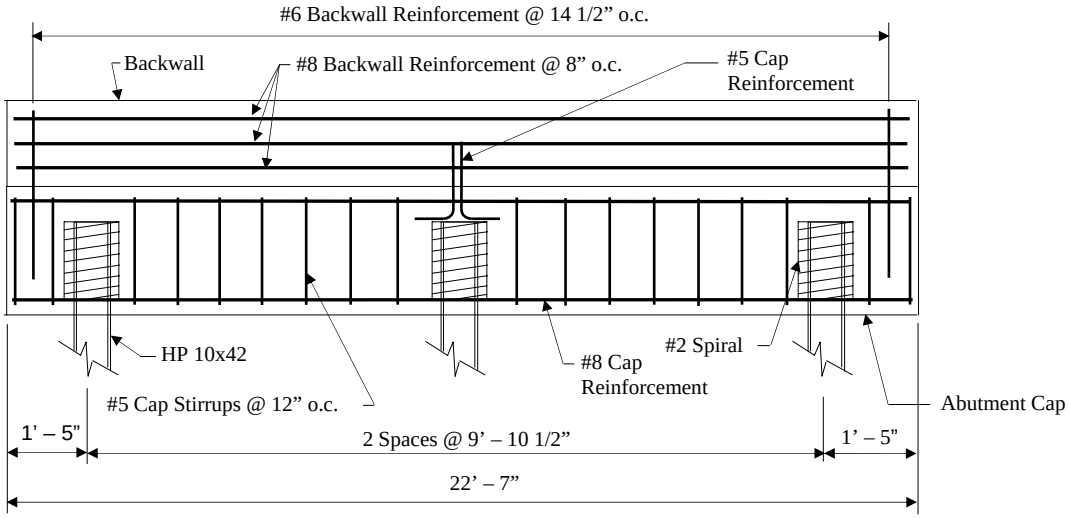


a. End view showing reinforcement in abutments [4]

**Figure 2.4. Details of BCB2 reinforced concrete abutments**

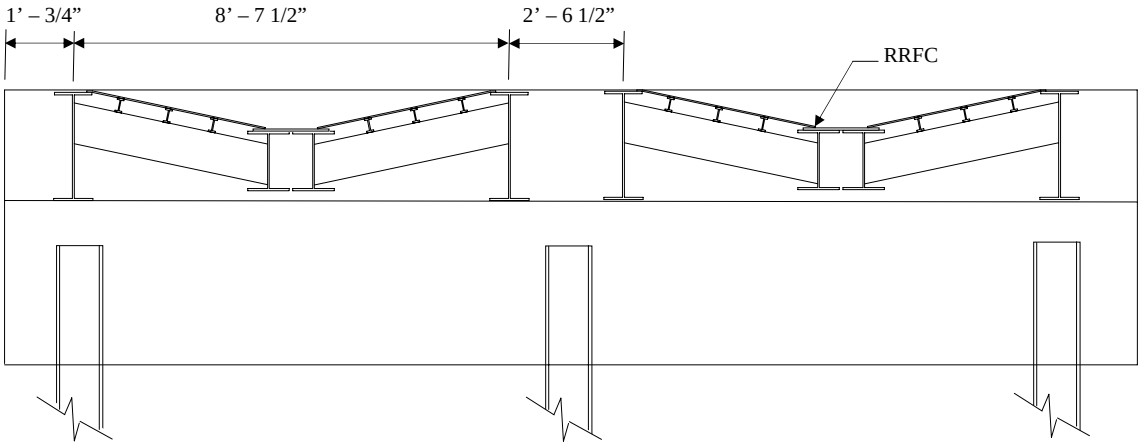


b. Location of RRFCs on abutment [4]

c. Side view of concrete abutment

**Figure 2.4. Continued**

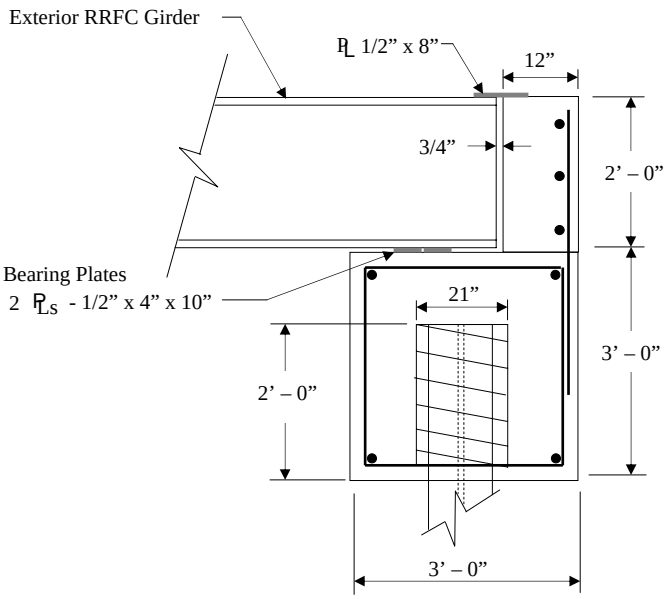


a. Side view of expansion joint (both abutments)

b. View of interior girder resting on abutment cap beam

**Figure 2.5. Details of BCB2 abutment cap beam**

Another difference between the abutments of the two bridges is the interior girder support at the abutments. As shown in Figure 2.5a, both the interior and exterior girders rest on bearing plates; however, at the abutments, the elevation of the bottom flanges of the interior girders is 1 1/2 in. higher than that of the bottom flanges of the exterior girders. Based on a recommendation in the demonstration project, TR-444, additional 1-in. plates were placed beneath the interior girders at the BCB2 abutments as seen in the photograph in Figure 2.5b. At the BCB1 abutments, the interior girders rest on a concrete seat rather than

additional bearing plates [4]; this detail was modified for ease of construction. The LFC between the RRFCs in the BCB2 is a reinforced concrete (R/C) beam which was based on the LFC in the BCB1. The structural adequacy of the BCB1 LFC was verified with a laboratory specimen for the demonstration project, TR-444 [4]. Shown in Figure 2.6a is the cross-section of the BCB2 and the LFC between the two RRFCs. The R/C beam has a width of 30 1/2 in. and a depth of 24 in. The reinforcement consists of two #11 bars for tension reinforcement and two #5 bars for compression reinforcement positioned as shown in Figure 2.6b. With this reinforcement, the concrete beam can support its own weight. As with the BCB1, the adjacent RRFCs are also "tied" together with 3/4-in. threaded rods on 2-ft intervals along the length of the connection.

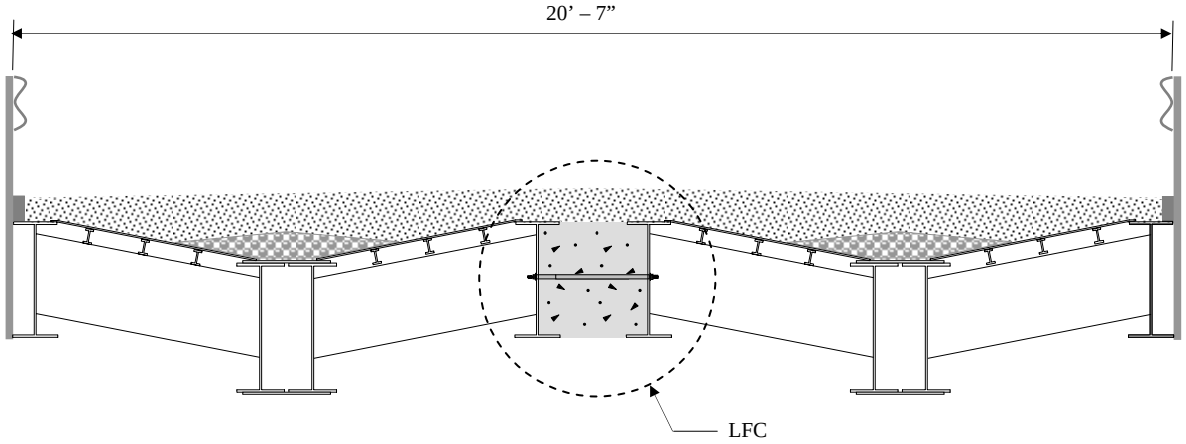


a. Cross-section of BCB2

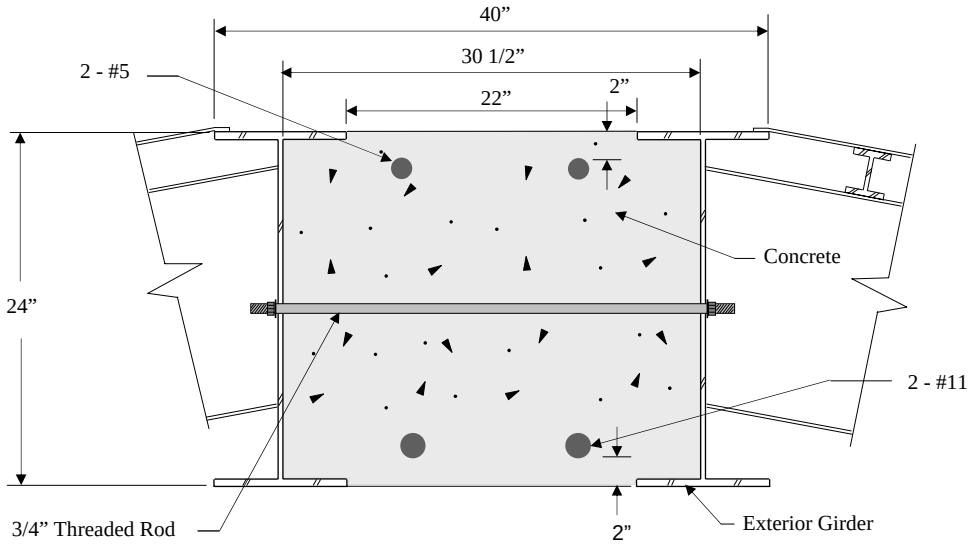


b. Details of LFC

**Figure 2.6. Longitudinal RRFC connection used in BCB2**

*2.2.2. BCB2 Construction*

The BCB2 was constructed by the Buchanan County construction crew, who followed the process for constructing a RRFC bridge developed in the demonstration project, TR-444 [4]. However, recommendations from TR-444 were incorporated into the construction of the BCB2 to simplify construction. In addition to using additional bearing plates beneath the interior girders at the abutments rather than a concrete seat, the formwork for the LFC was left in place once the LFC was completed.

As shown in Figure 2.7a, the 56-ft V-deck RRFCs have protrusions above the deck; however, in order for the RRFCs to be used in a bridge, the protrusions must be removed. Therefore, before the RRFCs were shipped to Buchanan County for use in the BCB2, the protrusions were cut off. A photograph of a 56-ft V-deck RRFC at the bridge site without the protrusions is shown in Figure 2.7b.

As described in further detail in the final report for the demonstration project, the abutments were first constructed, and then the RRFCs were positioned on the abutments as described in Section 2.2.1. Once the RRFCs were in place, the LFC was constructed utilizing leave-in-place formwork. Shoring was not used for the construction of the R/C beam. After the LFC was completed, pea gravel was placed on the RRFC decks over the interior girders to aid drainage and to fill in the V-deck. A layer of gravel was placed over the remaining RRFC deck and the pea gravel for the driving surface. Finally, the guardrail system, which consists of guardrail posts on 6-ft intervals welded to the flanges of the exterior girders with a thrie beam attached to the guardrail posts, was installed. The completed BCB2 is shown in Figure 2.8.

a. The 56-ft V-deck RRFC prior to trimming

**Figure 2.7. Photographs of the 56-ft. V-deck RRFC**

b. The 56-ft V-deck RRFC after trimming

**Figure 2.7. Continued**

a. Side view of BCB2

b. End view of BCB2

**Figure 2.8. Completed BCB2**

c. Underneath BCB2

**Figure 2.8. Continued**

## 2.3 BCB2 Field Testing

The behavior of the BCB2 was determined by loading the bridge with a tandem-axle truck loaded with gravel. The width of the truck's front tires was 15 in., the width of the individual tandem tires was 9 in., and the overall width of the rear tandem tires was 2 ft – 0 in. Truck dimensions and the axle weights of the truck used in the tests are presented in Figure 2.9. The field load tests on the BCB2 will be discussed in the following sections.

### *2.3.1 BCB2 Instrumentation*

In order to determine the structural strength and behavior of the bridge, girder strains in the BCB2 were measured and recorded during the field load tests using strain transducers and a data acquisition system, respectively. For additional bridge behavior data and to determine the load distribution to the primary girders, girder deflections were measured during the tests using deflection transducers. Throughout each test, deflections and strains were measured and recorded continuously. As the tandem axle of the test truck crossed reference lines on the bridge, a feature of the data acquisition system was used to specially mark the strain data for use in the analysis. The reference lines were: the centerline of the west abutment, the 1/4 span, the midspan, the 3/4 span, and the centerline of the east abutment.

The instrumentation plan used in testing BCB2 is illustrated in Figure 2.10. To verify transverse symmetry, the LFC and the bottom flanges of the six primary girders of the bridge were instrumented with strain transducers and deflection transducers at midspan; see Detail C in Figure 2.10a. The deflection

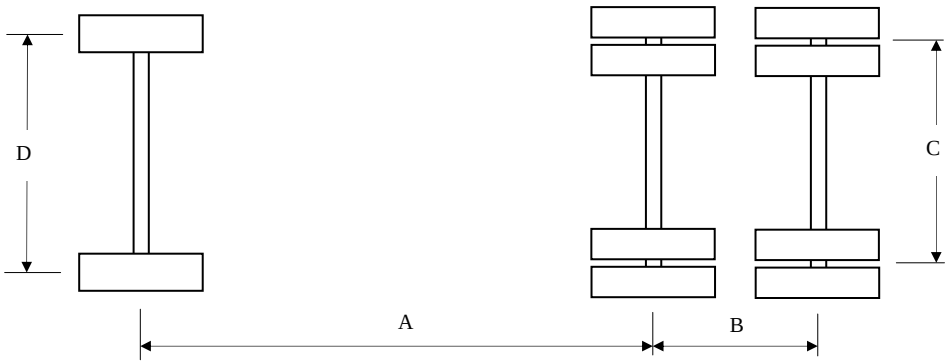


a. Top view


b. Side view

| Bridge | Dimensions | | | | Load (lbs) | | |
|---|---|---|---|---|---|---|---|
| | A | B | C | D | F | T | Gross |
| BCB2 | 13' -11" | 4' - 5" | 6' - 0" | 6' - 9 1/2" | 15,200 | 34,320 | 49,520 |

**Figure 2.9. Dimensions and weights of test trucks used in BCB2 field tests**

transducers were only attached to the bottom flange of each of the six primary girders, not the LFC. The location of the strain transducers across the midspan is shown in Figure 2.10d; the strain transducers usedto verify transverse bridge behavior are transducers 10 through 16. Photographs of a strain transducer and a deflection transducer on the bottom flange of an exterior girder are shown in Figures 2.11a and 2.11b, respectively. In addition to the bottom flanges, the top flanges of the three primary girders of the north RRFC were also instrumented with strain transducers, identified as transducers 17 through 19 in Figure 2.10d. The top and bottom flanges of the three primary girders on the north RRFC were instrumented with transducers 14 through 19 in order to determine the neutral axis of each girder.

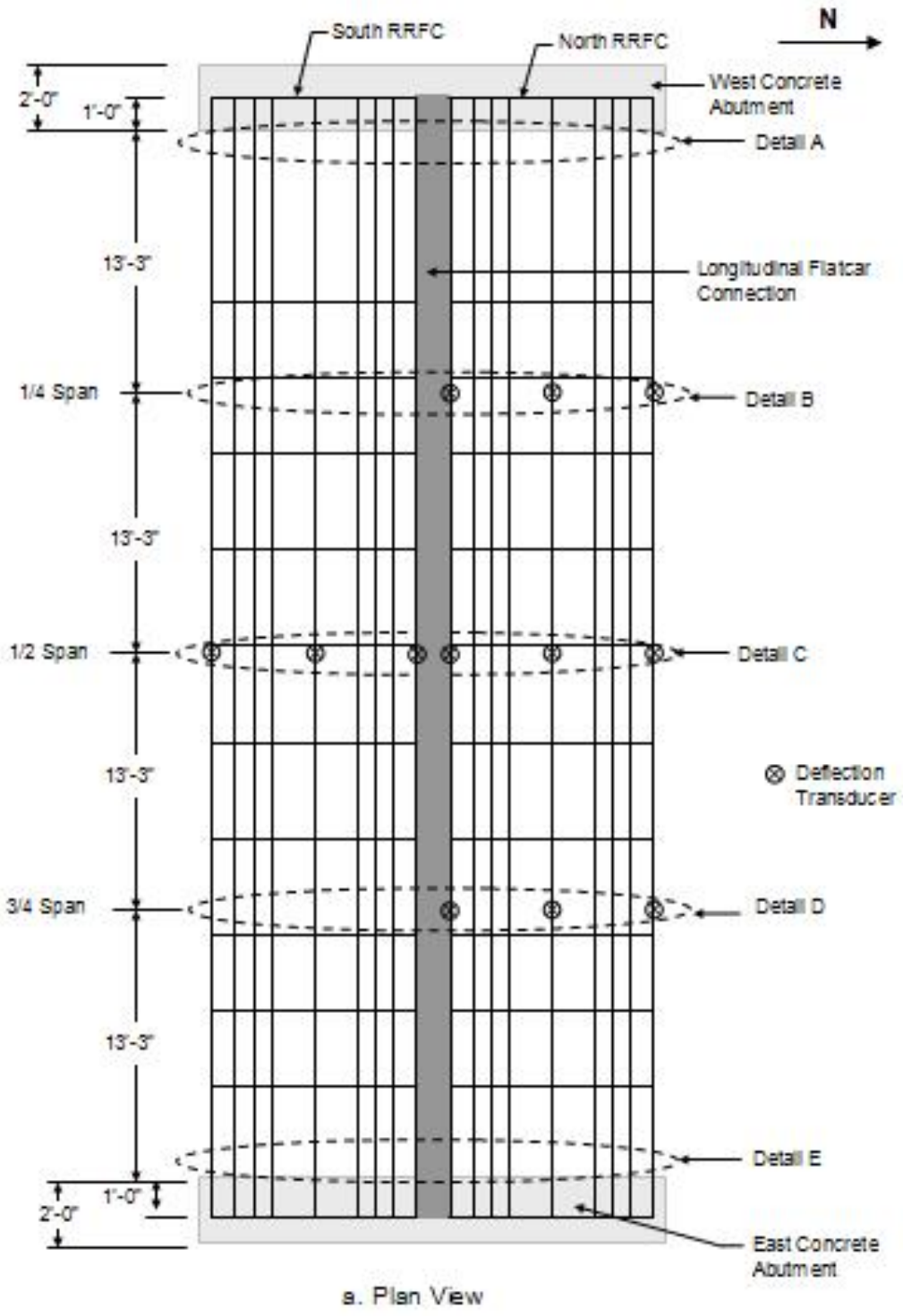


**Figure 2.10. Location of instrumentation in BCB2 tests**

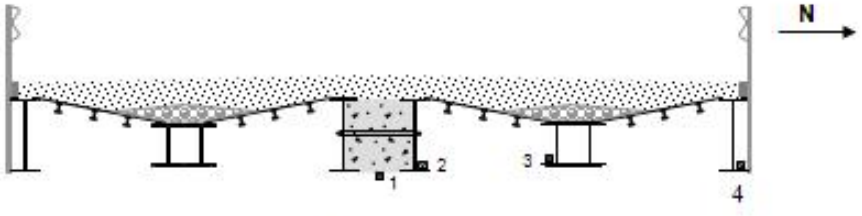


b. Details A and E

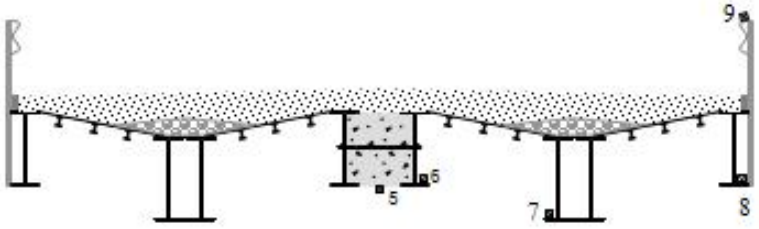


c. Details B and D

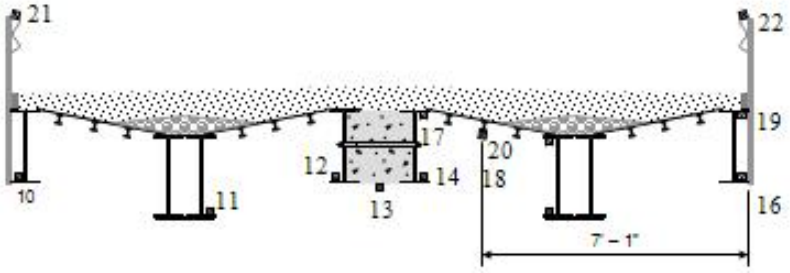


d. Detail C

Notes:

- Strain Transducers 1, 2, and 4 are in Detail E only.
- Strain Transducer 3 is in Details A and E.

**Figure 2.10. Continued**

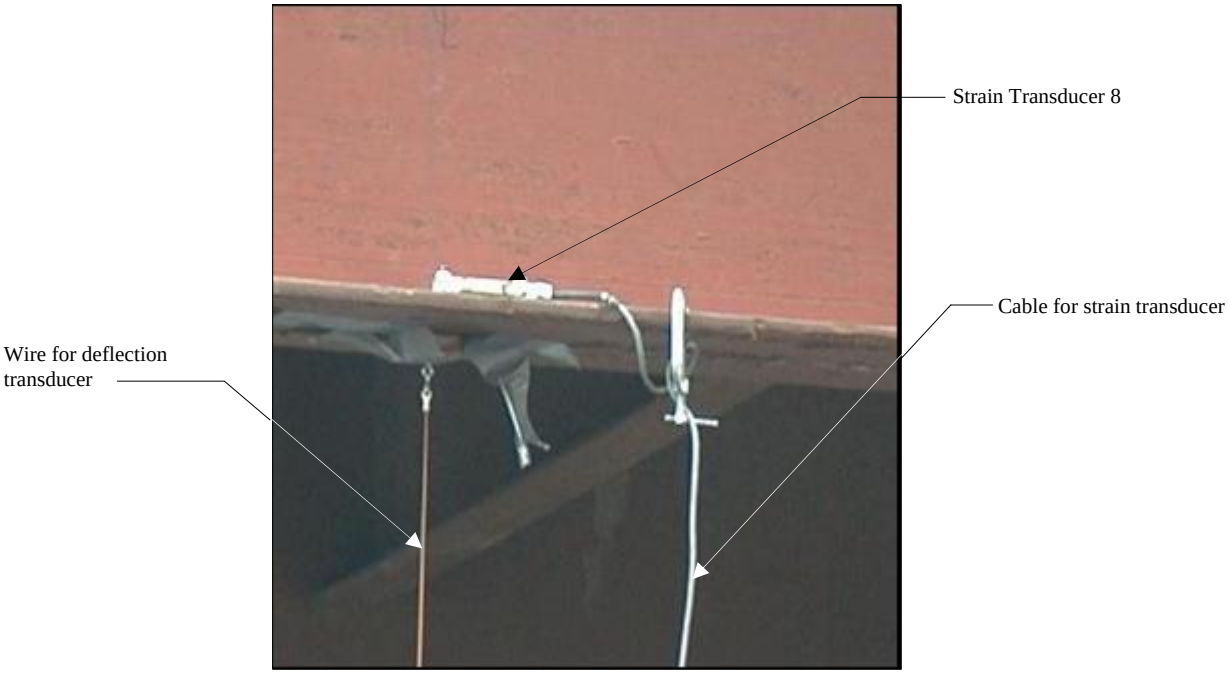


a. Strain transducer 8 on the bottom flange of the exterior girder


b. Deflection transducer for the exterior girder at the 1/4 span

**Figure 2.11. Instrumentation used on BCB2**

In order to verify longitudinal symmetry, the interior girder of the north RRFC was instrumented with strain transducers along the length of the BCB2. One strain transducer was positioned at each of the following locations: 18 in. from the face of the west abutment, the 1/4 span, the midspan, the 3/4 span, and 18 in. from the face of the east abutment. As presented in Figure 2.10, these locations correspond with Details A through E, respectively; the strain transducers used to determine the longitudinal bridge behavior are identified as transducers 3, 7, and 15.

At the quarter spans, the bottom flanges of the primary girders of the north RRFC and the LFC were instrumented with strain transducers and deflection transducers to determine the strains and deflections at these locations. In Figure 2.10, the 1/4 span and the 3/4 span are identified as Details B and D, respectively. The strain transducers located at the quarter spans are labeled as transducers 5 through 8 in Figure 2.10c. Also, to determine the behavior of the bridge at the abutments, the LFC and the bottom flanges of the primary girders of the north RRFC were instrumented with strain transducers at the east abutment. Because mounting the strain transducers at the centerline of the abutment was not feasible, the transducers were mounted 18 in. from the face of the east abutment; see Detail E in Figure 2.10. The strain transducers located at the east abutment are labeled as transducers 1 through 4 in Figure 2.10b.

In addition to the primary girders, a secondary member was instrumented with one strain transducer to determine the strains in the secondary members. The secondary member that was instrumented was located 7 ft – 1 in. from the north edge of the BCB2. As seen in Figure 2.10d, the strain transducer, identified as transducer 20, was mounted on the secondary member at midspan of the bridge. Finally, to determine the strains in the guardrail, the guardrail on the north edge of the BCB2 was instrumented with strain transducers at the midspan, the 1/4 span, and the 3/4 span and the guardrail on the south edge of the BCB2 was instrumented with a strain transducer at the midspan. The placement of the strain transducers is shown in Figure 2.10; the strain transducers on the guardrail are labeled 9, 21, and 22. A photograph of a strain transducer on the south guardrail is shown in Figure 2.12a.

As discussed in Section 2.2.2, the formwork for the LFC was left in place; thus, the plywood had to be cut so that the strain transducers mentioned in this section could be mounted on the concrete. A photograph showing the plywood removed from the LFC and a strain transducer mounted on the concrete LFC is presented in Figure 2.12b.

### *2.3.2 BCB2 Testing*

The BCB2 was divided into three lanes as shown in Figure 2.13 to determine the behavior of the bridge under different load conditions. As may be seen in Figures 2.13a and 2.13c, when in Lanes 1 or 3, the truck was positioned with the edge of the double tires 2 ft from the north or south edge of the bridge, respectively. With the truck positioned on the edge of the bridge, an eccentric load condition is created. The results from the test with the truck positioned in Lane 1 can be compared to the results from the test with the truck positioned in Lane 3 in order to verify transverse symmetry in the BCB2. The results from the tests with an eccentric load condition can also be used to determine the effectiveness of the LFC. A photograph of the test truck positioned in Lane 3 is shown in Figure 2.14a. As may be seen in Figure 2.13b, the truck was centered transversely on the bridge when in Lane 2. The results from the test with a centered load condition can be used to verify transverse symmetry. A photograph of the test truck positioned in Lane 2 is shown in Figure 2.14b.


a. Strain transducer at midspan on the south guardrail

b. Strain transducer on the concrete LFC

**Figure 2.12. Strain transducers used on BCB2**

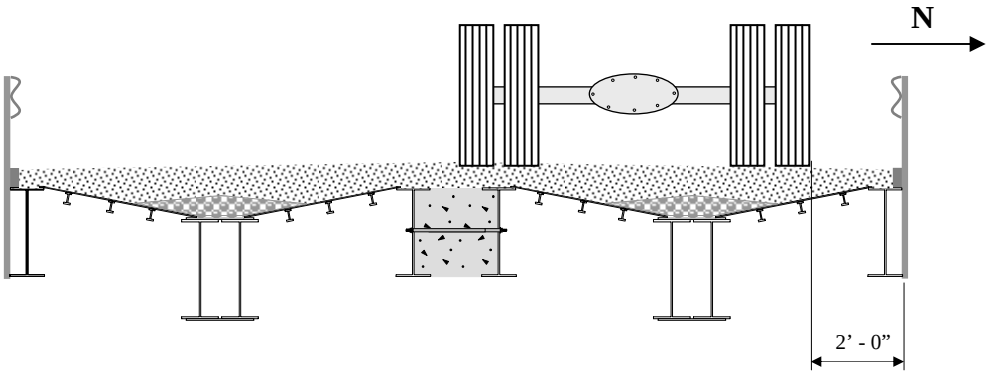


a. Lane 1

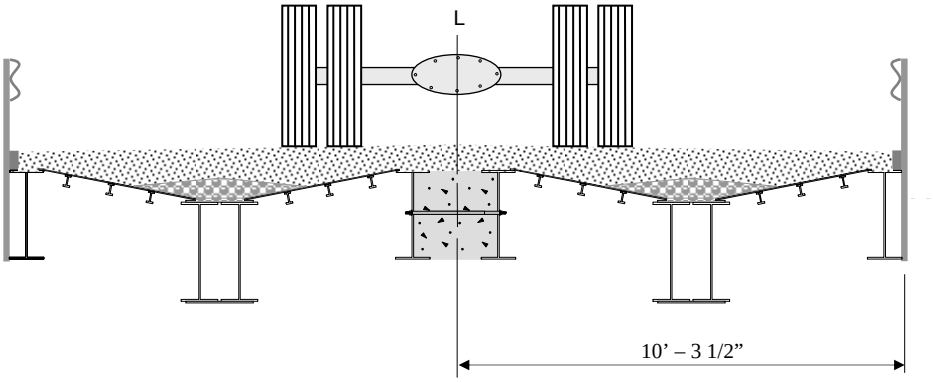


b. Lane 2

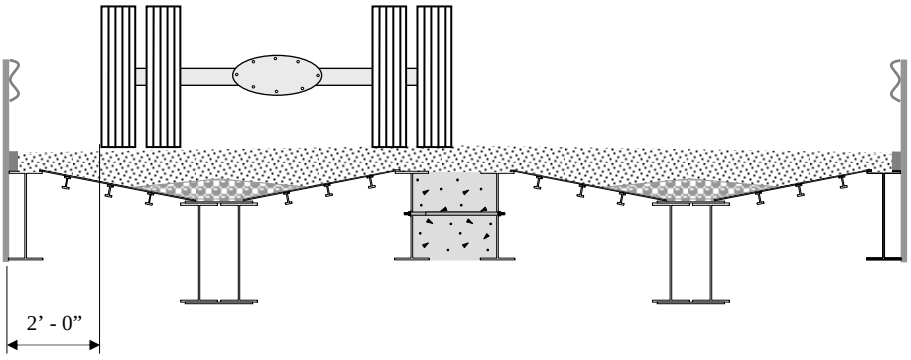


c. Lane 3

**Figure 2.13. Transverse locations of truck in the BCB2 tests**

For the field load tests, the truck, shown in Figure 2.14c, was driven slowly across the bridge in each of the three lanes while the data acquisition system recorded the strains and deflections measured by the strain and deflection transducers. The tests on the BCB2 were essentially static load tests because when traveling slowly, the truck did not produce dynamic amplification to the girder strains and deflections.

a. Loading BCB2 with truck on south RRFC (Lane 3)

b. Truck centered on BCB2 (Lane 2)

c. Photograph of BCB2 test truck

**Figure 2.14. Photographs of the truck used in the BCB2 tests**

## 2.4 Dead Load Analysis

The total stress in the BCB2 is the stress caused by the test truck during the field load test plus the stress due to the dead load on the bridge. To determine the total stresses in the primary girders of the BCB2, a dead load analysis was performed. To simplify this analysis, several assumptions were made. First, it was assumed that each primary girder supported its self-weight along with the weight of the secondary girders and transverse members within the tributary width of the primary girder. Since the 56-ft V-deck RRFC has three primary girders, the RRFC width was divided into tributary widths as shown in Figure 2.15. Thus, the tributary width of an exterior girder was about 2 ft – 4 in. and the tributary width of the interior girder was about 4 ft – 8 in.

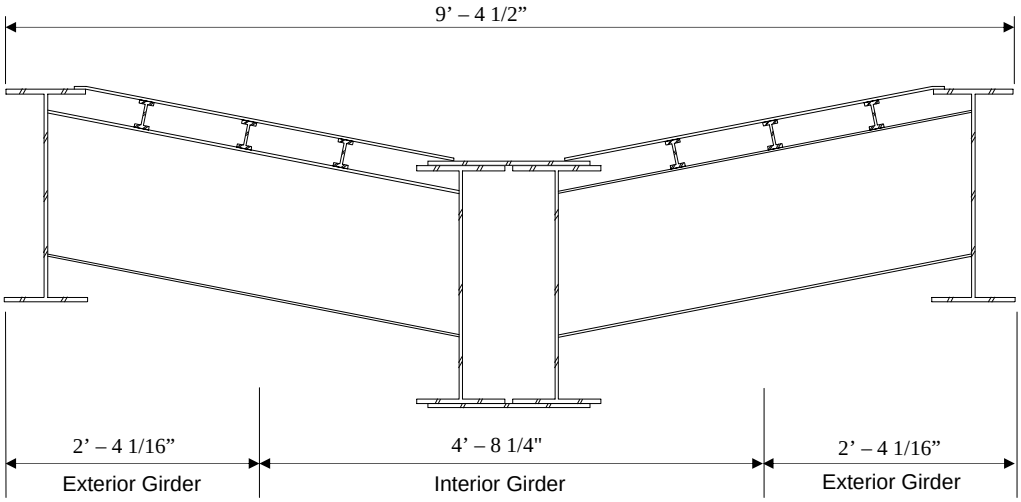


**Figure 2.15. Tributary width of RRFC girders for dead load analysis**

Following conventional methods of bridge design, the connected RRFCs were assumed to form a rigid cross-section such that any additional dead load could be considered uniform on the bridge. Thus, the total weight of the pea gravel and the gravel driving surface was assumed to be uniform on the bridge even though the pea gravel was only located in the V-deck above the interior girders as described in Section 2.2.2. Based on quantities and weights from the demonstration project, the total weight of the pea gravel and the gravel driving surface was assumed to be 98 lb/ft$^2$ and the weight of the RRFC was taken as its delivery weight, 35,000 lbs [4]. Finally, the BCB2 was assumed to be simply supported.

In order to determine the dead load stresses in the interior and exterior girders of one RRFC, two analyses were completed, one for an interior girder and one for an exterior girder. The dead loads in the tributary width of the girder were used to determine the moment at the midspan of the simply-supported girder. With the midspan moment and the section modulus of the girder, the dead load stress at the midspan of the girder was determined using Equation 2.1.

$$\sigma_{DL} = \frac{M}{S} \tag{2.1}$$

where:

DL = The dead load stress at the midspan of the girder

M = The midspan dead load moment

S = The section modulus of the girder

Using this procedure, the tensile dead load stresses in the bottom flanges of the interior and exterior girders of the BCB2 were determined to be 5.9 ksi and 11.0 ksi, respectively.

## 2.5 Field Load Test Results

As discussed in Section 2.3, deflections and strains were measured in longitudinal girders and secondary and transverse members of the BCB2. In the following sections, the deflection and strain results from the field load tests will be presented and analyzed in order to determine the structural behavior of the BCB2 (i.e., Objective 2 of this project).

In order to determine the stresses in the girders from the strains measured during the field load tests, the elastic modulus of the steel in the RRFCs must be known. To determine the acceptability of these stresses, the strength of the steel must be known. In the demonstration project, TR-444, tensile tests were performed on steel coupons from a 56-ft V-deck RRFC to determine that the modulus of elasticity and the yield strength were 29,000 ksi and 40 ksi, respectively [4]. As stated in the 2003 AASHTO Standard Specifications for Highway Bridges, the allowable flexural stress for compact steel members not subjected to lateral-torsional buckling is 55 percent of the yield strength [7]. The girders in both types of RRFCs used in this study are compact and not subjected to lateral-torsional buckling; therefore, the allowable flexural stress in the steel members of the RRFCs used in the BCB2 was 22 ksi, 55 percent of 40 ksi.

### *2.5.1 Static Test Results*

The BCB2 instrumentation plan described in Section 2.3.1 included measuring the strain in one secondary member and the interior girders at the abutments (18 in. from the face of the abutments). The maximum strains at the abutments occurred in the bottom flanges of the interior girders. At the east abutment, the maximum strain was 33 MII (1.0 ksi), and at the west abutment, the maximum strain was 24 MII (0.7 ksi). The presence of strain in the sections close to the abutments indicates that end restraint is present in the BCB2 even though it was designed to be simply supported. However, the maximum strain in the girders at the abutments was considerably less than the maximum strains experienced in the interior and exterior primary girders at the midspan of the bridge; the maximum stresses in the interior girders at the abutments were also significantly less than 22 ksi, the allowable stress in the steel. Although end restraint reduces the midspan strains, the effect is minimal because the strains at the abutments were significantly less than the strains at midspan. Thus, the abutment strains will not be discussed further.

As shown previously in Figure 2.10, the secondary member that was instrumented with Strain Transducer 20 was located 7 ft – 1 in. from the north edge of the bridge, or approximately half way between the interior girder of the north RRFC and the LFC. The maximum strain experienced in this member was 57 MII (1.6 ksi) and occurred when the truck was positioned in Lane 2, with the truck tires located directly above the transducer. Since the maximum strain in the secondary member was significantly less than the maximum strains experienced in the interior and exterior primary girders, the secondary members were determined to be not critical and will be excluded from additional discussion.

The maximum midspan deflections and strains that were measured when the truck was in Lanes 1 – 3 on the bridge are presented in Figures 2.16 – 2.18, respectively. As described in Section 2.3.1, the midspan of BCB2 was instrumented with six deflection transducers and seven strain transducers. The deflections and strains measured with these transducers are represented in Figures 2.16 – 2.18 by small diamonds.

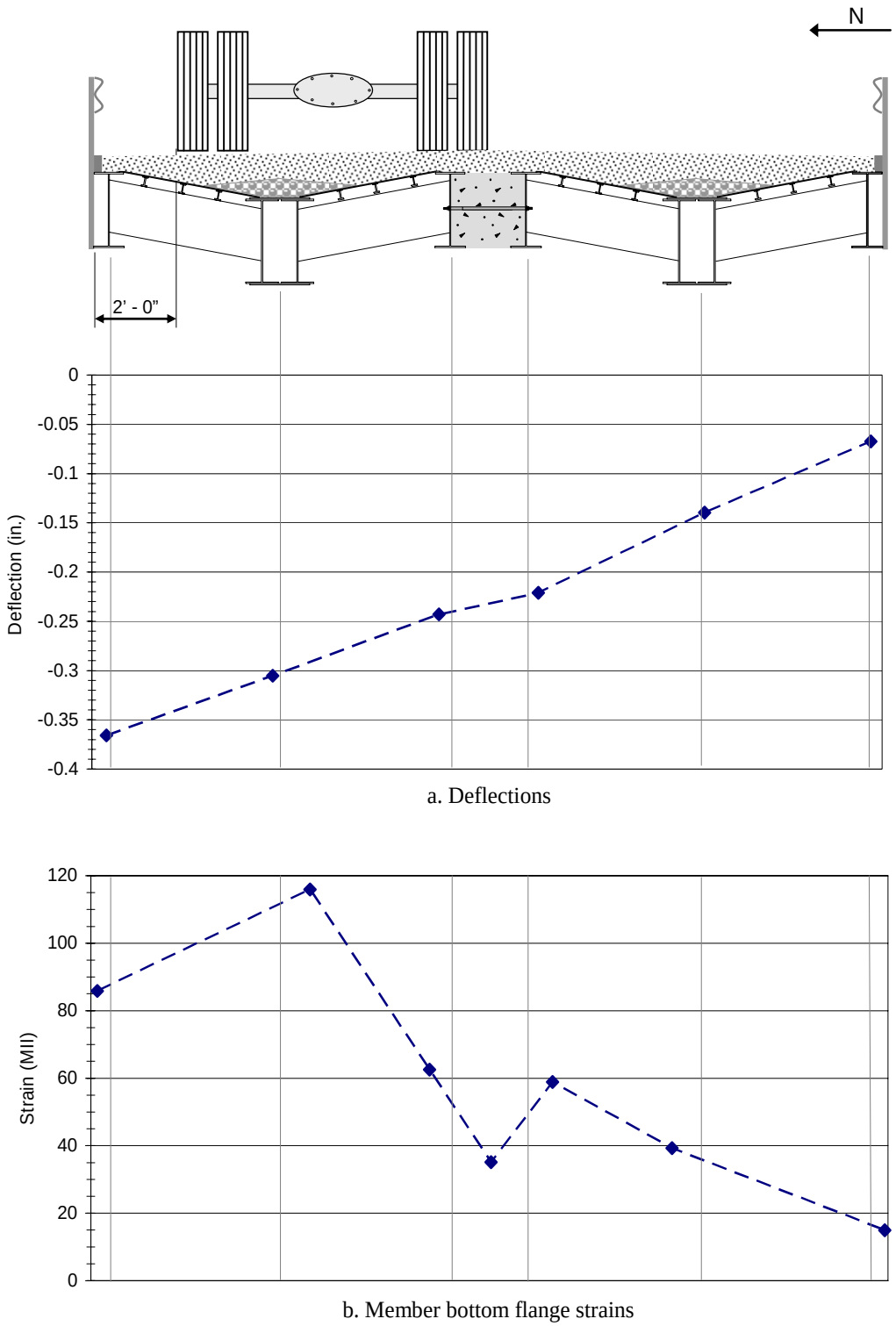


a. Deflections

b. Member bottom flange strains

**Figure 2.16. BCB2 Lane 1 midspan deflections and strains**

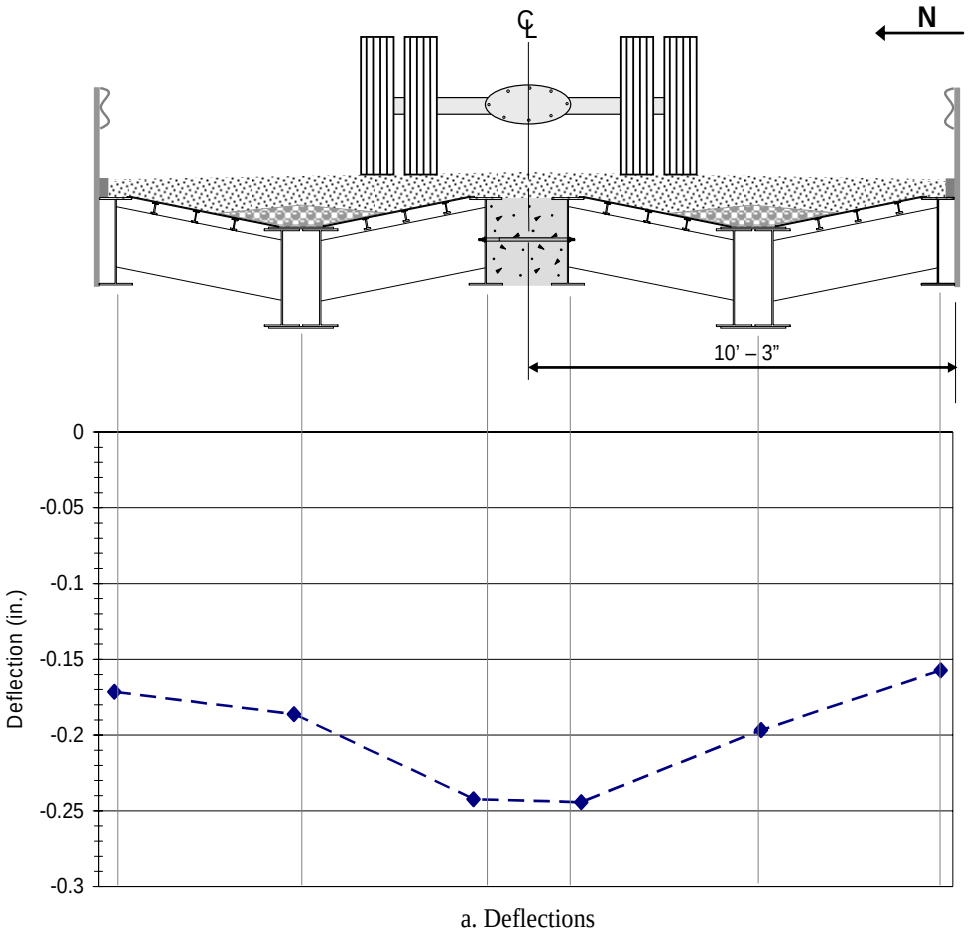


a. Deflections

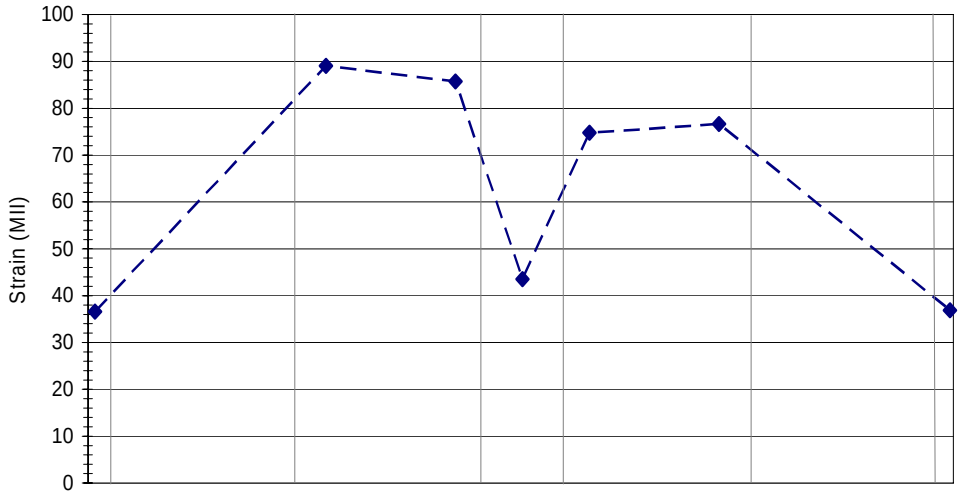


b. Member bottom flange strains

**Figure 2.17. BCB2 Lane 2 midspan deflections and strains**

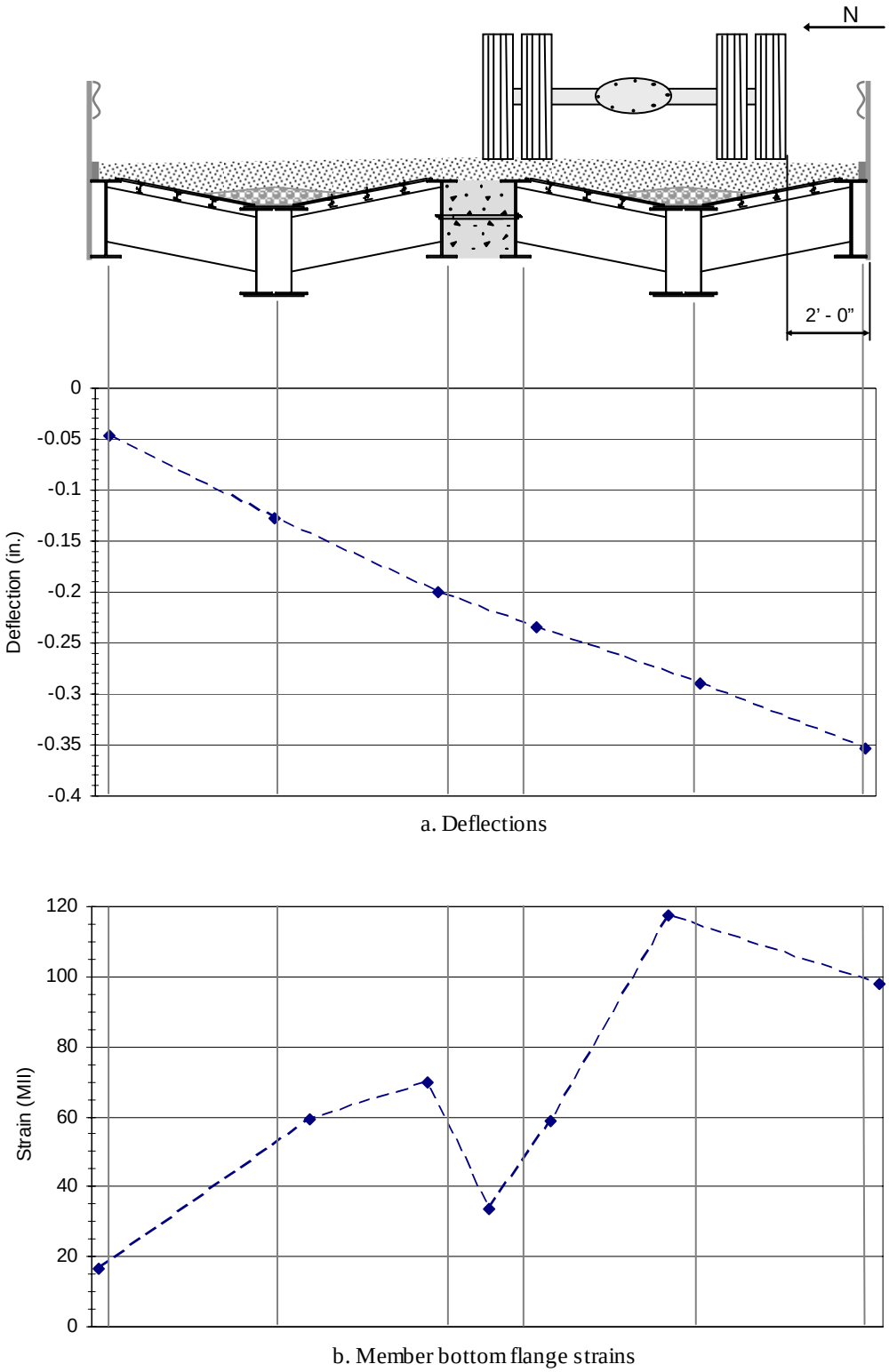


**Figure 2.18. BCB2 Lane 3 midspan deflections and strains**

The dashed lines represent a trend that may occur between the measured deflections and strains and thus, do not represent measured deflections or strains. The measured deflections and strains shown in Figures 2.16 – 2.18 occurred when the center of the tandem axle of the truck was at the midspan of the bridge. As can be seen in Figures 2.16 and 2.18, the maximum deflection of the BCB2 was 0.37 in. and 0.35 in. when the truck was in Lane 1 or 3, respectively, and occurred at the exterior girder on the north or south edge of the bridge, respectively. When the truck was positioned in Lane 2, the maximum deflection as seen in Figure 2.17 was 0.24 in. and occurred at the LFC.

According to the 2003 AASHTO Standard Specifications for Highway Bridges, an optional limit for the deflection of a bridge is 1/800 of the span length [7]. This optional limit is not a strict requirement for legal bridges but rather a guideline. For a 54 ft – 0 in. span, the optional limit is 0.81 in. However, the load of the test truck was not the maximum load that may cross the BCB2 and thus cannot be compared to the deflection limit. The maximum load is most likely that of an AASHTO HS-20 truck. In order to determine the maximum deflection of the BCB2, the deflections recorded during the field tests were multiplied by a load adjustment factor. To determine the load adjustment factor for the BCB2, the maximum moments at the midspan of a simply-supported beam due to point loads representing the BCB2 test truck axle loads and due to point loads representing an HS-20 truck were calculated. The load adjustment factor was then determined using Equation 2.2.

$$\beta = \frac{M_{HS-20}}{M_{TT}} \tag{2.2}$$

where:

$\beta$ = The load adjustment factor

$M_{HS-20}$ = The maximum midspan moment of a simply-supported beam due to an HS-20 truck

$M_{TT}$ = The maximum midspan moment of a simply-supported beam due to the test truck

Using Equation 2.2, the load adjustment factor for the BCB2 was determined to be 1.26. Therefore, the adjusted maximum deflection of the BCB2 was 0.46 in. which is below the optional AASHTO deflection limit of 0.81 in.

In each test, the maximum strain in the bridge occurred in the interior girder beneath the test truck. When the test truck was in Lane 1 or 3, the maximum exterior girder strain occurred in the exterior girder on the north or south edge of the bridge, as seen in Figures 2.16 and 2.18. With the truck positioned in Lane 2, the maximum exterior girder strain occurred at the LFC. As presented in Figures 2.16 – 2.18 and summarized in Table 2.2, the maximum interior and exterior girder strains recorded during the field tests were 116 MII (3.4 ksi) in tension and 97 MII (2.8 ksi) in tension, respectively, and occurred in the north interior girder when the truck was in Lane 1. When the dead load stresses were combined with the live load stresses determined from the field test results, the maximum total stresses in the longitudinal interior and exterior girders were both tensile stresses, 9.3 ksi and 13.8 ksi, respectively.

As mentioned previously, the test truck was not an AASHTO HS-20 truck which is likely the maximum load that will cross the BCB2. Therefore, the maximum strains measured in the field tests were adjusted using the previously described adjustment factor of 1.26. The adjusted maximum strains in the interior and exterior girders were 146 MII (4.2 ksi) in tension and 122 MII (3.5 ksi) in tension, respectively. The

adjusted maximum stresses were then added to the dead load stresses; the adjusted maximum total stresses in the interior and exterior girders were 10.1 ksi and 14.5 ksi, respectively, which are below 22 ksi, the allowable flexural stress.

**Table 2.2. BCB2 midspan strains recorded during field load tests**

| Girder | Position of Test Truck | | |
|---|---|---|---|
| | Lane 1 | Lane 2 | Lane 3 |
| Interior | 115 MII (3.3 ksi) | 89 MII (2.6 ksi) | 116 MII (3.4 ksi) |
| Exterior at Bridge Edge | 86 MII (2.5 ksi) | 36 MII (1.0 ksi) | 97 MII (2.8 ksi) |
| Exterior at LFC | 62 MII (1.8 ksi) | 86 MII (2.5 ksi) | 70 MII (2.0 ksi) |

As seen in Figures 2.16 – 2.18, the strain in the R/C beam LFC was less than the strains in the two adjacent RRFC girders. If the R/C beam was composite with the RRFC girders, the strain in the R/C beam would be about the same as the strain in the girders. Because the strains shown in Figures 2.16 – 2.18 could have been anomalies, the strain-time histories of the three strain transducers at the LFC for each of the three lanes were plotted and are presented in Figure A.1 in Appendix A. The strain-time histories revealed that the strains shown in Figures 2.16 – 2.18 are not anomalies; the strain in the R/C beam was less than the strain in the two RRFC girders consistently throughout each test. Thus, the R/C beam is not behaving compositely with the RRFC girders since, probably, there is insufficient connection between the two materials.

As expected, the maximum deflections and strains for each test occurred in the girders directly below the axle loads of the test truck. One would expect an effective lateral load distribution to be demonstrated with linearly varying strain and deflection patterns across the cross-section of the bridge. This behavior is demonstrated in the girder deflections and strain patterns shown in Figures 2.16 – 2.18. Thus, the BCB2 effectively distributes load through the LFC. In Figure 2.17, the deflections and strain patterns reveal symmetrical bridge behavior, and in Figures 2.16 and 2.18, transverse symmetry is demonstrated by the mirrored deflection and strain patterns.

*2.5.2 Comparison of BCB2 with BCB1*

As mentioned in Section 2.2.1, the BCB2 design was based on the BCB1 designed, constructed, and tested for the demonstration project, TR-444 [4]. Because the BCB1 is composed of three RRFCs, more tests were run, including tests with two trucks. However, load tests were run with one test truck traveling down the center of the bridge and 2 ft off either side of the bridge. These tests can be compared with the load tests on BCB2 with the truck positioned in Lanes 1 – 3 because the positions of the trucks and the loads carried by the trucks were approximately the same.

The final report for the demonstration project, TR-444, noted that the north edge of the BCB1 deflected upward when the test truck crossed the bridge 2 ft from the south edge of the bridge. Likewise, the south edge of the BCB1 deflected upward when the test truck crossed the bridge 2 ft from the north edge of the bridge [4]. Although the same behavior does not occur in the BCB2, the deflection patterns of the two bridges are similar. For the comparison of the behavior of the two bridges, the north edge of the bridges were aligned as shown in Figures 2.19a and 2.19b. Because the BCB1 consists of three RRFCs while the BCB2 has two RRFCs and the width of the LFCs used in the two bridges is different, the south exterior girder of the BCB2 most closely corresponds to the south girder in the south LFC of the BCB1. In both bridges, the maximum deflection occurred at the exterior girder at the north edge of the bridge on which the truck was positioned. As shown in Figure 2.19, the maximum deflection of the both the BCB1 and

BCB2 was 0.37 in. Although the deflections of the BCB2 are not identical to the deflections of the BCB1, the deflection patterns are both nearly linear. Thus, the BCB1 and BCB2 exhibit similar deflection behavior when the deflections (which are very small) in the third RRFC of the BCB1 are neglected; the third RRFC was the exterior RRFC on which the truck was not positioned.

Similar stress patterns should also be expected in the two bridges because in the BCB1, the live load strain in the third RRFC was nearly zero. As seen in Figure 2.20c, the strain patterns of the BCB1 and BCB2 are similar, but they have two major differences. In the BCB1, the maximum live load strain occurred in the exterior girder along the edge of the bridge beneath the test truck rather than in the interior girder beneath the test truck as the in BCB2. The difference in the location of the maximum strain is due to the position of the test truck along the edge of each bridge. As shown in Figures 2.20a and 2.20b, for the BCB1 field tests, the center of the tandem axle double tires was positioned 2 ft from the edge of the bridge, but in the BCB2 field tests, the edge of the tandem axle double tires was positioned 2 ft from the edge of the bridge. Thus, the center of the double tires at the tandem axle was positioned 3 ft from the edge of the bridge. By shifting the truck this 1 ft farther from the edge of the bridge, it was positioned partially on the LFC. Also, because in the BCB2 test, the truck was farther away from the edge, less strain occurred in the exterior girder at the edge of the bridge than in the interior girder.

Although the location of the maximum live load strain was different in the BCB1 and BCB2, the maximum total stress in both bridges occurred in the exterior girder at the north edge of the bridge while the truck was positioned along that edge of the bridge. The maximum stresses due to the combined dead and live loads on the BCB1 and BCB2 were 12.7 ksi and 13.8 ksi, respectively. The difference in stresses is due to the difference in the amount of dead load on each bridge as well as the difference in truck position.

By reviewing the strains in the R/C beams in the two bridges in Figure 2.20c, one observes the better composite action in the BCB1 connection. The lack of composite action in the BCB2 connection has been previously noted.

The strain and deflection patterns from the tests with the truck positioned in the center of the bridge reveal symmetrical bridge behavior in both the BCB1 and BCB2. In tests with the truck positioned along the edge of the bridge (with the center of the tandem axle double tires positioned 2 ft from the edge of the bridge in the BCB1 and with the edge of the tandem axle double tires positioned 2 ft from the edge of the bridge in the BCB2), the strain and deflection patterns were mirrored. Thus, transverse symmetry is displayed in the behavior of both bridges. This similarity indicates that the wider R/C beam acting as the BCB2 LFC is as effective as the narrower R/C beam acting as the BCB1 LFC. The comparison of the BCB1 and BCB2 field test results reveals that the modifications in the BCB1 design did not significantly alter the structural strength or bridge behavior of the BCB2.

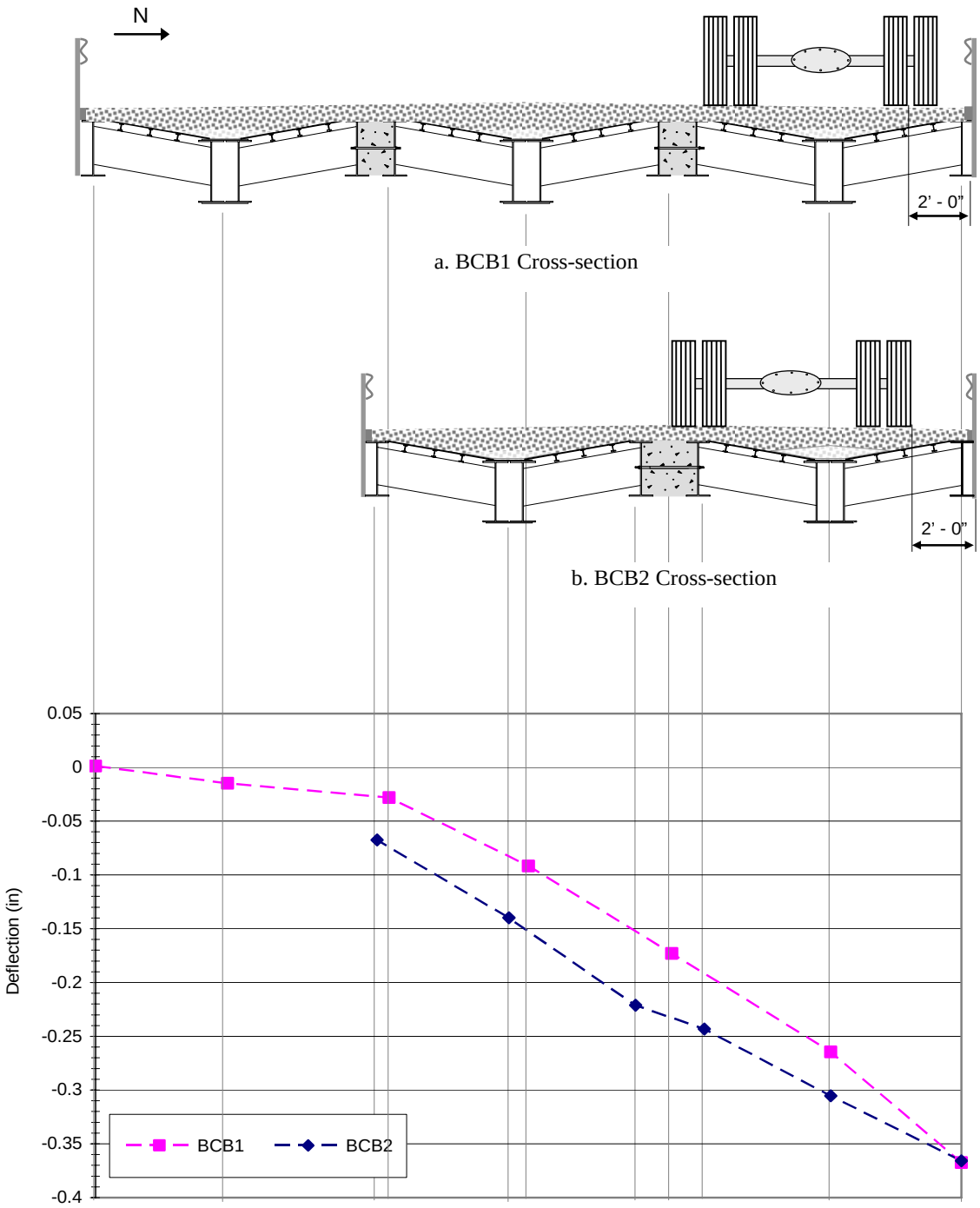


**Figure 2.19. BCB1 and BCB2 deflection comparison**

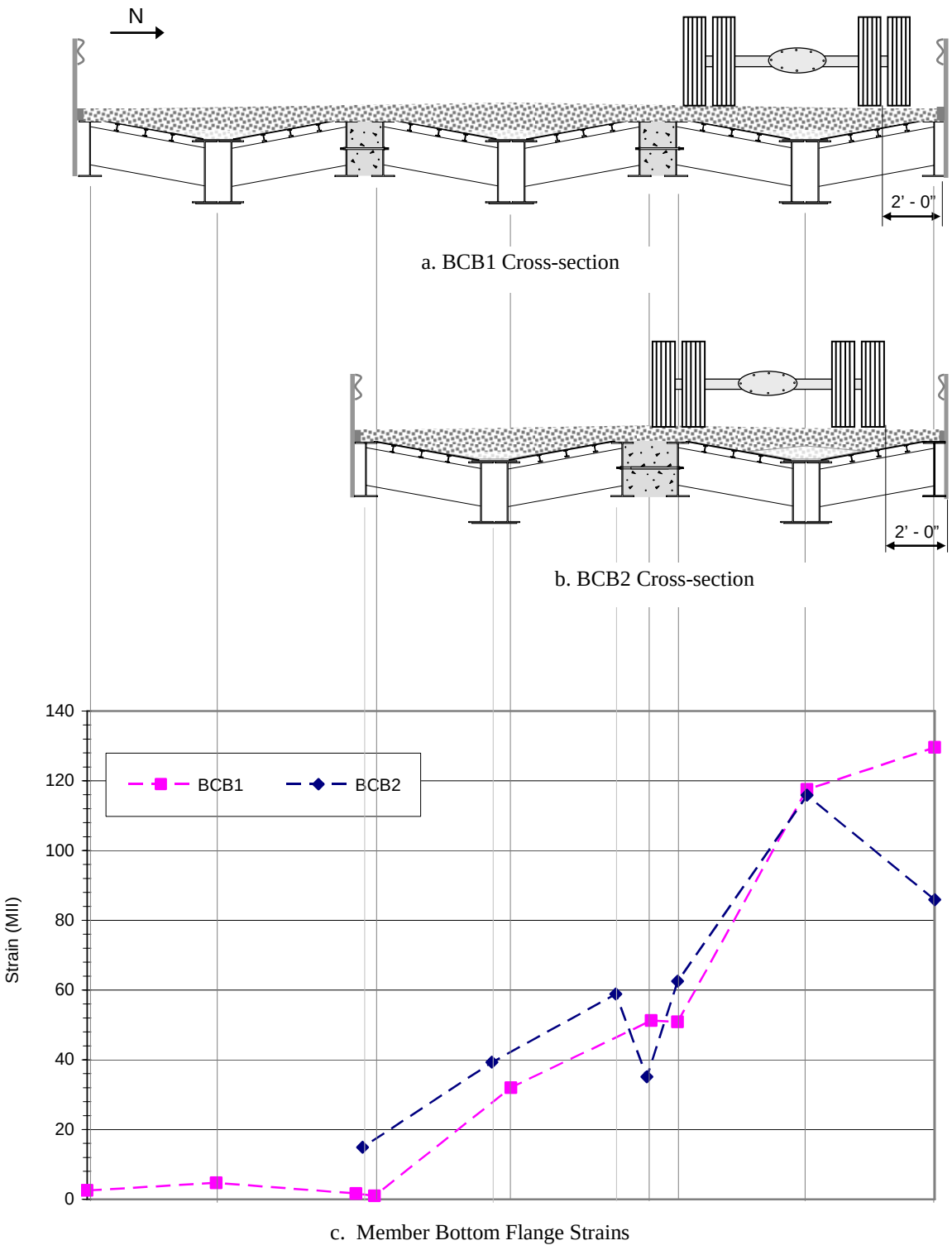


**Figure 2.20. BCB1 and BCB2 strain comparison**

## 3.0 DELAWARE COUNTY BRIDGE ON RAINBOW RD

### 3.1 Background

The Delaware County Bridge, referred to as DCB, crosses the Elk Creek approximately three miles northeast of Greeley, Iowa, at the intersection of 270th Avenue and Rainbow Road. Presented in Figure 3.1a is a map of a portion of Delaware County showing the major highways in that portion of the county. The general location of the bridge is identified with a dashed rectangle and labeled Detail A, which is presented as Figure 3.1b; the approximate location of the bridge is identified with a dashed circle in this figure. Details on the design and construction of DCB are presented in Section 3.2.


a. Map of a Portion of Delaware County

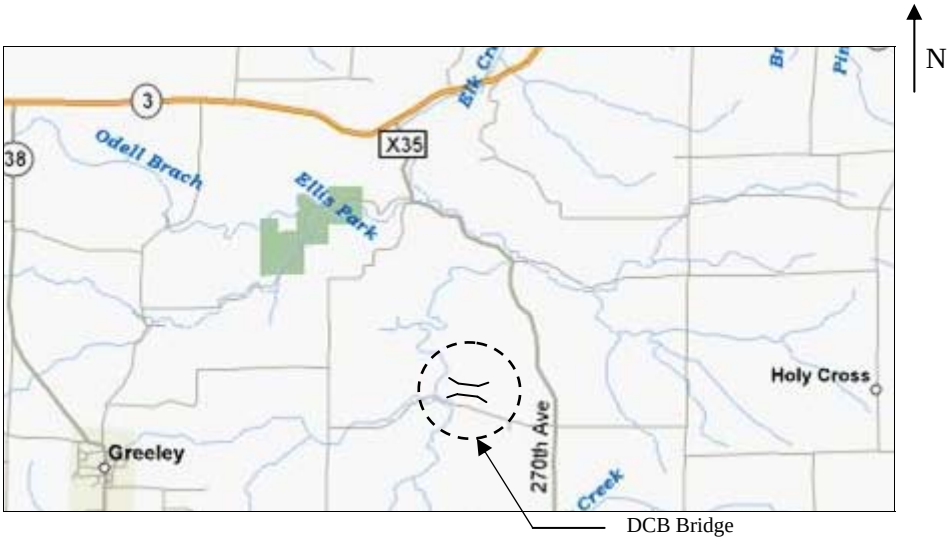


b. Detail A

**Figure 3.1. Location of the DCB site [6]**

## 3.2 DCB Design and Construction

### *3.2.1 DCB Design*

The DCB, which was designed by the Delaware County Engineering Department, consists of two 89-ft RRFCs and has a width of 18 ft – 4 in. Because the DCB did not require an 89-ft span, only a 67 ft – 6 in. portion of each RRFC was used. In order to keep the RRFCs symmetric, 10 ft – 9 in. were removed from each end of both RRFCs; from center to center of the abutments, the DCB spans 66 ft – 4 in.

As may be seen in Figure 3.2a, the 89-ft flatcars have three primary girders, two exterior and one interior, which are W-shapes, and six small secondary girders, which are inverted T-shapes. Also shown in Figure 3.2 are the three different transverse members that connect the primary girders: S-shaped members (Cross-section D), L-shaped members (Cross-section E), and U-shaped members (Cross-section F). The depth of the interior girder varies along the length of the RRFC; these dimensions are shown in Figure 3.3. The depths of the exterior girders remain constant (d = 15 in.) along the entire length of the RRFC. On the DCB, the south RRFC has an additional 1-in. steel plate welded to the bottom flange of the interior girder.

Both of the abutments are composed of a built-up cap beam supported by seven HP10x42 piles which are positioned beneath the primary girders of the RRFCs as shown in Figure 3.4a. As may be seen in Figure 3.4b, each cap beam consists of two C12x30 channels with a 14-in. x 1-in. steel plate welded to the top of the channels. The cap beam channels are connected to the piles with 3/4-in. bolts. Each bolster of the RRFCs rests on the cap beam while pieces of HP8x36 piles are positioned between the exterior girders and the cap beam as shown in Figure 3.4a. The pieces of HP8x36 piles are required beneath the exterior girders because the elevation of the bottom flanges of the exterior girders is 8 in. higher than the elevation of the bottom of the bolsters at the interior girders. The backwall, seen in Figure 3.5a, and the wing walls, seen in Figure 3.5b, consist of 3-in. x 12-in. wood planks. The backwall is held in place by the HP8x36 piles while timber piles are used to support the wing walls.

Unlike the BCB2, a R/C beam was not used as the LFC in the DCB. Instead, as shown in Figure 3.6, the RRFCs were positioned with no space between the bottom flanges of the exterior girders. The two exterior girders that comprise the connection were trimmed so that the top of the girders were even with the top of the deck and thus not extending into the driving surface. Although no space was present between the bottom flanges of the exterior girders at the connection, the trimming of the top half of the exterior girders created a 7-in. gap between the two RRFCs. In order to connect the two RRFCs and to provide a flat deck, a 14-in. by 1/2-in. plate was positioned over the adjacent exterior girders and was welded the full length of the RRFC. To complete the LFC, the transverse members, which are spaced approximately 4 ft apart, were welded together across the RRFCs.

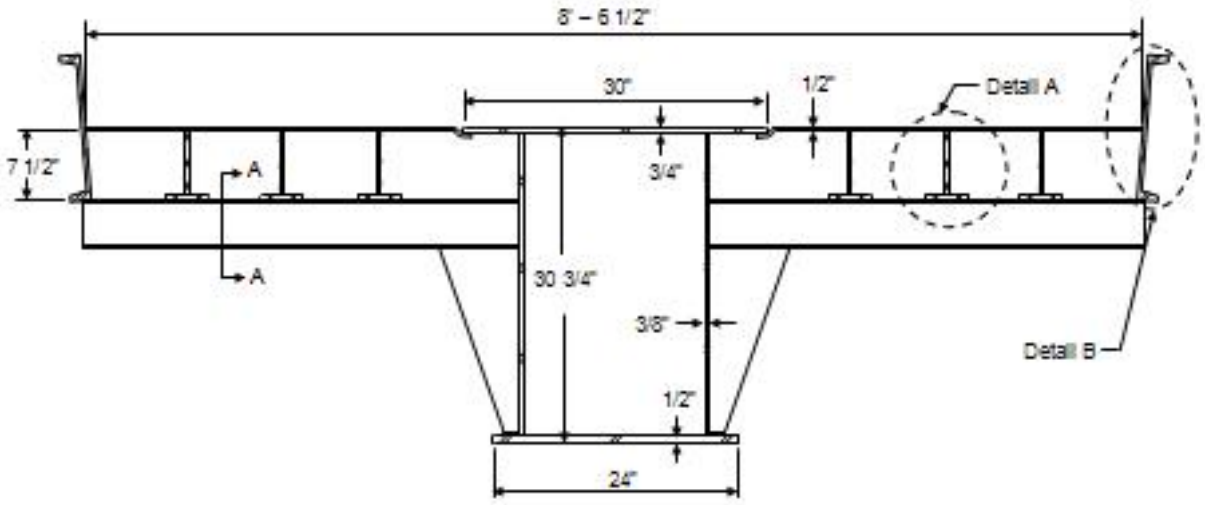


a. Cross-section with S-shape transverse member (Cross-section D)

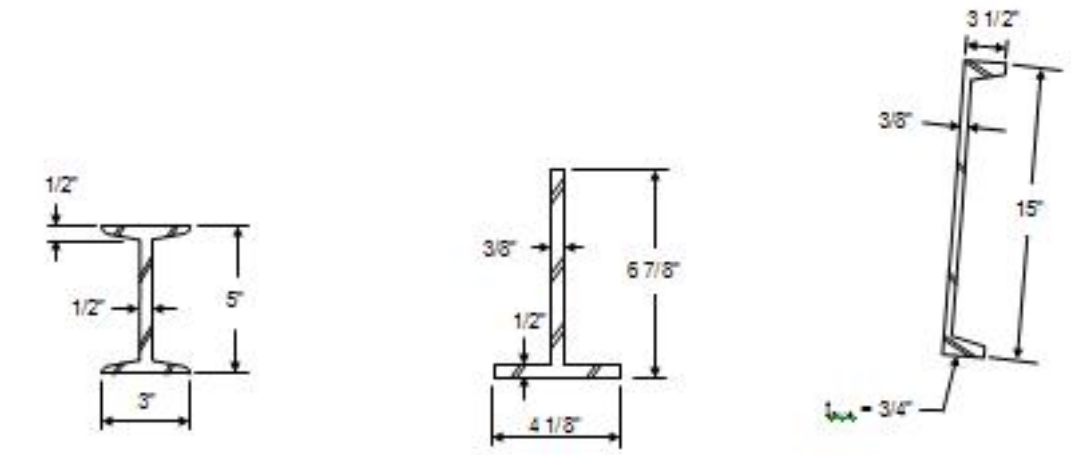


b. Section A – A (S-shape) c. Detail A (Tee-shape) d. Detail B

**Figure 3.2. Details of the 89-ft RRFCs used in the DCB [4]**

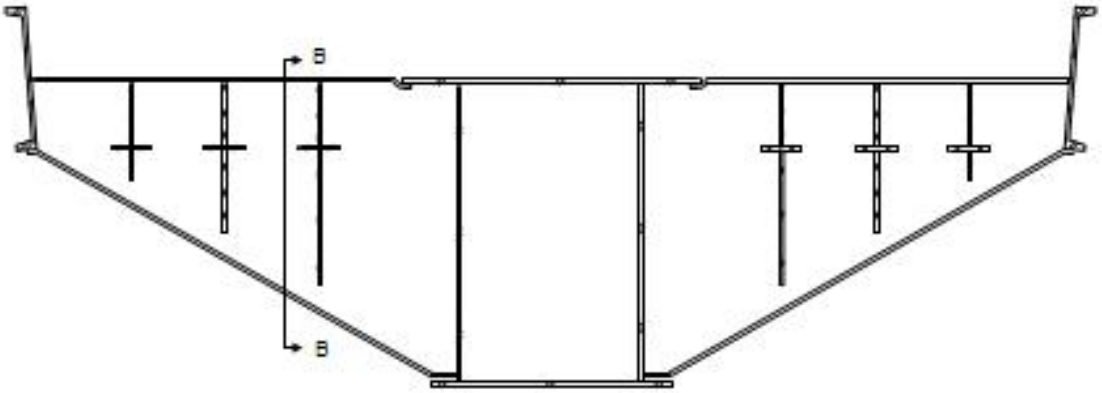


e. Cross-section with L-shaped transverse member (Cross-section E)

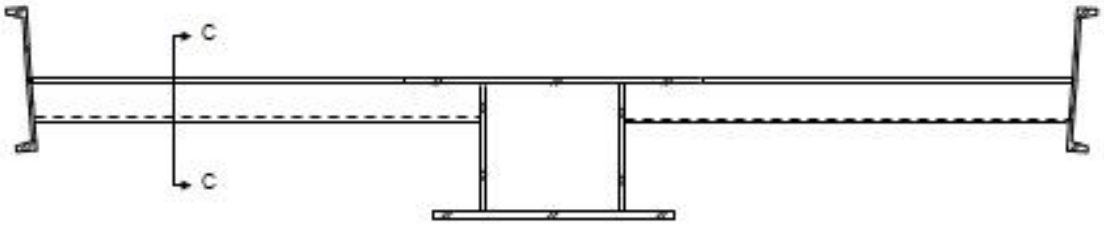


f. Cross-section with U-shaped transverse member (Cross-section F)


g. Section B – B (L-shape)

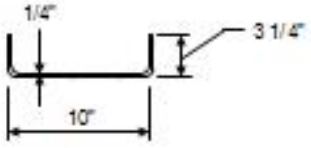


h. Section C – C (U-shape)

**Figure 3.2. Continued**

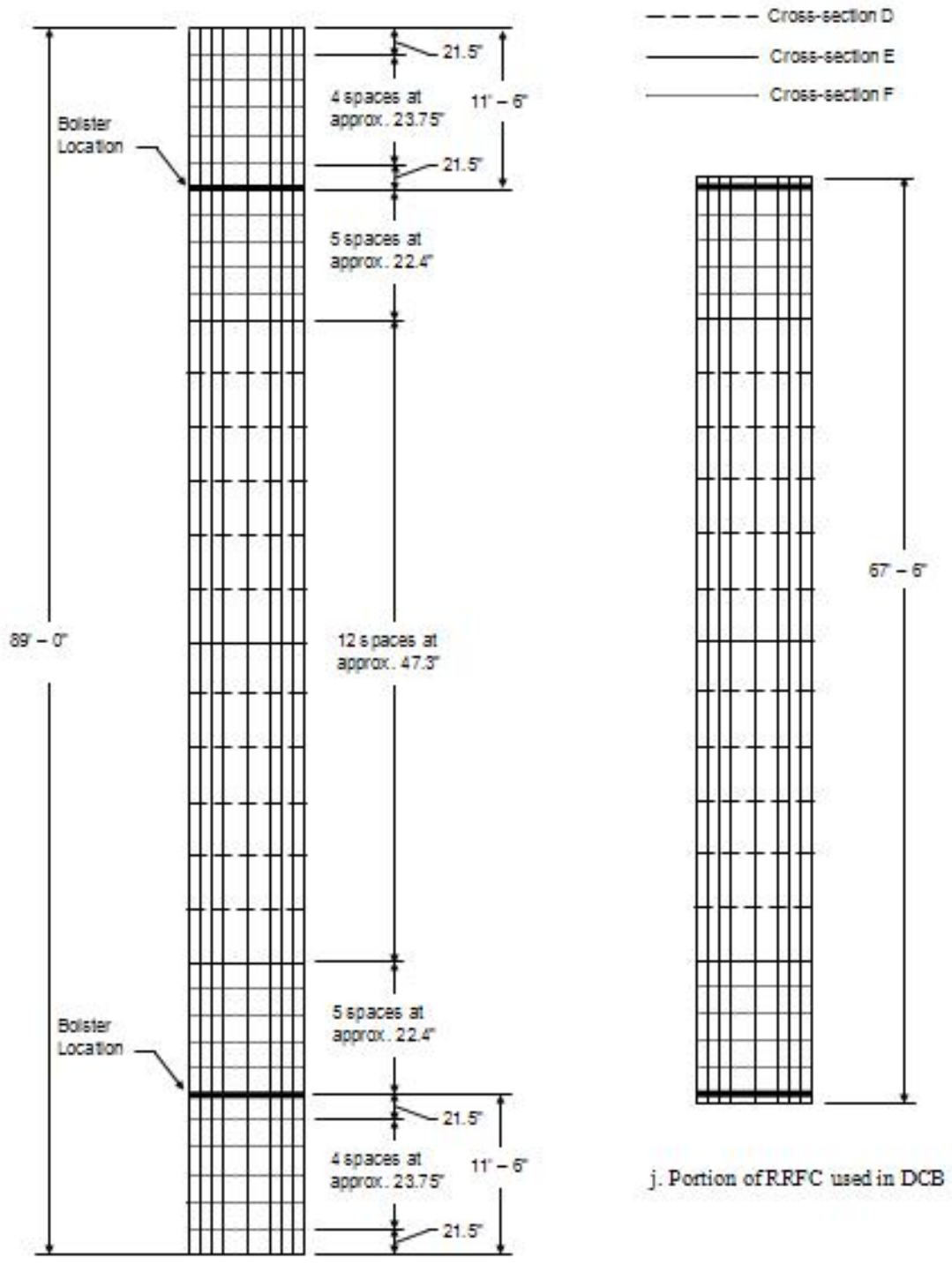


**Figure 3.2. Continued**

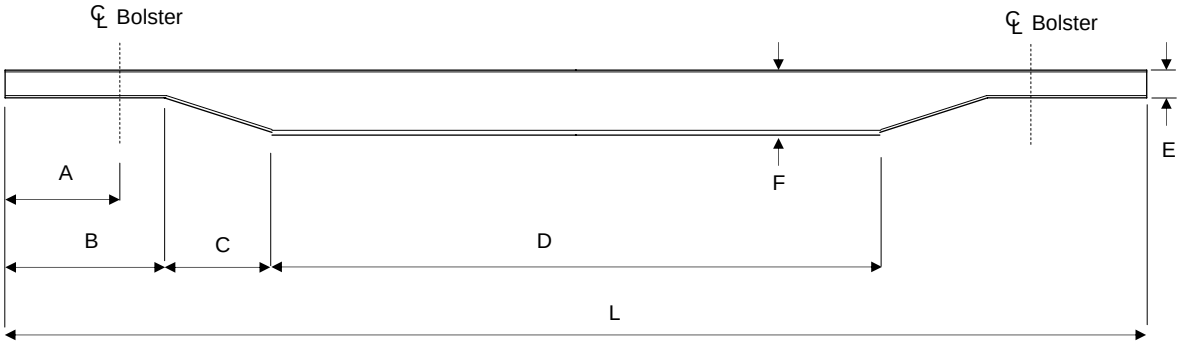


A = Distance from end to bolster
B = Minor Cross-Section Region
C = Transition Region
D = Major Cross-Section Region
L = Length of RRFC

| Bridge | Dimensions | | | | | | |
|---|---|---|---|---|---|---|---|
| | A | B | C | D | E | F | L |
| BCB2 | 0' - 9" | 1' - 9" | 8' - 4" | 47' - 4" | 1' - 1 3/4" | 2' - 6 1/4" | 67' - 6" |

**Figure 3.3. Dimensions of the interior girders in the RRFCs used in DCB**

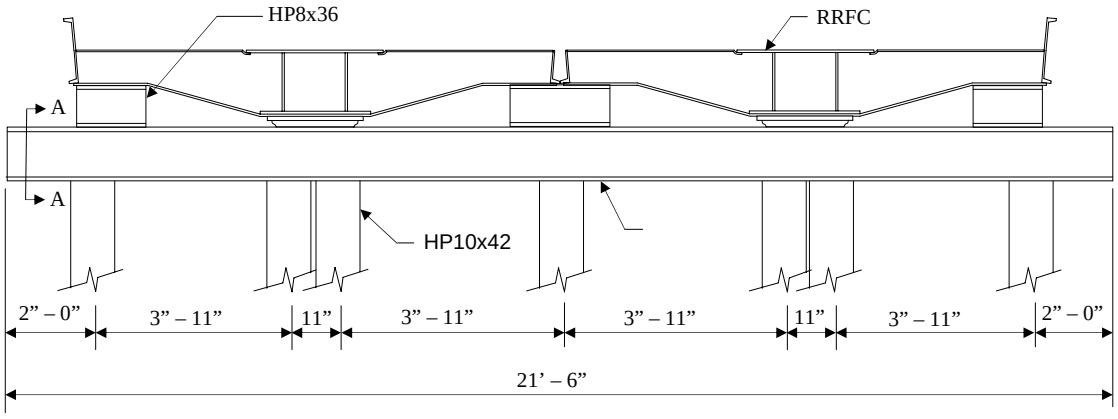


a. RRFC placement [4]

**Figure 3.4. Details of DCB abutments**

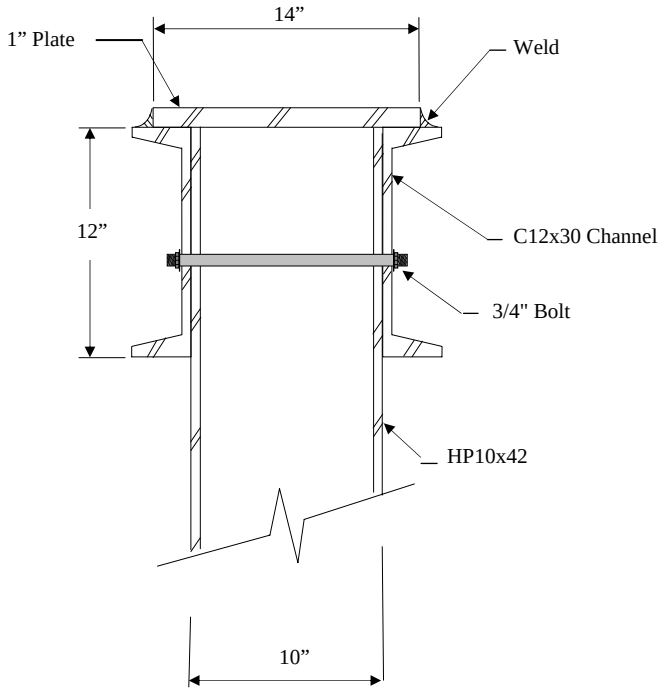


b. Section A-A

**Figure 3.4. Continued**

a. Photograph of abutment and backwall

**Figure 3.5. Photographs of DCB abutments**

b. Photograph of wing wall and side view of cap beam

**Figure 3.5. Continued**

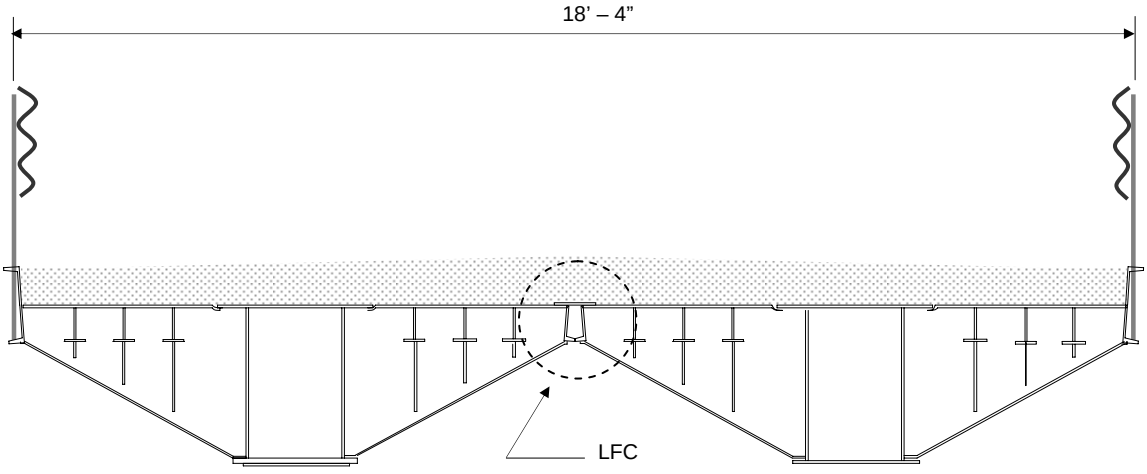


a. Cross-section of DCB

**Figure 3.6. Longitudinal RRFC connection used in the DCB**

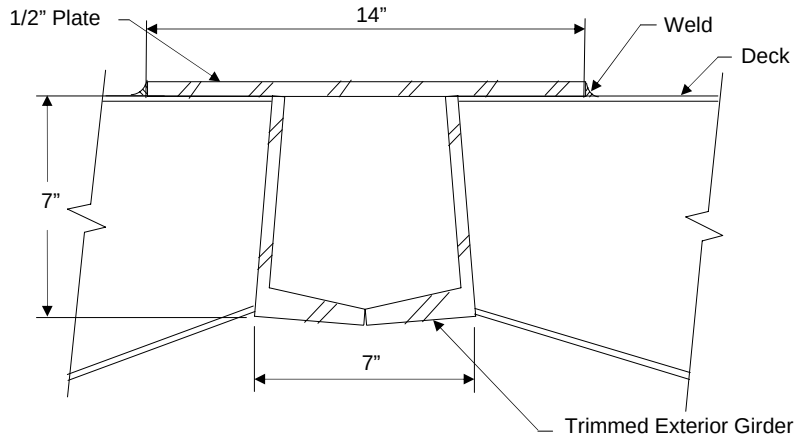


b. Details of LFC

**Figure 3.6. Continued**

*3.2.2 DCB Construction*

The DCB was constructed by a contractor hired by Delaware County. The construction process for the DCB differed from the process used for the BCB2 because the DCB LFC is not comprised of a R/C beam, and the type of RRFCs used is different. The DCB more closely resembles the WCB1, which was designed, constructed, and tested in the demonstration project, TR-444, and also consists of 89-ft RRFCs. However, the WCB1 LFC utilizes a small R/C beam in addition to steel plates welded at the connection [4]. Despite the difference in the LFC, the basic process used for constructing the DCB essentially followed the process developed in the demonstration project, TR-444, for the WCB1 [4].

As shown in Figure 3.7a, the 89-ft RRFCs have protrusions above the deck; however, in order for the RRFCs to be used in a bridge, the protrusions must be removed. Therefore, before the RRFCs were shipped to Delaware County for use in the DCB, the protrusions were trimmed off. The 89-ft RRFCs were also cut to the required 67 ft – 6 in. length before being shipped to Delaware County. A photograph of a trimmed 89-ft RRFC without the protrusions is shown in Figure 3.7b.

As described in further detail in the final report for the demonstration project, the abutments were first constructed, and then the RRFCs were positioned on the abutments as described in Section 3.2.1. Once the RRFCs were in place, the 14-in. by 1/2-in. plate was welded over the trimmed exterior girders to form the LFC. After the LFC was completed, a fabric liner was placed over the RRFC deck to prevent gravel from falling through small holes in the deck. A layer of gravel was then placed over the fabric liner for the driving surface. The layer of gravel has a 3-in. crown; the thickness of the gravel layer is 10 in. along the center of the bridge and 7 in. along the edges of the bridge. Finally, a guardrail system, which consists of guardrail posts welded on 6-ft intervals to the flanges of the exterior girders with a thrie beam attached to the guardrail posts, was installed. The completed DCB is shown in Figure 3.8.

a. The 89-ft RRFC prior to trimming

b. The trimmed 89-ft RRFC

**Figure 3.7. Photographs of the 89-ft RRFC**

### 3.3 DCB Field Testing

The behavior of the DCB was determined by loading the bridge with a tandem-axle truck loaded with gravel. The width of the front tires was 15 in., the width of the individual tandem tires was 9 in., and the overall width of the rear tandem tires was 2 ft – 0 in. Truck dimensions and the axle weights of the truck used in the tests are shown in Figure 3.9. Unlike the BCB2, both static and dynamic field load tests were conducted on the DCB. The following sections will describe the instrumentation and testing methods used for the static and dynamic tests.

a. Side view of DCB

b. End view of DCB


c. Underneath DCB

**Figure 3.8. Completed DCB**

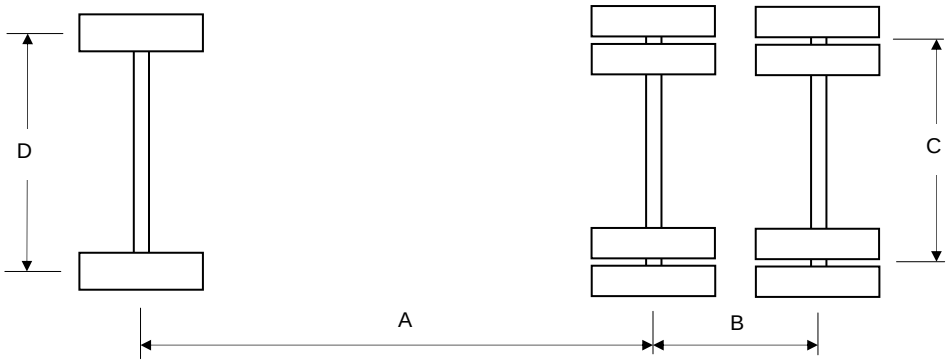


a. Top view


b. Side view

| Bridge | Dimensions | | | | Load (lbs) | | |
|---|---|---|---|---|---|---|---|
| | A | B | C | D | F | T | Gross |
| BCB2 | 13' -11" | 4' - 5" | 6' - 0" | 6' - 9 1/2" | 15,200 | 34,320 | 49,520 |

**Figure 3.9. Dimensions and weights of test trucks used in DCB field tests**

*3.3.1 DCB Instrumentation for Static Tests*

As with the BCB2 field load test, to determine the structural strength and behavior of the bridge, girder strains in the DCB were measured and recorded during the static field load tests using strain transducers and a data acquisition system, respectively. For additional bridge behavior data and to determine the load distribution to the primary girders, girder deflections were measured during the tests using deflection transducers. Throughout each test, deflections and strains were measured and recorded continuously. As the tandem axle of the test truck crossed reference lines on the bridge, a feature of the data acquisition system was used to specially mark the strain data for use in the analysis. The reference lines were the centerline of the west abutment, the 1/4 span, the midspan, the 3/4 span, and the centerline of the east abutment.

The instrumentation plan used in testing the DCB, illustrated in Figure 3.10, is similar to the plan used in testing the BCB2. To verify transverse symmetry, the bottom flanges of the six primary girders of the bridge were instrumented with strain transducers and deflection transducers at midspan, Detail E in Figure 3.10a.

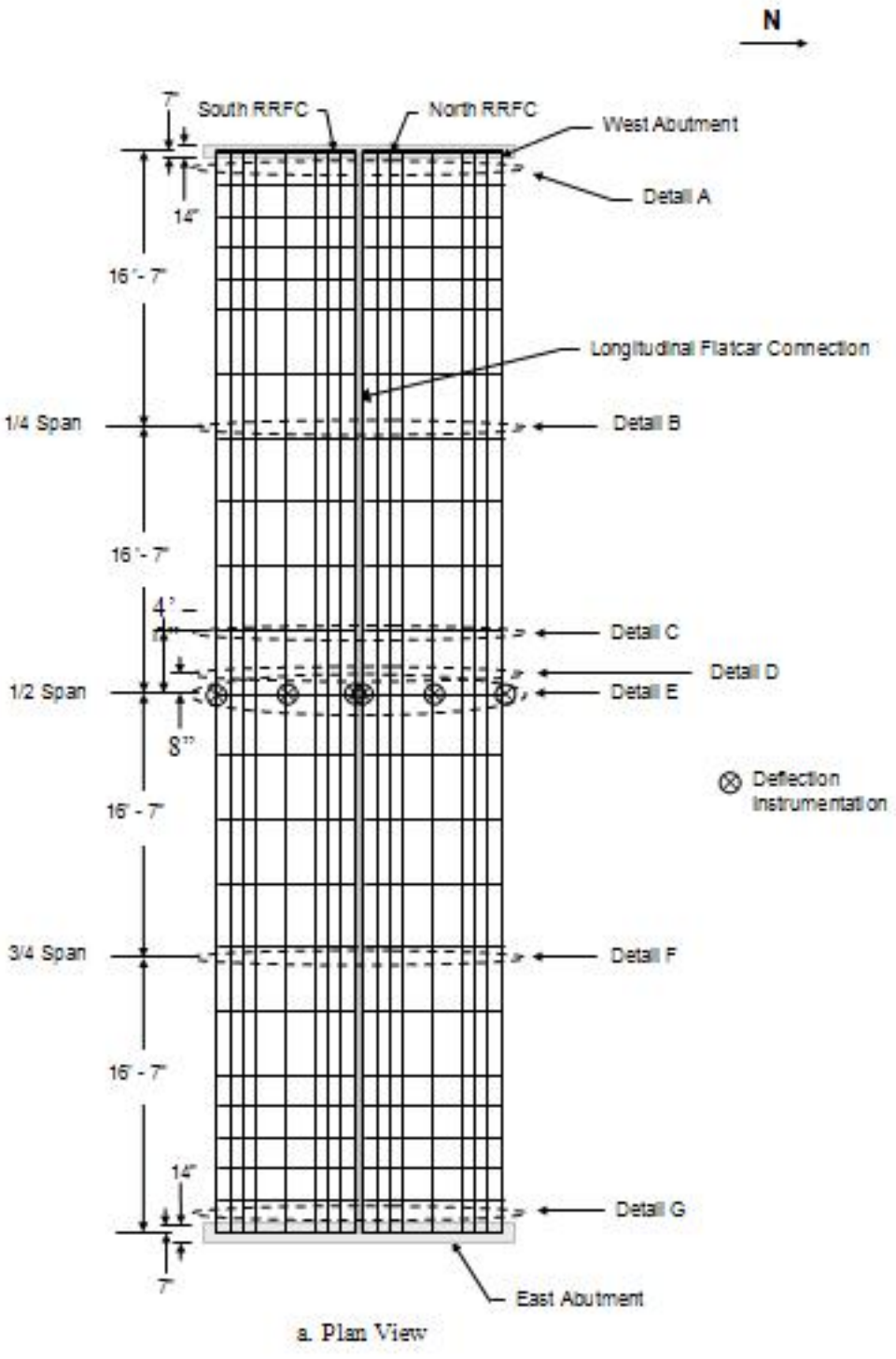


**Figure 3.10. Location of instrumentation in DCB tests**

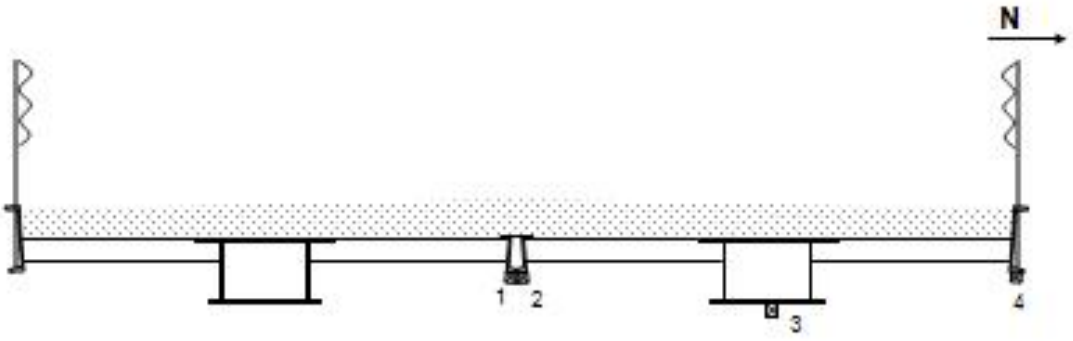


b. Details A and G

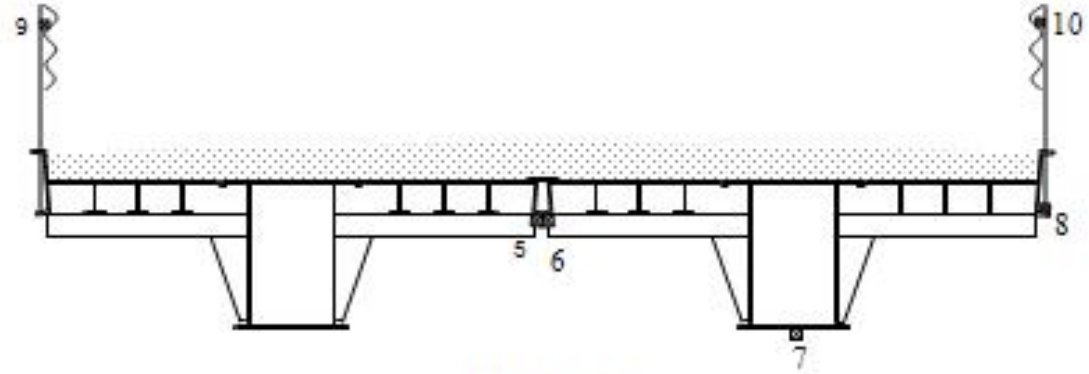


c. Details B and F

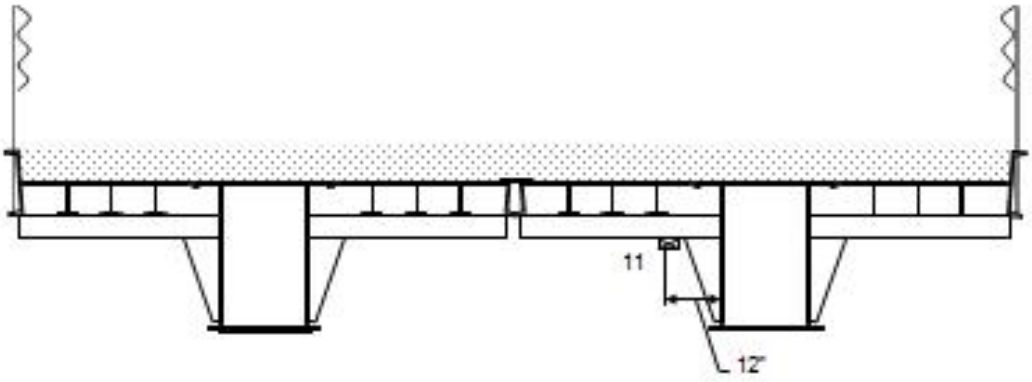


d. Detail C

**Figure 3.10. Continued**

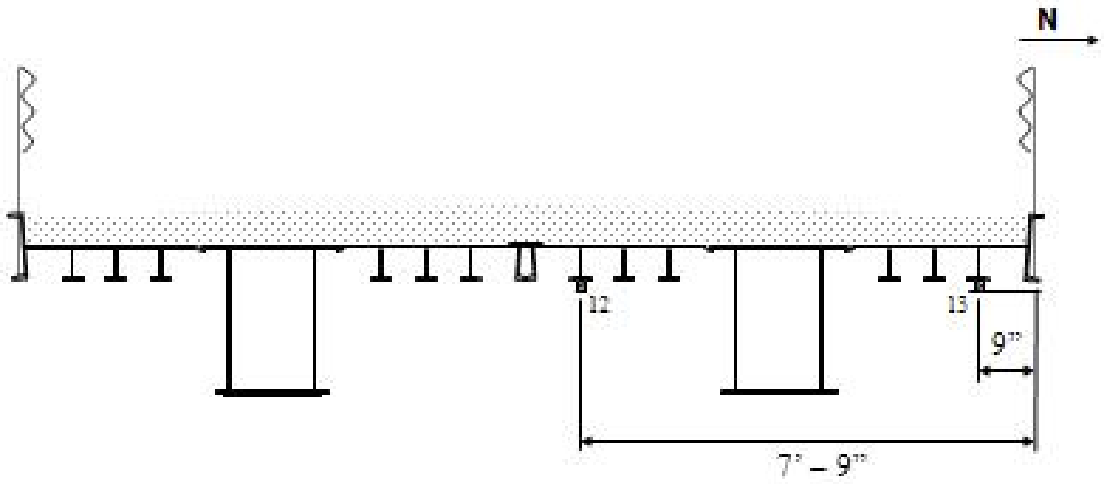


e. Detail D

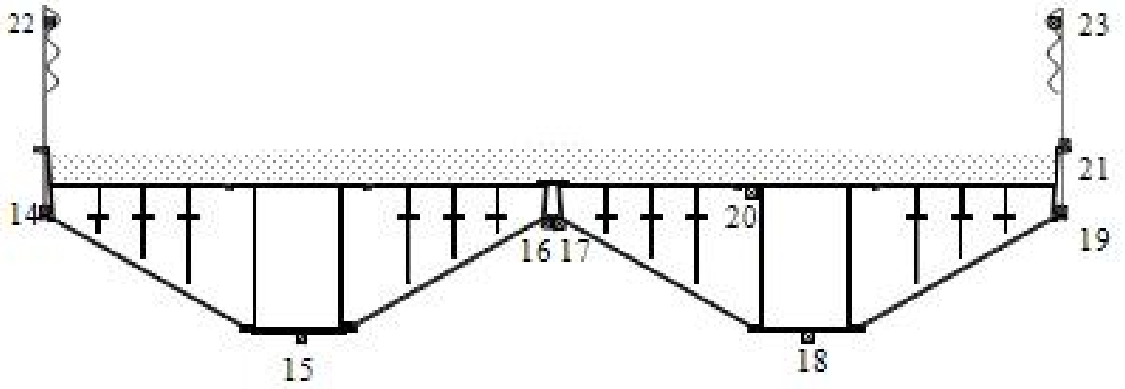


f. Detail E

Notes:

- Strain Transducers 1, 2, and 4 are in Detail G only.
- Strain Transducers 5, 6, and 10 are in Detail F only.

**Figure 3.10. Continued**

The deflection transducers were attached to the bottom flange of each of the six primary girders. A photograph of the deflection transducers for the LFC and interior girder of the south RRFC is presented as Figure 3.11. The placement of the strain transducers across the midspan is shown in Figure 3.10f. The strain transducers used to verify transverse bridge behavior are transducers 14 through 19. Photographs of strain transducers 16 and 17 at the midspan of the two girders at the LFC and strain transducer 7 on the interior girder are shown in Figure 3.12. In addition to the bottom flanges, the top flanges of the interior girder of the north RRFC and the exterior girder on the north edge of the DCB were instrumented with strain transducers, identified as transducers 20 and 21 in Figure 3.10f. The top and bottom flanges of the interior girder of the north RRFC and the exterior girder on the north edge of the bridge were instrumented with transducers 18 through 21 to determine the neutral axis of each girder.

In order to verify longitudinal symmetry, the interior girder of the north RRFC was instrumented with strain transducers along the length of the DCB. One strain transducer was positioned at each of the following locations: 12 in. from the face of the west abutment, the 1/4 span, the midspan, the 3/4 span, and 12 in. from the face of the east abutment. As presented in Figure 3.10, the locations correspond with Details A, B, E, F, and G, respectively; the strain transducers used to determine the longitudinal bridge behavior are identified as transducers 3, 8, and 18.

At the quarter spans, the bottom flanges of the primary girders of the north RRFC were instrumented with strain transducers to determine the strains and deflections at these locations. At the 3/4 span, both girders at the LFC were instrumented with strain transducers. In Figure 3.10, the 1/4 span and the 3/4 span are identified as Details B and F, respectively, and the strain transducers located at the quarter spans are labeled as transducers 5 through 8 in Figure 3.10c. Also, to determine the behavior of the bridge at the abutments, the bottom flanges of the primary girders of the north RRFC were instrumented with strain transducers at the east abutment. Because mounting the strain transducers at the centerline of the abutment was not feasible, the transducers were mounted 12 in. from the face of the east abutment, Detail G in Figure 3.10. The strain transducers located at the east abutment are labeled as transducers 1 through 4 in Figure 3.10b.

In addition to the primary girders, two secondary members and one S-shaped transverse member were instrumented with strain transducers to determine the strains in the secondary and S-shaped transverse members. As seen in Figure 3.10e, strain transducers 12 and 13 were mounted on the secondary members that were located 7 ft – 9 in. and 9 1/2 in. from the north edge of the DCB, respectively. The longitudinal position of the strain transducers, identified as Detail D in Figure 3.10a, is 8 in. west of the midspan. A photograph of strain transducer 13 on the secondary member is shown in Figure 3.13a. The transverse member that was instrumented is identified as Detail C in Figure 3.10a and was approximately 4 ft west of the midspan. As shown in Figure 3.10d, the strain transducer on the transverse member, transducer 11, is mounted 12 in. south of the web of the interior girder of the north RRFC. In Figure 3.13b, a photograph of strain transducer 11 on the S-shaped transverse member is shown.

Finally, to determine the strains in the guardrail, both the north and south guardrails of the DCB were instrumented with strain transducers at the midspan and the 3/4 span. The placement of the strain transducers is shown in Figure 3.10; the strain transducers on the guardrail are labeled 9, 10, 22, and 23.

### *3.3.2 DCB Static Testing*

As with the BCB2, the DCB was divided into the three lanes shown in Figure 3.14 to determine the behavior of the bridge under different load conditions. As may be seen in Figures 3.14a and c, when in Lanes 1 or 3, the truck was positioned with the center of one set of the double tires 2 ft from the south or north edge of the bridge, respectively. With the truck positioned in Lane 1 or 3, an eccentric load condition is created; the results from test with the truck positioned in Lane 1 can be compared to the

results from the test with the truck in Lane 3 to verify transverse symmetry in the DCB. The effectiveness of the LFC can also be determined with the results from the tests with an eccentric load condition.


**Figure 3.11. Deflection transducers used on DCB**


a. Strain transducers 16 and 17 on bottom flanges of girders at LFC

**Figure 3.12. Strain transducers on the DCB LFC**

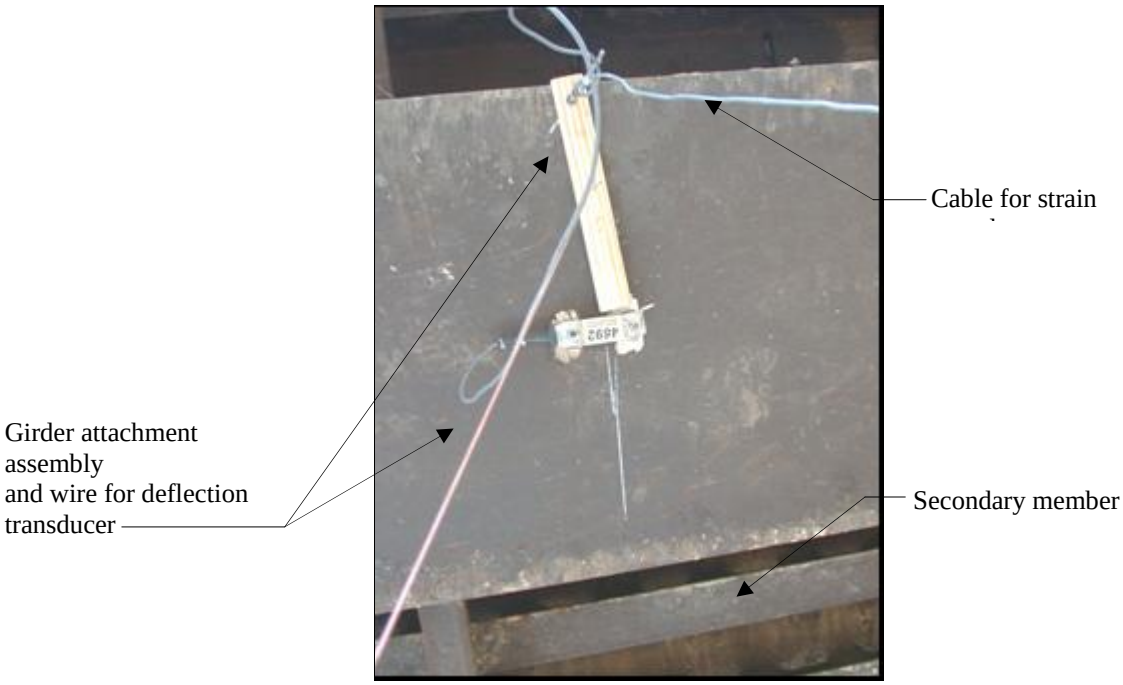


b. Strain transducer 7 on bottom flange of interior girder

**Figure 3.12. Continued**

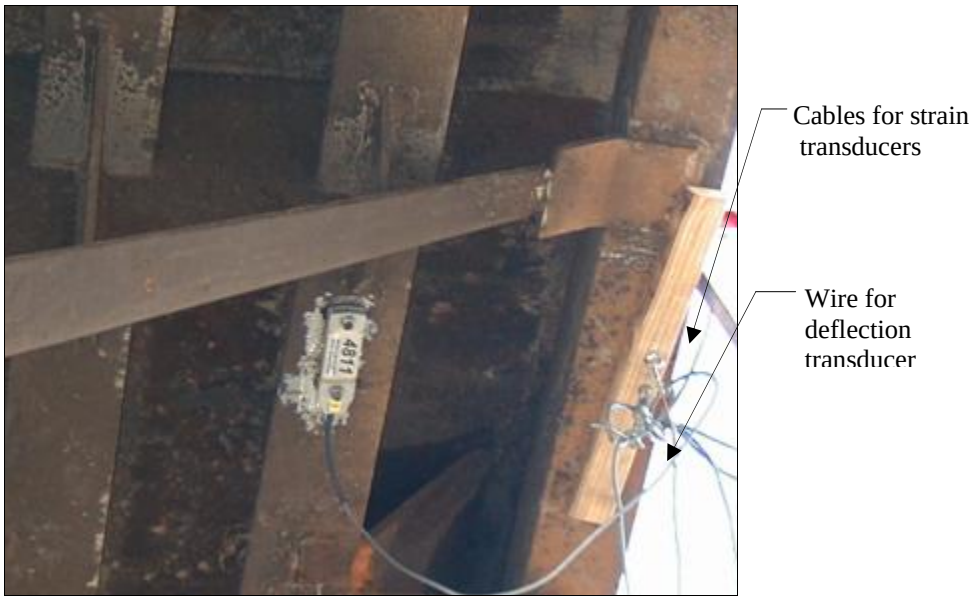


a. Strain transducer 13 on a secondary member

**Figure 3.13. Photographs of strain transducers used on DCB**

b. Strain transducer 11 on an S-shaped transverse member

**Figure 3.13. Continued**

As may be seen in Figure 3.14b, the test truck was centered transversely on the DCB when in Lane 2, creating a centered load condition. The results from the test with a centered load condition can be used to verify transverse symmetry. Photographs of the test truck positioned in Lanes 2 and 3 are shown in Figures 3.15 and b, respectively.

For the static field load tests, the truck, shown in Figure 3.15c, was driven slowly across the bridge in each of the three lanes while the data acquisition system recorded the strains and deflections measured by the strain and deflection transducers. The tests were considered static because when traveling at a slow speed, the truck did not cause significant dynamic effects in the bridge.

*3.3.3 DCB Instrumentation for Dynamic Tests*

To determine the dynamic behavior of the bridge, girder strains in the DCB were measured and recorded during the dynamic field load tests using strain transducers and a data acquisition system, respectively. For additional bridge behavior data, girder deflections were measured during the tests using deflection transducers. Throughout each test, deflections and strains were measured and recorded continuously. As the front axle of the test truck crossed the centerline of the west abutment of the bridge, a feature of the data acquisition system was used to specially mark the strain data for use in the analysis.

The instrumentation plan for the dynamic field load tests of the DCB is identical to the instrumentation plan for the static field load tests which was described in Section 3.3.1 and shown in Figure 3.10. The strains and deflections measured with the strain and deflection transducers shown in Figure 3.10 during the dynamic load tests can be used to determine the behavior of the bridge under dynamic loads. Also, the data collected during the dynamic load tests can be compared with the data from the static load tests in order to determine the dynamic amplification factors for the girder strains and deflections due to the test truck traveling at faster speeds.

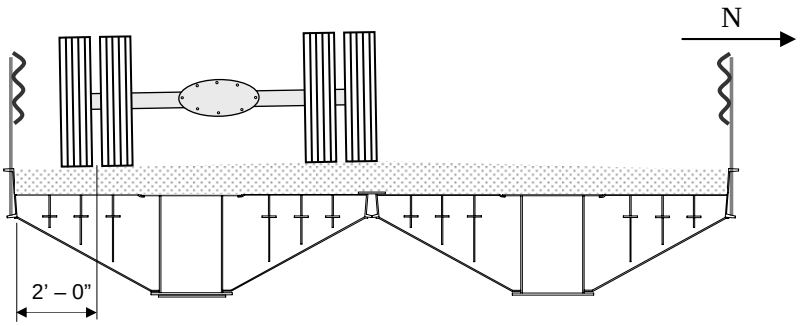


a. Lane 1

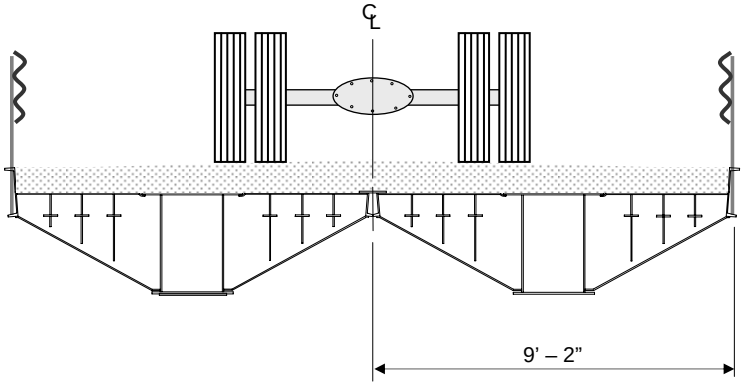


b. Lane 2

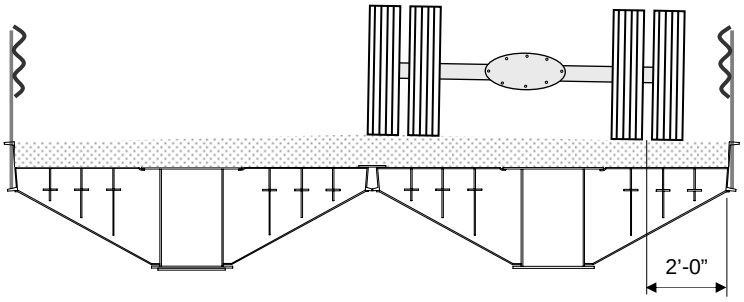


c. Lane 3

**Figure 3.14. Transverse locations of truck in DCB tests**

a. Truck centered on DCB (Lane 2)

b. Loading DCB with truck on north RRFC (Lane 3)

c. Photograph of DCB test truck

**Figure 3.15. Photographs of the truck used in the DCB tests**

*3.3.4 DCB Dynamic Tests*

Because the DCB is only 18 ft – 4 in. wide and is on a low-volume road, the daily traffic on the bridge is most likely to cross the DCB while centered transversely on the bridge. Thus, for the dynamic field load tests, the truck was driven across the bridge while centered on the bridge. This position of the test truck corresponds to Lane 2 of the static tests which was shown in Figure 3.14b.

Two dynamic load tests were run on the DCB. In the first dynamic test, the test truck was driven across the DCB traveling at 10 mph. In the second dynamic test, the test truck was driven across the DCB at 15 mph. At these speeds, the girder strains and deflections of the DCB will be amplified due to the dynamic effects of the test truck.

### 3.4 DCB Dead Load Analysis

The total stress in the DCB is the stress caused by the test truck in the field load test plus the stress due to the dead load on the bridge. To determine the total stresses in the primary girders of the flatcar, a dead load analysis was performed. As with the BCB2 dead load analysis, several assumptions were made to simplify the analysis. Because the geometry of the 89-ft RRFCs is different from that of the 56-ft V-deck RRFCs, slightly different assumptions were made for the DCB dead load analysis. Due to the geometry, the exterior girders were assumed to be incapable of resisting the weight of the steel deck, secondary members, and transverse members and the driving surface. This assumption is based on the results of a grillage analysis in the demonstration project, TR-444, which determined that 99.9% of the bending moment was resisted by the interior girder [4]. Thus, for the dead load analysis of the DCB, the entire dead load was assumed to be resisted by the interior girders. As with the BCB2, the connected flatcars were assumed to form a rigid cross-section following conventional methods of bridge design. This allows any additional dead load to be considered uniform on the bridge. The driving surface of the DCB consists of a layer of 120-pcf gravel which is 10 in. deep at the centerline of the bridge and 7 in. at the edges of the bridge. Based on a weight of 42,000 lbs for one 89-ft RRFC [4], the DCB was assumed to weigh 944 lb/ft. Finally, the DCB was assumed to be simply supported.

In order to determine the dead load stresses present in the interior girder of one RRFC, half of the dead load on the DCB was applied as a distributed load to a simply-supported model of the girder. The moment at the midspan of the girder was then calculated. With the midspan moment and the section modulus of the interior girder, the dead load stress in the interior girder at midspan was calculated using Equation 2.1, as in the BCB2 analysis. Using this procedure, the maximum dead load stress in the bottom flange of the interior girders at the midspan was determined to be 16.1 ksi in tension.

### 3.5 DCB Field Testing Results

As discussed in Section 3.3, deflections and strains were measured in the longitudinal girders and the secondary and transverse members of the DCB. In the following sections, the deflection and strain results from the field load tests will be presented and analyzed in order to determine the structural behavior of the DCB (i.e. (Objective 2 of this project).

In order to determine the stresses in the girders from the strains measured during the field load tests, the elastic modulus of the steel in the RRFCs must be known. To determine the acceptability of these stresses, the strength of the steel must be known. In the demonstration project, TR-444, tensile tests were performed on steel coupons from an 89-ft RRFC. The results of the tensile tests showed that the modulus of elasticity and the yield strength were 29,000 ksi and 40 ksi, respectively [4]. As stated in the 2003 AASHTO Standard Specifications for Highway Bridges, the allowable flexural stress for compact steel members not subjected to lateral-torsional buckling is 55 percent of the yield strength [7]. The girders in both types of RRFCs used in this study are compact and not subjected to lateral-torsional buckling; therefore, the allowable flexural stress in the steel members of the RRFCs used in the DCB was 22 ksi, 55 percent of 40 ksi.

#### *3.5.1 Static Field Load Test Results*

Besides instrumenting the primary girders at midspan, the DCB instrumentation plan described in Section 3.3.1 included measuring the strain in two secondary members, one transverse member, and one interior girder at both abutments (12 in. from the face of the abutments). The maximum strains at the abutments occurred in the bottom flanges of the interior girders. The maximum strain at the east abutment was 43 MII (1.2 ksi), and at the west abutment, the maximum strain was 55 MII (1.6 ksi). The presence of strain

in the girders close to the abutments indicates that some end restraint is present in the DCB, even though the bridge was designed to be simply-supported. However, the maximum strains in the interior girder at the abutments were considerably less than the maximum strains experienced in the interior and exterior primary girders at the midspan of the bridge. Also, the maximum stresses in the interior girder at the abutments were well below the allowable stress limit. Although end restraint reduces the midspan strains, the effect is minimal because the maximum strain at the abutments was significantly less than the maximum strain at midspan. Thus, the strains in the girders close to the abutments will not be discussed further.

As shown previously in Figure 3.10, the secondary members that were instrumented with Strain Transducers 12 and 13 were both located on the north RRFC, as was the S-shaped transverse member that was instrumented with Strain Transducer 11. The maximum strains that occurred in the two instrumented secondary members were 77 MII (2.2 ksi) and 34 MII (1.0 ksi) and occurred when the truck was positioned in Lane 3 on the north RRFC. The maximum strain that occurred in the transverse member was 47 MII (1.4 ksi) and occurred when the truck was positioned in Lane 2, with the truck tires directly above the transducer. The maximum strains in the secondary and S-shaped transverse member were significantly less than the maximum strains experienced in the interior primary girders, and the maximum stresses were well below the allowable stress limit. Thus, the secondary and S-shaped transverse members were determined to be not critical members and will be excluded from additional discussion.

The maximum midspan deflections and strains in the primary girders that were measured when the truck was in Lanes 1 – 3 on the DCB are presented in Figures 3.16 – 3.18, respectively. As described in Section 3.3.1, the midspan of DCB was instrumented with six deflection transducers and six strain transducers. The deflections and strains measured with these transducers are represented in Figures 3.16 – 3.18 by small diamonds. The dashed lines represent a trend that may occur between the measured deflections and strains and thus, do not represent actual measured deflections or strains. The deflections and strains shown in Figures 3.16 – 3.18 occurred when the center of the tandem axle of the truck was at the midspan of the bridge. As can be seen in Figures 3.16 and 3.18, the maximum deflection of the DCB was 0.69 in. and 0.84 in. when the truck was in Lane 1 or 3, respectively, and occurred at the exterior girder on the south or north edge of the bridge, respectively. When the truck was positioned in Lane 2, the maximum deflection as seen in Figure 3.17 was 0.6 in. and occurred at the LFC.

As previously noted, the 2003 AASHTO Standard Specifications for Highway Bridges states that an optional limit for the deflection of a bridge is 1/800 of the span length [8]. For a 66 ft – 4 in. span, this optional limit is 1.0 in. As with the BCB2 field tests, the test truck used in the DCB field tests was not an AASHTO HS-20 truck, which is one of the design loads used in bridge design. Using Equation 2.2, the load adjustment factor for the DCB was determined to be 1.37. By multiplying the measured deflections by the load adjustment factor, the adjusted maximum deflection of the DCB was determined to be 1.15 in., which is 15 percent over than the optional AASHTO deflection limit of 1.0 in. However, as stated in Section 2.5.1, the optional AASHTO deflection limit is a guideline, not a strict requirement for legal bridges. Because the DCB is a rural bridge on a low-volume road, exceeding the optional deflection limit was decided to be acceptable. If the deflections of the DCB were to be required to meet the AASHTO limit, the load of a truck with HS-20 axle spacings would have to be reduced to 30 tons.

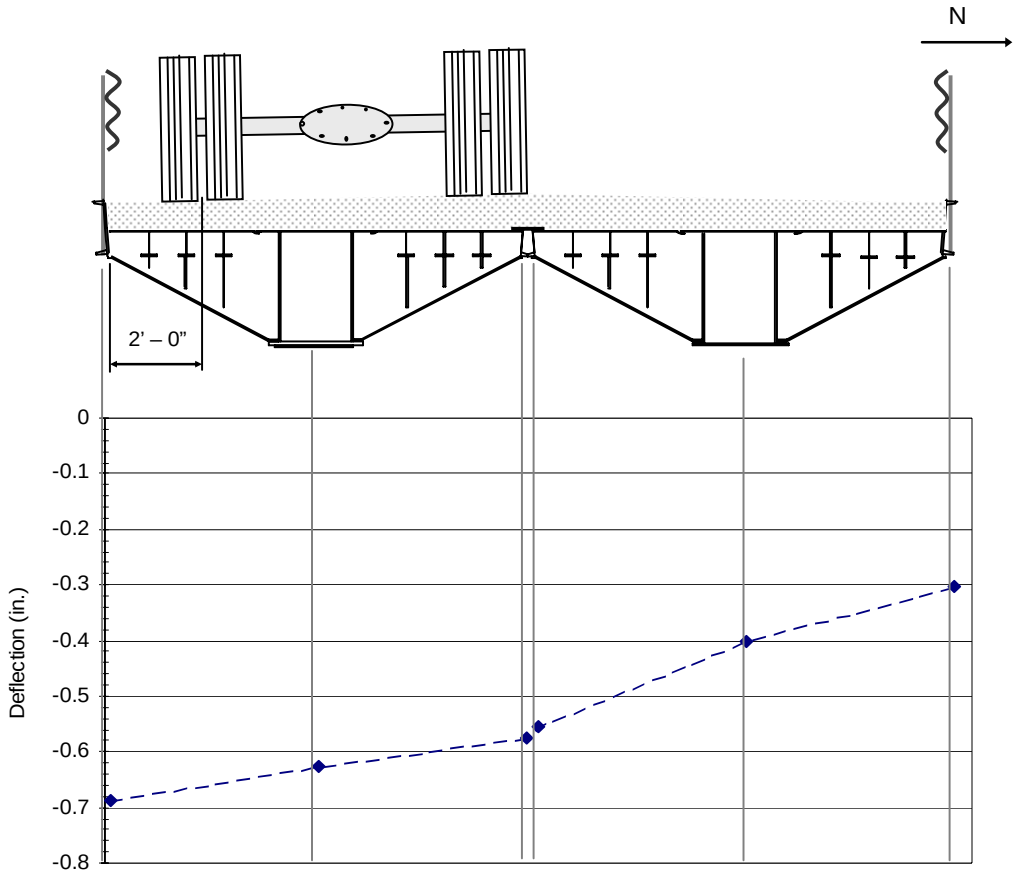


a. Deflections

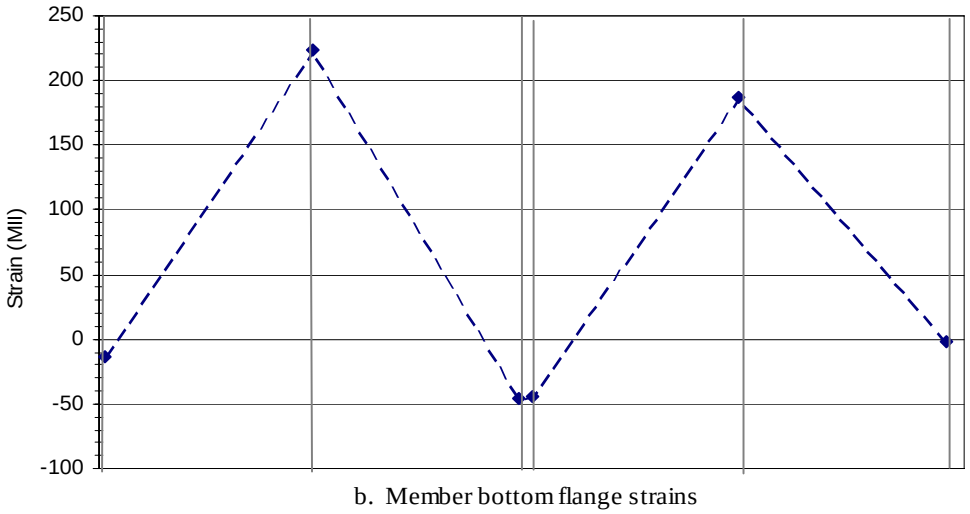


b. Member bottom flange strains

**Figure 3.16. DCB Lane 1 midspan deflections and strains**

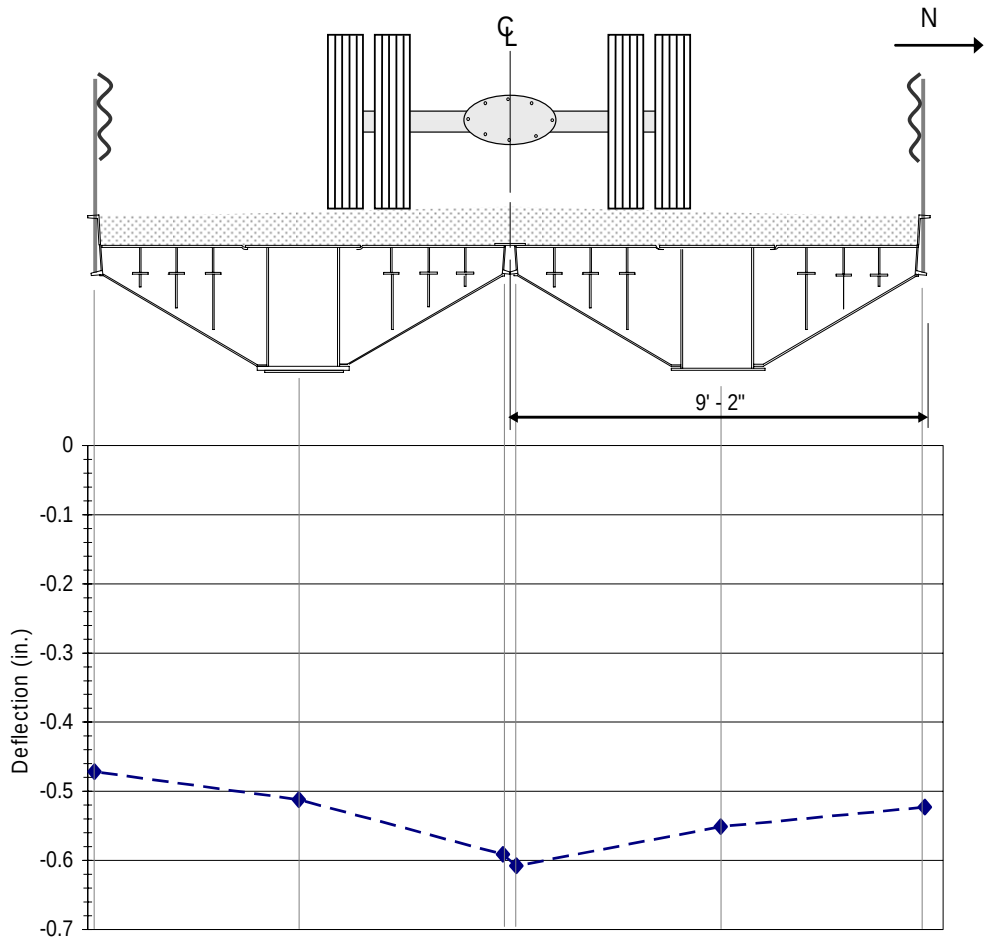


a. Deflections

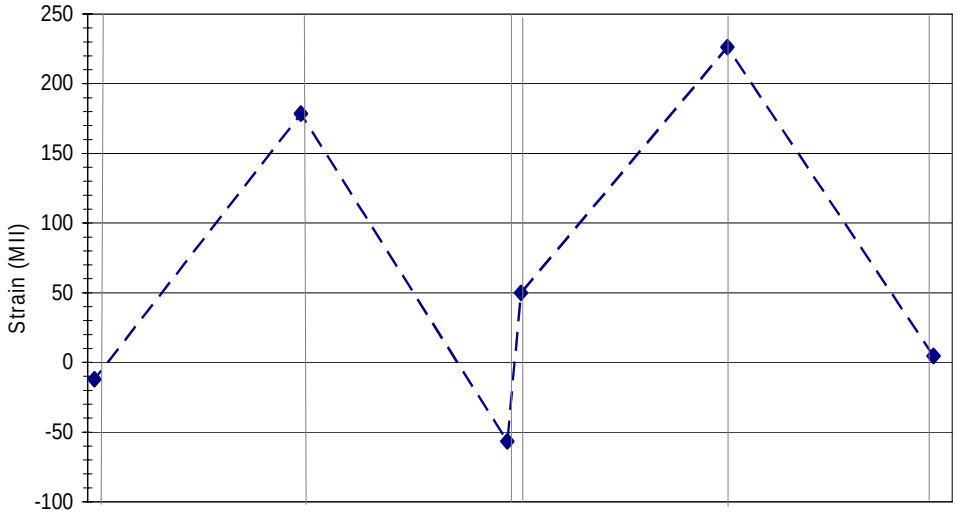


b. Member bottom flange strains

**Figure 3.17. DCB Lane 2 midspan deflections and strains**

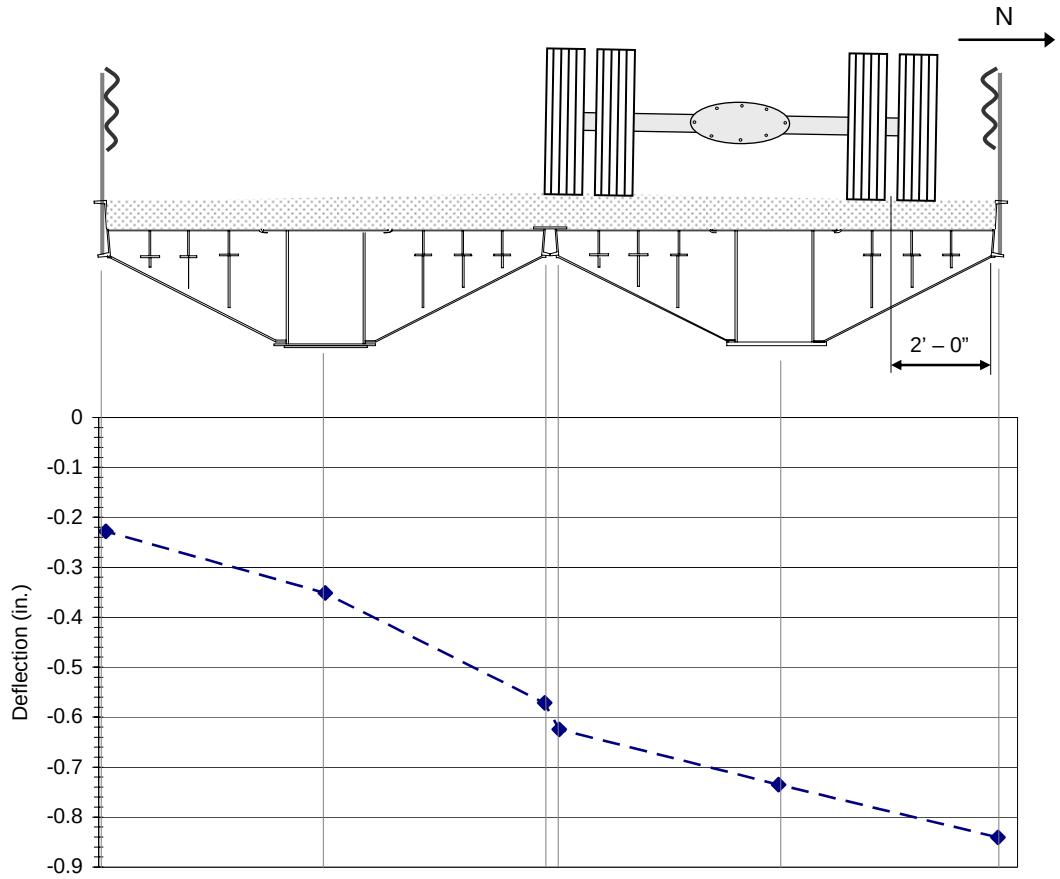


a. Deflections

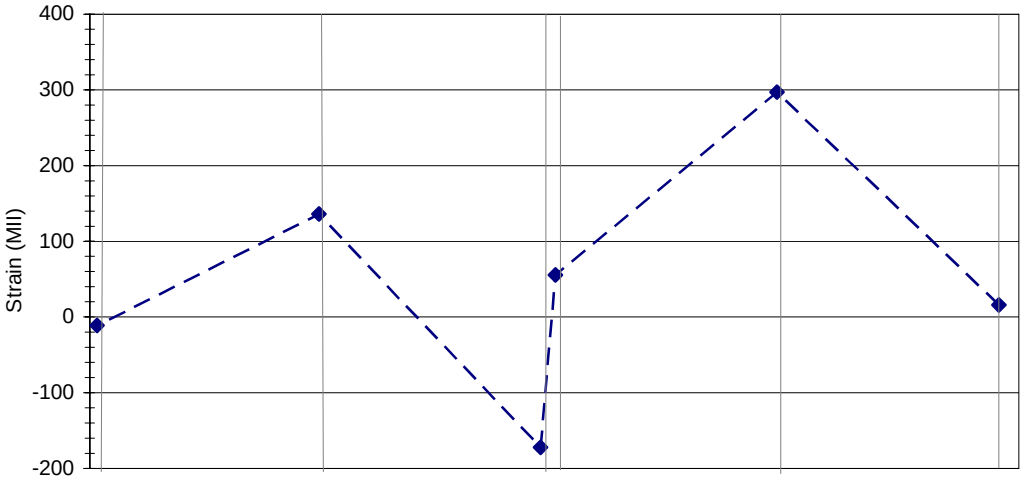


b. Member bottom flange strains

**Figure 3.18. DCB Lane 3 midspan deflections and strains**

In each test, the maximum strain in the DCB occurred in the interior girder beneath the test truck. Maximum strains occurred in the exterior girders at the LFC. As may be seen in Figure 3.18, the maximum strains measured in the interior and exterior girders due to the live loads were 297 MII (8.6 ksi) in tension and 172 MII (5.0 ksi) in compression, respectively. When the dead load stresses were combined with the live load stresses determined from the field test results, the maximum total stresses in the longitudinal interior and exterior girders were 24.7 ksi in tension and 5.0 ksi in compression, respectively. Thus, the maximum total stress in the DCB exceeds the allowable stress of 22 ksi by 12 percent.

As mentioned previously, the test truck was not an AASHTO HS-20 truck which is likely the maximum load that will cross the DCB. Therefore, the maximum strains measured in the field tests were adjusted using the load adjustment factor of 1.37 previously mentioned for the adjustment of the maximum deflections. The adjusted maximum strain in the interior girders was 408 MII (11.8 ksi) in tension. The adjusted maximum total stress in the interior girders was 27.9 ksi (27 percent greater than the allowable stress for flexure). In order to keep the maximum total stress below the allowable stress limit, the thickness of the gravel driving surface should be limited to 3 in. Decreasing the thickness of the gravel layer will reduce the dead load stress in the interior girder to 9.9 ksi which in turn will reduce the total stress in the interior girder to 21.7 ksi, which is less than the allowable flexural stress.

As expected, the midspan maximum strains and deflections for each test occurred in the girders directly below the test truck axle loads. As seen in Figures 3.16 and 3.18, the north edge of the bridge deflected downward when the truck was positioned in Lane 1, and the south edge of the bridge deflected downward when the truck was positioned in Lane 3. This behavior demonstrates effective lateral load distribution through the longitudinal flatcar connection.

Symmetrical bridge behavior is shown in the deflection patterns in Figure 3.17 and the mirrored deflection and strain patterns in Figures 3.16 and 3.18. Although the strain patterns in these figures are mostly symmetric, the strains in the exterior girders at the LFC are not symmetric. In Figures 3.15 and 3.18, the strain in the bottom flange of the south girder is compressive while the strain in the bottom flange of the north girder is tensile. As can be seen in Figures 3.15 and 3.18, the deflections of the two girders at the LFC are not equal; thus, the two RRFCs do not act as a rigid structure. The strain difference is likely due to the relationship of the bottom flange of the girder with the different neutral axes for the two RRFCs. The neutral axes of the two RRFCs are not equal because, as noted in Section 3.2.1, the south RRFC has an additional 1-in. plate welded to the bottom flange of the interior girder. On the north RRFC, the bottom flange of the LFC girder is below the neutral axis so the flange is in tension. However, on the south RRFC, the bottom flange of the LFC girder is above the neutral axis so the flange is in compression.

Another asymmetrical aspect of the DCB behavior is that the magnitudes of the strains and deflections in the girders of the south RRFC are less than the corresponding strains and deflections in the girders of the north RRFC. This difference is due to the additional 1-in. plate welded to the bottom flange of the interior girder of the south RRFC. The plate increases the stiffness of the interior girder, and thus, the south RRFC will experience smaller strains and deflections than the north RRFC.

### *3.5.2 Dynamic Load Test Results*

As described in Sections 3.3.3 and 3.3.4, dynamic load tests were run on the DCB with the test truck traveling across the bridge in Lane 2 at 10 mph and 15 mph. The maximum strain measured in the primary girders due to the test truck traveling at 10 mph was 235 MII (6.8 ksi) in an interior girder. When the test truck was driven at 15 mph across the bridge, the maximum interior girder strain in the DCB increased slightly to 240 MII (7.0 ksi). As with the static load tests, the stresses measured during the

dynamic load tests must be adjusted to represent the stresses due to an HS-20 truck using the 1.37 load adjustment factor from Section 3.5.1; the maximum adjusted strain during the dynamic tests was 329 MII (9.5 ksi) for the test with the truck traveling at 15 mph. When combined with the stresses due to the dead load of the bridge to accurately determine the total stresses in the DCB due to the dynamic load tests, the maximum adjusted total stress was 25.6 ksi (16 percent greater than the allowable stress for flexure), which is less than the maximum adjusted total stress determined in the static load tests. By decreasing the amount of gravel on the DCB as suggested in Section 3.5.1, the maximum adjusted total stress for the dynamic load test decreases to 19.9 ksi, which is less than the allowable stress limit.

The maximum deflections measured in the DCB when the test truck was driven across the bridge at 10 mph and 15 mph were 0.61 in. and 0.63 in., respectively. Again, these deflections were adjusted to represent the maximum deflection due to an HS-20 truck. The adjusted maximum deflections of the DCB during the dynamic load tests were 0.84 in. and 0.86 in. when the truck was traveling at 10 mph and 15 mph, respectively. These deflections are below the optional AASHTO limit of 1.0 in.

With the results from the both the static and dynamic load tests, the girder strains and deflections were compared to determine the dynamic amplification factors due to the faster speed of the test truck. In order to accurately determine the dynamic amplification factors, the deflections and strains from the dynamic load tests were compared with the maximum strains and deflections from Figure 3.17, the static load test with the truck positioned in Lane 2. Thus, for the purpose of determining the dynamic amplification factors for the girder strains and deflections, the maximum strain in the DCB was 226 MII (6.6 ksi) in an interior girder and the maximum deflection was 0.60 in.

The dynamic amplification factors, DAF, were determined using Equation 3.1 by calculating the percent difference between the static and dynamic load test results.

$$DAF = \frac{\text{Dynamic Result} - \text{Static Result}}{\text{Static Result}} * 100\% \quad (3.1)$$

Because the strains and deflections were larger in the load test with the truck traveling across the bridge at 15 mph, this load test was used to determine the dynamic amplification factors. The dynamic amplification factors for the girder strains and deflections were 6.2 percent and 5.0 percent, respectively.

In addition to the dynamic amplification factors for the DCB, the results from the dynamic load tests were used to analyze the dynamic deflection behavior of the DCB. For both dynamic load tests, the maximum deflections due to the test truck were located at midspan of the north girder in the LFC. Since the load test with the truck traveling at 15 mph resulted in larger deflections, the deflection behavior from this load test was used in the analysis. In Figure 3.17, the deflection behavior of the DCB is presented. The deflection of the exterior girder of the north RRFC at the LFC during the load test is shown in Figure 3.19a. The large spike in Figure 3.19a represents the deflection of the DCB as the test truck crosses the bridge. As expected, the maximum deflection of the bridge occurs when the truck is approximately at midspan, shown graphically in Figure 3.19a as the spike occurs halfway through the test. The free vibration of the DCB measured at the midspan of the bridge in the north RRFC in the exterior girder at the LFC, shown in Figure 3.19b, was recorded for approximately 11 seconds after the test truck crossed the bridge. As seen in Figure 3.19b, the DCB completed 11 cycles of vibration during the first 4 seconds of free vibration. Finally, using Equations 3.2 and 3.3, the period, $T_D$, and the damped frequency, $f_D$, of the DCB were determined to be 0.36 seconds and 2.75 Hz, respectively.

$$T_D = \frac{t}{n} \tag{3.2}$$

where:

t = time required to complete n cycles of free vibration

n = number of cycles of free vibration

$$f_D = \frac{1}{T_D} \tag{3.3}$$

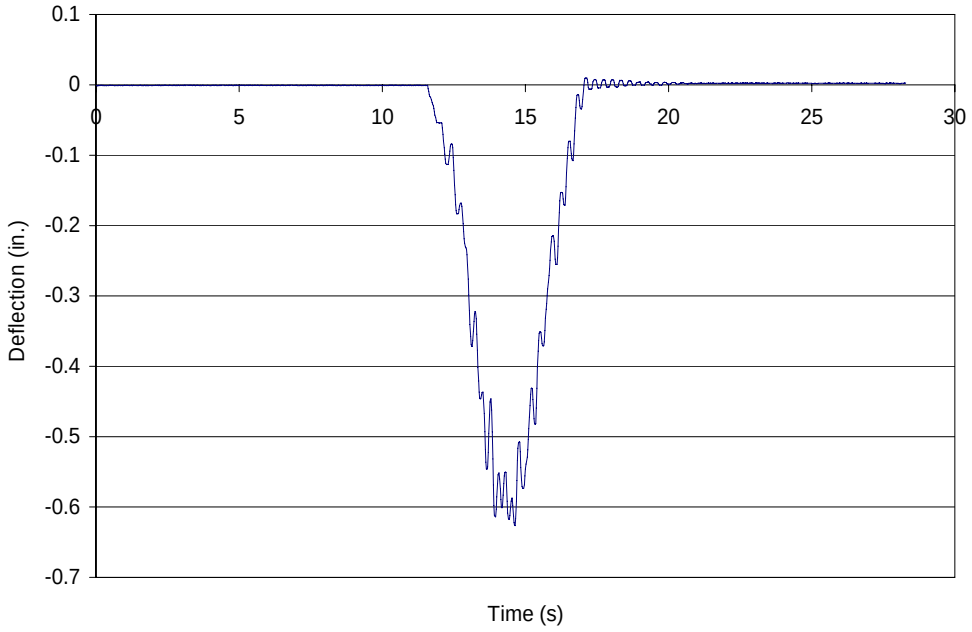


a. Deflection response during dynamic load test

**Figure 3.19. Deflection results of DCB 15 mph dynamic load test**

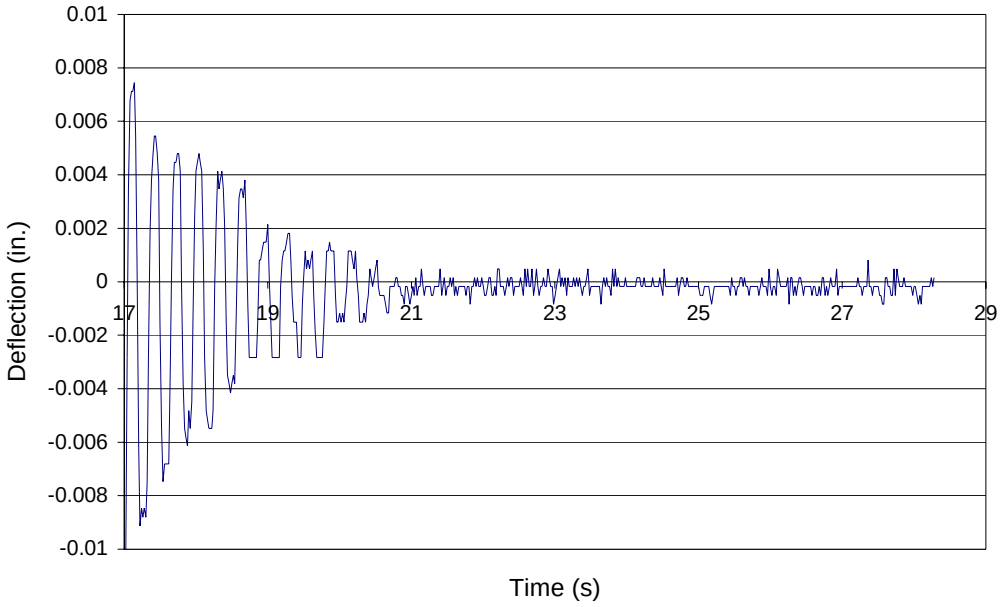


b. Free vibration of DCB after dynamic load test (50 samples per second)

**Figure 3.19. Continued**

## 4.0 BUCHANAN COUNTY BRIDGE 3 ON 270TH ST

### 4.1 Introduction

In the fall of 2004, construction of a RRFC bridge that crosses Smith Creek 1.5 miles east of Quasqueton, Iowa, on 270th St. was completed. This bridge will be referred to as Buchanan County Bridge 3 (BCB3) since it is the third RRFC bridge constructed in Buchanan County and tested by ISU. A map of the BCB3 location is presented in Figure 4.1.


a. Quasqueton, Iowa

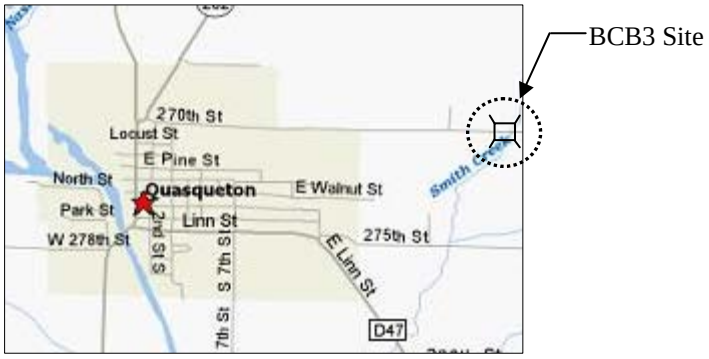


b. Detail A

**Figure 4.1. Location of the Buchanan County RRFC Bridge 3 [9]**

The BCB3 replaced a two-span timber bridge (19 ft – 0 in. and 22 ft – 6 in. spans) with a 20-ft wide deck that was constructed in 1948 (FWHA No. 082160). A sketch of the previous structure is presented in Figure 4.2. Five timber pilings at the abutments and pier were capped with a 12x12 timber section. Throughout the bridge length there were 11 equally spaced stringers; however, the west, smaller span was comprised of 6x16 timber stringers and the east, larger span had 4x16 timber stringers. Timber planks and gravel created the driving surface.

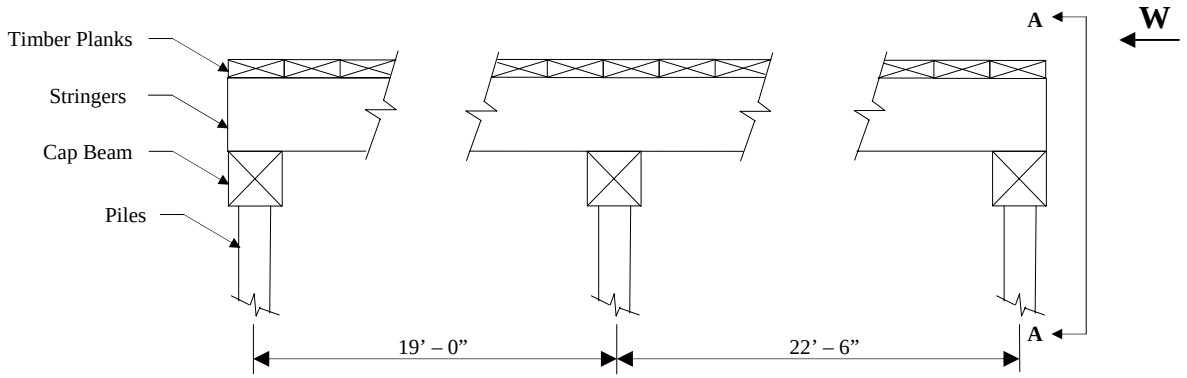


a. Elevation View

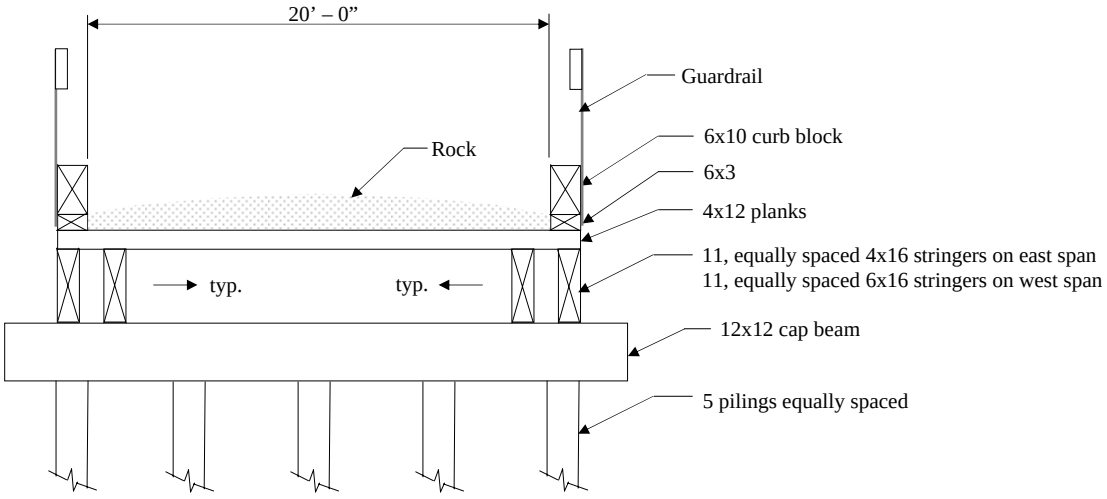


b. Section A-A

**Figure 4.2. Original Buchanan County Bridge on 270th St**

## 4.2 Design and Construction

The BCB3 was constructed using three RRFCs that were positioned side-by-side and were connected using bolts between adjacent cars. As shown in Figure 4.3, the BCB3 spanned 66 ft – 2 in. from center-to-center of abutments and had a deck width of 26 ft – 5 1/2 in.

The abutment and backwall details for the BCB3 are presented in Figure 4.4. The abutment was a modification of the Iowa Department of Transportation (Iowa DOT) standard stub abutment with zero skew [10]. The constructed concrete abutment was 3 ft tall, 4 ft wide, and 30 ft long. Five HP 10x42 piles were extended 24 in. into the concrete cap and surrounded with spiral reinforcement within the cap.

a. Photograph of the BCB3

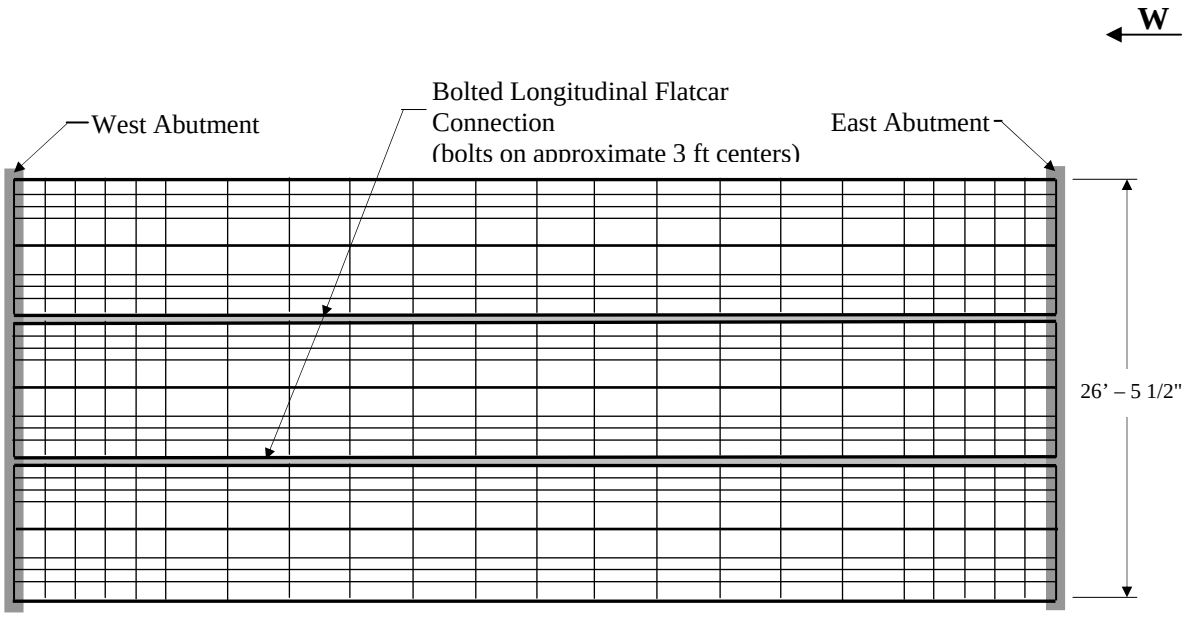


b. Plan View

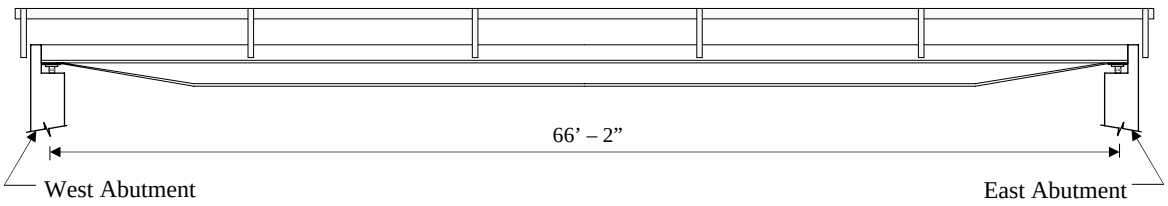


c. Elevation View

**Figure 4.3. Buchanan County RRFC Bridge 3**

**Figure 4.4. Details of the BCB3 concrete abutments**

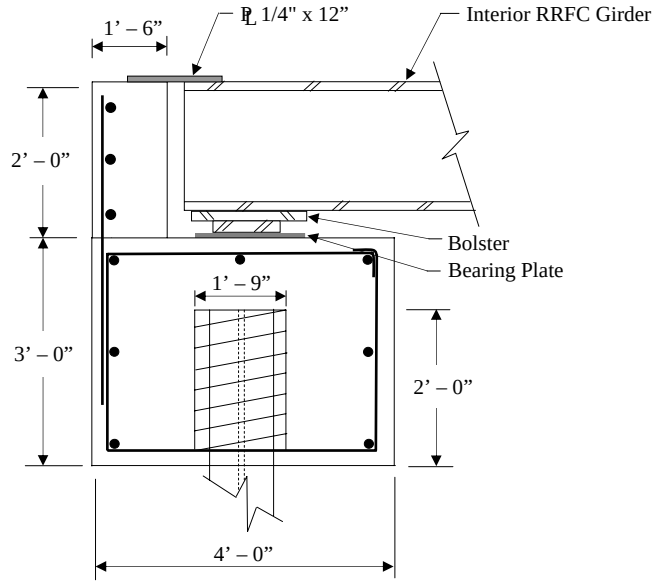


c. Side view of abutment

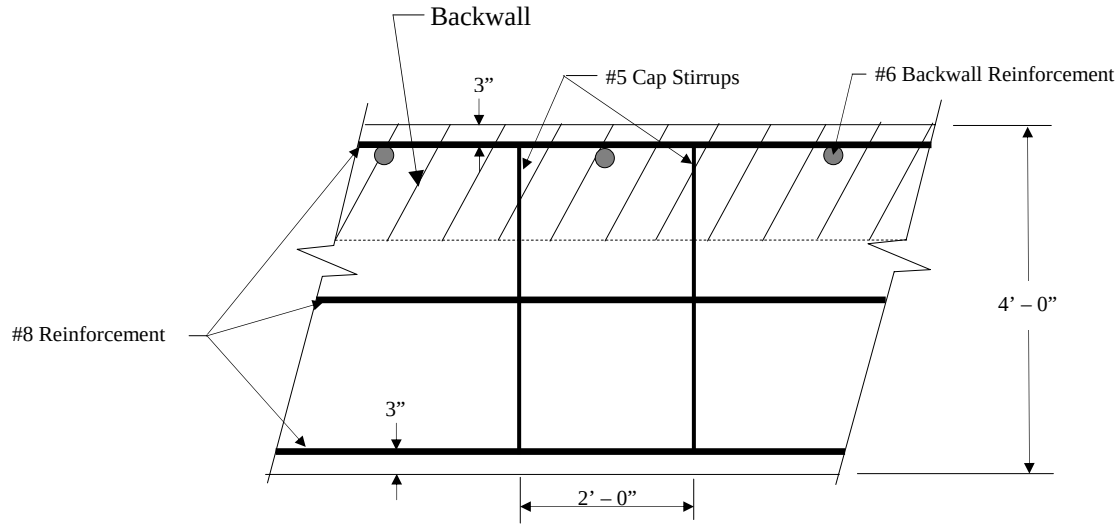


d.. Top view of abutment

**Figure 4.4. Continued**

Cap beam reinforcement included #8 longitudinal bars for flexure and #5 stirrups for shear resistance. The backwall was connected to the cap using #6 reinforcement. A ¼-in. thick, 12-in. wide, and 30-ft long plate (shown in Figure 4.4c) was welded to the top of the RRFCs to prevent foreign material from falling in the expansion joint between the backwall and the railcars.

The RRFCs used for the bridge superstructure were 89-ft railcars (identical to those used for the BCB2), trimmed near the bolsters to create the 66 ft – 2 in. span. Details of the 89-ft RRFCs were previously

presented in Figure 3.2. All exterior girders of the BCB3, except those located on the north and south exterior faces of the bridge, had the top portion of the girder trimmed flush with the top surface of the RRFC deck. To connect the adjacent exterior girders together at the bolted connections, the bottom flanges of the exterior girders were also trimmed. The longitudinal connection used to join the RRFCs (See Figure 4.5) was created with bolts (1 1/4 in. diameter), spaced approximately on 3 ft centers, connecting the webs of the adjacent RRFCs' exterior girders. Approximately 22 bolts were required in each longitudinal connection.

a. Photograph of the bolted connection

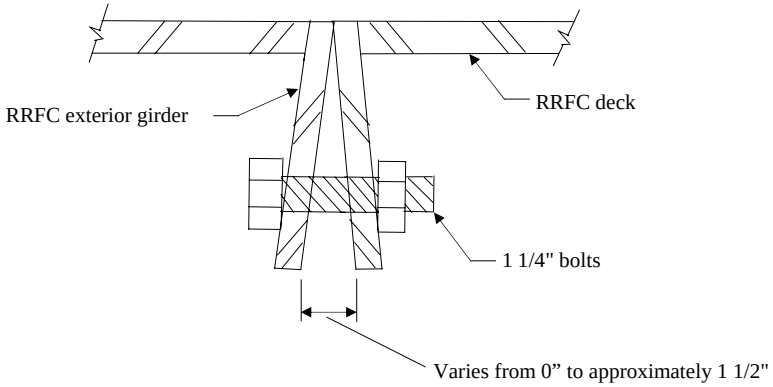


b. Bolted connection sketch

**Figure 4.5. Bolted longitudinal connection**

Supports at the abutments for the exterior, longitudinal RRFC girders are shown in Figure 4.6. They were created from a W-section confined on top and bottom with inverted channel sections. A set of built-up bearing sections was located at the connection location, while bearing plates were placed under the interior girders.

a. Photograph of bearings at a longitudinal bolted connection

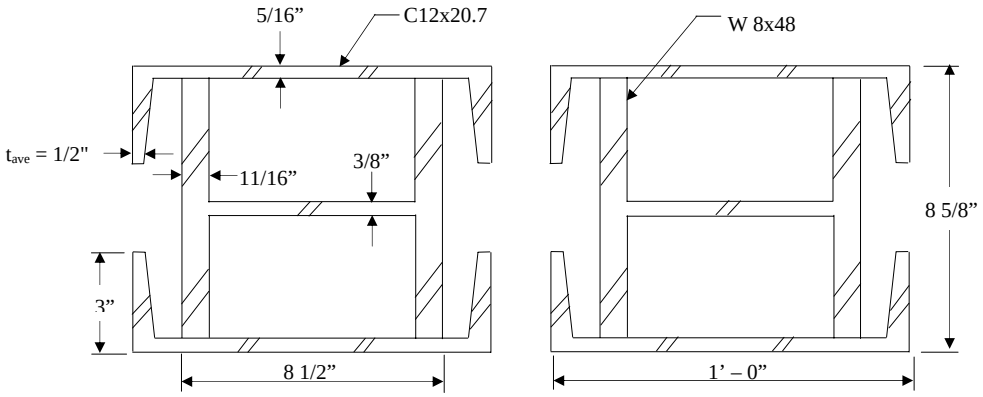


b. Bearing dimensions

**Figure 4.6. Built-up bearing sections at the abutments of the BCB3**

### 4.3 BCB3 Field Testing

The field testing of the 270th St. BCB3 involved both dynamic and static testing using a tandem county truck. Dimensions and weights of the tandem truck used in the field tests are presented in Figure 4.7, and a photograph of the truck is shown in Figure 4.8. The front tires were 1 ft – 2 in. wide, the individual rear tires were 10 in. wide, and a set of rear tandem tires had a width of 2 ft – 0 in. The truck had a gross weight of 48,200 lbs.

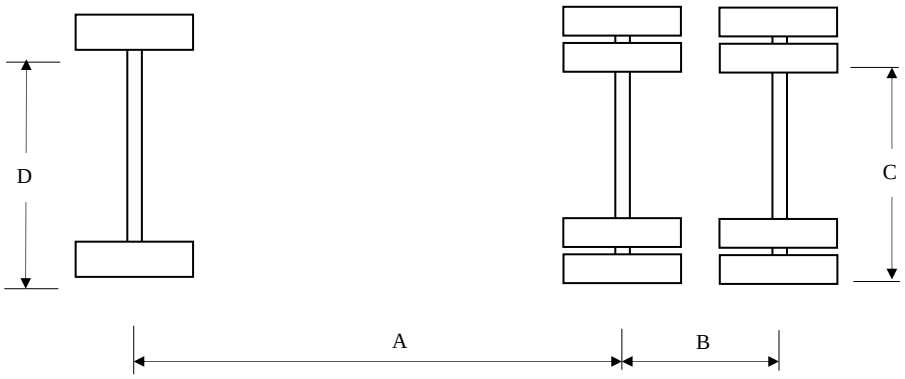


a. Top view


b. Side view

| Dimensions | | | | Load (lbs) | | |
|---|---|---|---|---|---|---|
| **A** | **B** | **C** | **D** | **F** | **T** | **Gross** |
| 13' - 6 1/2" | 4' - 5" | 6' - 0" | 6' - 11" | 11,940 | 36,260 | 48,200 |

**Figure 4.7. Dimensions and weights of test truck used in BCB3 field tests**

**Figure 4.8. Test truck used in BCB3 bridge field test**

The dynamic testing of the BCB3 was performed by driving the tandem test truck down the centerline of the bridge (See Figure 4.9). Five separate dynamic tests were completed; the first test was at a speed of 10

mph which was increased by 5 mph increments in subsequent tests until a maximum speed of 30 mph was reached in the final test. Through the dynamic tests, the dynamic amplification of the deflections and strains was determined. Static testing of the BCB3 included five different transverse positions of the tandem truck across the bridge which are illustrated in 4.10, and photographs of the test truck on the bridge are presented in Figure 4.11.

**Figure 4.9. Dynamic testing of the BCB3**

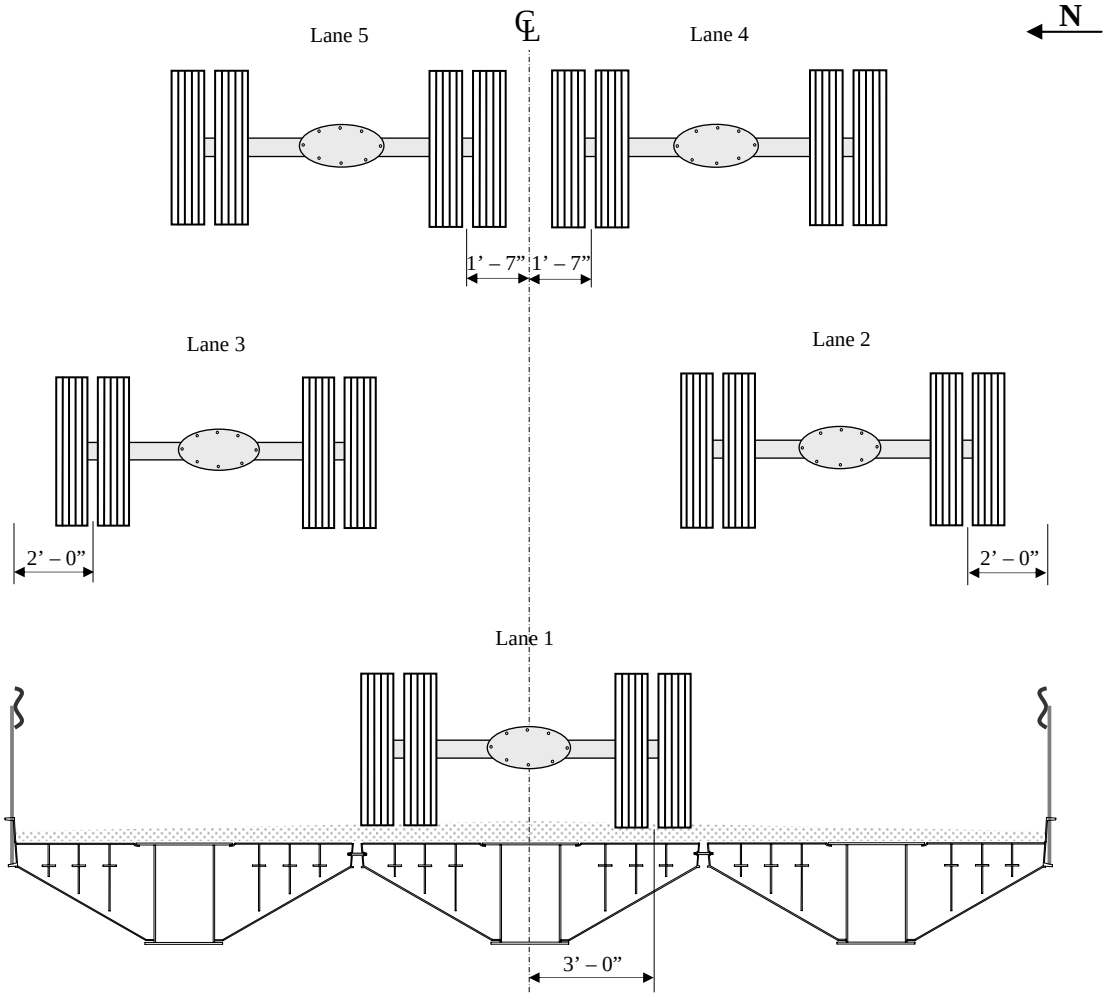


**Figure 4.10. Transverse locations of the truck used in field tests**

a. In Lane 1

b. In Lane 3

**Figure 4.11. Photographs of the test truck on BCB3**

Instrumentation for the BCB3 test included both deflection and strain transducers placed on the various RRFC girders. The full instrumentation plan is presented in Figure 4.12. At the bridge midspan, deflection and strain instrumentation was placed on all interior box girders and exterior members of the three RRFCs. These data were used to perform a complete cross-sectional analysis of the member deflections and strains at the midspan, the location where maximum stresses and deflections occurred in the girder. The interior box girder of the south RRFC was instrumented with strain transducers near each abutment, at the midspan, and also at the 1/4 and 3/4 span locations. Information from instrumenting along the length of one of the RRFC enabled a time history analysis of the member when the tandem truck crossed the bridge. At the 3/4 span location, deflection instruments were placed on all three interior box girders to determine how the bridge behavior at this location differed from that at the midspan. Strain transducers were placed on the outer side of the guardrail system at the 3/4 span location of the south RRFC to determine if the guardrail system provided added stiffness to the structure. Lastly, secondary longitudinal members and a transverse member near the midspan were instrumented with strain transducers to determine the live load strains. A total of 12 deflections and 24 strains were measured in the bridge tests.

### 4.4 BCB3 Dead Load Analysis

Total stresses in the RRFC members are obviously the combination of live and dead load stresses acting on the bridge. Live load stresses were determined from measured live load strains obtained in the field tests of the bridge previously described in Section 4.3. Dead load stresses, however, must be calculated using structural analysis procedures.

For the dead load analysis, it was necessary to make several assumptions. First, the bridge was assumed to be simply supported at the abutments. Secondly, the dead loads were assumed to be uniform across the width of the bridge and evenly distributed longitudinally along the bridge length; hence, each RRFC supported a uniform dead load force equal to 1/3 of the total distributed dead load. It was also assumed that although there were numerous smaller, secondary longitudinal members in each RRFC (See Figure 3.2), the three main longitudinal members (one interior box girder and the two exterior girders) support the entire bridge dead load. As stated previously, the exterior girders at the longitudinal connection were “trimmed” to accommodate the connection details. Both the “trimmed” and uncut exterior members were significantly smaller than the interior box girders, and thus were capable of supporting only a very small percentage of the dead loads. Therefore, the dead load on each RRFC was distributed to the main longitudinal girders based on their inertias.

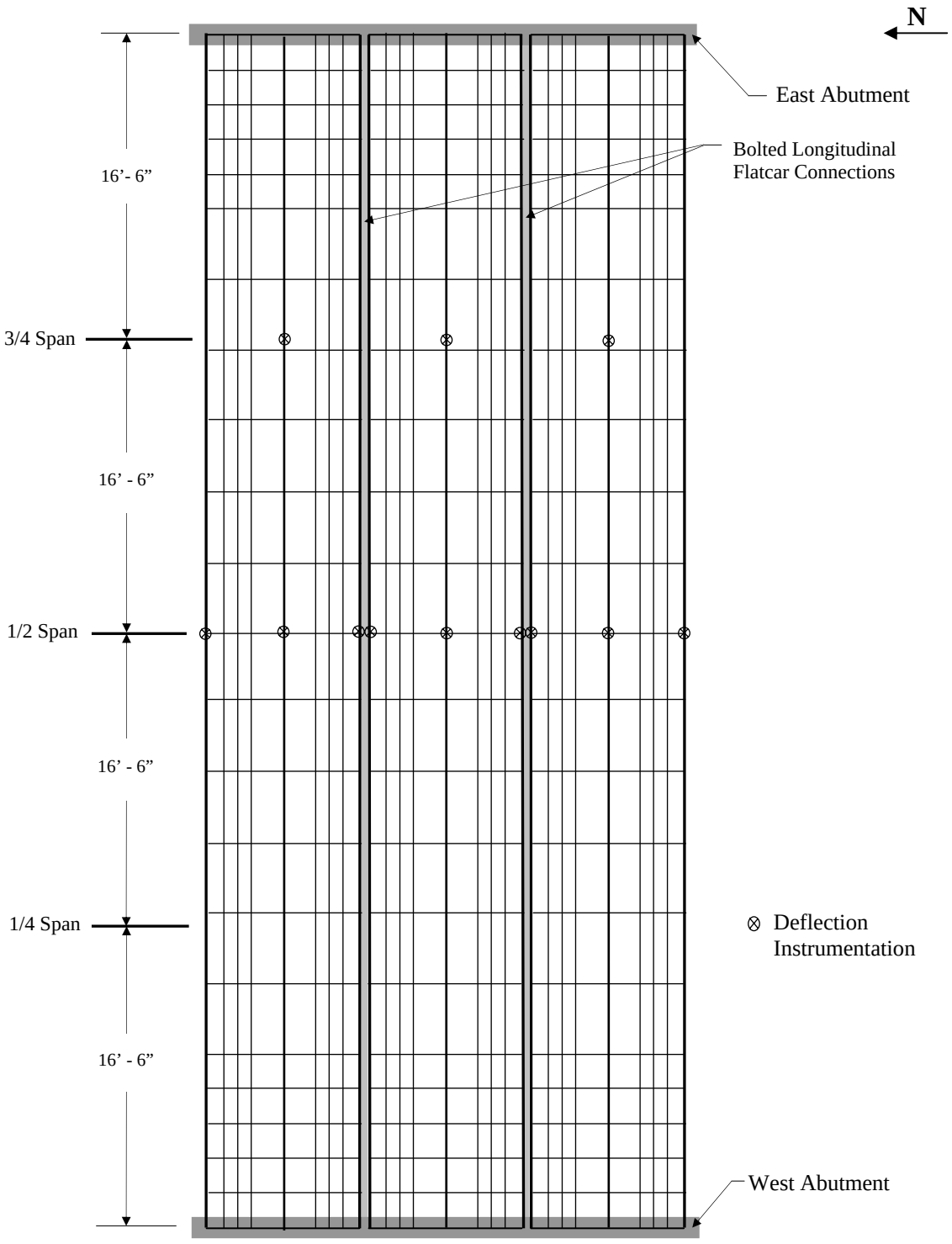


a. Deflection instrumentation

**Figure 4.12. Location of instrumentation used in BCB3 field test**

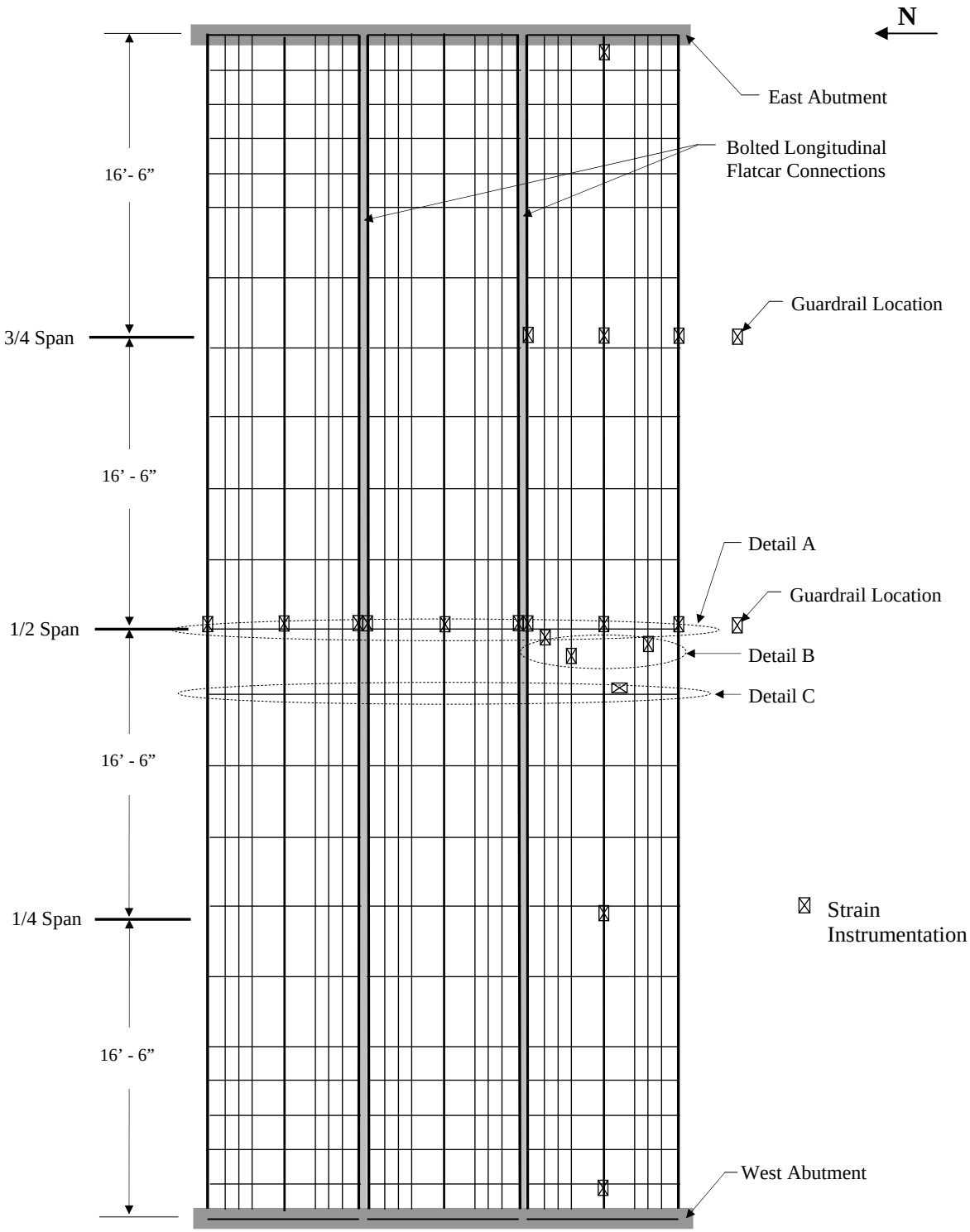


b. Strain Instrumentation

**Figure 4.12. Continued**

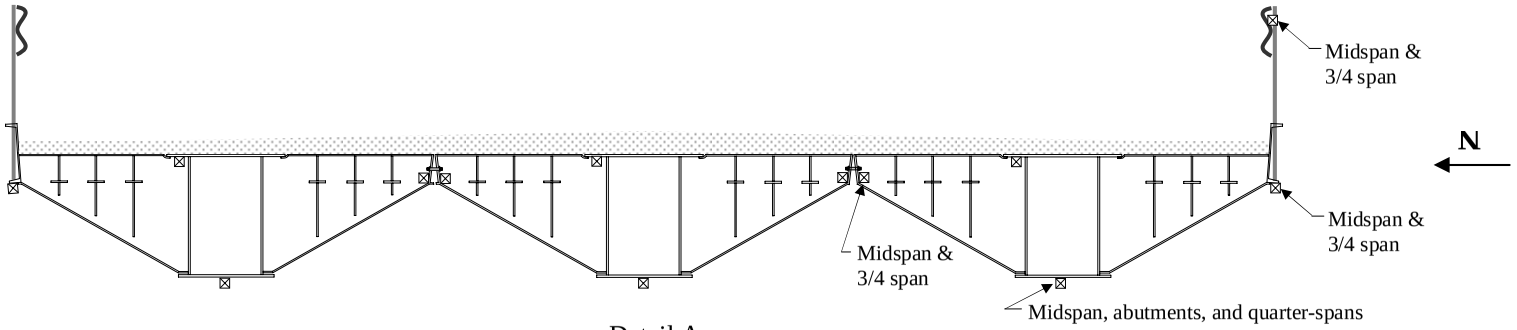


c. Detail A

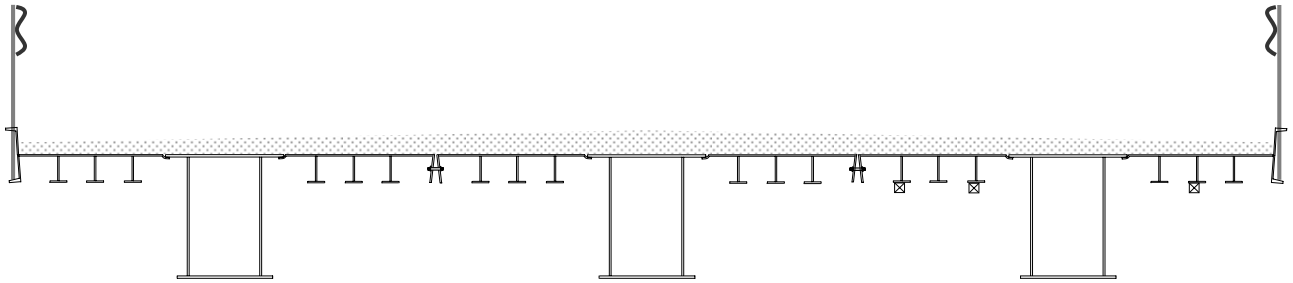

d. Detail B

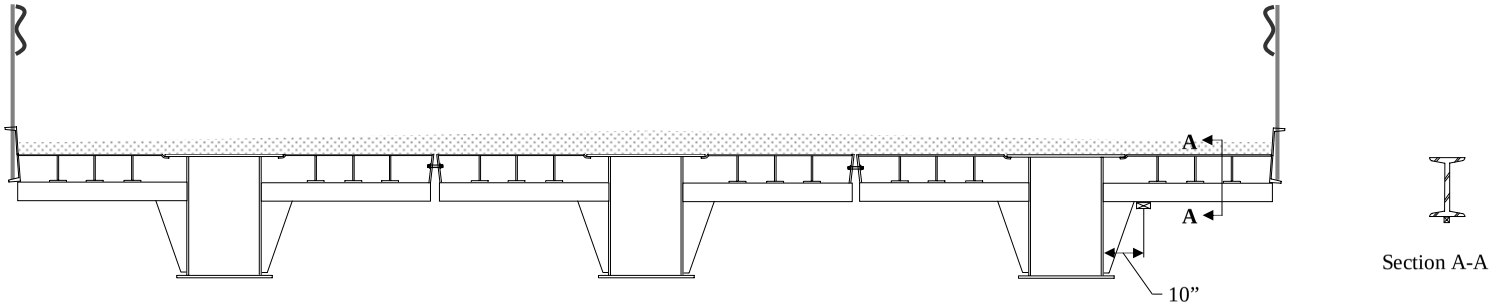


Note: Instrumentation illustrated at or near midspan unless otherwise indicated.

e. Detail C

Strain Transducer Orientation:

⊠ Longitudinal axis transverse to the bridge span.

⊠ Longitudinal axis parallel to the bridge span.

**Figure 4.12. Continued**

Dead loads considered were the weight of the RRFCs, the guardrail system, and the rock driving surface. According to weight tickets provided, the weight of each flatcar was 33,000 lbs. The weight per unit length of the guardrail system was estimated to be 100 lb/ft. The rock driving surface was approximately 5 in. thick and was estimated to have a unit weight of 130 lb/ft3.

Following the noted assumptions and procedures, analysis of the BCB3 due to the described dead loads resulted in midspan tensile stresses of +12.4 ksi in the bottom flange of the interior box girders, +1.9 ksi in the bottom flange of the "trimmed" exterior girders, and +5.15 ksi in the bottom flange of the uncut exterior girders.

## 4.5 BCB3 Field Testing Results

Deflection and strain data collected during the field testing were analyzed, and the RRFC bridge behavior was investigated. Maximum live load stresses determined from field testing data were combined with the calculated dead load stresses (presented in Section 4.4). The total stresses were then compared to the allowable stress limitations for the RRFC girders.

### *4.5.1 Static Testing*

The measured midspan deflections and strains in the exterior and interior members of the three RRFCs are presented in Figures 4.13 – 4.16. Dashed lines have been added to show trends between data points. The midspan location was selected for presentation since the structure is simply supported and deflections and strains are maximum near this location. As can be seen in these figures, maximum deflections and strains occur in the respective RRFC when the test truck is positioned on that flatcar, and the live load is distributed transversely across the bridge through the longitudinal bolted connection between the adjacent flatcars. The adequacy of the bolted connection in distributing live load distribution is illustrated in Figure 4.16.

During Lane 1 loading, the deflection and strain measurements appear symmetric to the two adjacent flatcars. However, when the truck is in Lane 2 the deflection of RRFC3 is significantly larger than that of RRFC1 when the truck is in Lane 3. Using the areas under the deflection cures, the moment distribution to an exterior RRFC when the truck was positioned on that side of the bridge was found to be 60%.

The maximum deflection (-0.88 in.) occurred in the south RRFC exterior girder when the test truck was located in Lane 2 (See Figure 4.16). The AASHTO LRFD Bridge Design Specifications [8] recommends a maximum deflection of 'span'/800 for legal truck loads. This limitation would be -0.99 in. for a clear span of 66 ft – 2 in.; hence, for this truck loading, the maximum measured deflection is below recommended values. If the measured deflection were increased in proportion of the test truck load to an HS-20 loading, the experimental deflection would be -1.31 in., which is significantly above AASHTO limits.

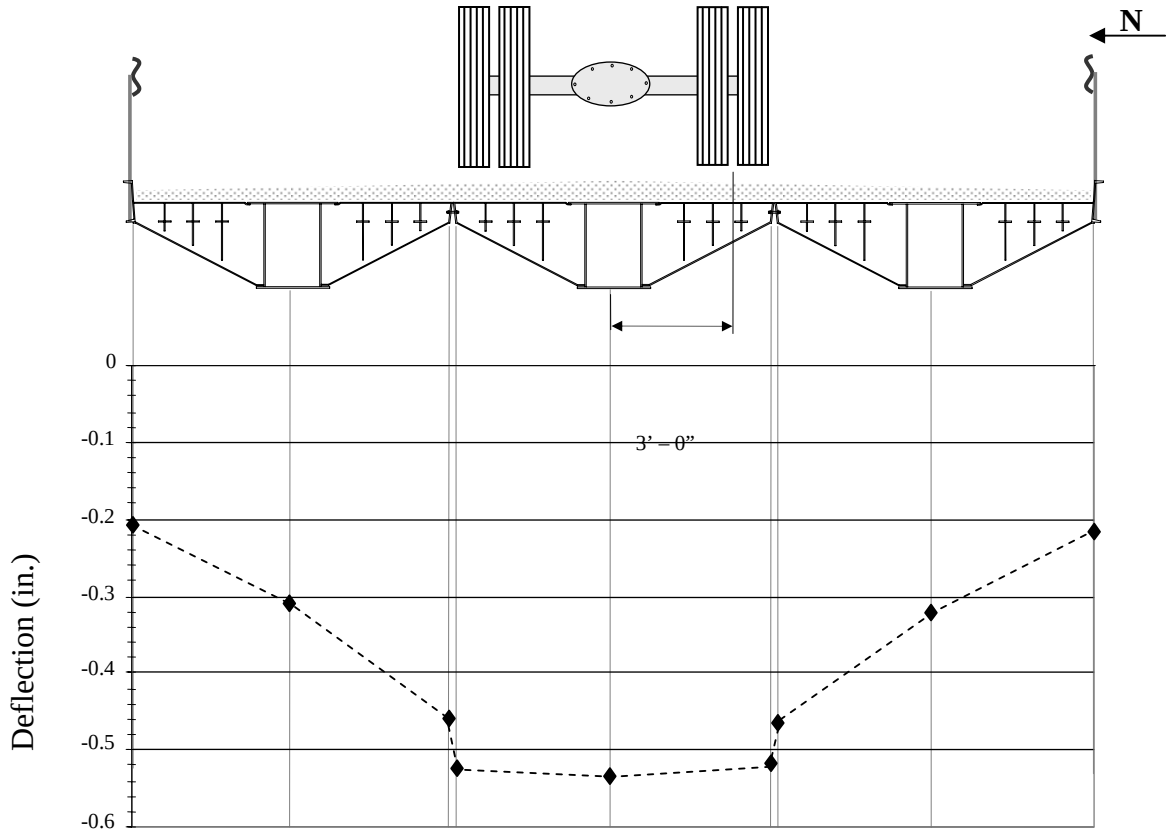


a. Deflections

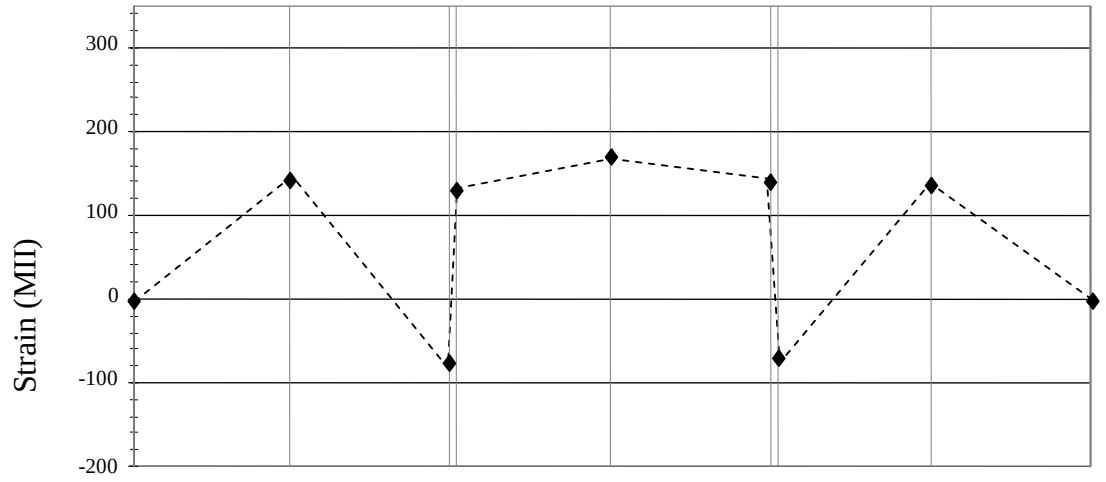


b. Member bottom flange strains

**Figure 4.13. BCB3 Lane 1 midspan deflections and strains**

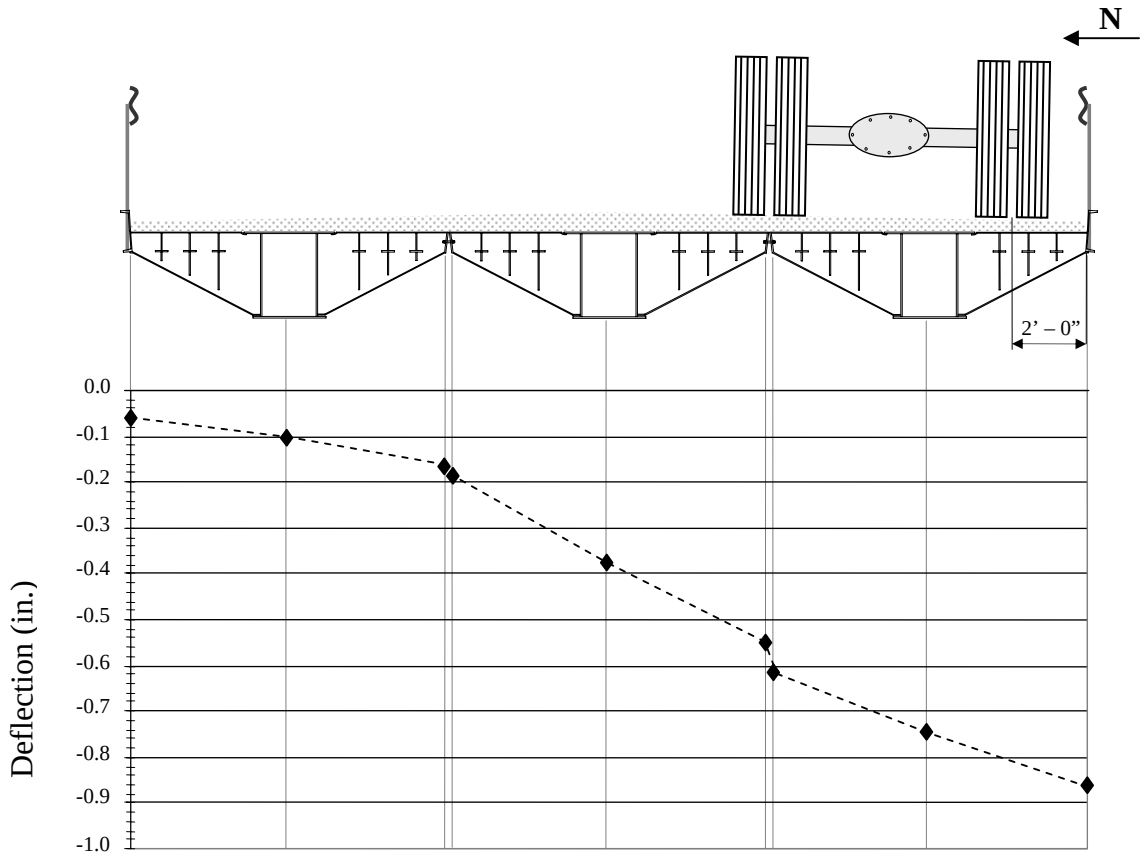


a. Deflections

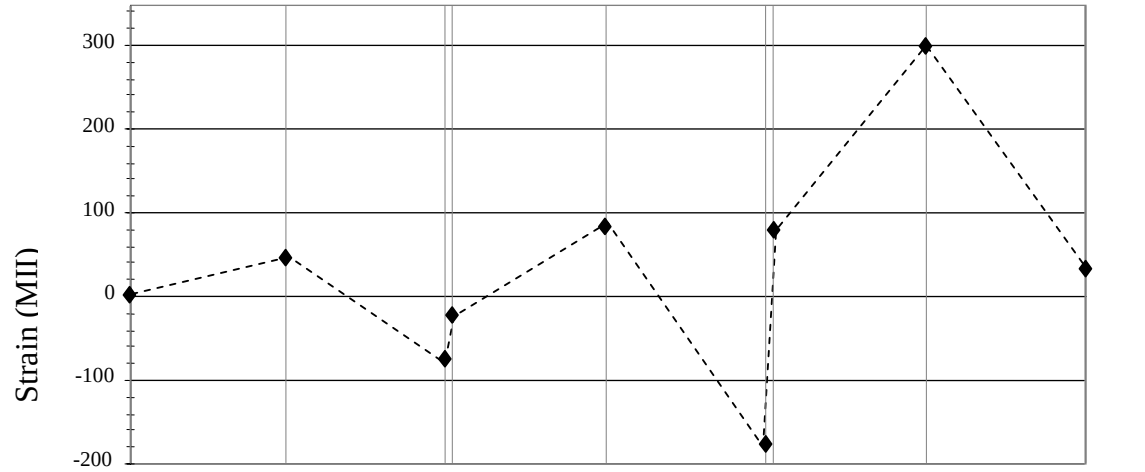


b. Member bottom flange strains

**Figure 4.14. BCB3 Lane 2 midspan deflections and strains**

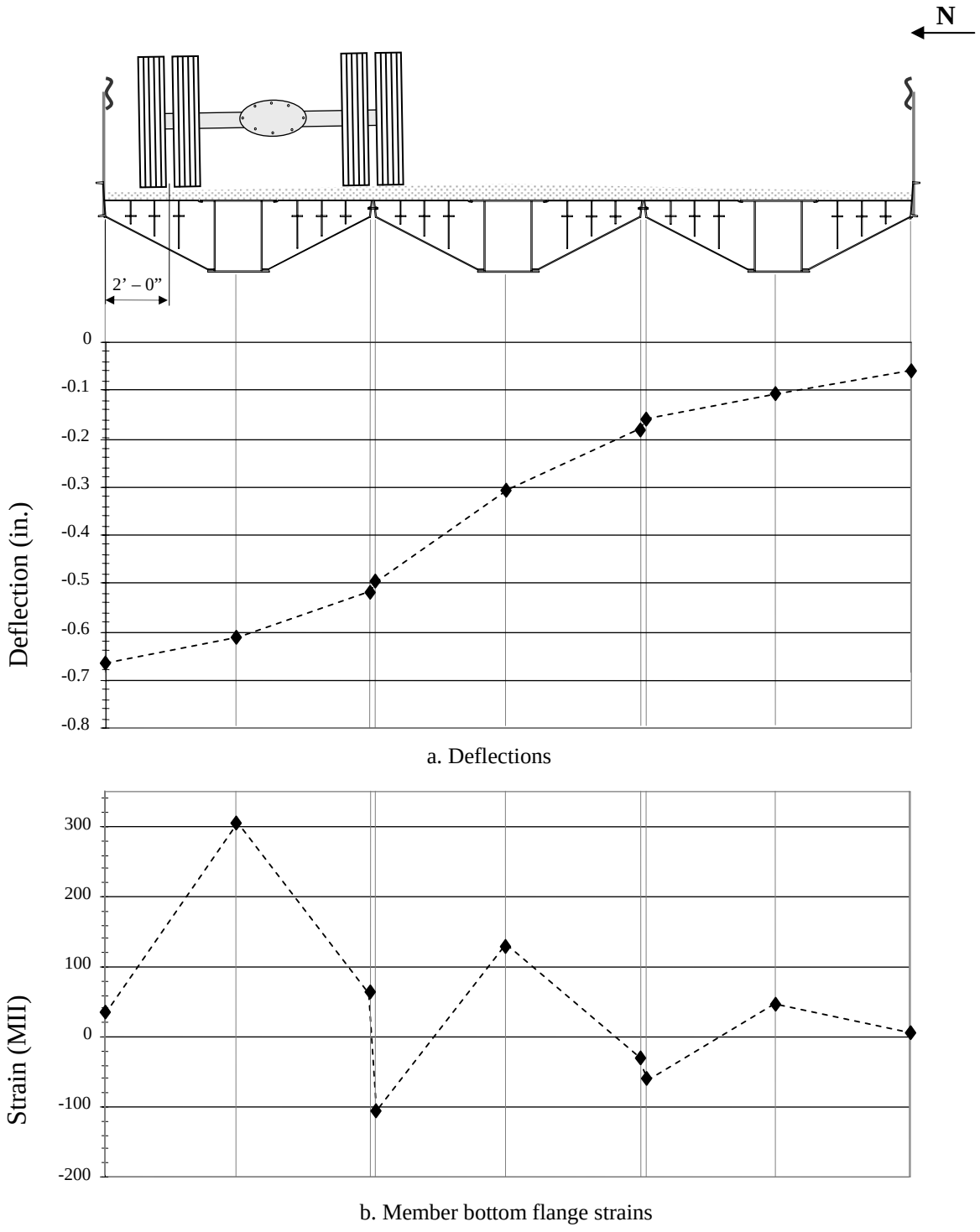


**Figure 4.15. BCB3 Lane 3 midspan deflections and strains**

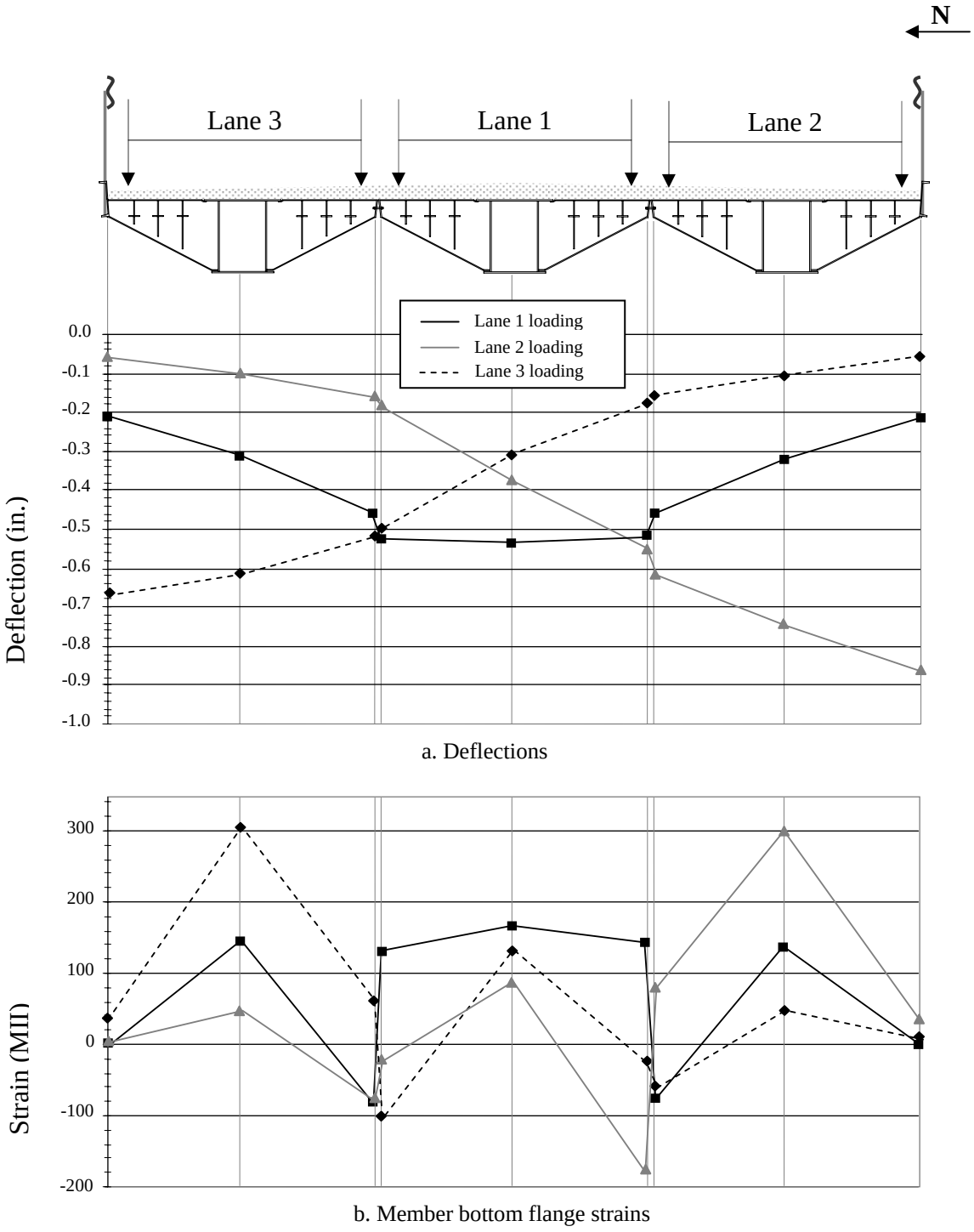


**Figure 4.16. BCB3 Lanes 1, 2 and 3 midspan deflections and strain**

Since the 89-ft RRFCs used for the BCB3 were similar to those used in previous projects [3,4], it was assumed that the material properties in these RRFCs were the same as those previously determined; the proportional limit and modulus of elasticity were assumed to be 40 ksi and 29,000 ksi, respectively. In the project, a conservative yield strength of the steel was assumed to be 36 ksi [4]. Through analysis of the field data, it was determined that the interior box girders experienced the largest strains (stresses) since they are larger than the exterior girders, the secondary longitudinal members, and the transverse members. The relative size of the RRFC structural members can be described by comparing their inertias as seen in Table 4.1. The maximum live load tensile strain (stress) for the bottom flanges of the interior box girders was +322 MII (+9.3 ksi), while the bottom flanges of the uncut exterior members on the outer south and north edges of the bridge experienced maximum tensile strains (stresses) of +38 MII (+1.1 ksi). The exterior girders at the longitudinal connection had maximum strains (stresses) in their bottom flanges varying from -193 MII (-5.6 ksi) to +148 MII (+4.3 ksi). Secondary longitudinal members and the transverse member experienced maximum live load strains (stresses) in their bottom flanges of +161 MII (+4.7 ksi) and +86 MII (+2.5 ksi), respectively.

**Table 4.1. Inertias of various RRFC members**

| RRFC Structural Member | Inertia ($in^4$) |
|---|---|
| Interior Box Girder | 8999.2 |
| Exterior Uncut Girder | 345.1 |
| Exterior "Trimmed" Girder | 12.0 |
| T-Shape Secondary Member | 20.7 |
| S-Shape Transverse Member | 14.7 |

The total stresses for the girders were computed by combining the theoretical dead load stresses with the live load stresses calculated from the measured live load strains. The interior box girder had a maximum total stress in the bottom flange of +21.7 ksi, while a maximum total stress of +6.3 ksi was determined for the bottom flange of the exterior girder on the outer edge of the bridge.

Theoretical analysis with an HS-20 design truck loading (not including impact) was performed to determine maximum stresses. The theoretical live load stresses were calculated from design truck loading for the bottom flanges of the interior girders (+12.8 ksi), exterior (uncut) girder bottom flanges (+5.3 ksi), and bottom flanges of the exterior (cut) girders (+2.5 ksi). Combining these values with the theoretical dead load stresses in the girders of an exterior RRFC, the maximum total stress due to an HS-20 design truck loading would be +25.2 ksi for the interior girder bottom flanges, +10.5 ksi for the uncut exterior girder bottom flanges, and +4.4 ksi for the trimmed exterior girder bottom flanges. If the allowable stress is calculated at 55% of the proportional limit (40 ksi), the maximum total stress in the interior girder bottom flanges (+25.2 ksi) is larger than the allowable limit of 22 ksi but the stresses in the exterior girder bottom flanges are below the allowable stress.

*4.5.2 BCB3 Longitudinal Connection Behavior*

As stated previously, the longitudinal connection between adjacent RRFCs is created by joining adjacent exterior girders with 1 1/4- in. diameter bolts spaced on approximately 36-in. centers. A cross-section of the BCB3 at midspan is illustrated in Figure 4.17. The RRFCs are referenced as follows: FC1 is the north RRFC, FC2 is the middle RRFC, and FC3 is the south RRFC. Joints A and B, near midspan of the bridge, are the north and south bolted connections between FC1 and FC2 and FC2 and FC3, respectively. The exterior girder of FC1 at Joint A is Girder 3; the exterior girders of FC2 are Girders 4 and 6 at Joints A

and B, respectively; the FC3 exterior girder at Joint B is Girder 7. Strain transducers (located 6 in. below the bridge deck) were placed near the midspan on the connected exterior girders of both longitudinal joints (Joints A and B in Figure 4.17). The theoretical neutral axis of the BCB3 was determined to be 10.37 in. below the deck. Since the exterior girders, and consequently also the strain transducers, are above this neutral axis, compressive strains should be measured when the girders are subjected to bending about the horizontal axis (See Figure 4.18). However, this is not always the case as shown in Figures 4.13b – 4.16b where some of the exterior girders experience tension when the truck is positioned at certain transverse locations on the bridge. A review of these three figures reveals that the tensile strains always occur in the exterior member of a longitudinal joint when the test vehicle is positioned on that RRFC. For example, in Figure 4.13b when the test vehicle is on FC2, tensile strains are recorded in Girders 4 (+131 MII) and 6 (+143 MII). In Figure 4.16b, when the test vehicle is on FC1, a strain of +61 MII is measured in Girder 3.

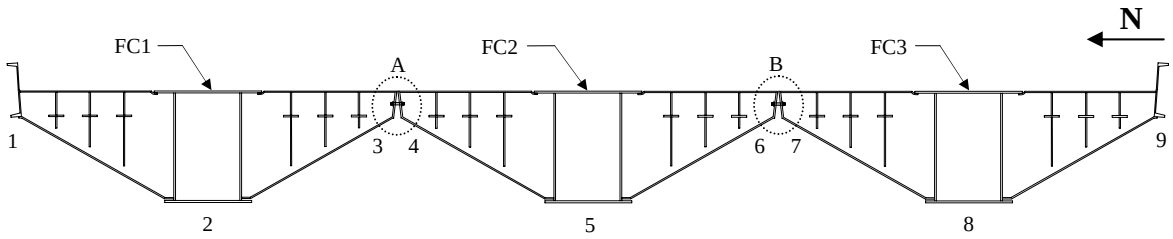


**Figure 4.17. Midspan cross-section of BCB3**

The strain transducers at these exterior girder locations are measuring the combination of the bending about the bridge's neutral axis (i.e. thehorizontal axis) and bending about the vertical axis (See Figure 4.18). In the cases previously discussed, tensile strains due to bending about the vertical axis were larger than the compressive strains resulting from bending about the bridge's neutral axis; the net effect (i.e. tensile strains) at these locations were thus measured by the strain transducers.

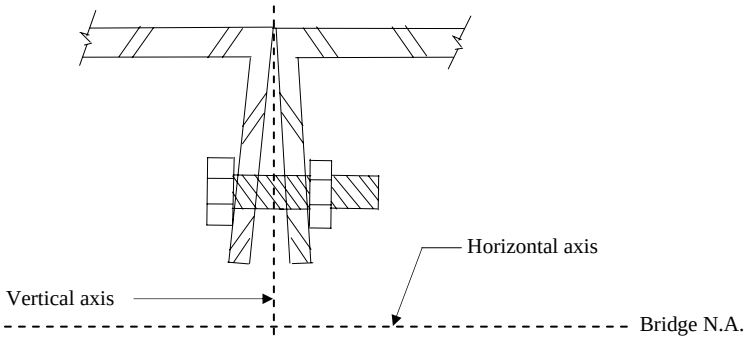


**Figure 4.18. Horizontal and vertical axes of bending**

The bending of the exterior girders about the vertical axis is influenced by three factors: differential displacements between adjacent RRFCs at a longitudinal joint, differences in rotations of the girders at

the longitudinal joint, and the presence of transverse stiffeners. Differential displacement and rotation at the joint are illustrated in Figure 4.19 where the differential rotation is defined as the algebraic sum of the change in rotation of the two RRFCs. The effect of the transverse stiffeners is illustrated in Figure 4.20; the strain transducer on the loaded RRFC has a net tensile strain while the unloaded RRFC has a net compressive strain since the loaded RRFC experiences larger bending about the vertical axis. As can be seen, the fact that the strain transducers were in close proximity to the transverse stiffeners obviously also influenced the measured strains.

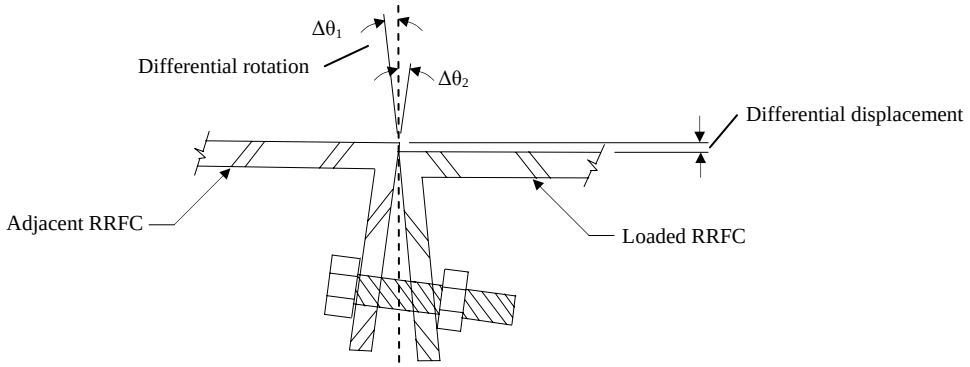


**Figure 4.19. End view of the longitudinal connection joint during loading**

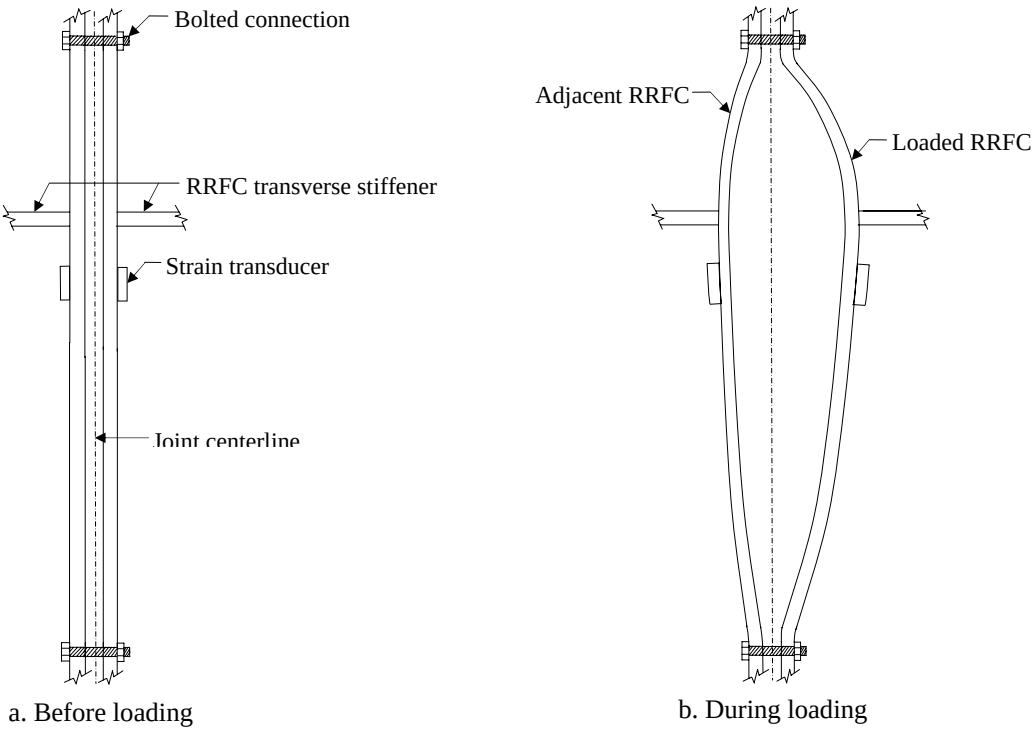


**Figure 4.20. Plan view of the longitudinal connection joint**

*4.5.3 Time History Analysis*

As stated previously in Section 4.3, strain transducers were installed at 5 locations on the bottom flange of the south RRFC interior girder. These locations shown in Figure 4.21 were 12 in. from the west abutment, at the 1/4 span, 1/2 span, 3/4 span, and 12 in. from the east abutment.

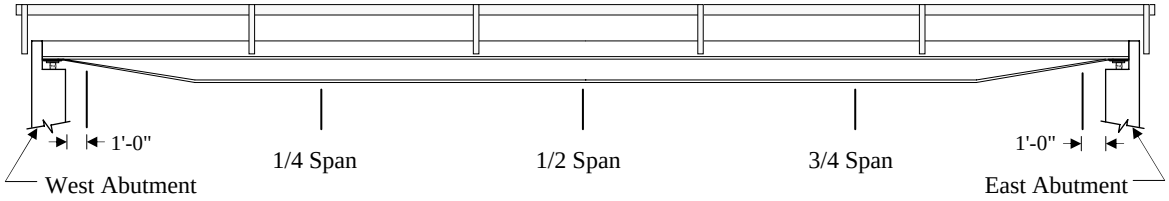


**Figure 4.21. Strain instrumentation locations for BCB3 time history analysis**

Time history plots of the strains from the south RRFC's interior girder are shown in Figure 4.22. The maximum strains were measured at the midspan location which was expected since the maximum moment for a simply supported structure occurs near midspan. Strains measured at the abutment locations should be essentially zero in an idealized situation. However, the strain instrumentation was placed 1ft – 0 in. from the abutment face due to inaccessibility, so strains were measured at these locations.

Maximum strains of +69 MII were measured at both abutments when the truck was in Lane 2. The largest strains measured at the quarter points also occurred during Lane 2 loading: +224 MII at the 1/4 span and +220 MII at the 3/4 span location. The maximum strain when the truck is on the south RRFC is +306 MII, and when the truck is in Lanes 1 and 3, these maximum strains are +145 MII and +53 MII respectively.

*4.5.4 Dynamic Testing*

Dynamic testing of the BCB3 was also performed during the field testing; this enabled the structural dynamic properties of the bridge to be determined along with the dynamic amplification of deflections and strains in the girders. The free vibration of the interior girders can be seen from the oscillating strains when the tandem truck has exited the bridge. Based on this free vibrational response, the period, frequency, and damping of the interior girders were determined. The period was found to be 1.3 seconds, resulting in a member frequency of 0.77 Hz, and the damping of the interior girders was approximately 4%.

Of the five dynamic test runs that were performed, it was found that the maximum dynamic amplification occurred at a truck speed of 25 mph. A plot of the time history comparison of the deflections and strains during the static and dynamic field testing are presented in Figures 4.23 and 4.24, respectively. These graphs illustrate the dynamic amplification that occurred in the interior box girders of the north, middle, and south RRFCs.

The largest amplification of both deflection (17%) and strain (17%) was experienced in the south RRFC. This likely occurred due to the tandem truck not positioned precisely in Lane 1 (centered on the roadway). Assuming the truck is positioned slightly south of the centerline during the dynamic testing, this

misalignment would have placed more load on the south RRFC and thus increasing both the strains and deflections measured in the south interior girder.

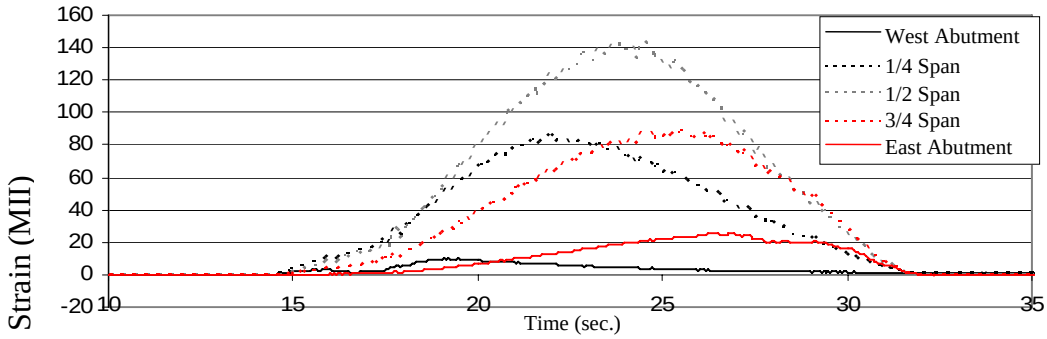


a. Truck in Lane 1

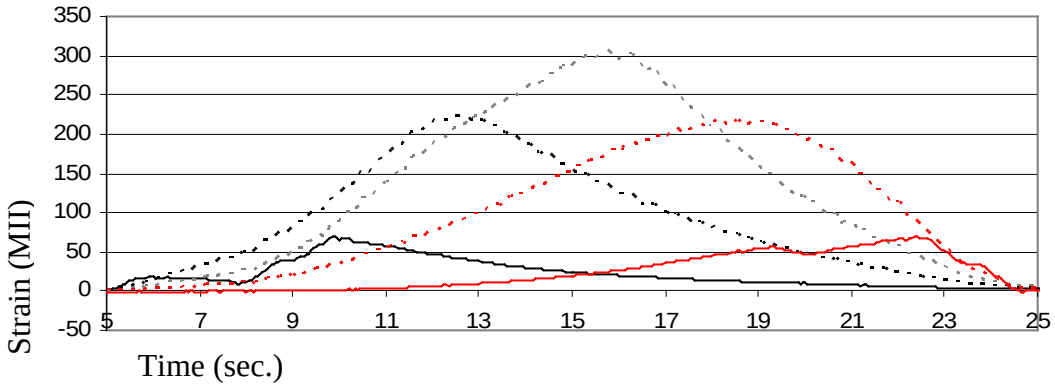


b. Truck in Lane 2

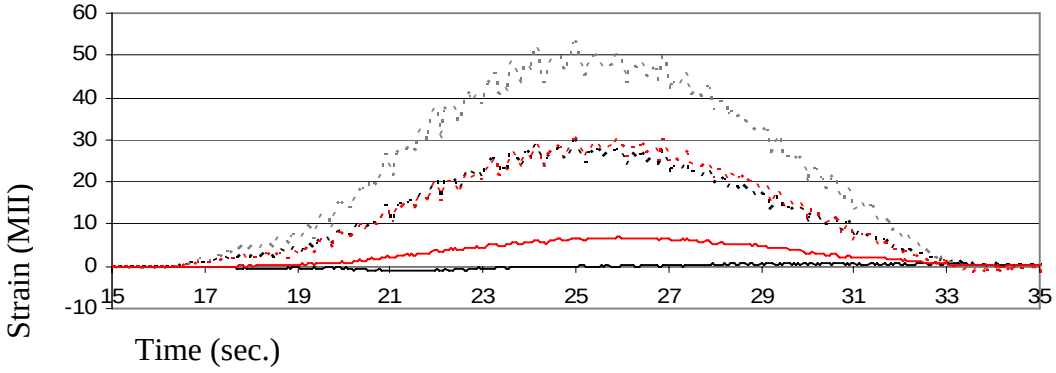


c. Truck in Lane 3

**Figure 4.22. Time history of bottom flange strains in the south RRFC interior girder**

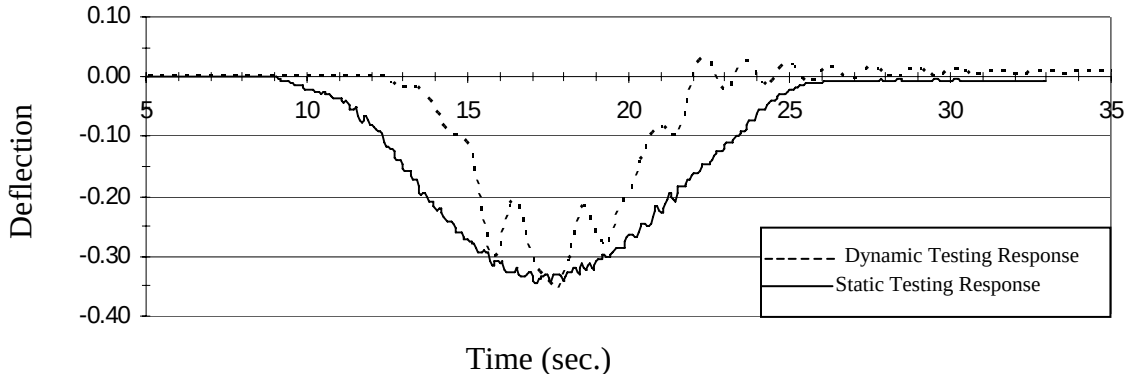


a. North RRFC interior girder

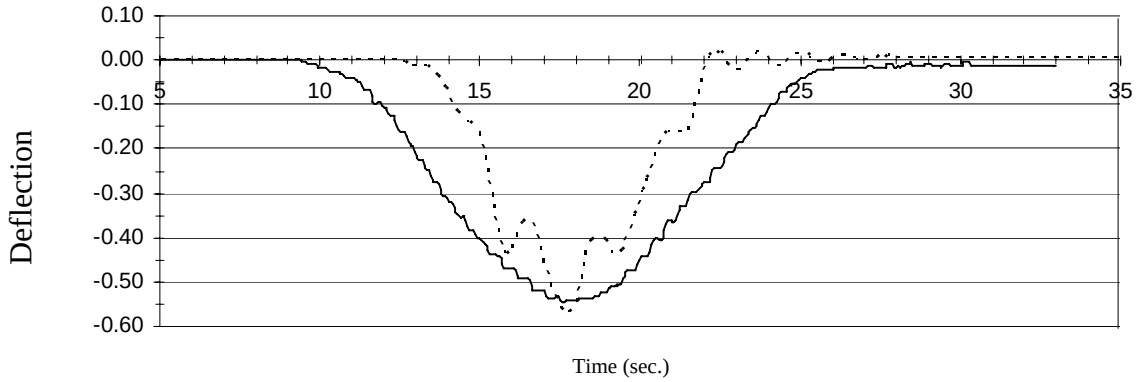


b. Middle RRFC interior girder

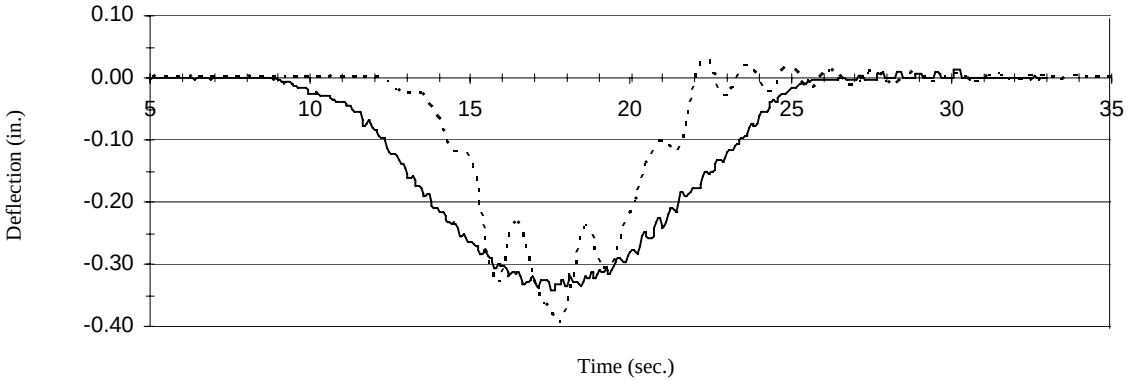


c. South RRFC interior girder

**Figure 4.23. Comparison of the measured interior girder deflections of the north, middle, and south RRFCs from static and dynamic field tests (Lane 1 loading)**

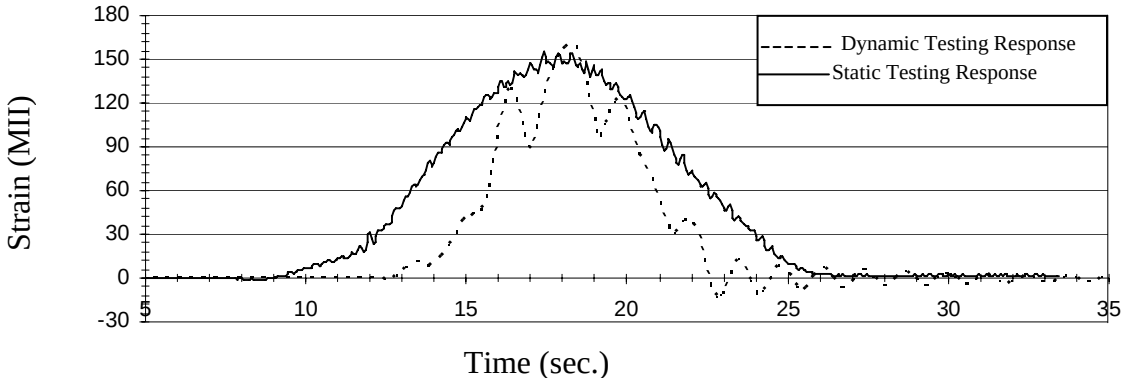


a. North RRFC interior girder

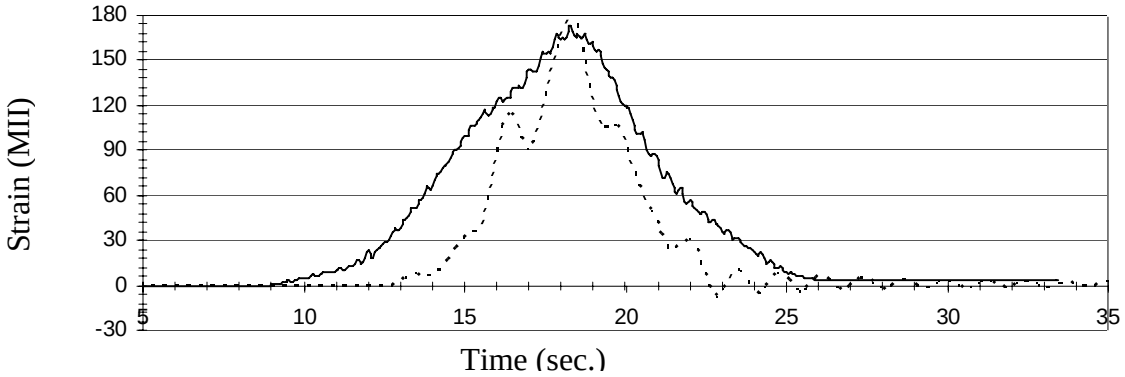


b. Middle RRFC interior girder

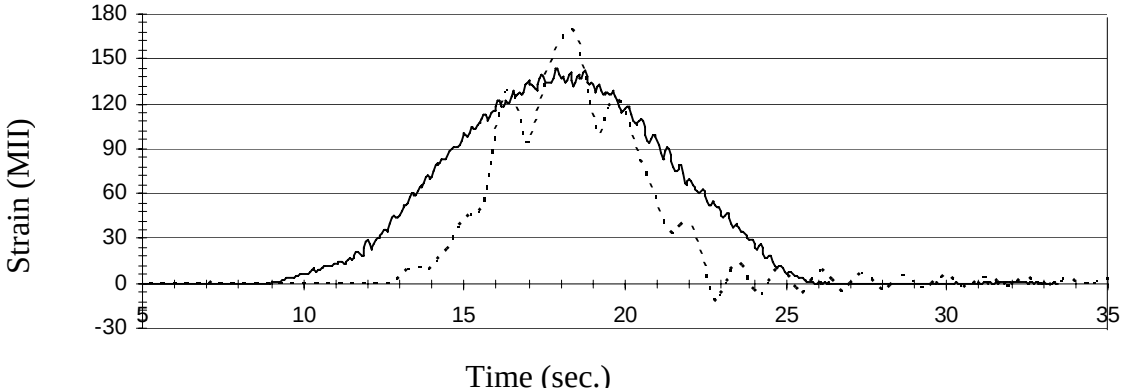


c. South RRFC interior girder

**Figure 4.24. Comparison of the measured interior girder bottom flange strains of the north, middle, and south RRFCs from static and dynamic field tests (Lane 1 loading)**

## 5.0 WINNEBAGO COUNTY BRIDGE 2 ON 460TH ST

### 5.1 Introduction

In the summer of 2005, a RRFC bridge was constructed in Winnebago County, Iowa. This is the second RRFC bridge in Winnebago County tested by ISU and will be referred to as Winnebago County Bridge 2 (WCB2). Maps showing the location of the WCB2 are presented in Figure 5.1; the bridge is located approximately 5.5 miles west and 1 mile north of Lake Mills, Iowa, on 460th St.


a. Lake Mills, Iowa

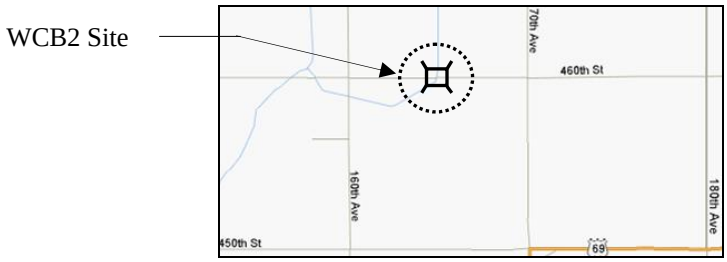


b. Detail A

**Figure 5.1. Location of the Winnebago County RRFC Bridge 2 [11]**

The previous three-span timber bridge (FWHA No. 344890) at the WBC2 site (See Figure 5.2) had a total length of 62 ft from center to center of the abutments and a central span length of 23 ft. The timber substructure consisted of 6 timber piles at each abutment and pier, and 12x12 creosoted timbers were used for the abutment caps. The stringers were 6x16 creosoted timber and the deck was constructed with 3x12 creosoted timber planks.

**Figure 5.2. Original three-span, timber bridge at the WBC2 site**

## 5.2 Design and Construction

The WCB2 shown in Figure 5.3 was constructed using the superstructure from three RRFCs that were positioned side-by-side and connected with a reinforced concrete beams. The span length is 66 ft – 4 in. from center to center of abutments with 2 ft – 1 3/4-in. overhangs at each end; the bridge width is 27 ft (26 ft – 5-in. driving surface). End abutments consist of 6 steel HP12x53 piles and HP12x53 steel caps (See Figure 5.3d) with sheetpile backwalls at the end of the overhangs for soil retainment. The 70 ft – 7 1/2-in. lengths of RRFCs, cut from 89-ft RRFCs, used in the WCB2 were the same as those for the BCB2 as described in Chapter 3 (Figure 3.2).

a. Photograph of the WCB2

**Figure 5.3. Winnebago County RRFC Bridge 2**

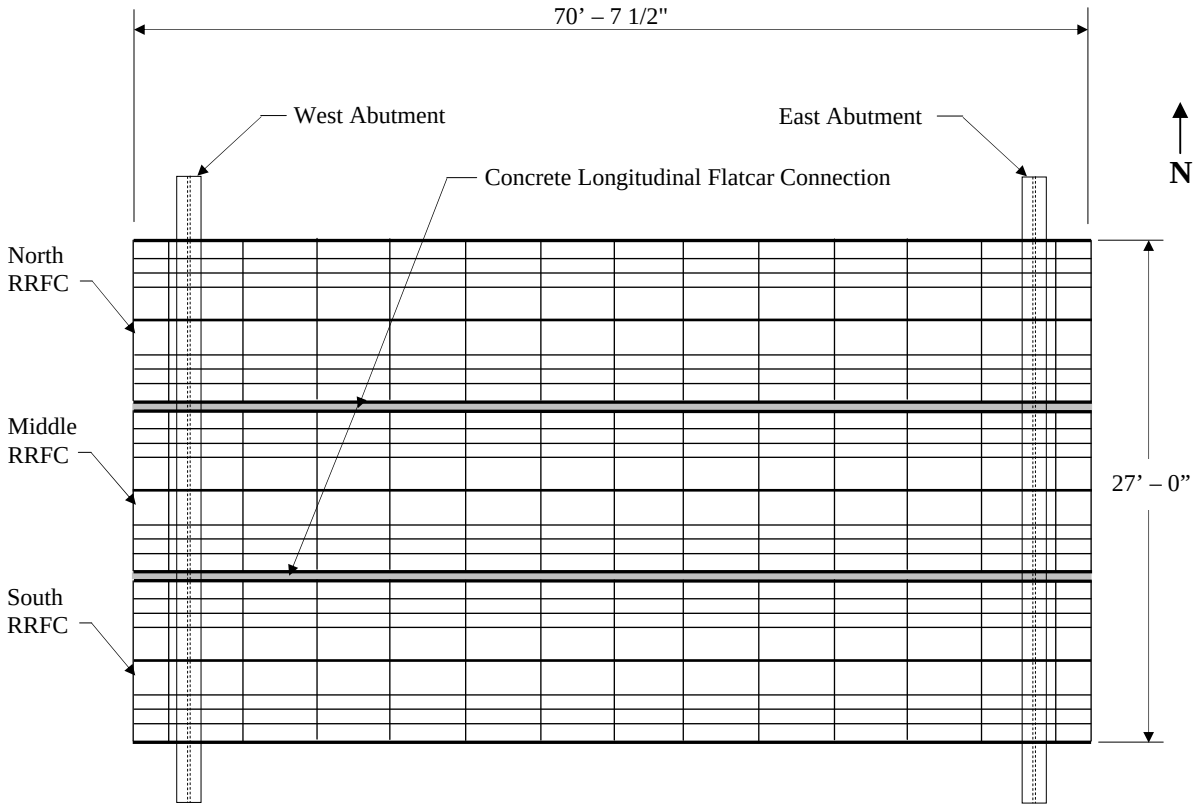


b. Plan View

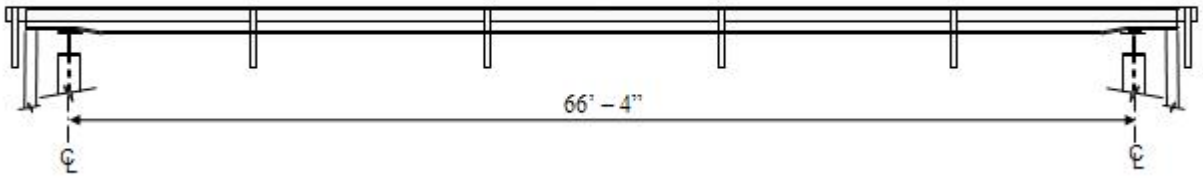


c. Side View

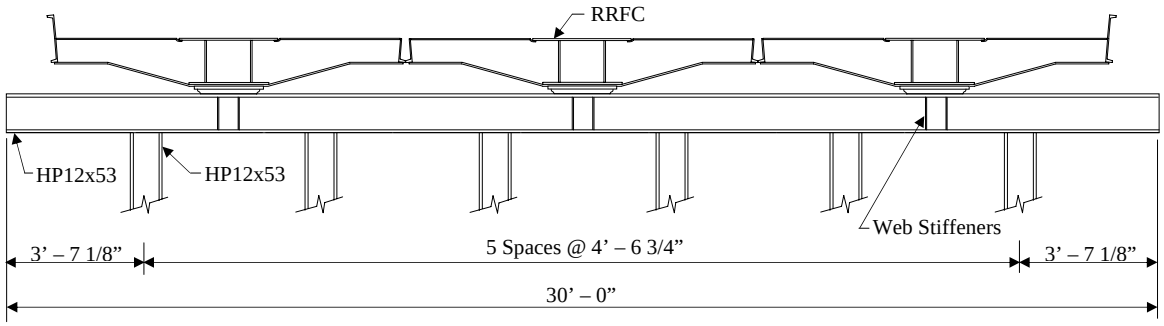


d. Abutment cross-section

**Figure 5.3. Continued**

The driving surface was constructed using timber planks with gravel. The north half of the bridge had 3x12 timber plans butted against one another while the south side had 4x12 tongue-and-groove timber planks. The depth of the gravel driving surface varied randomly across the bridge from a minimum of 1 1/4 in. to a maximum of 5 1/2 in.

Exterior girders of adjacent flatcars were joined using 3/4 in. diameter threaded rods located 2 1/2 in. below the deck on approximately two foot centers. Details of the reinforced concrete beam connection between adjacent RRFCs are presented in Figure 5.4. The void between the adjacent exterior girders was framed with 24-in. steel plates and filled with reinforced concrete and a #5 reinforcement bar to complete the connection between the flatcars. The bottom plates begin at the end of the RRFCs and are spaced on 24-in. centers. The top plates are also on 24-in. centers and are staggered from the bottom plates. This connection is similar to that of the WCB1 with the exception of the location of the reinforcement bar and the plate details [4].

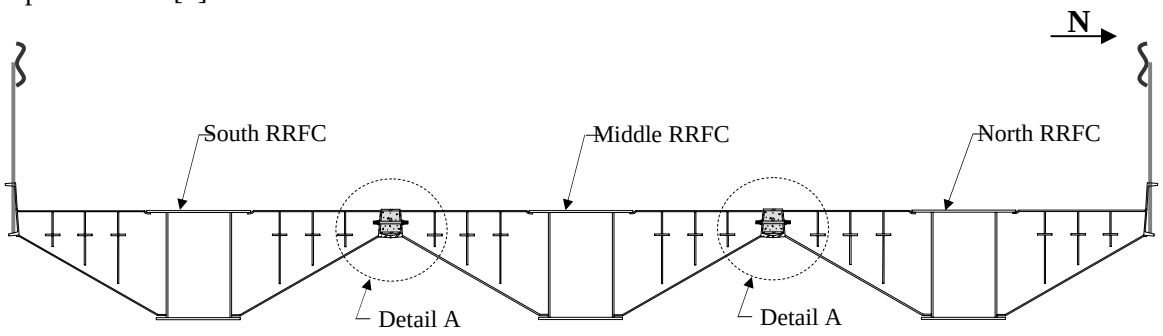


a. Cross-section

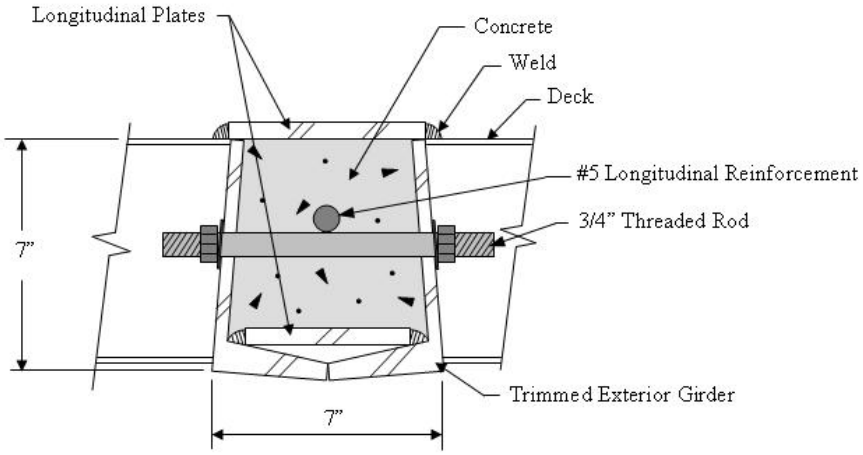


b. Detail A

**Figure 5.4. Longitudinal concrete beam connection used in the WCB2**

Supports for the exterior girders were necessary at the abutments because the elevation of the bottom of these girders was higher than rest of the RRFC. Recycled HP12x53 sections from the abutments and piles, which are shown in Figure 5.5, were used to create the needed supports. The supports at the east abutment were welded to the steel cap beam. At the west abutment, a roller condition was created to allow for expansion and contraction of the bridge. Recycled flanges from the trimmed portions of the exterior girders were welded on to either side of the west support. A "box" fabricated out of 3/8-in plates allows the recycled RRFC flange on either side of the support to move horizontally (parallel to the bridge length) and restricts movement vertically and horizontally (perpendicular to the bridge length).

### 5.3 WCB2 Field Testing

On July 6, 2005, a week after completion of the bridge construction, a field test of the WCB2 was conducted by loading the bridge with a tandem truck. Truck dimensions and axle weights are presented in Figure 5.6. The front tires on the test truck were 12 in. wide while each set of tandem tires was 22 in. wide. Spacing between the centers of the front tires was 7 ft – 3 in. and the spacing between centers of the tandem tire pairs was 6 ft – 0 in. The gross weight of the truck was 52,020 lbs, with 17,100 lbs distributed to the front axle. It was noted during testing that the gravel was not uniformly distributed in the truck's box. A larger portion of the gravel was positioned on the south side of the truck, thus increasing the weight of the truck on its south side and consequently increasing loading applied to the bridge on that side of the truck. Therefore, in all load tests, a larger portion of the truck's load was on the south side of the truck.

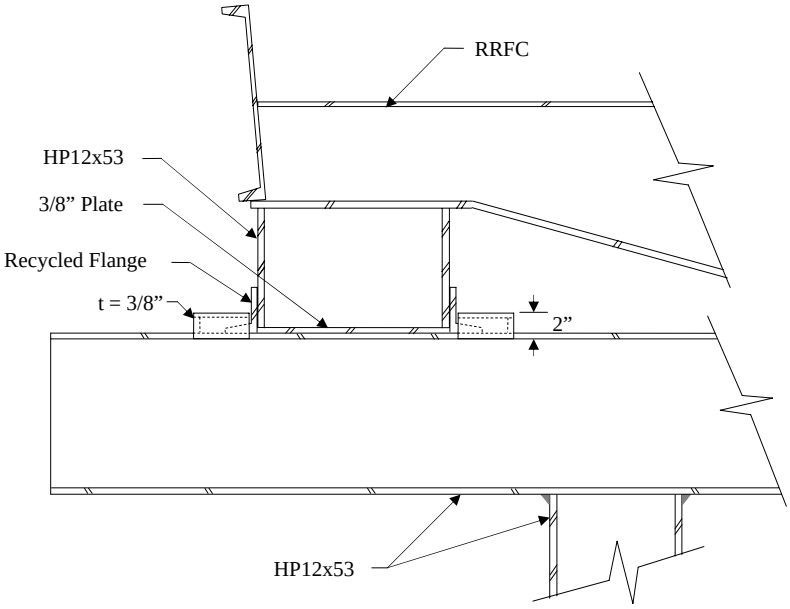


a. Exterior girder support at the west abutment

**Figure 5.5. Exterior girder supports for the WCB2**

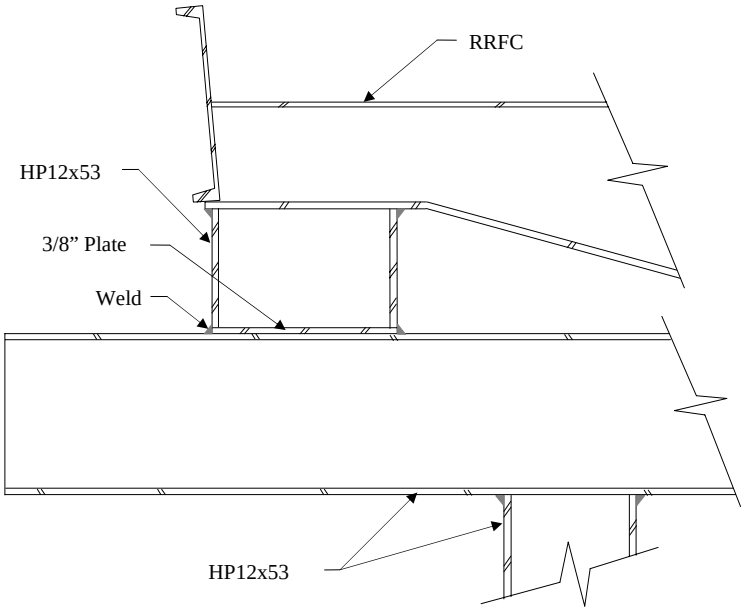


b. Exterior girder support at the east abutment

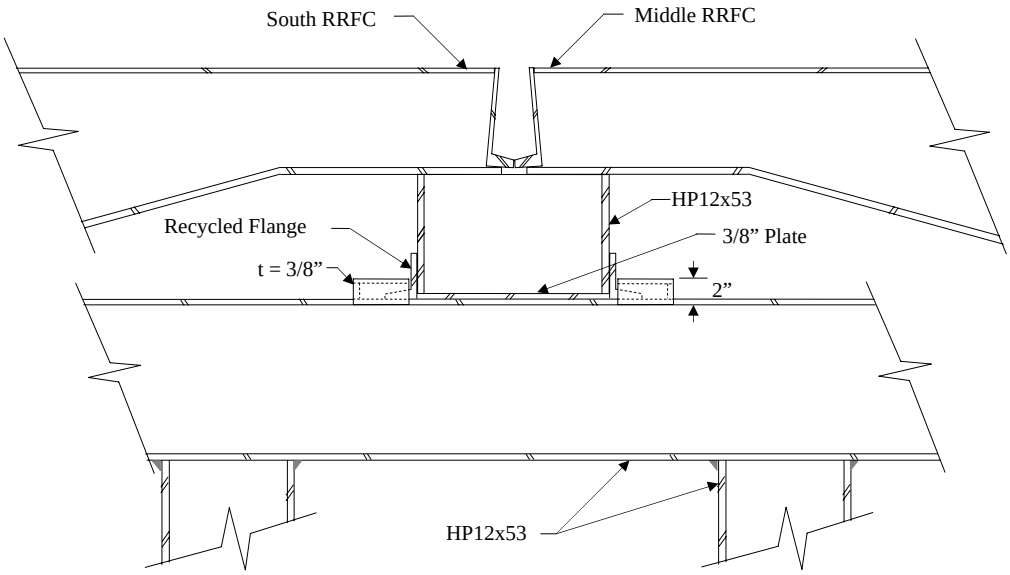


c. Connection support at the west abutment

**Figure 5.5. Continued**

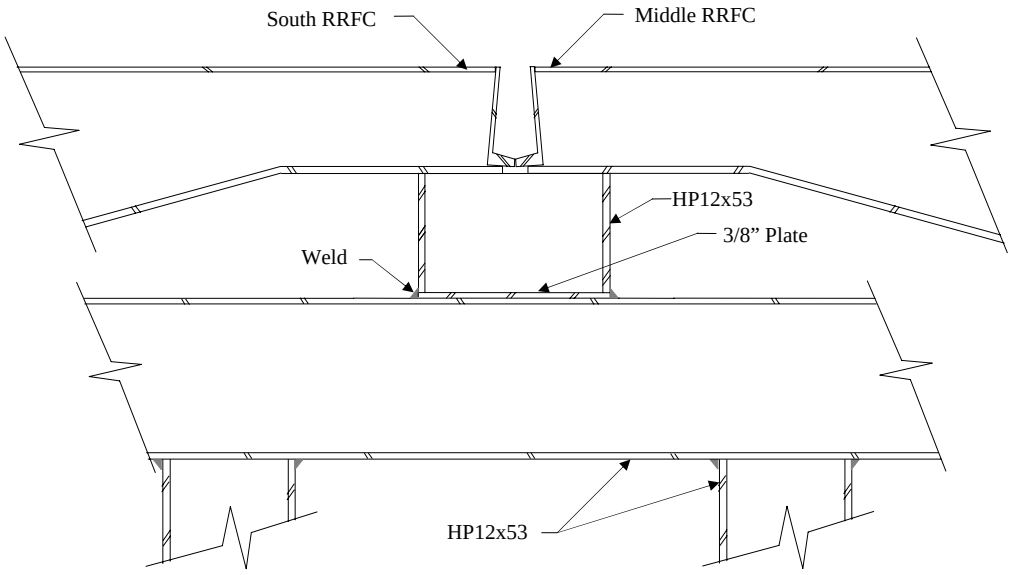


d. Connection support at the east abutment

e. East abutment edge support

f. West abutment connection support

**Figure 5.5. Continued**

Instrumentation for the WCB2 field test involved both strain and deflection transducers placed on the RRFC girders. Strains and deflections were measured at 20 and 9 locations on the bridge, respectively. Specific locations of the deflection and instrumentation on the respective girders, along with photographs of some of the instrumentation are presented in Figures 5.7 and 5.8, respectively. Deflection transducers were placed along the midspan cross-section at all the interior and exterior girders of the three flatcars. Strain data were collected on the interior girder of the south RRFC near the abutments and at the 1/4, 1/2, and 3/4 spans. At the 3/4 span location, strain instrumentation was also placed on the exterior girders of the south RRFC.

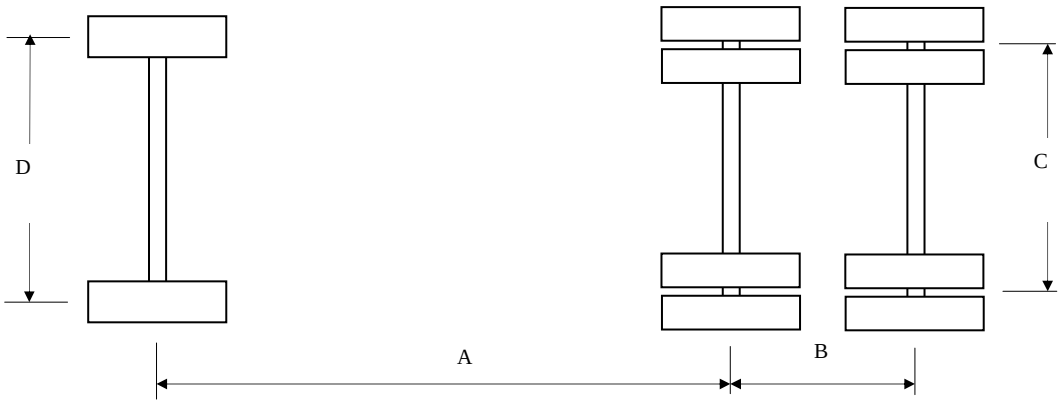


a. Top view

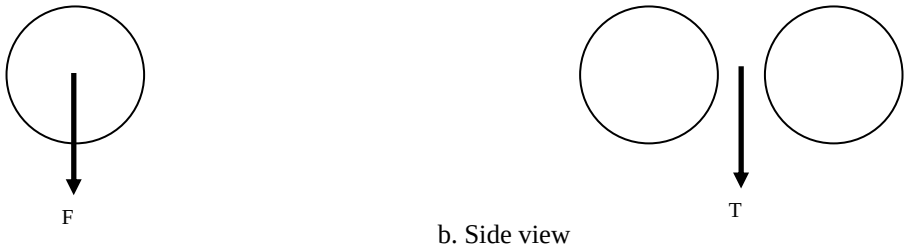


b. Side view

| Dimensions | | | | Load (lbs) | | |
|---|---|---|---|---|---|---|
| **A** | **B** | **C** | **D** | **F** | **T** | **Gross** |
| 14' - 1" | 4' - 7" | 6' - 0" | 7' - 3" | 17,100 | 34,920 | 52,020 |

**Figure 5.6. Dimensions and weights of truck used in WCB2 field test**

Strain transducers at midspan were placed on all the interior and exterior members of the three RRFCs and near the top of the south guardrail. Also, strain transducers were placed on two secondary longitudinal members located 12 in. east of midspan and on a transverse member located approximately 4 ft west of the midspan. Data (deflections and strains) were collected across the width of the bridge at the midspan so that the load distribution among the flatcars could be determined.

Continuous data were measured and recorded as the tandem truck traveled across the bridge during each test run. Data were recorded as the truck's tandem crossed each abutment and at 1/4, 1/2, and 3/4 span locations. To determine the bridge's behavior at different transverse loading locations, four transverse truck positions across the width of the bridge were used as illustrated in Figures 5.9 and 5.10.

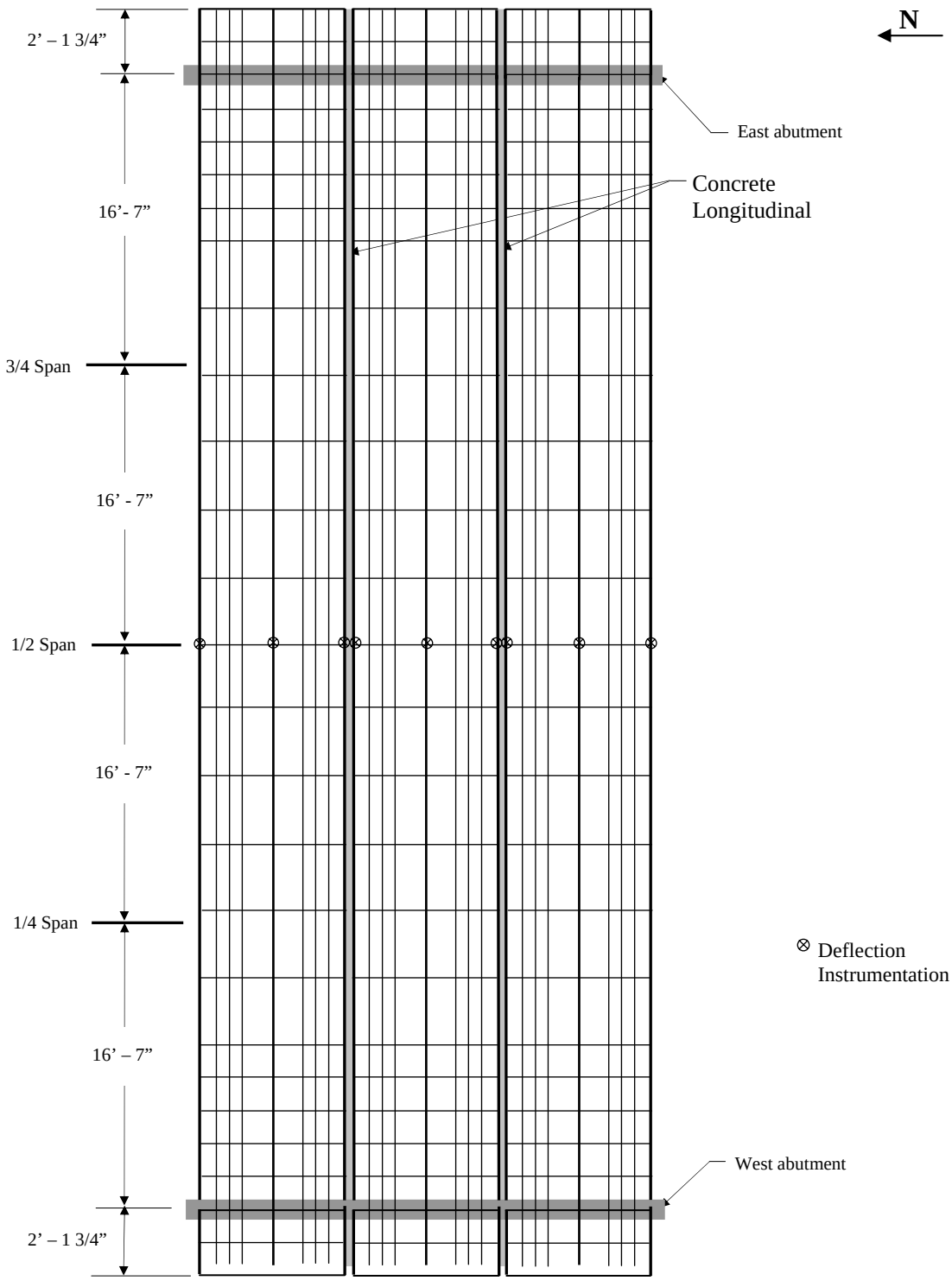


a. Deflection Instrumentation

**Figure 5.7. Location of instrumentation used on the WCB2**

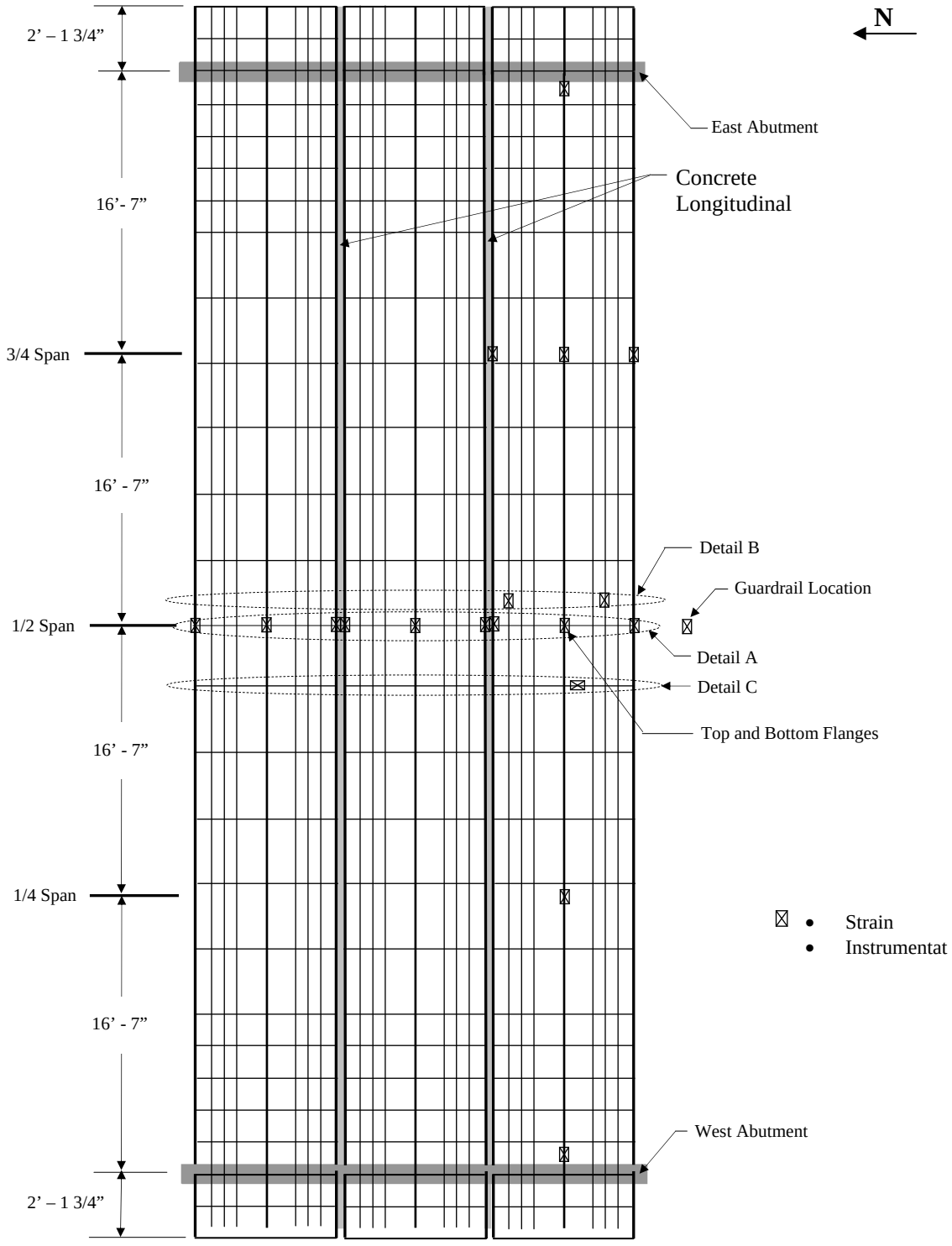


b. Strain Instrumentation

**Figure 5.7. Continued**

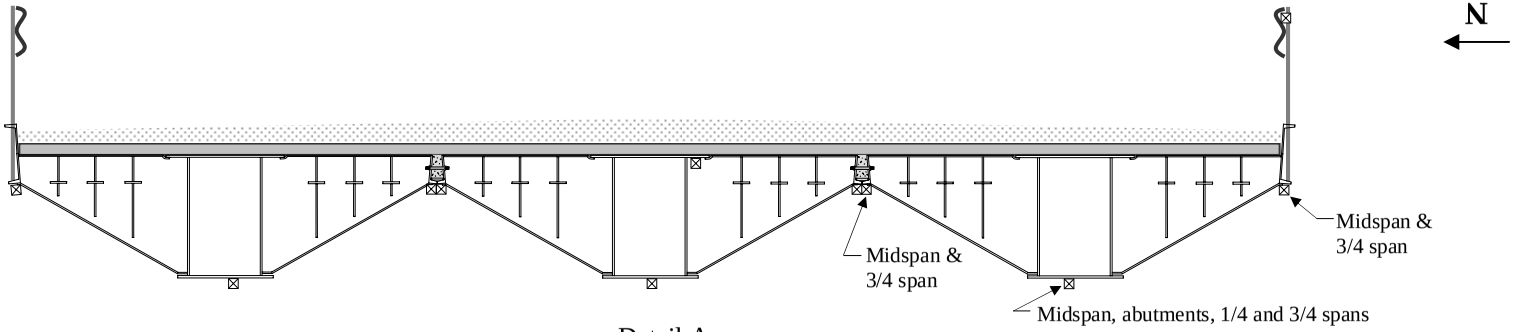


c. Detail A

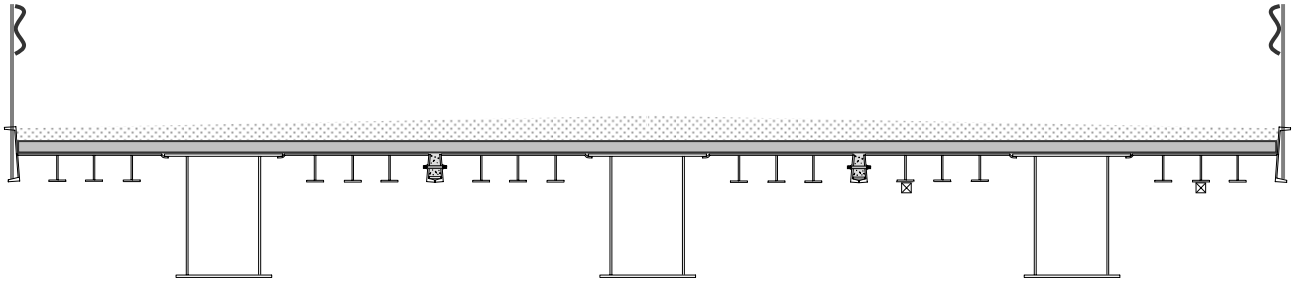

d. Detail B

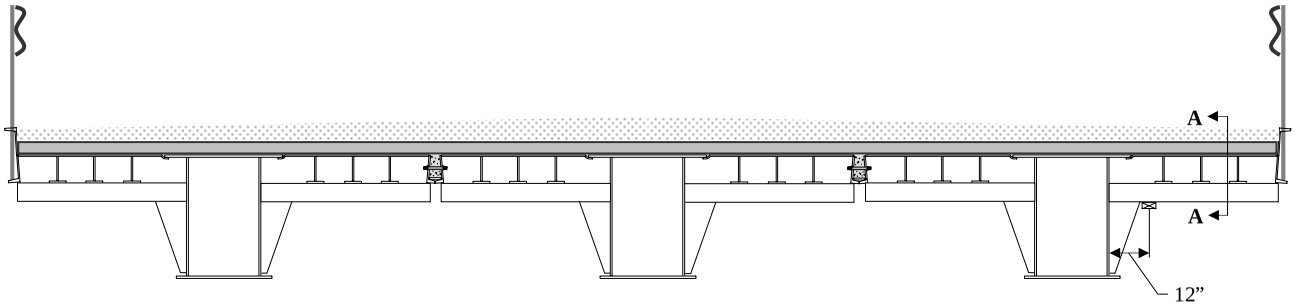


Section A-A

Note: Instrumentation illustrated at or near midspan unless otherwise indicated.

e. Detail C

Strain Transducer Orientation:

⊠ Longitudinal axis transverse to the bridge span.

⊠ Longitudinal axis parallel to the bridge span.

**Figure 5.7. Continued**

a. Installed deflection instrumentation on the WCB2

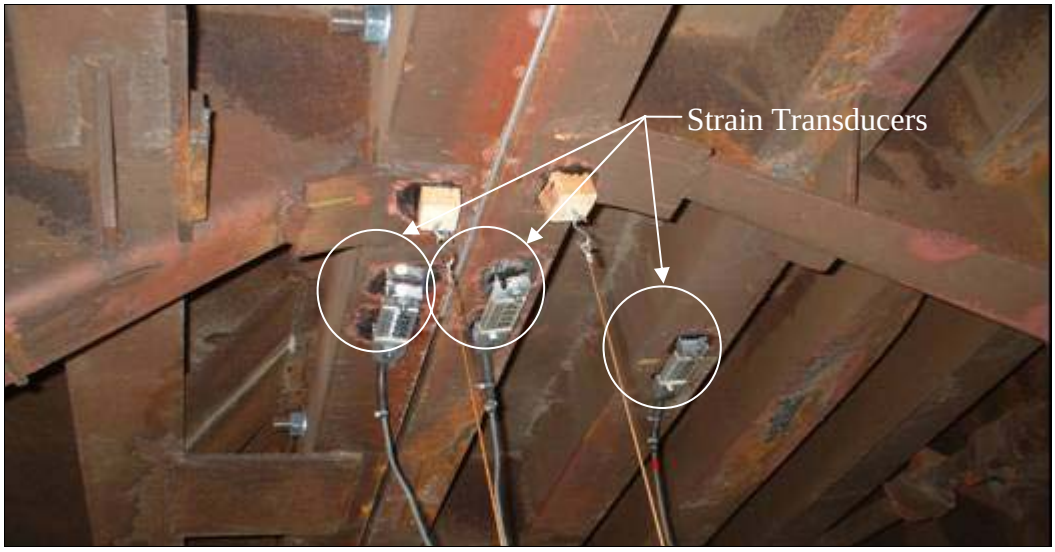


b. Instrumentation at the south longitudinal concrete connection

**Figure 5.8. Deflection and strain instrumentation on the WCB2**

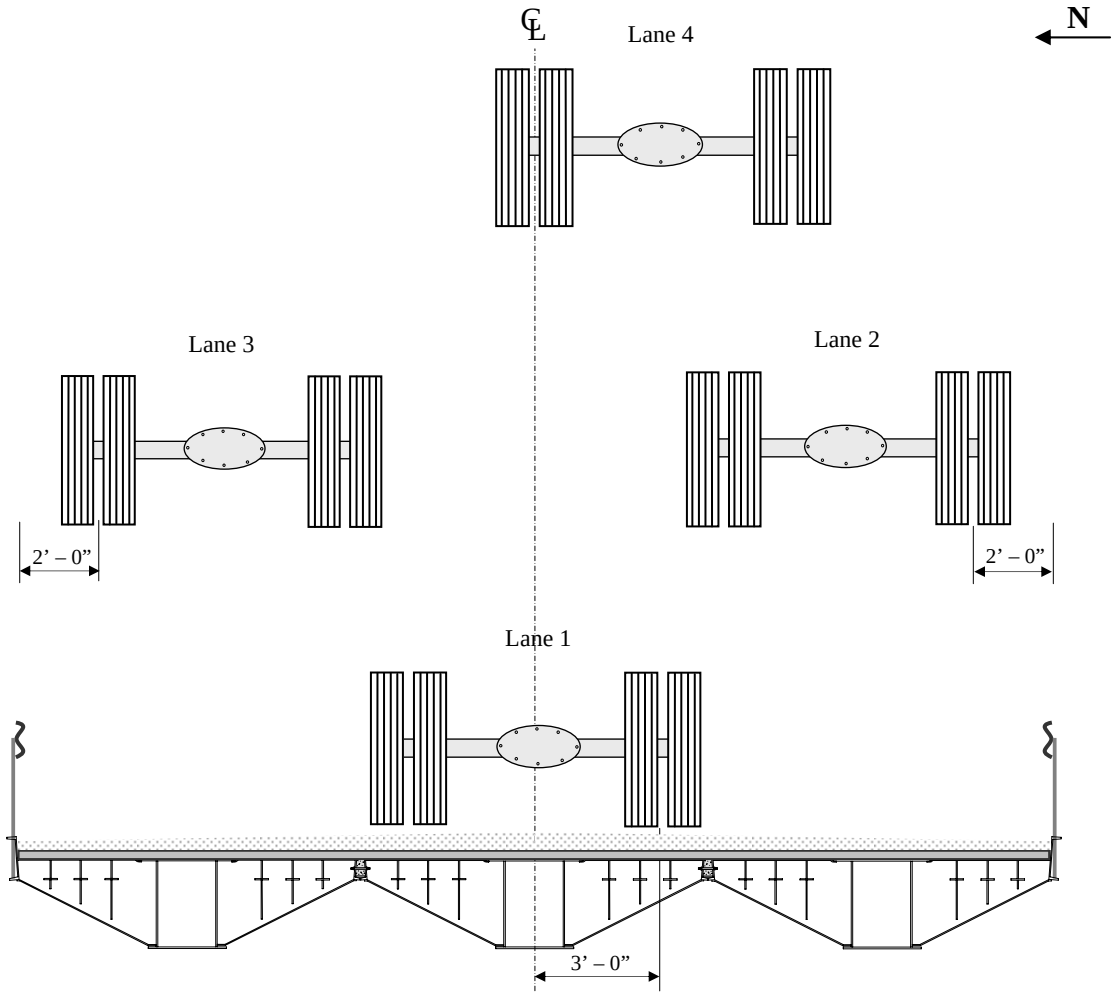


**Figure 5.9. Transverse truck locations during the WCB2 load testing**

a. Test truck in Lane 1

**Figure 5.10. Photographs of WCB2 field testing**

b. Test truck in Lane 3

c. Test truck in Lane 2

**Figure 5.10. Continued**

## 5.4 WCB2 Dead Load Analysis

Dead load analysis for the primary girders (interior box girders and exterior girders) was performed using various assumptions. The WCB2 was assumed to be simply supported at the abutments with a 66 ft – 4-in. clear span and 2 ft – 1 3/4-in. overhangs. Since the timber planks on the north and south halves of the bridge were different (3x12 timber planks were used on the north side and 4x12 tongue-and-groove planks were used on the south side), it was assumed that the dead loads on the each side were evenly distributed transversely only along that half of the bridge. However, all dead loads were assumed to be evenly distributed along the length of the bridge on each side. As discussed in Section 4.4 with the BCB3, the three main longitudinal members were assumed to support the entire bridge dead load, and their inertia ratios were used to distribute these loads to the girders. The girder inertias are similar to those in Table 4.1 with the exception of the exterior "trimmed" girder's inertia being 24.5 $in^4$ for the WCB2.

Conventional bridge design methods include analysis of a continuous, rigid structure across the width of the bridge. Hence, for the WCB2, it was assumed that the concrete connection between the flatcars was rigid and thus the dead load across the connection was uniformly distributed to the adjacent flatcars. After trimming excess material from the RRFCs and installation of guardrail posts, the weight of each railcar

was 33,120 lbs. The guardrail system was assumed to be 100 lbs/ft while the gravel driving surface was estimated have a unit weight of 110 lbs/ft$^3$ and the timber planks were approximated at 36.3 lbs/ft$^3$. Field measurements estimated the gravel thickness to be 3.6 in. thick on the north half of the bridge and 4.2 in. thick on the south side. As stated previously, the timber planks on the north and south sides were 3 in. thick and 4 in. thick, respectively.

Because the bridge is simply supported and the dead load was assumed to be evenly distributed along the bridge length, the maximum dead load stresses for the exterior and interior girders of each flatcar occurred at the bridge midspan. Maximum dead load stresses for the north, middle, and south RRFCs are given in Table 5.1.

**Table 5.1. WCB2 bottom flange dead load stresses**

| North RRFC | | | Middle RRFC | | | South RRFC | | |
|---|---|---|---|---|---|---|---|---|
| Exterior Girder (uncut) | Interior Girder | Exterior Girder (trimmed) | Exterior Girder (trimmed) | Interior Girder | Exterior Girder (trimmed) | Exterior Girder (trimmed) | Interior Girder | Exterior Girder (uncut) |
| +4.8 ksi | +11.4 ksi | +3.6 ksi | +3 ksi | +12.6 ksi | +3.3 ksi | +3.8 ksi | +12.3 ksi | +5.1 ksi |

## 5.5 WCB2 Field Testing Results

As stated previously, the WCB2 was instrumented with deflection transducers across the midspan on interior and exterior girders, and strain transducers were placed on numerous interior and exterior girders, the south guardrail near midspan, and on two secondary longitudinal members and one transverse member of the south RRFC. Data collected from the field testing were reviewed and it was determined that the maximum deflections and strains occurred near midspan of the major members when the test truck tandem was at the midspan. Therefore, all analyses of live load deflections and strains are based on the data collected in the members at the bridge midspan when the truck tandem was also at midspan.

### *5.5.1 Static Testing*

The midspan deflections and strains that were measured on the interior and exterior girders across the width of the bridge are presented in Figures 5.11 – 5.14. In these figures, trend lines are used to connect deflection and strain data points measured during the field testing. The maximum midspan deflection (-0.86 in.) occurred at the exterior girder of the south RRFC when the truck was in Lane 2 (See Figure 5.12), and the maximum midspan strain (+343.7 MII) occurred during the Lane 3 loading at the interior girder of the north RRFC (See Figure 5.13). As can be seen in Figures 5.11 – 5.14, measured midspan strain and deflection values that occurred when the truck load was in Lanes 1-4 (truck rear tandem at midspan) for all other members are below the maximum midspan values previously noted.

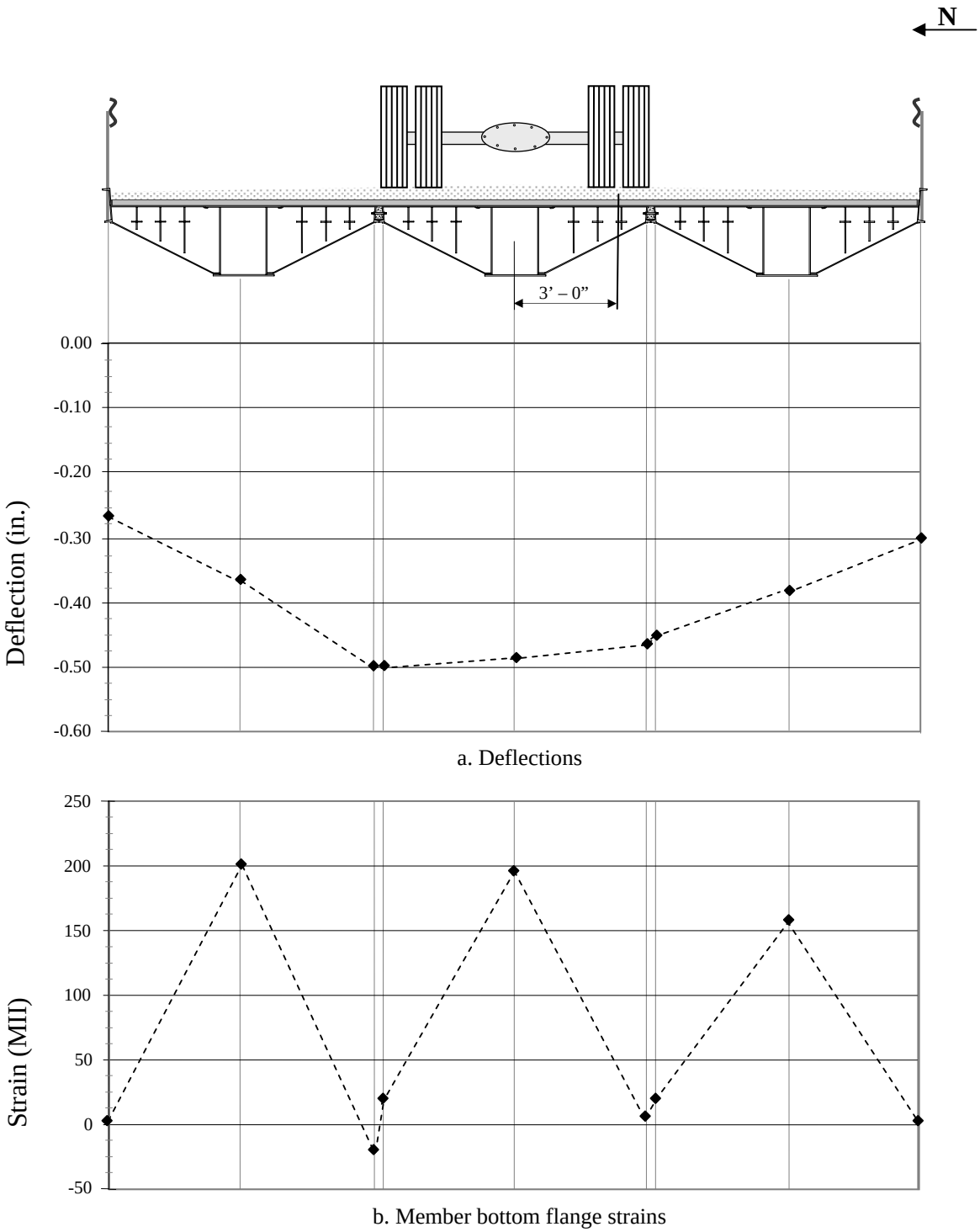


**Figure 5.11. WCB2 Lane 1 midspan deflections and strains**

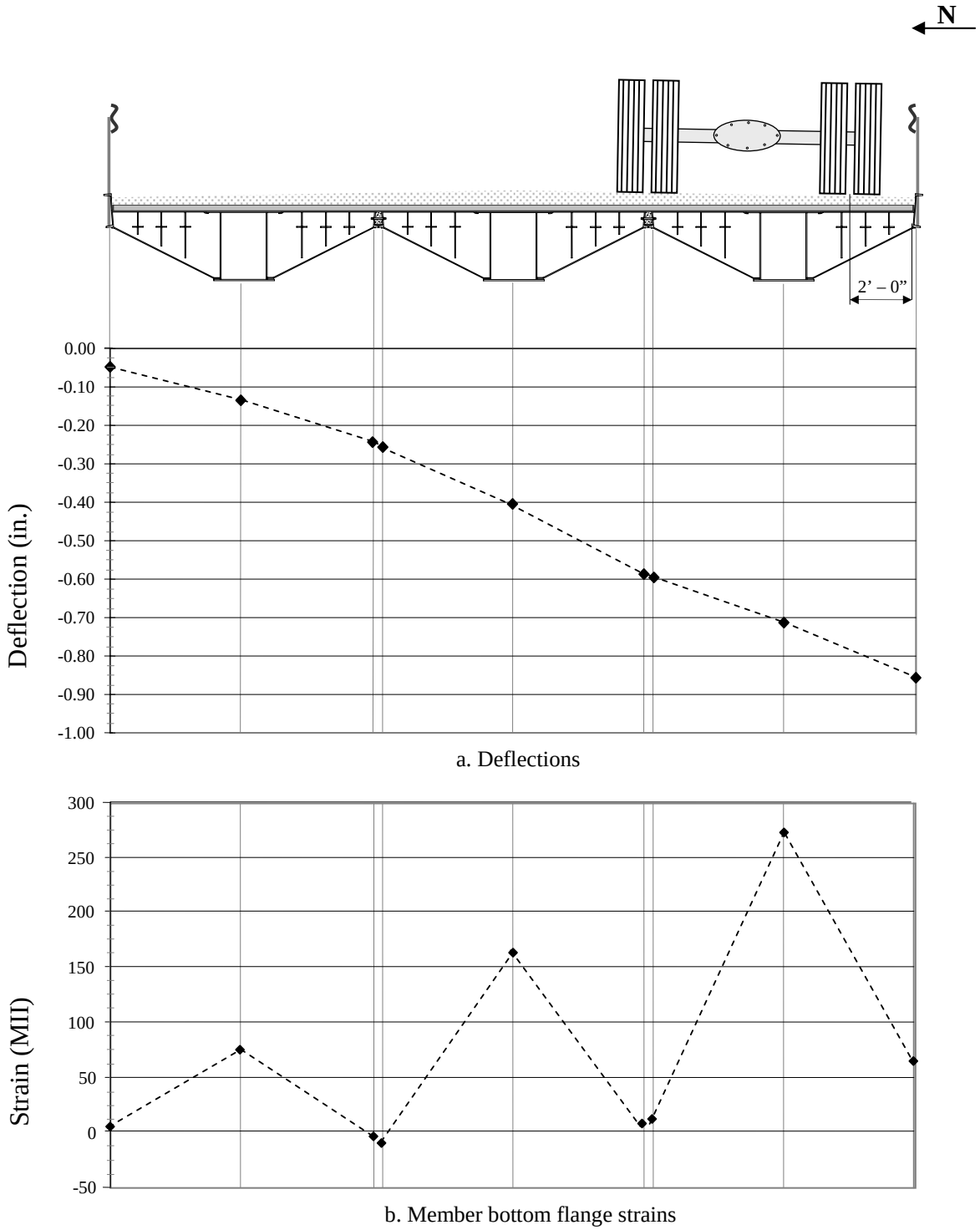


**Figure 5.12. WCB2 Lane 2 midspan deflections and strains**

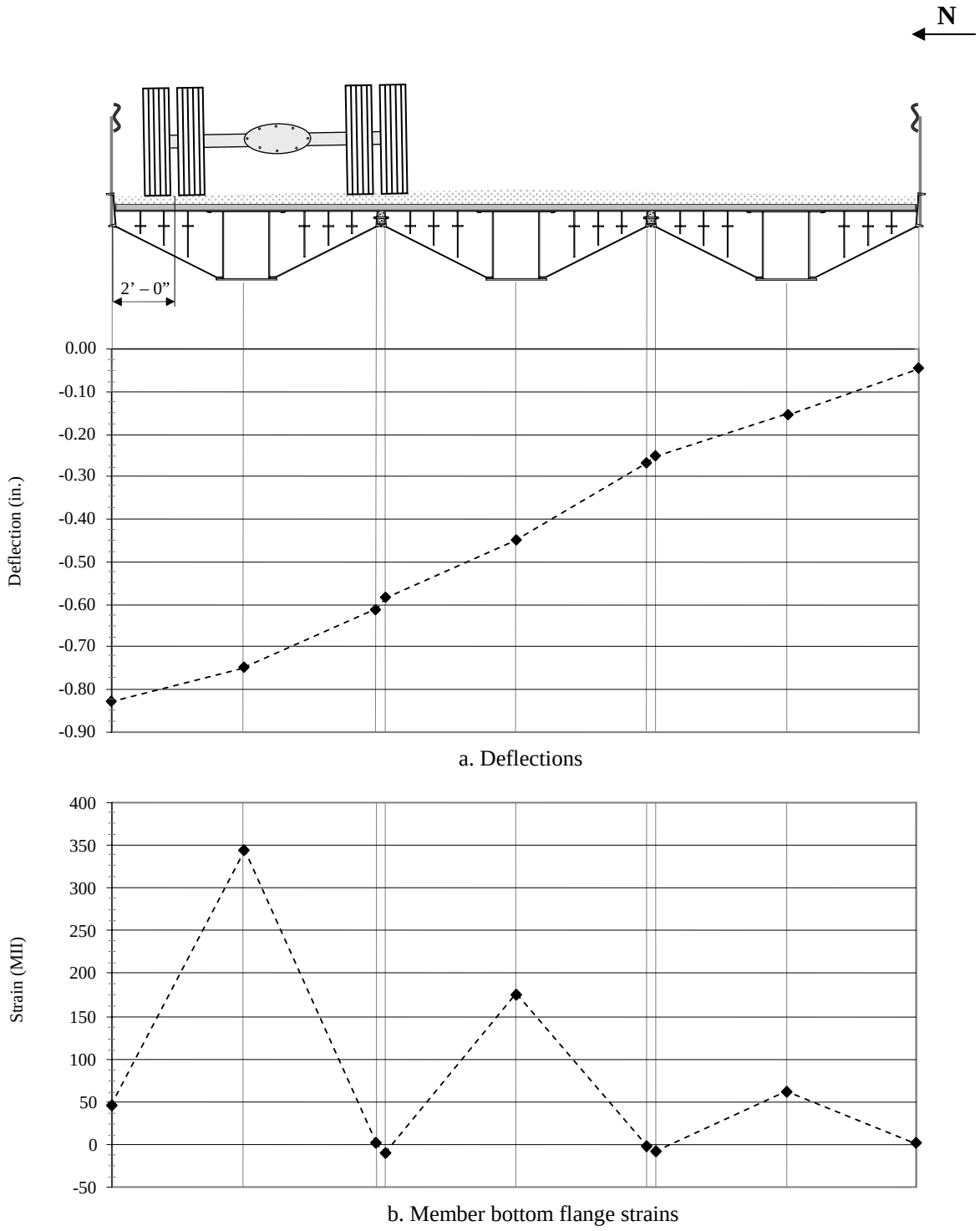


**Figure 5.13. WCB2 Lane 3 midspan deflections and strains**

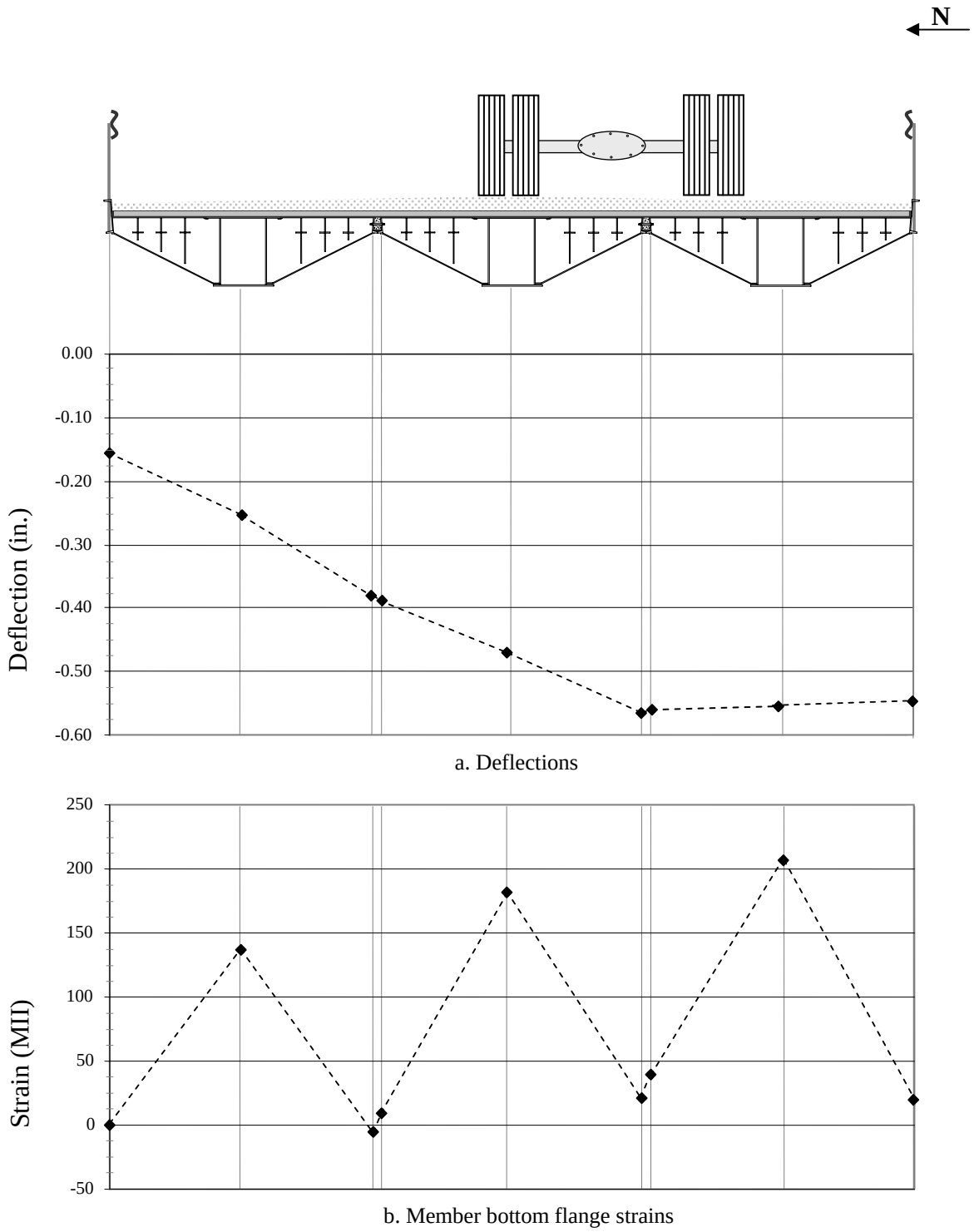


**Figure 5.14. WCB2 Lane 4 midspan deflections and strains**

As can be seen from Figures 5.11 – 5.14, the location of maximum deflection in each case occured directly below the wheel position. The deflection decreased as the transverse distance between the girder and the truck wheel increased. In general, the same can be said for the strains, where the greatest strains occurred at the wheel location. An exception is the interior girder of the north RRFC during Lane 1 loading which had a slightly higher strain value (4 MII) than the interior girder of the middle RRFC. This may be the result of the lower rigidity of the north portion of the bridge due to the timber planking on that side of the bridge and/or the truck being positioned slightly to the north of the bridge's centerline.

Lateral load distribution as shown in Figure 5.15 was different on the north and south sides of the WCB2 because of the different timber planking used on each side of the centerline of the bridge. The south side, which had tongue-and-groove plank, distributed loads better than the north side planks. When the truck was positioned in Lane 1, larger deflections and strains were measured in the north RRFC than the south RRFC due to the better distribution on the south side. The tongue-and-groove timber planks could also distribute loads longitudinally to other secondary members, thus decreasing the deflections and strains on the bridge's south side. When the truck was in Lane 3, the distribution of loads was less, thus the interior girder of the north RRFC resisted more of the load and little was transferred to other members. This distribution can also be seen in the south RRFC's interior girder during Lane 2 loading in which there was better distribution and the load was transferred to other members, thus reducing the strains measured in the interior girder of the south RRFC. The live load distribution factor needed for design was found from analyses of the deflection data from the various loading positions. The maximum live load strains (stresses) and deflections occurred on the interior and exterior girders of an exterior RRFC when the truck was positioned on that side of the bridge. The live load moments in each girder, resulting in the maximum strains (stresses) was a function of the live load distribution factor. Using the areas under the deflection curves during loading in these truck positions, the moment distribution was found to be 55%.

The maximum deflection measured (-0.92 in.) occurred near the midspan and was measured in the south RRFC exterior girder when the test truck was located in Lane 2. Following the AASHTO LRFD Bridge Design Specifications [8], a recommended maximum deflection was 'span'/800 for legal truck loads. For the WCB2 with a clear span of 66 ft – 4 in., this legal load deflection limitation would be -1.00 in. Hence, for this truck loading, the maximum measured deflection was below recommended values. If the measured deflection were increased in proportion of the test truck load to an HS-20 loading, the experimental deflection would be -1.27 in., which is significantly above AASHTO limits.

It was assumed that the material properties for these RRFCs are similar to those of the railroad flatcars used in previous projects [3,4]. The proportional limit and modulus of elasticity for these railcars used in previous research were determined from coupon tests to be 40 ksi and 29,000 ksi, respectively. A conservative yield strength of the material was assumed to be 36 ksi [4]. The maximum live load strains in the exterior and interior girders were +360 MII (+10.4 ksi) in the north RRFC interior girder near midspan (Lane 3 loading), and +83.4 MII (+2.4 ksi) in the south RRFC exterior girder at the longitudinal connection at the 3/4 span location (Lane 1 loading). The maximum exterior girder strain occurred at the south longitudinal connection because, as previously noted, the truck load was concentrated more towards the south side of the truck's box. The maximum strain occurred at the 3/4 span because it was near the location of the timber plank transition from 3x12 timber planks to 4x12 tongue-and-groove timber planks. Thus, the stiffness near this location was less, resulting in higher strains.

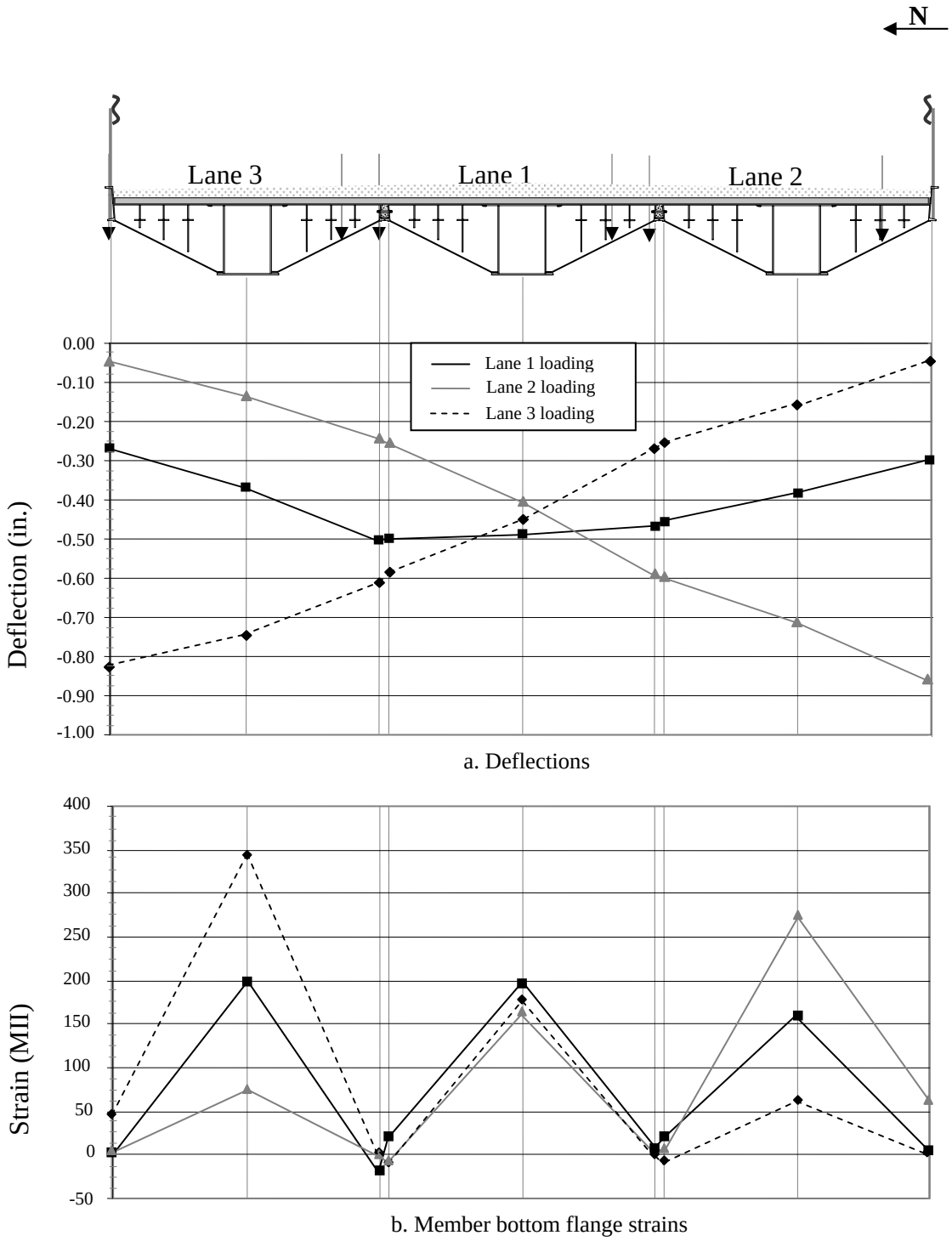


**Figure 5.15. WCB2 Lanes 1, 2, and 3 midspan deflections and strains**

The maximum strain in the transverse member instrumented near midspan was +42 MII (+1.2 ksi) and occurred when the truck was in Lane 4. The secondary members, also near midspan, had a maximum strain of +38 MII (+1.1 ksi) when the loading was in Lane 2. Maximum strains measured in other RRFC members were below these, and thus are not presented.

Combining the calculated dead load stresses with the live load stresses determined from the measured live load strains, the total member stresses were determined and are presented in Table 5.2.

**Table 5.2. WCB2 bottom flange total stresses**

| North RRFC | | | Middle RRFC | | | South RRFC | | |
|---|---|---|---|---|---|---|---|---|
| Exterior Girder (uncut) | Interior Girder | Exterior Girder (trimmed) | Exterior Girder (trimmed) | Interior Girder | Exterior Girder (trimmed) | Exterior Girder (trimmed) | Interior Girder | Exterior Girder (uncut) |
| +6.3 ksi | +21.8 ksi | +4.5 ksi | +4.8 ksi | +18.6 ksi | +4.1 ksi | +5.3 ksi | +20.5 ksi | +7.1 ksi |

The maximum total stresses in the north RRFC girders all occurred when the truck was positioned in Lane 3. The maximum stresses in the interior and north exterior girders of the middle RRFC occurred during Lane 1 loading. The exterior girders at the south longitudinal connection between the middle and south RRFCs had maximum stresses when the truck was in Lane 4. Lane 2 loading produced the maximum total stresses in the interior girder and exterior (uncut) girder of the south RRFC. The overall maximum stress of +21.8 ksi occurred in the interior girder of a side RRFC when the truck was positioned on that side of the bridge. This is the same condition which resulted in a maximum stress of +16.7 ksi in the interior girder of a side RRFC of the 3-span WCB1 bridge described in Section 1.2.2.3.

Theoretical analysis of an HS-20 design truck loading (not including impact) was performed to determine maximum stresses of an exterior RRFC near the midspan. The design live load stress (+11.7 ksi) was calculated for the interior girder using the distribution factor determined using field test results. Combining this with the theoretical dead load stress in the interior girder, the maximum total stress due to an HS-20 design truck loading would be +24.0 ksi in the bottom flange of the interior girder of the south RRFC. As stated previously, the allowable stress was computed to be 22 ksi; therefore, the stress of +24 ksi for the interior girder's bottom flange exceeds this limit by approximately 9%.

*5.5.2 Time History Analysis*

With continuous data collected during a truck crawl speed (approximately 4 mph test), a time history analysis of the interior girder of the south RRFC was performed using data from strain transducers placed 1 ft from both abutments, at the 1/4 span, midspan, and 3/4 span locations (See Figure 5.16). It should be noted that the test truck traveled westward; hence peak values in the girders occurred first near the east abutment and lastly near the west abutment.

The time history strain data recorded during field testing is plotted in Figure 5.17. It can be seen that the maximum bottom flange strain was measured at the interior girder's midspan, since the structure is simply supported and maximum moments would occur near this location. Also, the fixity at the two abutments

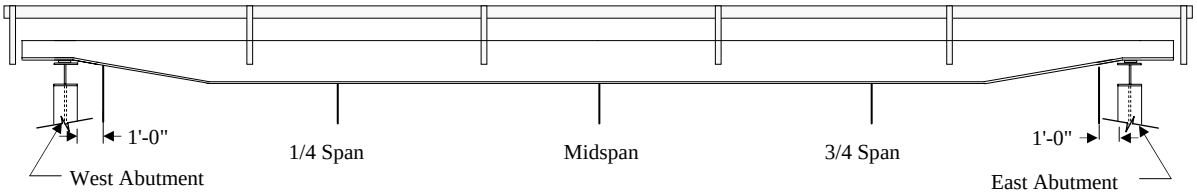


**Figure 5.16. Strain instrumentation locations for WCB2 time history analysis**

can be analyzed from the time history data. The east abutment is welded (restraining translations and rotations) while the west abutment allows for horizontal movement parallel to the bridge and some rotation. Strain instrumentation placed 12 in. from the supports at both abutments measured small strains signifying some restraint at the abutments.

*5.5.3 Dynamic Analysis*

The structural dynamic properties of the WCB2 were determined through the dynamic testing performed during the filed testing. Four dynamic tests were conducted at 10, 15, 20, and 25 mph truck speeds. Because of the flexibility of the WCB2, the 10 mph truck speed created the greatest dynamic amplification in the girders' deflections and strains.

The free vibration of the interior girders was used to determine their period, frequency, and damping. The oscillating strains when the tandem truck had exited the bridge indicated the free vibration of the bridge. Based on this data the period was found to be 1.4 seconds, resulting in a member frequency of 0.70 Hz, and the damping of the interior girders was approximately 1.5%.

As previously noted, the maximum dynamic deflections and strains occurred at a truck speed of 10 mph. A plot of the time history comparison of the deflections and strains during the static and dynamic field testing are presented in Figures 5.18 and 5.19, respectively. The dynamic testing was performed in Lane 1; therefore, the data from static load testing are also from Lane 1 loading. The largest amplification occurred in the north RRFC interior box girder: the deflection was increased by 41% while the strain was amplified by 27%. As seen in Figures 5.18 and 5.19, the dynamic effects on the north RRFC are significantly more apparent with the large sinusoidal fluctuation of deflections and strains as the truck crosses the bridge. This is because the bridge's north side is less stiff than the south due to the tongue-and-groove timber planks positioned on the south side of the bridge. The increased flexibility of the north side of the bridge makes it more susceptible to dynamic amplification at the 10 mph truck speed.

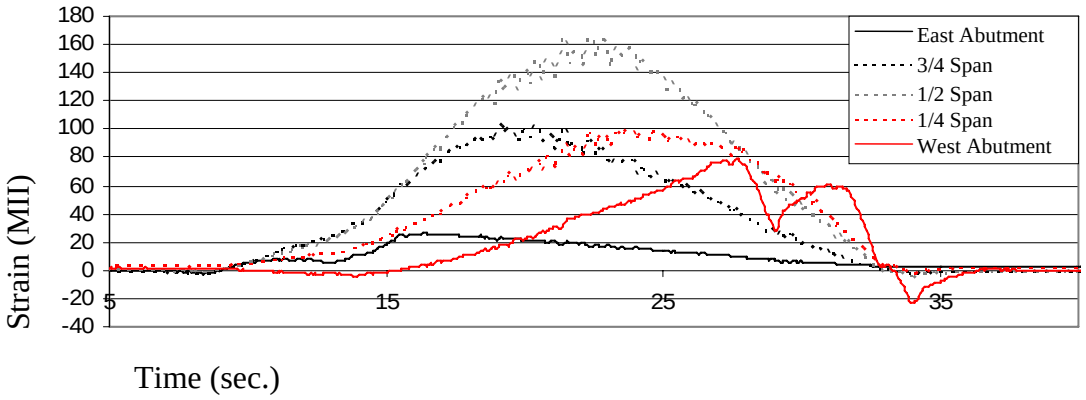


a. Truck in Lane 1

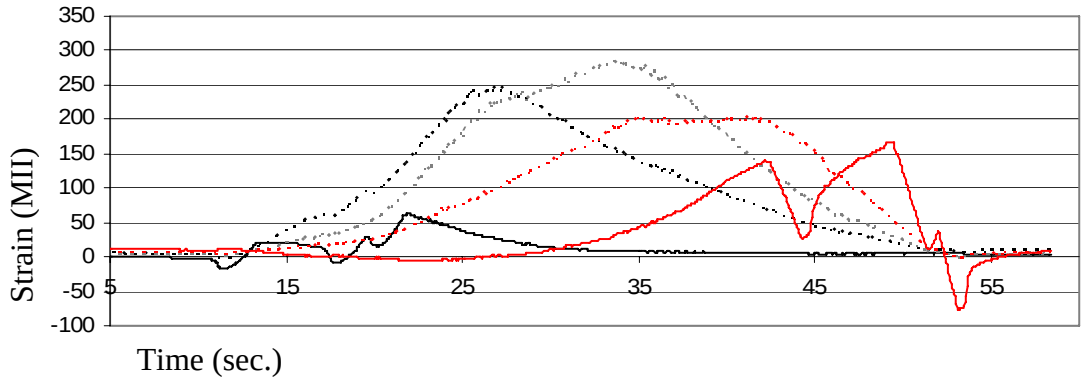


b. Truck in Lane 2

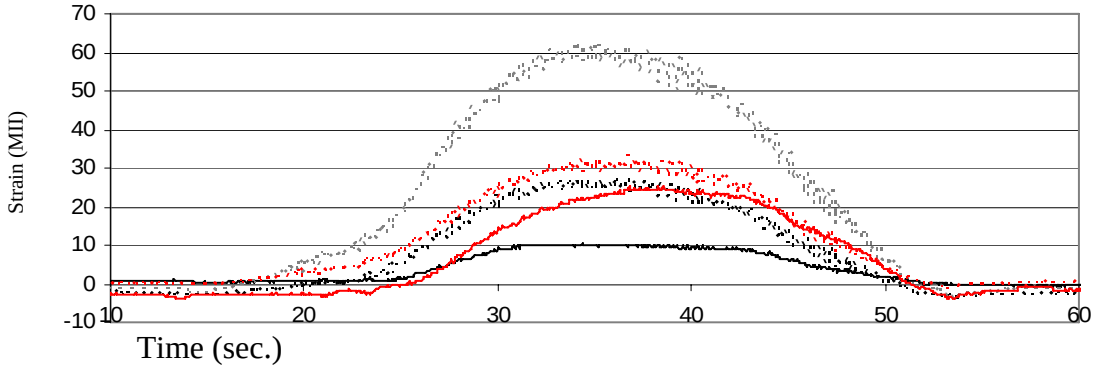


c. Truck in Lane 3

**Figure 5.17. WCB2 strain vs. time for the south RRFC's interior girder bottom flange**

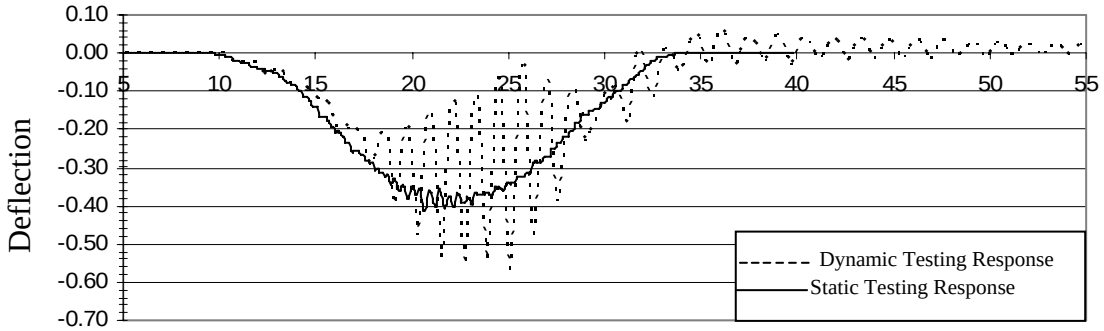


a. North RRFC interior girder

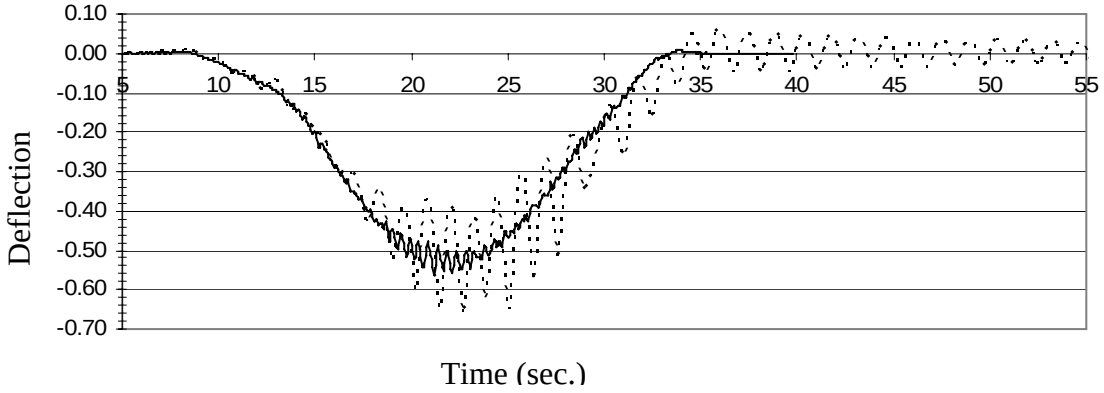


b. Middle RRFC interior girder

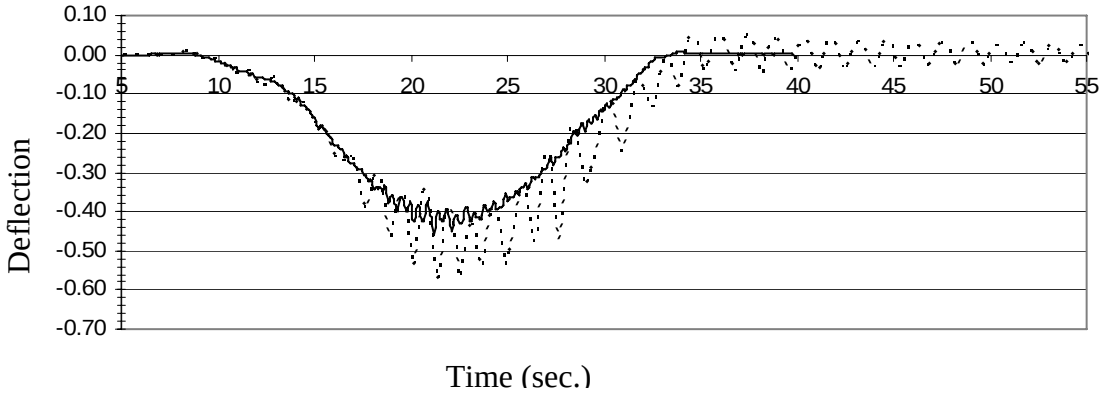


c. South RRFC interior girder

**Figure 5.18. Comparison of the measured interior girder deflections of the north, middle, and south RRFCs from static and dynamic field tests (Lane 1 loading)**

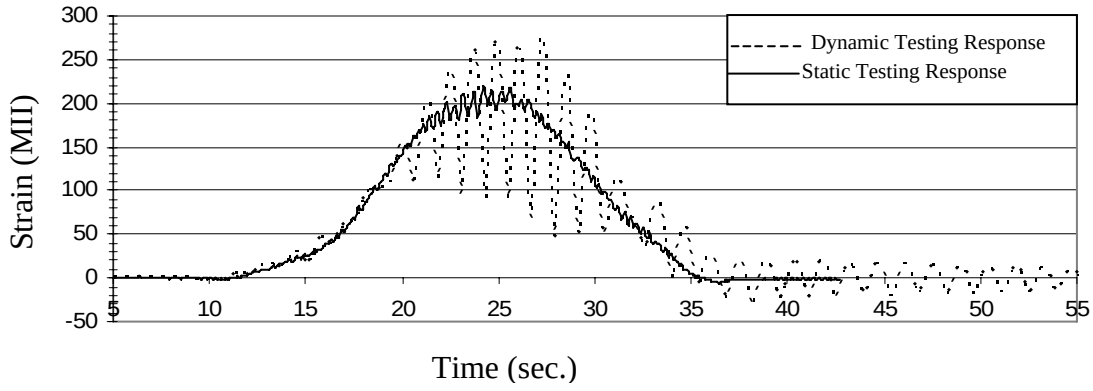


a. North RRFC interior girder

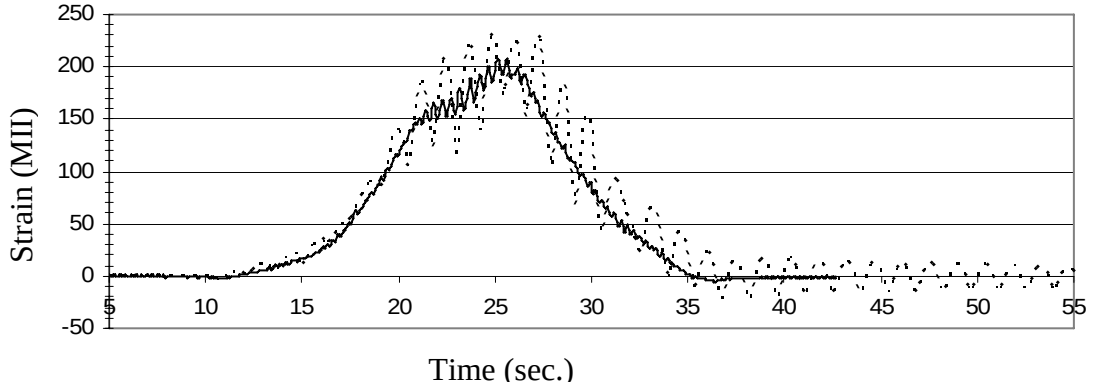


b. Middle RRFC interior girder

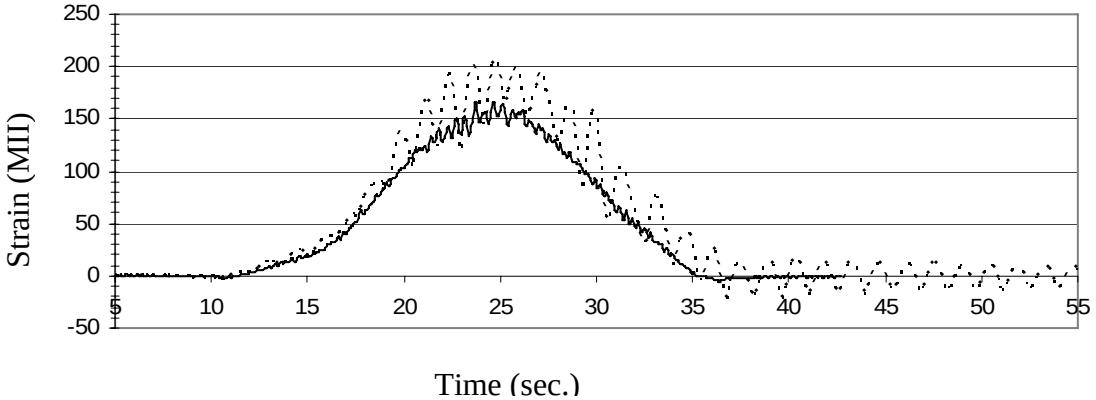


c. South RRFC interior girder

**Figure 5.19. Comparison of the measured interior girder bottom flange strains of the north, middle, and south RRFCs from static and dynamic field tests (Lane 1 loading)**

*5.5.4 Comparison of WCB1 with WCB2*

A comparison of midspan field data collected from WCB1 and WCB2 during load testing is presented in Figures 5.20 – 5.22. The WCB1 and WCB2 bridges both have reinforced concrete longitudinal connections between adjacent railcars and are composed of three 89-ft RRFC superstructures; the length of the WCB2 railcars were "trimmed" to satisfy site requirements while the WCB1 utilized the entire railcars' lengths. The WCB2 bridge construction resulted in simply supported conditions while the WCB1 bridge was a three span continuous bridge. The difference in structural behavior of these two bridges was representative of these different support conditions, although the trends tended to be similar. The smaller deflections and strains measured in the WCB1 were expected due to the continuity of the bridge. Since there was very little difference in the field truck weights used to test the two bridges (WCB1 = 51.1 k, WCB2 = 52.0 k), the increase in bridge length and support conditions were the controlling factors in the deflection and strain values. During Lane 1 loading, the deflection from WCB1 field test was, on average, 71% of that measured in the WCB2 test, while the strains measured in WCB1 were approximately 64% of WCB2 strains.

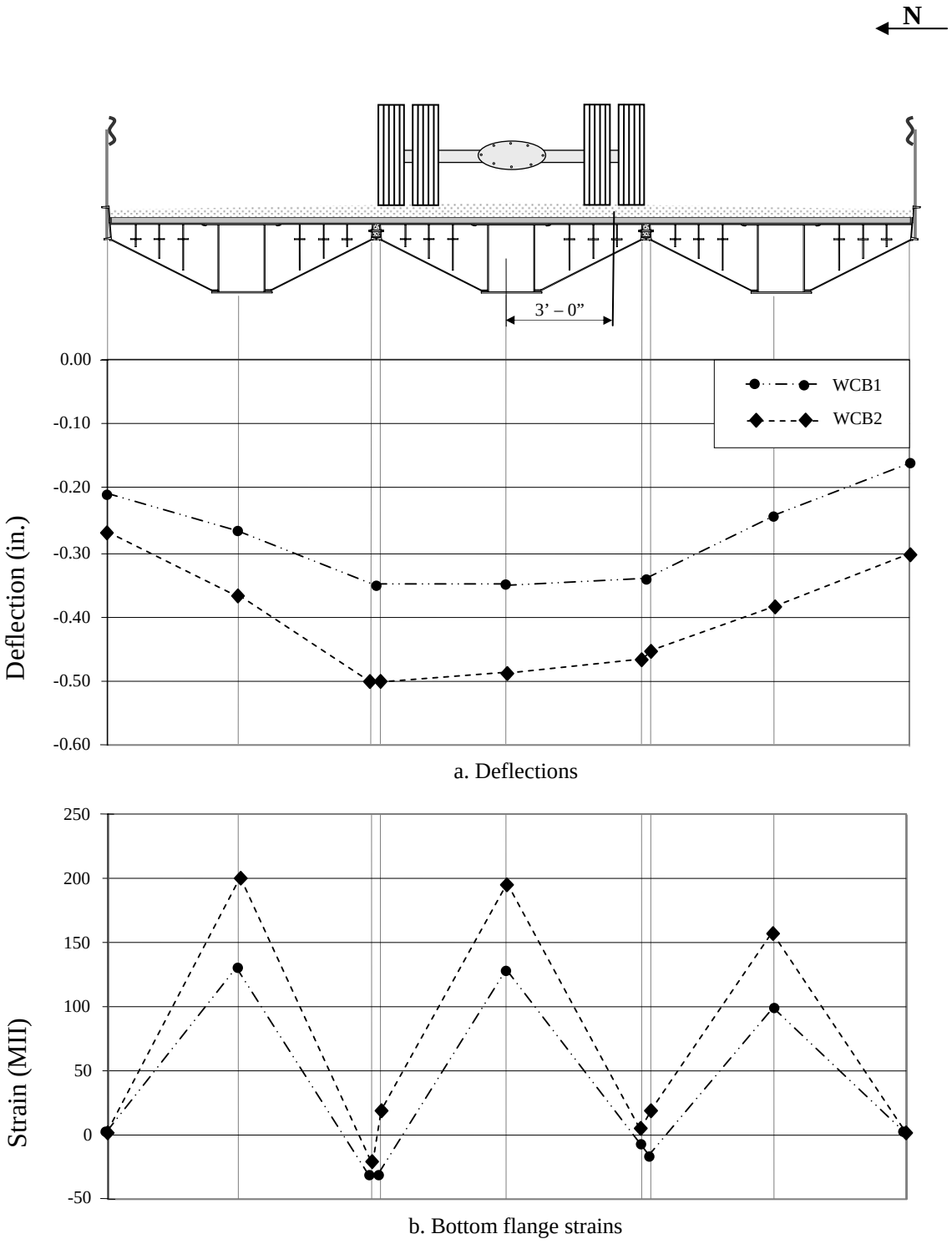


**Figure 5.20. Comparison of field data from WCB1 and WCB2 (Lane 1)**

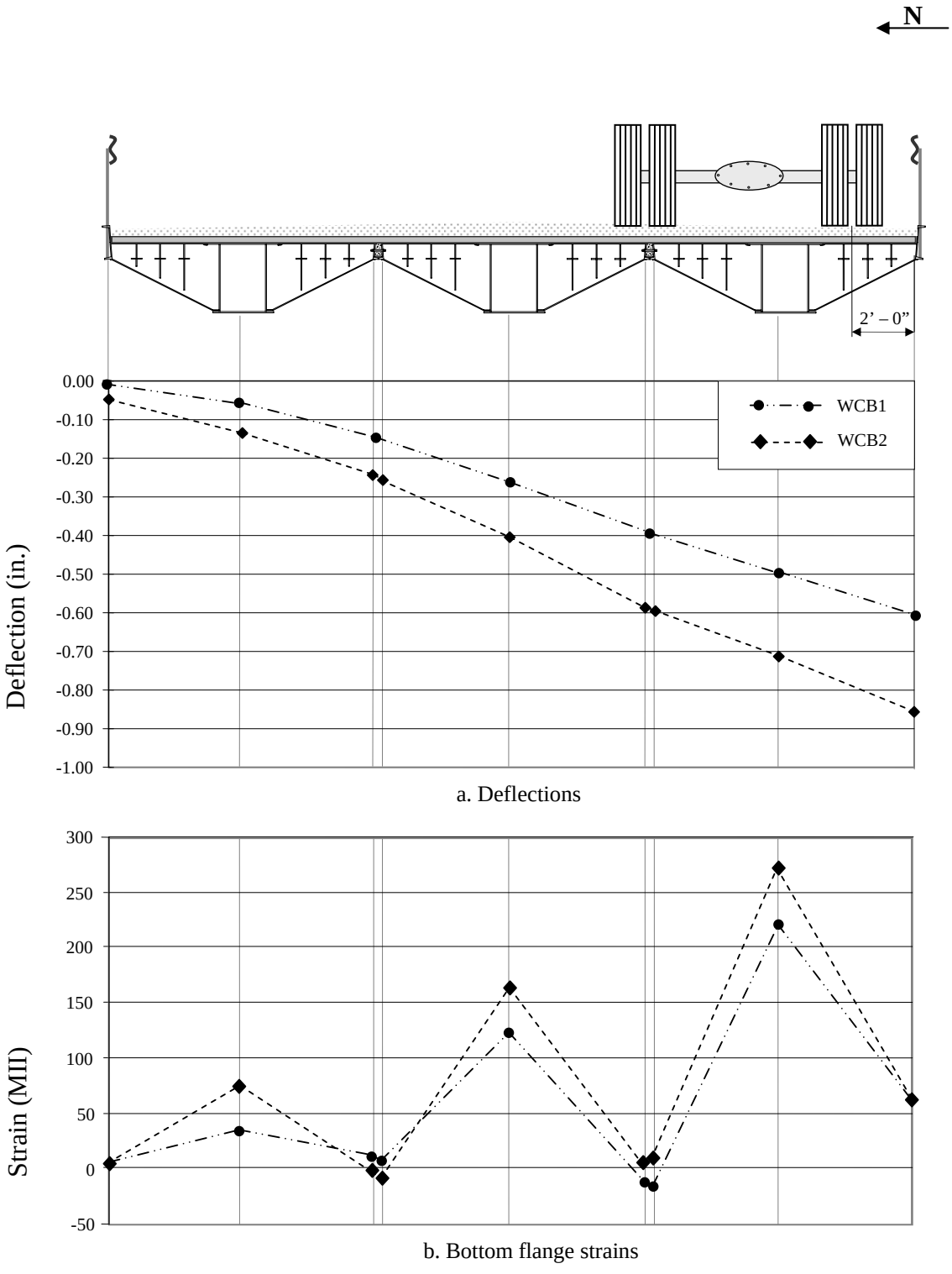


**Figure 5.21. Comparison of field data from WCB1 and WCB2 (Lane 2)**

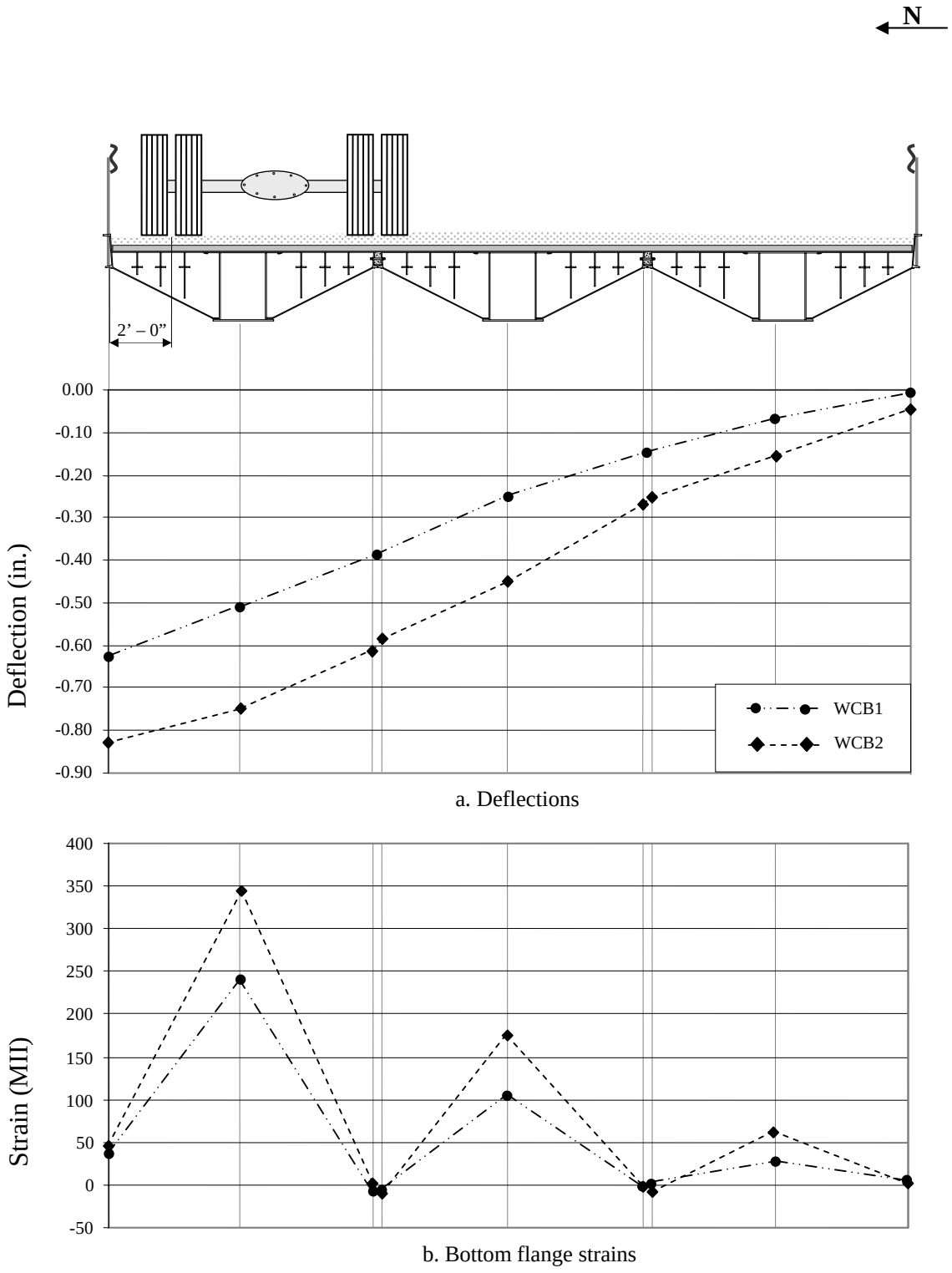


**Figure 5.22. Comparison of field data from WCB1 and WCB2 (Lane 3)**

## 6.0 DESIGN AND ANALYSIS OF THE RRFC BRIDGES

### 6.1 Recommendations for Live Load Distribution

In the demonstration project, equations for the live load moments were presented; these equations were developed for the bridges and LFCs described in the report [4]. The BCB1 is a single-span simply-supported bridge composed of three 56-ft V-deck RRFCs, and the WCB1 is a three-span bridge composed of 89-ft RRFCs. Since the BCB2 and DCB are both single-span bridges composed of two RRFCs, the live load moment equations previously developed were modified to more accurately determine the live load moments in the interior and exterior girders in such bridges.

As determined in the results in Sections 2.5 and 3.5, the maximum stresses were recorded in the three primary girders of the RRFC. The live load moments in each girder can be determined with the following equation:

$$M_{LL} = \frac{2}{3}\omega\psi M_{SD} \tag{6.1}$$

where:

$M_{LL}$ = The actual, maximum midspan live load moment in the girder being investigated

$M_{SD}$ = The maximum, midspan live load moment in the statically determinate RRFC bridge based on the live load

$$\omega = \text{Inertia ratio} = \frac{I_D}{\Sigma I_{RRFC}} \tag{6.2}$$

$I_D$ = Strong-axis moment of inertia for the girder being investigated

$\Sigma I_{RRFC}$ = Sum of the girders' strong-axis moments of inertia in one RRFC

$$= (2)(I_{EXT})+I_{INT} \tag{6.3}$$

$I_{EXT}$ = Strong-axis moment of inertia for the exterior girder

$I_{INT}$ = Strong-axis moment of inertia for the interior girder

$\psi$ = Adjustment factor to correct for the simplified analysis [4]

For interior girders in RRFC bridges like the BCB2, $\psi = 0.8$

For exterior girders in RRFC bridges like the BCB2, $\psi = 0.75$

For interior girders without extra plates in RRFC bridges like the DCB, $\psi = 0.9$

For exterior girders in RRFC bridges like the DCB, $\psi = 0.4$

The preceding adjustment factors were determined as described in Appendix B so that the maximum live load moment at midspan calculated using Equation 6.1 would adequately approximate the actual live load moment measured during the field load test. Grillage models of the BCB1 and WCB1 were created for the demonstration project, so a variety of inertia ratios were examined for the two different LFCs used in the two bridges [4]. Thus, the adjustment factors that were provided for the BCB1 and WCB1 are equations based on the inertia ratio of the girder being investigated.

Summarized in Table 6.1 are the adjustment factors for the BCB1 and WCB1 interior and exterior girders determined using the equations in the demonstration project and the adjustment factors for the BCB2 and DCB interior and exterior girders determined as described in Appendix B. The adjustment factors for the interior girders of the BCB1 ($\psi$ = 0.809) and BCB2 ($\psi$= 0.8) are nearly identical, as are the adjustment factors for the interior girder of WCB1 ($\psi$=0.871) and DCB ($\psi$=.75) are significantly different, as are the adjustment factors for the exterior girders of the WCB1 ($\psi$=0.855) and DCB ($\psi$=0.4). These comparisons indicate, as one would expect, that the LFC has significantly more influence on the exterior girder adjustment factors than it does on the interior girder adjustment factors .

**Table 6.1. Summary of the live load distribution adjustment factors ($\psi$).**

| Bridge Design | Adjustment Factor ($\psi$) | |
|---|---|---|
| | Interior Girder | Exterior Girder |
| BCB1 | 0.809 | 1.107 |
| BCB2 | 0.8 | 0.75 |
| WCB1 | 0.871 | 0.855 |
| DCB | 0.9 | 0.4 |

The moment fraction equal to 2/3 in Equation 6.1 represents the fraction of the total area under the deflection curve for one railroad car when the truck is positioned on that car. This value was first determined in the demonstration project for bridges with three RRFCs, though the actual fraction was 0.69 for the BCB1 and 0.62 for the WCB1 [12]. The same method described in Appendix D of the Demonstration Project Using Railroad Flatcars for Low-Volume Road Bridges [12] was used to determine the moment fraction for the bridges with two RRFCs. For the BCB2, the fraction was 0.65 while for the DCB, the fraction was 0.66. Appendix C presents the calculations used to determine these moment fractions. The similar fractions developed for the three-RRFC bridges in the demonstration project and for the two-RRFC bridges investigated in this report are due to the minimal load carried by the exterior RRFC when the truck is positioned over the other exterior RRFC in a three-RRFC bridge, (i.e. the BCB1 and WCB1) [12]. Since the BCB2 and DCB moment fractions are also approximately 2/3, the moment fraction in the live load distribution factor was determined to be 2/3 for bridges with two RRFCs as for three RRFCs. Because of this, Equation 6.1 (with the appropriate values of $\psi$ an $\omega$ included) is valid for bridges composed of two or three RRFCs.

### 6.2 Rating Procedure for RRFC Bridges

The rating procedure for RRFC bridges follows the allowable stress method for rating bridges. Following the allowable stress method for rating bridges in the AASHTO Manual for Condition Evaluation of Bridges (Rating Manual) [13], the equation used to determine the rating of each member in a typical highway bridge is as follows:

$$RF = \frac{C - A_1 D}{A_2 L (1 + I)} \tag{6.4}$$

where:

RF = The rating factor for the live-load carrying capacity

C = The allowable stress capacity of the member

D = The dead load effect on the member

L = The live load effect on the member

I = The impact factor to be used with the live load effect = 0.33

$A_1$ = Factor for dead loads = 1.0 for the allowable stress method

$A_2$ = Factor for live load = 1.0 for the allowable stress method

The allowable stress capacity of the member, C, is determined using the properties in tables provided in the Rating Manual; for bridge materials or construction that is unknown, the engineer should determine the allowable stresses based on field investigations and/or material testing [13]. The dead load effect on the member, D, is calculated using standard bridge analysis methods and is based on the existing conditions of the bridge. Appendices are provided in the Rating Manual for determining the live load effect on girders and stringers in typical highway bridges. However, RRFC bridges are not composed of uniform girders at equal spacing like standard girders in slab on girder bridges; thus, a different method must be used to determine the live load effect. For RRFC bridges, the effect of the live load on a member, L, should be determined by multiplying the maximum live load moment by a distribution factor. The distribution factor to be used is the fraction of the live load transferred to the member. The distribution factors for the RRFCs used in the bridges tested for this investigation were presented in Section 6.1 as part of Equation 6.1 and now explicitly as Equation 6.5.

$$DF = \frac{2}{3} \omega \psi \tag{6.5}$$

The variables in Equation 6.5 are the same as in Equation 6.1.

The majority of the RRFCs have three primary girders and several secondary and transverse members. As assumed in Sections 2.5 and 3.5, primary girders carry nearly all the load on the bridge. Because of this, the primary girders are assumed to carry the entire load of the bridge for the distribution of the live load. Thus, no distribution factors are presented for the secondary members, and only the primary girders are given a numerical rating.

On a bridge composed of 89-ft RRFCs, the transverse members may be part of the critical load path of the bridge; however, more data must be collected and analyzed to accurately include the transverse members in the numerical load rating. For all RRFC bridges, all members of the bridge, including the secondary members and the transverse members, should be visually inspected for damage as described in the Rating Manual [13].

To determine the rating of each bridge member, the Rating Factor, RF, from Equation 6.4 should be

multiplied by the weight of the truck used in determining the live load effect, L. This will result in the bridge member rating in tons, and the actual bridge rating will be controlled by the bridge member with the lowest rating [13]. An example RRFC bridge rating is provided as Appendix D.

# 7.0 SUMMARY AND CONCLUSIONS

## 7.1 Summary

The focus of this part of the study was to investigate the structural behavior of simple span bridges constructed with RRFC superstructures. Specific objectives included investigating construction variables; testing RRFC bridges to determine live load strains (stresses) and deflections; using field testing data to revise the design methodology developed in previous research; and developing a load rating process for RRFC bridges. These objectives were accomplished by field testing four bridges - two in Buchanan County, Iowa, one in Delaware County, Iowa, and one in Winnebago County, Iowa - and examining the data obtained from those tests.

The BCB2 is composed of two 56-ft V-deck RRFCs supported by concrete abutments and a LFC between the RRFCs consisting of a 30.5-in. wide R/C beam and transverse threaded rods. The BCB2 has a width of 20 ft – 7 in. and spans 54 ft -0 in. The design of the BCB2 was based on the BCB1, which was designed and constructed as part of the demonstration project, TR-444 [4]. The DCB is composed of two 89-ft RRFCs; however, 10 ft – 9 in. were removed from each end of the RRFCs so that a symmetric 67 ft – 6 in. portion of the RRFC remained. The DCB has a width of 18 ft – 4 in. and spans 66 ft – 4 in. The LFC for the DCB consists of a 14-in. by 1/2-in. plate welded over the trimmed exterior girders of the adjacent RRFCs along the entire length of the connection.

Both the BCB3 and the WCB2 were constructed using three 89-ft RRFCs (the railcars were “trimmed” to meet the span requirements of each bridge); however, the construction details in each bridge were significantly different which greatly influenced their structural behavior. The BCB3 was 26 ft – 5 1/2 in. wide with a single span of 66 ft – 2 in. The constructed concrete abutment was 3 ft deep, 4 ft wide, and 30 ft long. Five HP 10x42 piles were extended 24 in. into the concrete cap and surrounded with spiral reinforcement within the cap. Supports at both concrete abutments were rollers and restricted only vertical movement. A bolted longitudinal connection (1 1/4 in. diameter bolts spaced on 3 ft centers) was used to join adjacent RRFCs and a gravel driving surface was added. On the other hand, the WCB2 was 27 ft – 0 in. wide with a main span length of 66 ft – 4 in. and 2 ft – 1 3/4 in. overhangs at each abutment. End abutments consisted of 6 steel HP12x53 piles and HP12x53 steel caps with sheetpile backwalls at the end of the overhangs for soil retainment. Supports at the east abutment were welded (restraining translations and rotations), while those at the west abutment restrained only vertical movement (rollers). Timber planks (3x12 planks on the north side and 4x12 tongue-and-groove planks on the south side) were added for additional transverse live load distribution. Adjacent RRFCs were joined by a longitudinal reinforced concrete connection with threaded rods spaced on 2 ft centers. To complete the bridge construction, a gravel diving surface was installed.

In order to determine the structural strength and behavior of the four bridges, strain transducers and deflection transducers were mounted on the RRFCs. The BCB2 was instrumented with 12 deflection and 20 strain transducers. Both deflection transducers and strain transducers were mounted on the primary girders at the midspan, the 1/4 span, and the 3/4 span. Strain transducers were also mounted on the R/C beam at the midspan, the 1/4 span, and the 3/4 span. The interior girder of one RRFC was instrumented with strain transducers near the abutments to determine the presence of end restraint at the abutments, and a secondary member was instrumented with a strain transducer to determine the strains in that member. Finally, strain transducers were mounted to the top channel of the guardrails at midspan.

The DCB was instrumented with 6 deflection and 23 strain transducers. Similar to the BCB2 instrumentation plan, both deflection transducers and strain transducers were mounted on the primary girders at the midspan, the 1/4 span, and the 3/4 span. In addition to the primary girders, secondary

members and a transverse member in the DCB were instrumented with strain transducers to determine the strains in those members. The interior girder of one RRFC was instrumented with strain transducers near the abutments to determine the presence of end restraint at the abutments. Finally, strain transducers were mounted to the top channel of the guardrails at midspan to determine the structural contribution of the guadrails.

The BCB3 was instrumented with 12 deflection and 24 strain transducers. At the bridge's midspan, deflection and strain instrumentation was placed on all interior box girders and exterior members of the three RRFCs. The interior box girder of the south RRFC was instrumented with strain transducers near each abutment, at the midspan, and also at the 1/4 and 3/4 span locations. At the 3/4 span location, deflection instruments were placed on all three interior box girders; a strain transducer was also placed on the outer side of the south guardrail's top channel. Lastly, secondary longitudinal members and a transverse member near the midspan were instrumented with strain transducers.

The RRFC girders of the WCB2 were instrumented with 20 strain and 9 deflection transducers. Similar to instrumentation on the BCB3, deflection and strain transducers were placed along the midspan cross-section at all the interior and exterior girders of the three flatcars. Additional strain data were collected on the interior girder of the south RRFC near the abutments and at the 1/4 and 3/4 span locations. Two secondary longitudinal members, a transverse member, and the south guardrail all near the bridge midspan were also instrumented with strain transducers.

During the field load tests of the four bridges, strains and deflections were continuously measured by the transducers and recorded with a data acquisition system. With the data acquisition system, it was possible to specially mark the data as desired during the tests. The specially marked data were then used as reference points in the analysis of the results. For the static load tests, the strain data were specially marked as the tandem axle of the test truck crossed the centerline of the west abutment, the 1/4 span, the midspan, the 3/4 span, and the centerline of the east abutment.

In the demonstration project, tensile tests on coupons from a 56-ft V-deck RRFC and an 89-ft RRFC determined that the modulus of elasticity and yield strength of the steel used in both RRFCs was 29,000 ksi and 40 ksi, respectively [4]. This information was required so that the stresses in the girders from the strains recorded during the field tests could be calculated and then compared to the allowable stress of the steel used in the RRFCs. Following the 2003 AASHTO Standard Specifications for Highway Bridges as a guideline, the allowable stress of the steel used in the BCB2 and DCB was determined to be 22 ksi, 55 percent of the yield strength [7]. The Standard Specifications for Highway Bridges was also used as a guideline for determining the optional deflection limit, 1/800 of the bridge span [7].

In order to determine the total stresses that occurred in the bridges during the field load tests, a dead load analysis was performed for all bridges. Because the exterior girders in the BCB2 are of a substantial size, both the interior and exterior girders were assumed to carry the dead load of the BCB2. This was not the case in the other three bridges where the exterior girders are much smaller than the interior girder, thus, only the interior girders were assumed to carry the dead load of the DCB, BCB3, and WCB2.

As expected, the maximum strains and deflections measured during the static load tests on the BCB2 and DCB occurred in the girders directly below the axle loads of the test truck when the center of the tandem axle of the test truck was at the midspan of the bridge. The weights of the test trucks used in the load tests on the BCB2 and DCB were not the legal load that may cross either bridge. Thus, the maximum strains and deflections recorded during the load tests were multiplied by a load adjustment factor to determine an approximation of the maximum strains and deflections caused by an HS-20 truck, the maximum load likely to cross either bridge. The load adjustment factor was the ratio of the midspan moment of a simply-supported beam due to the load of an HS-20 truck to the midspan moment of a simply-supported beam

due to the loaded test truck.

In the BCB2, the maximum total stress occurred in an exterior girder at the edge of the bridge and was 14.5 ksi, which is less than the allowable flexural stress, 22 ksi. The maximum deflection of the bridge occurred in an exterior girder at the edge of the bridge and was 0.46 in., which is less than 0.81 in., the AASHTO optional limit of 1/800 of a 54 ft – 0 in. span. In the DCB, the maximum total stress occurred in an interior girder and was 27.9 ksi, which exceeds the allowable stress limit by 27 percent. In order to keep the maximum total stress below the allowable stress, the gravel driving surface on the DCB should be limited to 3 in. The maximum deflection of the DCB was 1.15 in., which slightly exceeds 1.0 in., the optional AASHTO limit of 1/800 of a 66 ft – 4 in. span. However, the optional limit is a guideline, not a requirement, and because the DCB is a rural bridge on a low-volume road, slightly exceeding the optional limit is acceptable. If the deflection of the DCB were to be required to meet the optional limit, the weight of a truck with HS-20 spacings would have to be limited to 30 tons.

Gross truck weights of 48.2 kips and 52.0 kips were used in the testing of the BCB3 and WCB2, respectively. An HS-20 design truck, without impact, has a gross weight of 72 kips, which is approximately 49% larger than the BCB3 loading and 38% larger than the WCB2 loading. A maximum deflection of -0.88 in. occurred in the BCB3 field test, which is below the AASHTO recommendation of L/800 (-0.99 in. for a span length of 66 ft – 2 in.) for legal load (HS20 gross truck weight = 72.0 kip). The WCB2 had a maximum measured deflection of -0.92 in., which was also below that of AASHTO recommendations (-1.00 in with a clear span length of 66 ft – 4 in.) If the deflections of both the BCB3 and WCB2 were increased in proportion to the test truck weights and the HS-20 design truck, the maximum deflections would be -1.31 in. and -1.27 in., respectively. These deflections are both larger than the AASHTO recommendations for both bridges, which could result in serviceability issues. The interior girders of the BCB3 during field testing had a calculated maximum total stress of +21.7 ksi, while a maximum total stress of +6.3 ksi was computed for the exterior girders. Calculated maximum total stresses for the interior and exterior girders that occurred during WCB2 field testing were +21.8 ksi and +7.1 ksi, respectively. Assuming a 40 ksi yield stress capacity, these maximum stresses fall below allowable limits of 55% of yield (22 ksi for yield stress of 40 ksi). However, if considering an HS-20 design truck loading condition, the estimated maximum total stresses for the BCB3 (+25.2 ksi) and WCB2 (+24 ksi) are above the allowable limit by 15% and 9%, respectively.

In the dynamic load tests of the DCB, the adjusted maximum total stress and the adjusted maximum deflection were 25.3 ksi and 0.83 in., respectively, and occurred when the test truck was traveling at 15 mph. Although the maximum deflection is less than the optional limit of 1.0 in., the maximum total stress exceeds the allowable stress limit. However, the maximum total stress in the static load test was greater than that in the dynamic load test; thus, by changing the thickness of the driving surface as suggested for the static load tests, the adjusted maximum total stress in the dynamic load test decreases to 19.6 ksi, which is below the allowable stress limit. The results of the dynamic load tests of the DCB were also compared to the results of the static load tests in order to determine the dynamic amplification factor for the girder strains and deflections. Through this comparison, it was determined that the dynamic amplification factor for the girder strains was 6 percent and the dynamic amplification factor for the girder deflections was 5 percent. Finally, the dynamic deflection behavior of the DCB revealed that the damped period and damped frequency of the bridge were 0.36 seconds and 2.75 Hz, respectively.

Dynamic load testing of the BCB3 and WCB2 was performed to determine the dynamic properties of the bridges, along with the dynamic amplification of their deflections and strains. The period of the BCB3 was found to be 1.3 seconds, resulting in an interior girder frequency of 0.77 Hz, and the damping of the interior girders was approximately 4%. Maximum dynamic amplification occurred at a truck speed of 25 mph on the BCB3; the maximum strain amplification was 17% and occurred in the south RRFC. Based on the free vibration of the interior girders, the dynamic properties of the WCB2 were determined. The

period was found to be 1.4 seconds, resulting in a member frequency of 0.70 Hz, and the damping of the interior girders was approximately 1.5%. A truck speed of 10 mph produced the maximum dynamic amplification in the WCB2. The largest strain amplification (27%) occurred in the north RRFC interior box girder.

Using field test data, live load distribution was determined for the BCB3 and WCB2. The additional timber planks and reinforced concrete connection in the WCB2 increased the distribution of live load forces transversely across the bridge, thus lowering the moment distribution factor. The BCB3 distribution factor was 60% while the WCB2 has a 55% distribution factor.

The third and fourth objectives of this study were met using the results from the field load tests of the BCB2 and DCB. To satisfy the third objective, the refinement of the design methodology first presented in the demonstration project [4], load distribution factors were determined for the interior and exterior members of the RRFCs. As part of the determination of the load distribution factors, it was determined that a moment fraction equal to 2/3 is valid for RRFC bridges composed of two RRFCs as well as three RRFCs. Thus, with the appropriate adjustment factors, the equation for the live load distribution factor developed for the demonstration project [4] is valid for bridges with two or three RRFCs.

After the determination of the distribution factors, a procedure for rating RRFC bridges was developed. In this procedure, all members of the bridge should be visually inspected, but only the interior and exterior primary girders are assigned a numerical rating. This rating should be found following the AASHTO Manual for Condition Evaluation of Bridges [13]. However, due to the variation of the size of girders and girder spacing, the live load effect of a member cannot be determined with the tables provided in the Rating Manual. Instead, the live load effect should be determined using the load distribution factors developed either for this report or for the demonstration project [4].

### 7.2 Conclusions

The following conclusions can be drawn from the information and analysis obtained in this investigation on the use of RRFCs in low-volume road bridges:

- The maximum girder stresses in RRFC bridges designed like the BCB2 are less than the allowable stress of the steel used in the 56-ft V-deck RRFCs.

- The maximum deflection due to an HS-20 truck on RRFC bridges designed like the BCB2 is less than the optional limit suggested in the AASHTO Standard Specifications for Highway Bridges [7].

- The maximum girder stresses in bridges designed like the DCB, which has an 8.5-in. driving surface, slightly exceed the allowable stress of the steel used in the 89-ft RRFCs. However, if the gravel driving surface is reduced or limited to 3 in., the maximum girder stresses will be less than the allowable stress.

- The maximum deflection of the DCB exceeds the optional limit suggested in the AASHTO Standard Specifications for Highway Bridges [7]. However, the optional limit is a guideline, not a requirement, and because the DCB is a rural bridge on a low-volume road, the maximum deflection of the DCB is acceptable.

- The maximum strains (stresses) and deflections measured in both the BCB3 and WCB2 bridges during testing were below the allowable stresses and AASHTO deflection

recommendations. However, the estimated strains (stresses) and deflections for an HS-20 truck loading were above these limiting values. It is recommended to reduce the span lengths so that girder strains (stresses) and deflections are below the allowable stresses and AASHTO deflection recommended values, respectively.

- The RRFC interior girder resists the majority of both the live and dead loads due to its large size in comparison to that of the other members. Thus, it is very important that this member be essentially free of any defects prior to bridge construction.

- The 22-in. wide R/C beam (BCB2 LFC) effectively transfers the live load forces transversely across the bridge.

- Welding a 1/2-in. plate to the decks of the RRFCs at the connection (DCB LFC) effectively transfers the live load forces transversely across the bridge.

- The longitudinal reinforced concrete beams connecting adjacent RRFCs, along with transverse timber planks on the bridge deck (BCB3 and WCB2 LFC) effectively transfer the live load forces transversely across the bridge.

- Tongue-and-groove timber planks on the bridge deck reduce deflections and strains by increasing the distribution of live load forces to other RRFC members.

- The use of bolted longitudinal connections between RRFCs must be properly designed (i.e. determining the spacing between bolts and large transverse members) due to the susceptibility of out-of-plane bending that may occur between bolts at these locations.

- RRFC bridges, with little or no overhangs at the abutments, should be restricted to clear span lengths of less than 66 ft. Increasing the clear span lengths would obviously increase the total maximum stresses beyond the allowable stresses in the steel.

- Using the load distribution factors presented in this investigation, the live load moments developed in the primary girders of bridges designed like the BCB2 and DCB can be determined.

- RRFC bridges can be rated by following the AASHTO Manual for Condition Evaluation of Bridges [13] and using the load distribution factors presented in this investigation to determine the live load effects.

- RRFC bridges composed of two or three RRFCs are an economical solution to bridge replacement if the longitudinal connections and bridge span length are correctly engineered. Timber planking should also be considered for additional load distribution for wider bridges composed of three railcars.

## 8.0 REFERENCES


1. National Bridge Inventory Study Foundation. NBI Report 2004. http://www.nationalbridgeinventory.com/nbi_report_200414.htm. Accessed February 1, 2005.

2. US Census Bureau. State Rankings—Statistical Abstract of the United States—Resident Population. http://www.census.gov/statab/ranks/rank01.html. Accessed September 7, 2004.

3. Wipf, T. J., F. W. Klaiber, and T. L. Threadgold. Use of Railroad Flat Cars for Low-Volume Road Bridges. Iowa DOT Project TR-421. Iowa Department of Transportation. August, 1999. 141 pp. May be accessed electronically at http://www.dot.state.ia.us/materials/research/reports/ihrb_by_topic/transportation_structures.html

4. Wipf, T. J., F. W. Klaiber, J. D. Witt, and J. D. Doornink. Demonstration Project Using Railroad Flatcars for Low-Volume Road Bridges. Iowa DOT Project TR-444. Iowa Department of Transportation. February 2003. 193 pp. May be accessed electronically at http://www.dot.state.ia.us/materials/research/reports/ihrb_by_topic/transportation_structures.html

5. Quasqueton, Iowa [map]. http://www.mapquest.com/maps/map.adp?searchtype=address&country=US&addtohistory=&searchtab=home&address=&city=Quasqueton&state=IA&zipcode=. Accessed July 7, 2004.

6. Greeley, Iowa [map]. http://www.mapquest.com/maps/map.adp?searchtype=address&country=US&addtohistory=&searchtab=home&address=&city=Greeley&state=IA&zipcode=. Accessed July 7, 2004.

7. American Association of State Highway and Transportation Officials (AASHTO). Standard Specifications for Highway Bridges, 17th Edition. Washington, D.C. 2003.

8. American Association of State Highway and Transportation Officials (AASHTO). AASHTO LRFD Bridge Design Specifications, Second Edition, Customary US Units. Washington, D.C. 1998.

9. Quasqueton, Iowa [map]. http://www.mapquest.com/maps/map.adp?searchtype=address&country=US&addtohistory=&searchtab=home&address=&city=quasqueton&state=ia&zipcode=. Accessed October 25, 2004.

10. Iowa Department of Transportation, Highway Division. Standard Designs. Abutment Details 0° skew – Steel Piling, Standard No., J30C-17-87. December 2004.

11. Lake Mills, Iowa [map]. http://www.mapquest.com/maps/map.adp?searchtype=address&country=US&addtohistory=&searchtab=home&address=&city=lakemillls&state=ia&zipcode=. Accessed September 13, 2004.

12. Doornink, J. D. Demonstration Project Using Railroad Flatcars for Low-Volume Road Bridges. M.S. Thesis, Iowa State University, 2003.

13. American Association of State Highway and Transportation Officials (AASHTO). Manual for Condition Evaluation of Bridges. Washington, D.C. 1994.

14. Carle, R., and S. Whitaker. Sheet Piling Bridge Abutments. Deep Foundations Institute Annual Meeting, Baltimore, Maryland. Oct. 1989, 16 pp.

15. Skyline Steel, LLC. Case Histories: Sprout Brook Bridge: Permanent Sheet Piling provides the Answer. Online article: http://www.skylinesteel.com/info_ch1.htm.

16. Sassel, R. Fast Track Construction with Less Traffic Disruption. Structural Engineer, October 2000. pp. 1-2.

17. United States Steel Corporation. USS Steel Sheet Piling Design Manual. Federal Highway Administration (FHWA). July 1984, 132 pp.

18. Bustamante, M., and L. Gianeselli. Predicting the Bearing Capacity of Sheet Piles Under Vertical Load. Proceedings of the 4th International Conference on Piling and Deep Foundations, Stresa, Italy. April 1991, 8 pp.

19. McShane, G. Steel Sheet Piling Used in the Combined Role of Bearing Piles and Earth Retaining Members. Proceedings of the 4th International Conference on Piling and Deep Foundations, Stresa, Italy. April 1991.

20. Doss, Robert E. and Shiping Yang. Subsurface Exploration Bridge G-2-N Winnebago County, Iowa. TEAM No. 1-1361. TEAM Services: Soil, Environmental and Material Consultants. March 1, 2004, 12 pp.

21. Anderson, J.B., F.C. Townsend, and B. Grajales. Case History Evaluation of Laterally Loaded Piles. Journal of Geotechnical and Geoenvironmental Engineering, American Society of Civil Engineers (ASCE). March 2003, pp. 187-189.

22. Office of Bridges and Structures. Bridge Design Manual. Iowa Department of Transportation. January 28, 2004.

23. Das, Braja M. Principles of Foundation Engineering, 4th Edition. Brooks/Cole Publishing Company. 1999, p598.

24. Contech Construction Products, Inc. Metric Sheeting. Middletown, Ohio. 1989.

# APPENDIX A. BCB2 LFC STRAIN-TIME HISTORIES

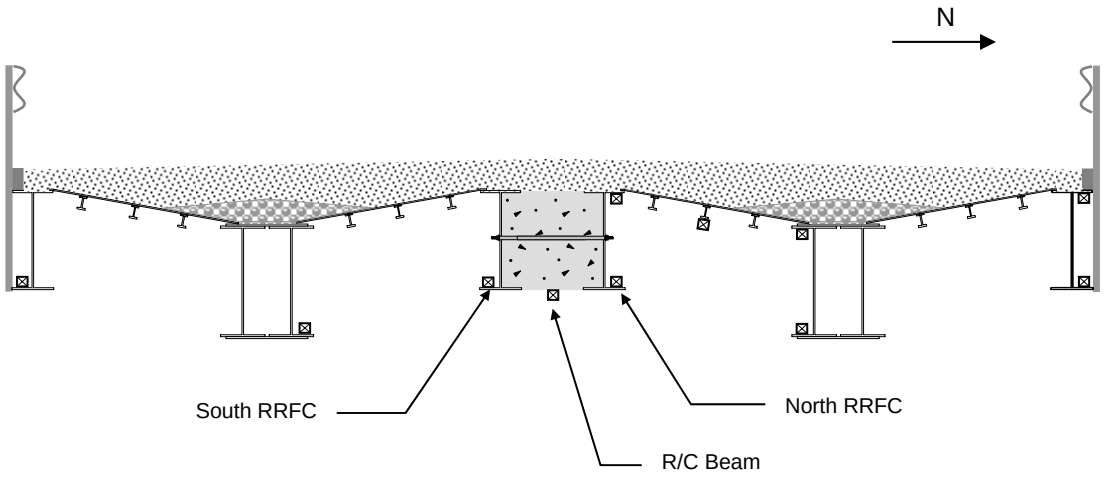


a. BCB2 cross-section at midspan

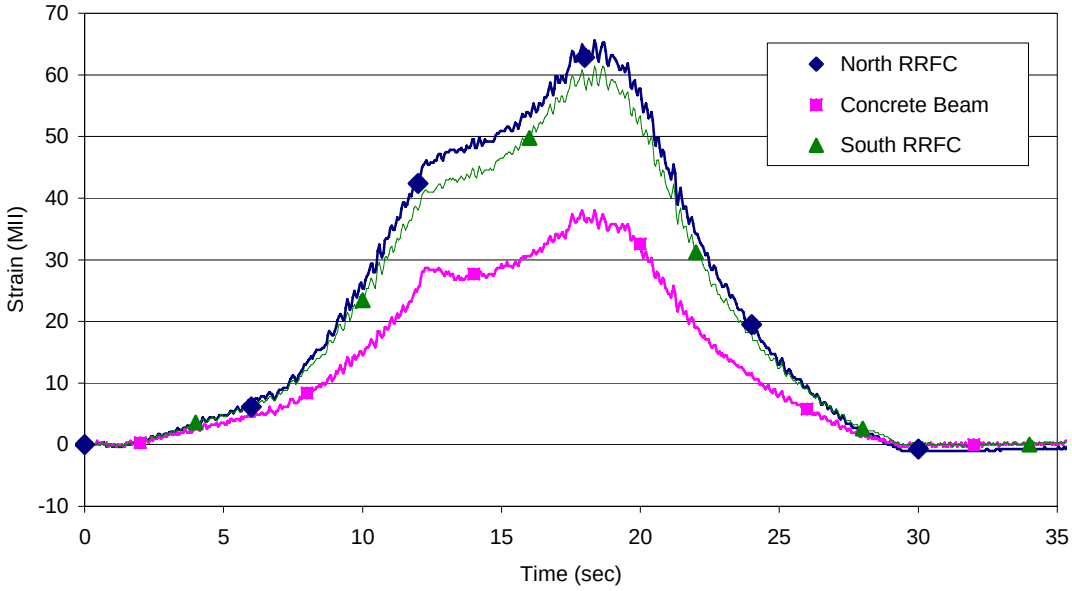


b. Lane 1 strain-time history

**Figure A.1. BCB2 LFC strain-time history**

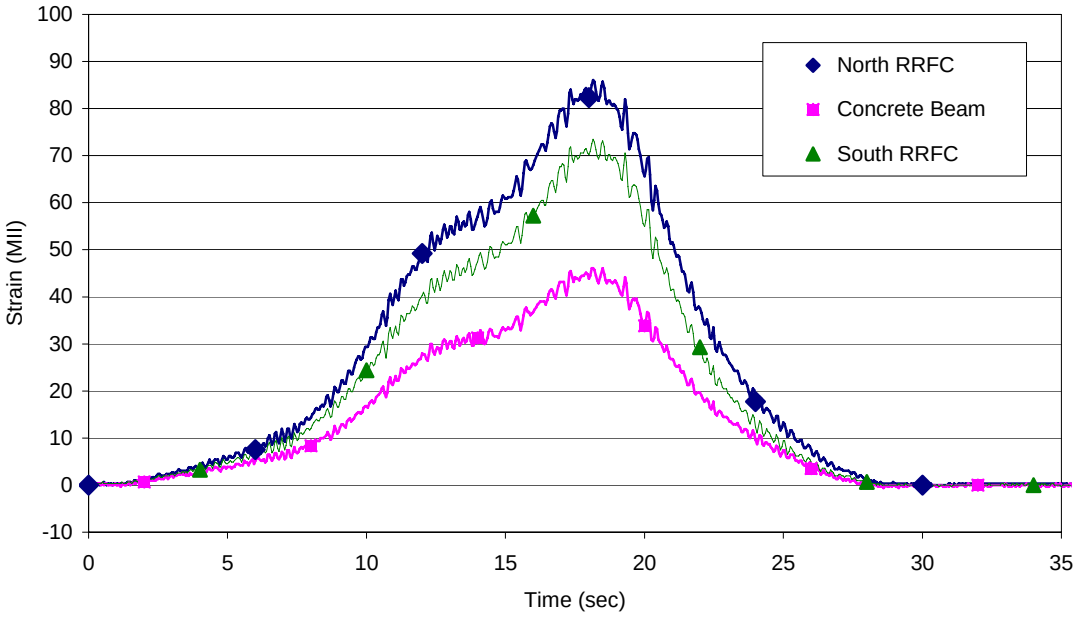


c. Lane 2 strain-time history

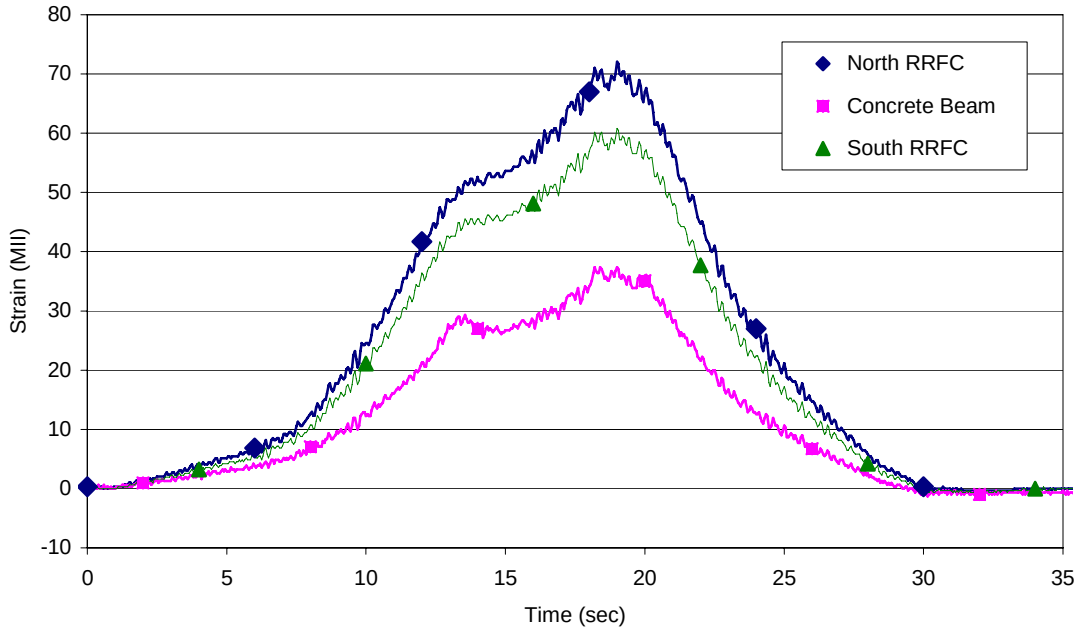


d. Lane 3 strain-time history

**Figure A1. Continued**

# APPENDIX B. DETERMINATION OF THE ADJUSTMENT FACTOR

In order to determine the adjustment factor, ψ, required for the live load distribution factor in Equations 6.1 and 6.5, a trial-and-error process was used. As reported in Section 6.1, separate adjustment factors were determined for the interior and exterior girders of both the BCB2 and the DCB. The trial-and-error process will be described using the equations presented in Section 6.1 and the calculation for the BCB2 interior girder live load distribution factor.

First, develop a statically determinate structure for the BCB2. Center the tandem axle loads of the test truck used in the field load tests over the center of the span and analyze the BCB2 as a simply-supported structure:

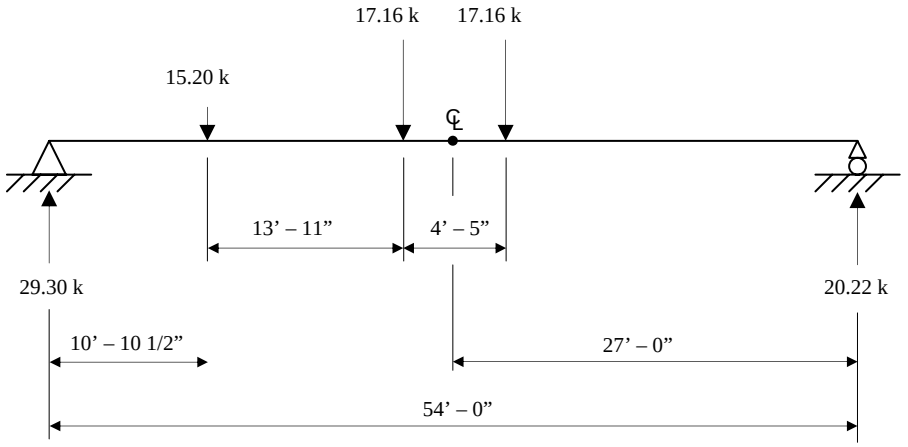


Determine the maximum live load moment, $M_{SD}$, at midspan of the BCB2 with the center of the tandem axles at midspan:

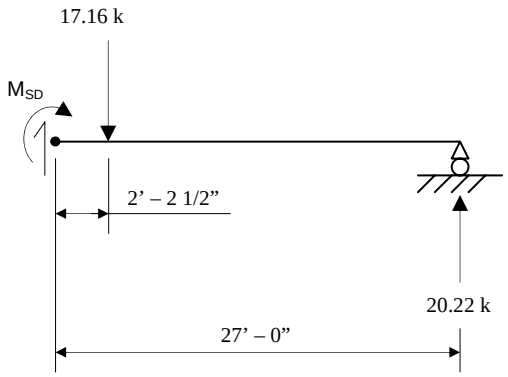


$M_{SD}$ = (20.22 k)(27.00 ft) – (17.16 k)(2.208 ft) = 508.1 k-ft

Next, determine the section properties of the primary girders and the inertia ratio, ω, for the interior girder of one RRFC:

$c_{INT}$ = 13.7 in.

$I_{INT}$ = 8,322 $in^4$

$I_{EXT}$ = 1,964 $in^4$

$I_D$ = 8,322 $in^4$

$\Sigma I_{RRFC} = (2)(I_{EXT}) + I_{INT} = (2)(1{,}964) + 8{,}322 = 12{,}250\ in^4$

$$\omega = \frac{I_D}{\Sigma I_{RRFC}} = \frac{8{,}322\ in^4}{12{,}250\ in^4} = 0.679$$

Assume the adjustment factor, ψ, is equal to 1.0, and calculate the theoretical live load moment, $M_{LL}$, in the interior girder at midspan of the bridge:

$$M_{LL} = \frac{2}{3}\psi\omega M_{SD} = (\frac{2}{3})(1.0)(0.679)(508.1) = 230.0\ \text{k-ft}$$

Determine the theoretical strain in the interior girder at midspan:

$$\varepsilon_{theo} = \frac{M_{LL}}{S*E} = \frac{(230.0\ k\text{-}ft)(12\ in./ft)(13.7\ in.)}{(29{,}000\ ksi)(8{,}322\ in^4)}(10^6) = 157\ \text{MII}$$

Determine the relative error between the theoretical strain and the experimental strain measured during the field load test, $\varepsilon_{exp}$ = 116 MII:

$$\text{Error} = \frac{\varepsilon_{exp} - \varepsilon_{theo}}{\varepsilon_{exp}} * 100\% = \frac{(116 - 157)}{116} * 100\% = -35.3\%$$

A relative error less than zero indicates that the experimental strain is less than the theoretical strain; thus, the theoretical strain is conservative. For the assumed adjustment factor to be acceptable, the relative error between the two strains must be negative and the absolute value of the relative error must be less than 10 percent. With a relative error less than 10 percent, the theoretical live load moment can be assumed to adequately approximate the experimental live load moment. A sensitivity analysis on the effect of the relative error on the adjustment factor indicated that there is a minimal difference between adjustment factors determined with a maximum relative error of 10 percent and adjustment factors determined with a maximum relative error 1 percent. Because the relative error is 35.3 percent, which is more than 10 percent, assume a new value for the adjustment factor and recalculate the theoretical live load moment:

$\psi = 0.8$

$$M_{LL} = \frac{2}{3}\psi\omega M_{SD} = (\frac{2}{3})(0.8)(0.679)(508.1) = 184.0 \text{ k-ft}$$

Determine the revised theoretical strain in the interior girder at midspan:

$$\varepsilon_{theo} = \frac{M_{LL}}{S*E} = \frac{(184.0\,\text{k - ft})(12\,\text{in./ft})(13.7\,\text{in.})}{(29{,}000\,\text{ksi})(8{,}322\,\text{in}^4)}(10^6) = 125 \text{ MII}$$

Determine the relative error between the revised theoretical strain and the experimental strain measured during the field load test, $\varepsilon_{exp} = 116$ MII:

$$\text{Error} = \frac{\varepsilon_{exp} - \varepsilon_{theo}}{\varepsilon_{exp}} * 100\% = \frac{(116 - 125)}{116} * 100\% = -7.2\%$$

When the adjustment factor, $\psi$, is equal to 0.8, the relative error between the theoretical and experimental strains is negative and less than 10 percent. Thus, for interior girder of the BCB2, the adjustment factor, $\psi$, is 0.8.

This procedure was followed to determine the adjustment factors for an exterior girder of the BCB2 and the interior and exterior girders of the DCB.

# APPENDIX C. DETERMINATION OF THE MOMENT FRACTION

Equation 6.1, which is presented in Section 6.1 and used to determine the maximum live load moment at midspan of a bridge, includes a moment fraction of 2/3 as part of the live load distribution factor. The moment fraction is determined using the deflection curve that describes the maximum deflection of the bridge. The area beneath the deflection curve is the total energy of the system, and the moment fraction is the fraction of the system energy for one RRFC. The procedure for determining the moment fraction was first developed in the demonstration project for RRFC bridges consisting of three RRFCs [4]. To verify that the moment fraction is the same for bridges composed of two RRFCs, the procedure described in Appendix D of the Demonstration Project Using Railroad Flatcars for Low-Volume Road Bridges [12] is used in the following sections to determine the moment fractions for the BCB2 and DCB.

**C.1 BCB2 Moment Fraction**

To determine the moment fraction, one first plots the maximum deflections at midspan due to the test truck and fits a "best-fit" curve to the deflections; the "best-fit" curve for the BCB2 is shown in Figure C.1 using the deflections from the field load test with the truck in Lane 3. Using the equation of the "best-fit" curve, calculate the area under the "best-fit" curve for the unloaded RRFC (the system energy of the unloaded RRFC):

$$A_1 = \int_0^{134.5} (1.119)(10^{-6})(x^2) - (1.554)(10^{-3})(x) - (0.03976)dx = -19.01 \text{ in}^2$$

Calculate the area under the "best-fit" curve beneath the RRFC on which the test truck is positioned (the system energy of the loaded RRFC):

$$A_2 = \int_{134.5}^{247} (1.119)(10^{-6})(x^2) - (1.554)(10^{-3})(x) - (0.03976)dx = -34.60 \text{ in}^2$$

Determine the moment fraction for the BCB2 (the fraction of the system energy for the loaded RRFC):

$$MF_{BCB2} = \frac{A_2}{A_1 + A_2} = \frac{-34.60}{-19.01 - 34.60} = 0.65$$

**C.2 DCB Moment Fraction**

The "best-fit" curve for the DCB is shown in Figure C.2 using the deflections from the field load test with the truck in Lane 3. As with the BCB2, one calculates the area under the best-fit curve for the unloaded RRFC (the system energy of the unloaded RRFC):

$$A_1 = \int_0^{109.5} (7.880)(10^{-8})(x^3) - (2.113)(10^{-6})(x^2) - (1.905)(10^{-3})(x) - (0.2186)dx$$
$$= -41.89 \text{ in}^2$$

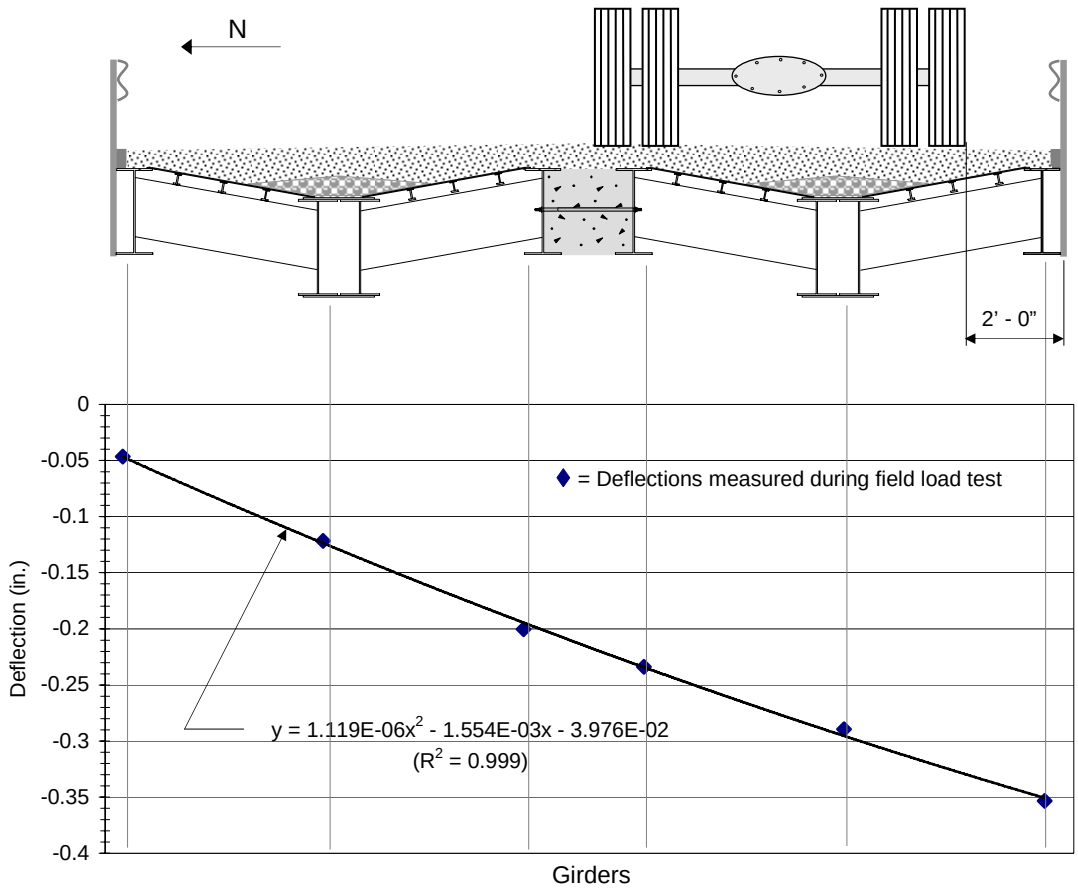


**Figure C.1. BCB2 midspan deflection "best-fit" curve**

Then, calculate the area under the "best-fit" curve beneath the RRFC on which the test truck is positioned (the system energy of the loaded RRFC):

$$A_2 = \int_{109.5}^{219} (7.880)(10^{-8})(x^3) - (2.113)(10^{-6})(x^2) - (1.905)(10^{-3})(x) - (0.2186)dx$$

$$= -81.25 \text{ in}^2$$

Determine the moment fraction for the DCB (the fraction of the system energy for the loaded RRFC):

$$MF_{DCB} = \frac{A_2}{A_1 + A_2} = \frac{-81.25}{-41.89 - 81.25} = 0.66$$

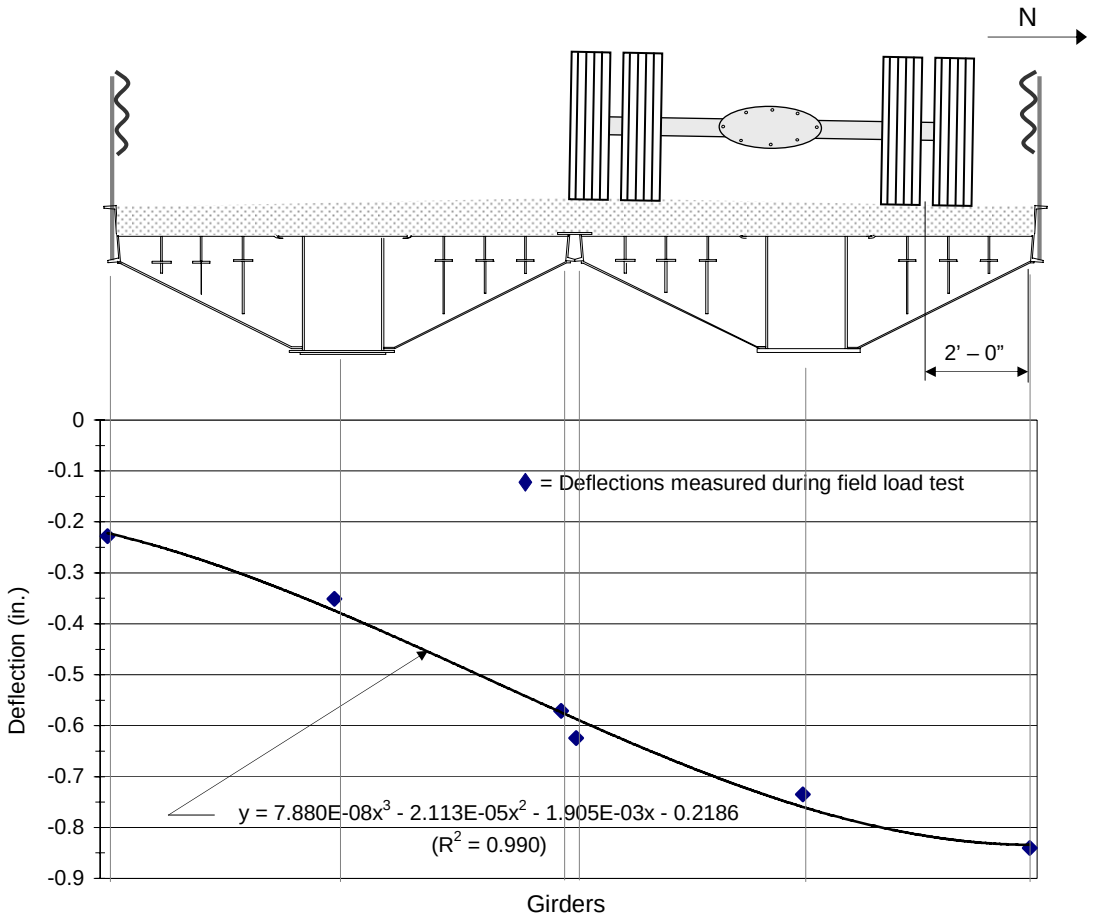


**Figure C.2. DCB midspan deflection "best-fit" curve**

# APPENDIX D. RRFC BRIDGE RATING EXAMPLE

Following the procedure of Section 6.2, the bridge inventory rating for the BCB2 will be determined as an example for rating RRFC bridges. First, determine the rating factor for an interior girder. To do so, determine the allowable stress capacity of the member, C, from the inventory rating table (Table 6.6.2.1-1) provided in the Rating Manual [13]:

$C = 0.55\ F_y = (0.55)(40\ \text{ksi}) = 22\ \text{ksi}$

Next, determine the dead load effect on the interior girder, D, using the assumptions and procedure described in Section 2.4. First, calculate the equivalent uniform dead load acting on the interior girder:

Gravel = 98 lb/ft$^2$

Guard Rail System = 100 lb/ft

RRFC = 35,000 lb

RRFC Length = 56 ft

Bridge Span = 54 ft

Bridge Width = 20.5 ft

Interior girder tributary width = 4.688 ft

$$w = \left(\frac{4.688\,\text{ft}}{20.5\,\text{ft}}\right)\left[(98\,\text{lb/ft}^2)(20.5\,\text{ft}) + (100\,\text{lb/ft}) + (2)\left(\frac{35{,}000\,\text{lb}}{56\,\text{ft}}\right)\right] = 769\ \text{lb/ft}$$

Develop a statically determinate structure for the girder, and analyze the girder with the uniform dead load:

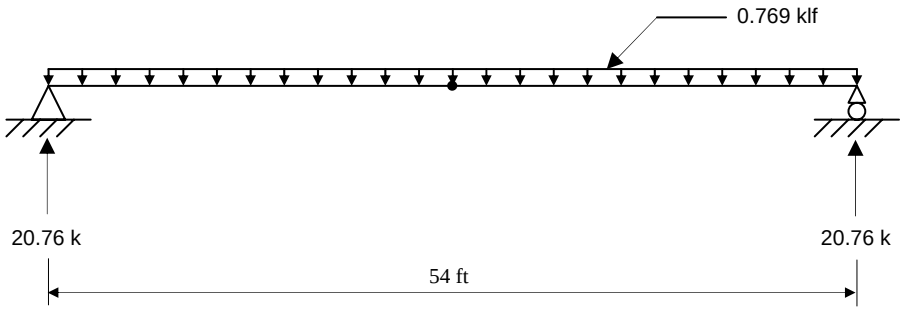

Determine the maximum dead load moment, M, at midspan of the bridge:

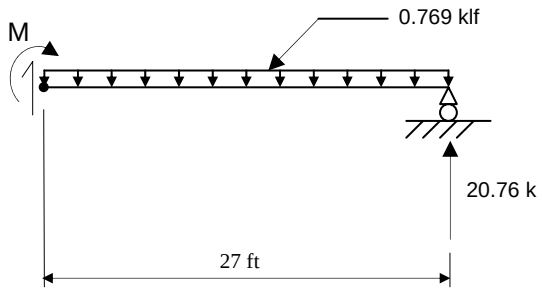


M = (20.76 k)(27 ft) – (0.769 klf)(27 ft)(0.5)(27 ft) = 280 k-ft

Determine the section modulus of the interior girder:

$I = 8{,}322\ \text{in.}^4$

c = 13.73 in. (to the bottom flange)

$$S = \frac{I}{c} = \frac{8{,}322\ \text{in}^4}{13.73\ \text{in.}} = 606\ \text{in.}^3$$

Calculate the dead load effect, the stress in the bottom flange of the interior girder:

$$D = \sigma_{DL} = \frac{M}{S} = \frac{(280\ \text{k - ft})(12\ \text{in./ft})}{606\ \text{in}^3} = 5.6\ \text{ksi}$$

In order to determine the live load effect on the interior girder of the BCB2, develop a statically determinate structure for the BCB2. Position the center of gravity of an HS-20 truck over the center of the span and analyze the bridge as simply supported over its clear span:

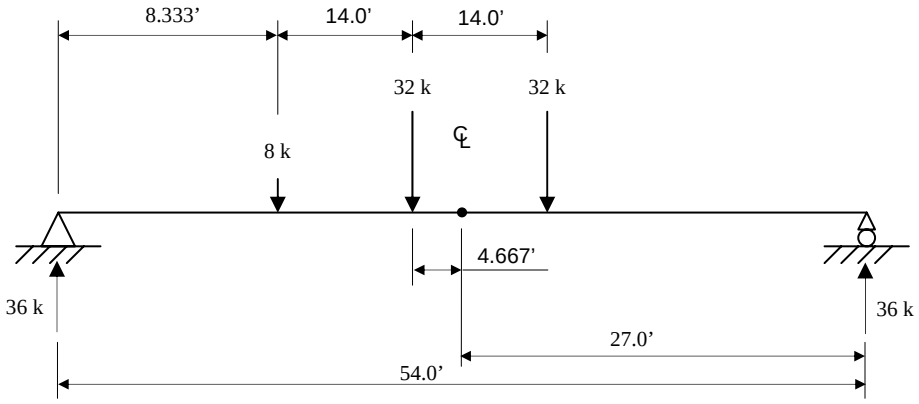

Determine the maximum midspan moment due to the HS-20 truck, $M_{HS-20}$:

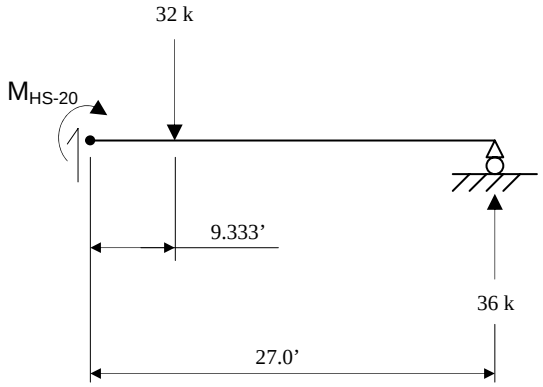


$M_{HS-20}$ = (36 k)(27.0 ft) – (32 k)(9.333 ft) = 673 k-ft

Next, determine the section properties of the primary girders and the inertia ratio, ω, and adjustment factor, ψ, for the interior girder of one RRFC:

$c_{INT}$ = 13.7 in.

$I_{INT} = 8{,}322\ \text{in}^4$

$I_{EXT} = 1{,}964\ \text{in}^4$

$I_D = 8{,}322\ \text{in}^4$

$\Sigma I_{RRFC}$ = (2)($I_{EXT}$) + $I_{INT}$ = (2)(1,964) + 8,322 = 12,250 in.$^4$

$$\omega = \frac{I_D}{\Sigma I_{RRFC}} = \frac{8{,}322\,\text{in}^4}{12{,}250\,\text{in}^4} = 0.679$$

ψ = 0.8 (from Section 5.1)

Calculate the distribution factor for the interior girder:

$$DF = \frac{2}{3}\psi\omega = \frac{2}{3}(0.8)(0.679) = 0.362$$

Determine the live load moment for the interior girder:

M = (DF)($M_{HS-20}$) = (0.362)(673 k-ft) = 244 k-ft

Calculate the live load effect, L, the stress in the bottom flange of the interior girder:

$$L = \sigma_{LL} = \frac{M}{S} = \frac{(244\,\text{k - ft})(12\,\text{in./ft})}{606\,\text{in}^3} = 4.83\ \text{ksi}$$

The values for the impact factor, I, and the factors for dead and live loads, $A_1$ and $A_2$, are provided in Section 6.2. With these values, and the calculated values of the allowable stress capacity, C, the dead load effect, D, and the live load effect, L, determine the rating factor for the interior girder:

$$RF = \frac{C - A_1 D}{A_2 L (1 + I)} = \frac{(22\ \text{ksi}) - (1.0)(5.6\ \text{ksi})}{(1.0)(4.83\ \text{ksi})(1 + 0.33)} = 2.55$$

Finally, determine the inventory rating of the interior girder of the BCB2:

Rating = (RF)(Weight of truck) = (2.55)(36 tons) = 91 tons

To determine the actual bridge rating of the BCB2, this example should be repeated to find the rating for the exterior girders of the BCB2. When repeated, using the properties of an exterior girder, the bridge rating is 80 tons. The BCB2 bridge rating is the lowest calculated rating; thus, the bridge rating for the BCB2 is 80 tons.

# APPENDIX E. DETERMINATION OF THE LOAD ADJUSTMENT FACTOR

Equation 2.2, presented in Section 2.5.1, is used to determine the load adjustment factor, which modifies the strains and deflections measured in field load tests to reflect the strains and deflections caused by Iowa legal loads, an HS-20 truck. The load adjustment factor is the ratio of the midspan moment due to an HS-20 truck to the midspan moment do to the test truck. The load adjustment factors for the BCB2 and DCB are calculated in the following sections.

**E.1 BCB2 Load Adjustment Factor**

First, develop a statically determinate structure for the BCB2. Position the center of gravity of an HS-20 truck over the center of the span and analyze the bridge as simply supported over its clear span:

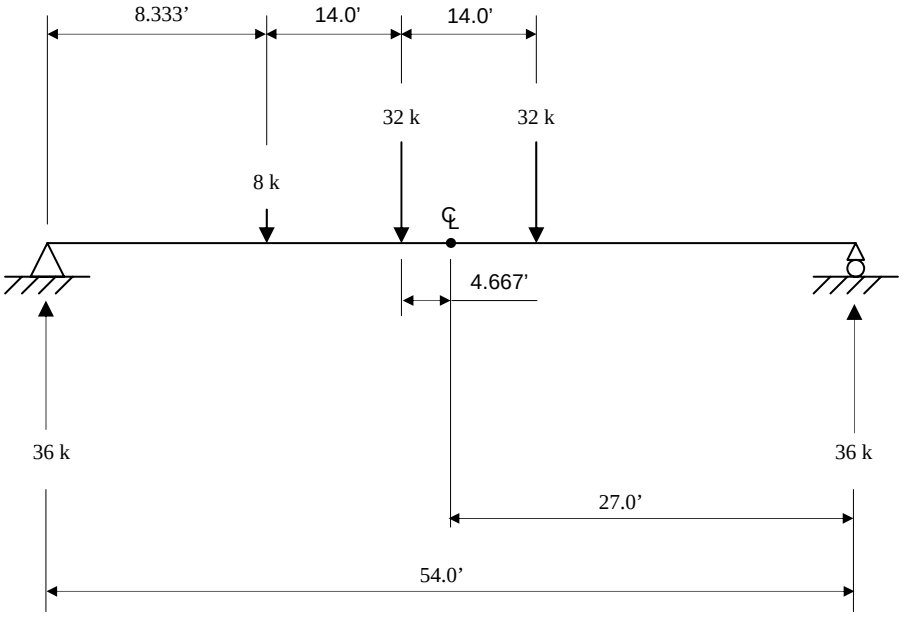


Determine the maximum midspan moment due to the HS-20 truck, $M_{HS-20}$:

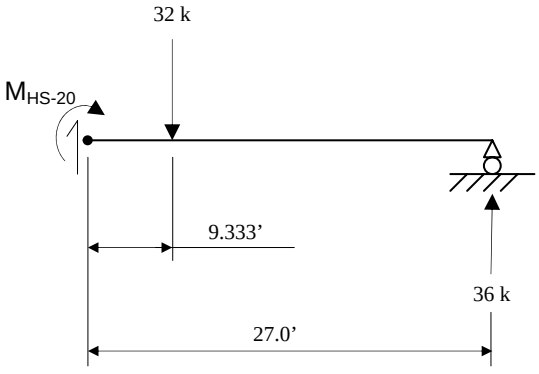


$M_{HS-20}$ = (36 k)(27.0 ft) – (32 k)(9.333 ft) = 673 k-ft

With the structurally determinate BCB2, position the center of gravity of the test truck over the center of the span and analyze the bridge as simply supported over its clear span:

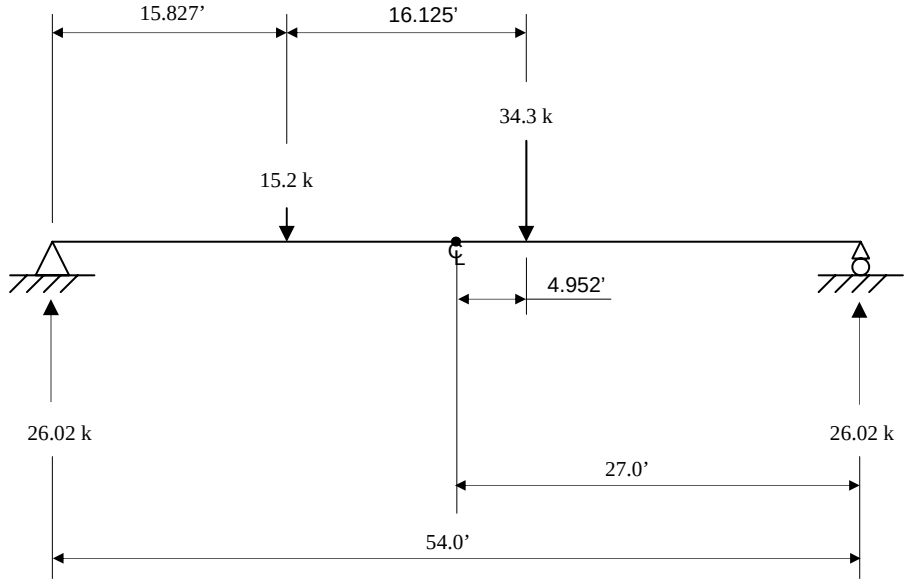


Determine the maximum midspan moment due to the test truck, $M_{TT}$:

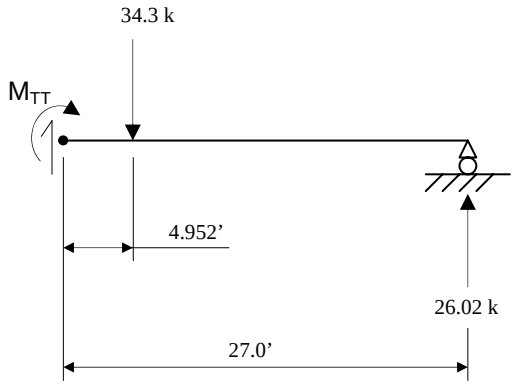


$M_{TT}$ = (26.02 k)(27.0 ft) – (34.3 k)(4.952 ft) = 533 k-ft

Calculate the load adjustment factor for the BCB2:

$$\beta = \frac{M_{HS-20}}{M_{TT}} = \frac{673\,\text{k - ft}}{533\,\text{k - ft}} = 1.26$$

**E.2 DCB Load Adjustment Factor**

Develop a statically determinate structure for the DCB. Position the center of gravity of an HS-20 truck over the center of the span and analyze the bridge as simply supported over its clear span:

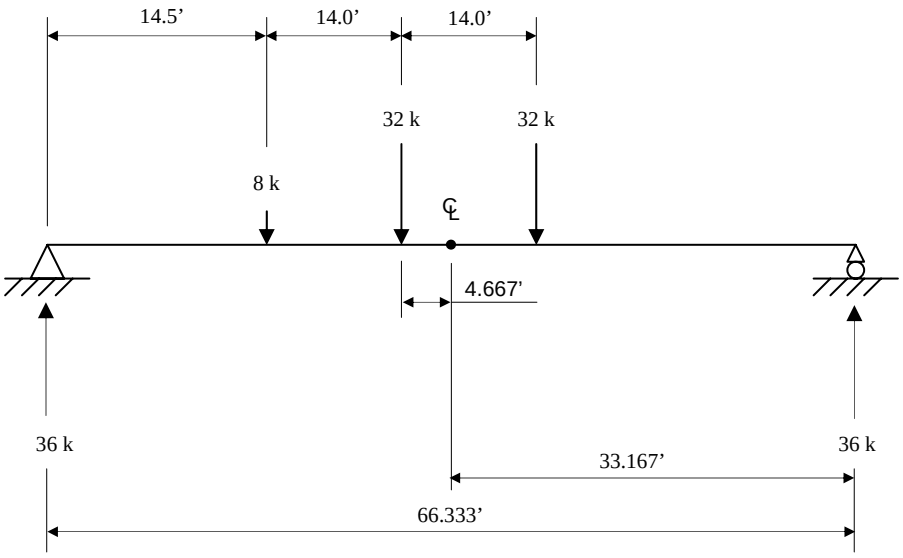


Determine the maximum midspan moment due to the HS-20 truck, $M_{HS-20}$:

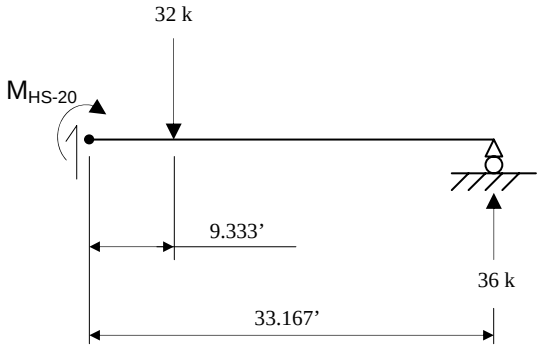


$M_{HS-20}$ = (36 k)(33.167 ft) – (32 k)(9.333 ft) = 895 k-ft

With the structurally determinate DCB, position the center of gravity of the test truck over the center of the span and analyze the bridge as simply supported over its clear span:

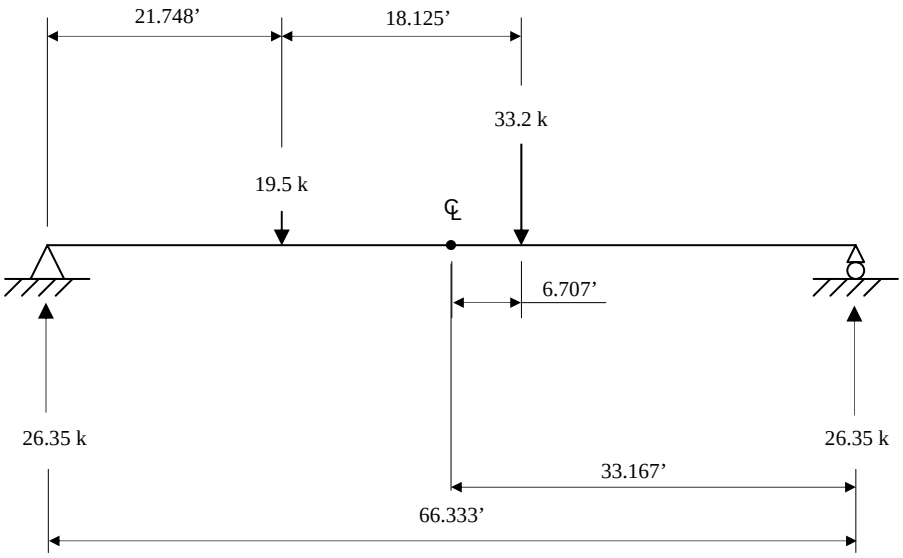


Determine the maximum midspan moment due to the test truck, MTT:

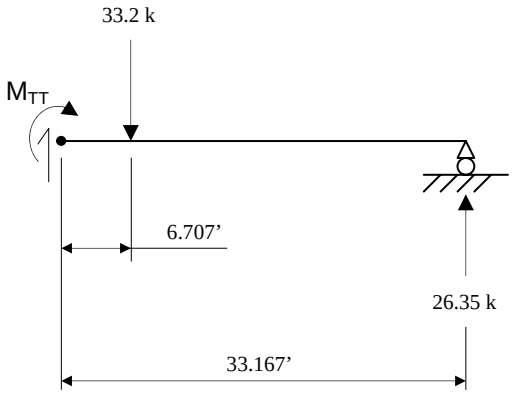


$M_{TT}$ = (26.35 k)(33.167 ft) – (33.2 k)(6.707 ft) = 651 k-ft

Calculate the load adjustment factor for the DCB:

$$\beta = \frac{M_{HS-20}}{M_{TT}} = \frac{895\,k\text{-}ft}{651\,k\text{-}ft} = 1.37$$

# APPENDIX F. DETERMINATION OF THE MAXIMUM SPAN FOR 89-FT RRFCS

The sections that follow present the assumptions and equations used to determine the maximum clear span of 89-ft RRFCs without building up the cross-section at the midspan of the bridge and without a center pier. AASTHO LRFD equations and load factors are used for the calculations, and the maximum clear span is designed based on the effects of an HS-20 truck as specified in the AASHTO LRFD Bridge Design Specifications [8].

## F.1 Assumptions

For the calculation in this appendix, the RRFCs are assumed to be symmetric about the midspan of the bridge, regardless of the clear span length. To theoretically determine the maximum stresses in the RRFC bridges, several other assumptions must be made. The assumptions made for the dead load on the bridge are:

1. One 89-ft RRFC weighs 42,000 lbs
2. 3.5 in. thick wood planks cover the entire deck
3. The unit weight of the wood planks is 36.3 pcf
4. A 6 in. layer of gravel covers the wood planks
5. The unit weight of the gravel is 110 pcf
6. The guard rail system weighs 100 lb/ft

These loads are converted to pounds per unit length by assuming the bridge is composed of two RRFCs with a total width of 18 ft. Using these assumptions, the total weight of the components is 1040 lb/ft and the total weight of the wearing surface is 700 lb/ft.

## F.2 Calculations

The maximum moment due to the uniform dead load occurs at midspan of a bridge. However, the maximum moment due to the concentrated live axle loads occurs beneath the load closest to the center of gravity of all the axle loads when the truck is positioned as described in the following section. Because the maximum moments due to the dead and live loads may not occur at the same point along the bridge, two cases must be considered. For Case 1, the dead and live load moments are determined at the midspan of the bridge; the maximum dead load moment and live load moment at midspan are combined. For Case 2, the dead and live load moments are determined at the point beneath one of the axle loads; the maximum live load moment is combined with the dead load moment at the same location.

### *F.2.1 Case 1 Calculations*

First, develop a statically determinate model of the bridge. Position an HS-20 truck such that midspan of the bridge is half way between the center of gravity of the three axle loads and the nearest axle load, increase the axle loads by 33 percent to account for the impact load, and analyze the bridge as simply supported over its clear span:

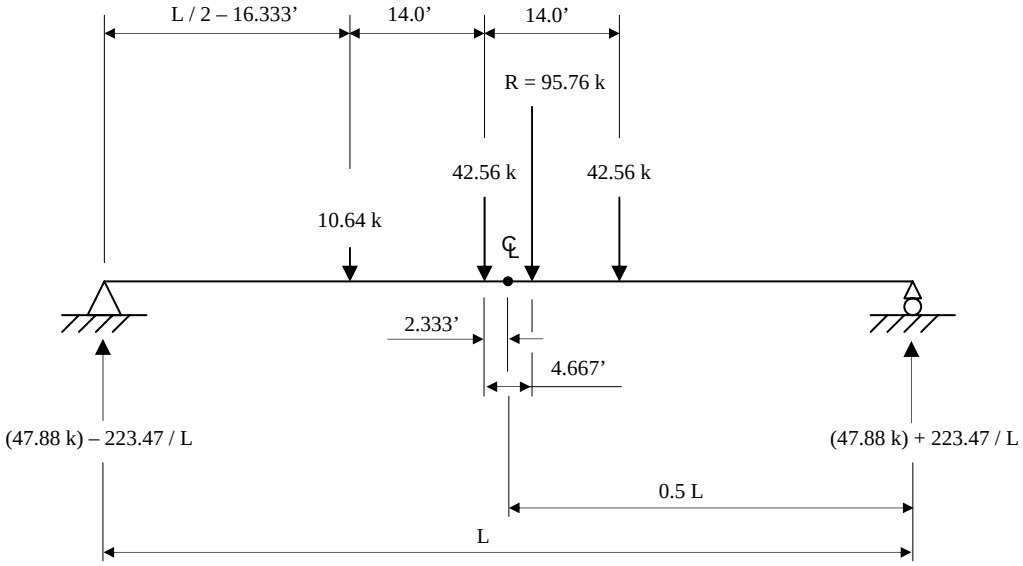


Determine the maximum live load moment, $M_{SD}$, at midspan of the bridge:

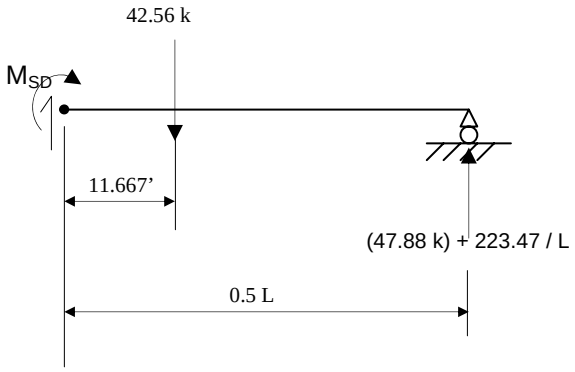


$$M_{SD} = (47.88 + \frac{223.47}{L})(0.5\ L) - (42.56)(11.667) = (23.94\ L - 384.8)\ k - ft$$

Next, determine the section properties of the primary girders and the inertia ratio, ω, for the interior girder and one exterior girder of one 89-ft RRFC:

$I_{INT} = 8{,}999\ in.^4$

$I_{EXT} = 346\ in.^4$

$\Sigma I_{RRFC} = (2)(I_{EXT}) + I_{INT} = (2)(346) + 8{,}999 = 9{,}691\ in.4$

$$\omega_{INT} = \frac{I_D}{\Sigma I_{RRFC}} = \frac{8{,}999\ in.^4}{9{,}961\ in.^4} = 0.929$$

$$\omega_{EXT} = \frac{I_D}{\Sigma I_{RRFC}} = \frac{346\,\text{in.}^4}{9{,}961\,\text{in.}^4} = 0.036$$

Because the inertia ratio for the interior girder is significantly larger than the inertia ratio for an exterior girder, assume that the capacity of the interior girder will control the maximum clear span. Also, assume the adjustment factor, $\psi$, is equal to 1.0, and calculate thelive load moment, $M_{LL}$, in the interior girder at midspan of the bridge:

$$M_{LL} = \frac{2}{3}\psi\omega M_{SD} = (\frac{2}{3})(1.0)(0.929)(23.94\,L - 384.8) = (14.83\,L - 238.3)\ k - ft$$

Next, analyze the bridge with the uniform dead load assumed in Section F.1, separating the dead load of the components (DC) from the dead load of the wearing surface (DW):

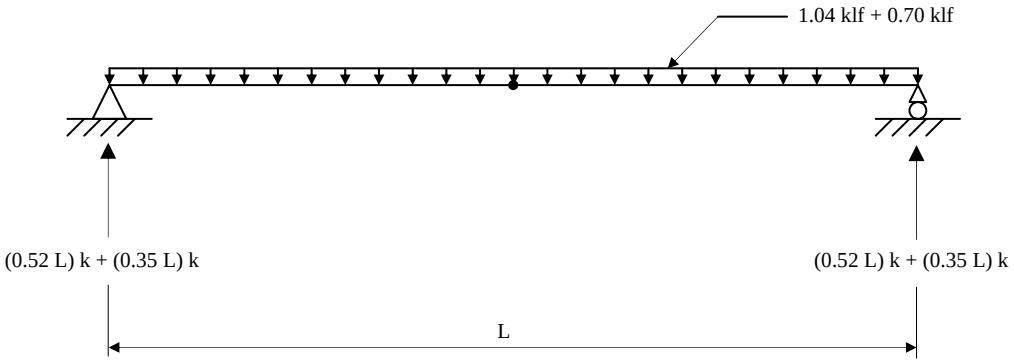


Determine the maximum dead load moment, $M_{SD}$, at midspan of the bridge:

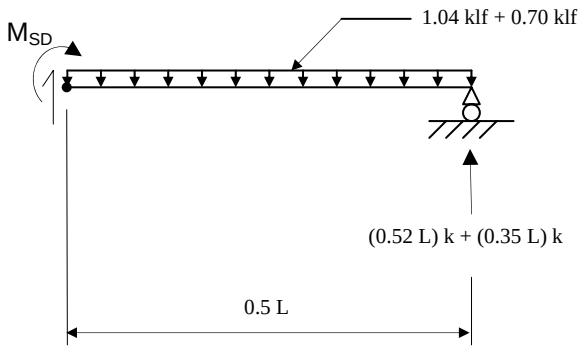


DC: $M_{SD} = (0.52\,L)(0.5\,L) - (1.04)(0.5\,L)(0.5)(0.5\,L) = (0.13\,L^2)\ k - ft$

DW: $M_{SD} = (0.35\,L)(0.5\,L) - (0.70)(0.5\,L)(0.5)(0.5\,L) = (0.088\,L^2)\ k - ft$

As with the live load analysis, the interior girders are assumed to carry the entire dead load on the bridge, thus, the maximum dead load moment in one interior girder at midspan of the bridge is:

$M_{DC} = (0.5)(M_{SD}) = (0.5)(0.13\ L^2) = (0.065\ L^2)$ k - ft

$M_{DW} = (0.5)(M_{SD}) = (0.5)(0.088\ L^2) = (0.044\ L^2)$ k - ft

Following the AASHTO LRFD Bridge Design Specifications [8], combine the maximum live load and dead load moments assuming the operational importance factor is 0.95 since RRFC bridges are used on low-volume roads:

$M_{MAX} = (0.95)(1.25*M_{DC} + 1.5*M_{DW} + 1.75*M_{LL})$

$= (0.95)[(1.25)(0.065\ L^2) + (1.5)(0.044\ L^2) + (1.75)(14.83\ L - 238.3)]$

$= (0.14\ L^2 + 24.65\ L - 396.17)$ k - ft

Determine the flexural capacity of an interior girder of an 89-ft RRFC following the procedure in the AASHTO LRFD Bridge Design Specifications [8]:

$M_r = 1{,}898$ k - ft

Calculate the maximum clear span, L, for which $M_{MAX}$ is less than $M_r$:

$M_{MAX} = M_r$

$(0.14\ L^2 + 24.65\ L - 396.17) = 1{,}898$

$L = 67.33$ ft

This is the maximum clear span for Case 1, using the maximum dead load and live load moments at the midspan of the bridge.

*F.2.2 Case 2 Calculations*

Using the statically-determinate structure developed for Case 1, determine the maximum live load moment, $M_{SD}$, at the point beneath the axle load closest to the center of gravity of the truck:

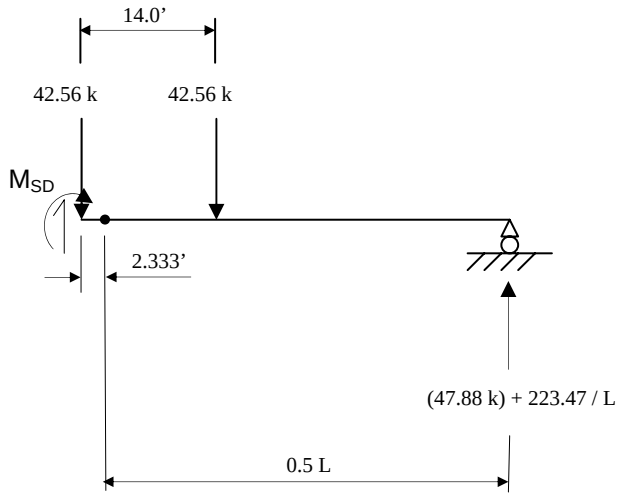

$$M_{SD} = (47.88 + \frac{223.47}{L})(0.5\,L + 2.333) - (42.56)(14.0)$$

$$= (23.94\,L + \frac{521.42}{L} - 372.40)\ \text{k - ft}$$

Use the section properties and inertia ratios used for the maximum dead load moment case, and again assume the adjustment factor, $\psi$, is equal to 1.0. Calculate the live load moment, $M_{LL}$, in the interior girder at midspan of the bridge:

$$M_{LL} = \frac{2}{3}\psi\omega M_{SD} = (\frac{2}{3})(1.0)(0.929)(23.94\,L + \frac{521.42}{L} - 372.40)$$

$$= (14.83\,L + \frac{322.93}{L} - 230.64)\ \text{k - ft}$$

Next, determine the maximum dead load moment, $M_{SD}$, at the point 2 ft – 4 in. from the midspan of the bridge:

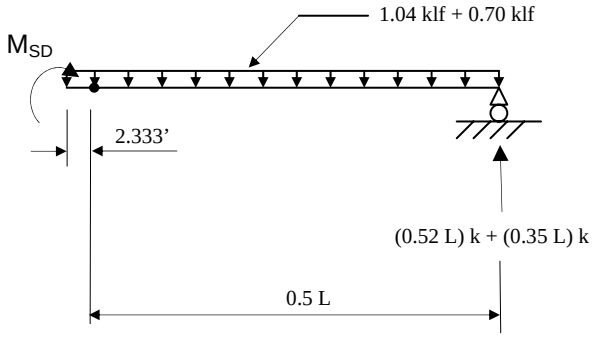


DC: $M_{SD} = (0.52\,L)(0.5\,L + 2.333) - (1.04)(0.5\,L + 2.333)(0.5)(0.5\,L + 2.333)$

$= (0.13\,L^2 - 2.83)$ k - ft

DW: $M_{SD} = (0.35\,L)(0.5\,L + 2.333) - (0.70)(0.5\,L + 2.333)(0.5)(0.5\,L + 2.333)$

$= (0.088\,L^2 - 1.91)$ k - ft

As with the live load analysis, the interior girders are assumed to carry the entire load on the bridge, thus, the maximum dead load moment in one interior girder at midspan of the bridge is:

$M_{DC} = (0.5)(M_{SD}) = (0.5)(0.13\,L^2 - 2.83) = (0.065\,L^2 - 1.41)$ k - ft

$M_{DW} = (0.5)(M_{SD}) = (0.5)(0.088\,L^2 - 1.91) = (0.044\,L^2 - 0.95)$ k - ft

Following the AASHTO LRFD Bridge Design Specifications [8], combine the maximum live load and dead load moments assuming the operational importance factor is 0.95 since RRFC bridges are used on low-volume roads:

$M_{MAX} = (0.95)(1.25*M_{DC} + 1.5*M_{DW} + 1.75*M_{LL})$

$$= (0.95)[(1.25)(0.065\ L^2 - 1.41) + (1.5)(0.044\ L^2 - 0.95)$$

$$+ (1.75)(\ 14.83\ L + \frac{322.93}{L} - 230.64)]$$

$$= (0.14\ L^2 + 24.65\ L + \frac{536.87}{L} - 386.47)\ k\text{-}ft$$

The flexural capacity of an interior girder of an 89-ft RRFC is the same as determined for Case 1:

$M_r = 1{,}898$ k - ft

Calculate the maximum clear span, L, for which $M_{MAX}$ is less than $M_r$:

$M_{MAX} = M_r$

$$(0.14\ L2 + 24.65\ L + \frac{536.87}{L} - 386.47) = 1{,}898$$

L = 66.93ft

This is the maximum clear span for Case 2, using the maximum live load moment. Because the shorter length controls the maximum clear span, Case 2 controls the maximum clear span. Thus, for a simply-supported bridge composed of two 89-ft RRFCs without building up the girders, the maximum clear span is 66 ft – 11 in. As stated in Section F.1, this clear span assumes that the RRFC is symmetric about the midspan of the bridge; the portion of the 89-ft RRFC used for the maximum clear span is shown in Figure F.1

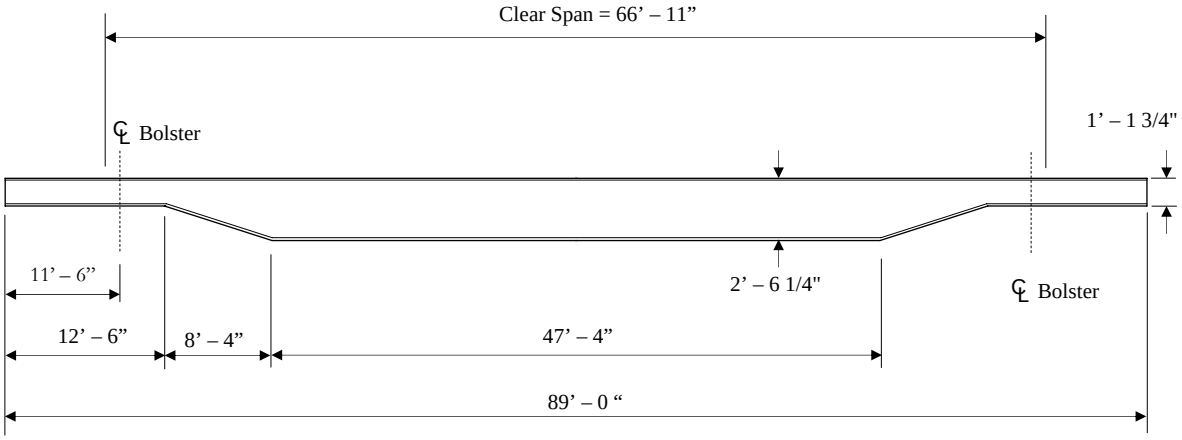


**Figure F.1. Maximum clear span possible from a “cut” 89-ft RRFC**